



**Bifunctional Nanocomposites:
Surface Modification of Reactive Matrices
with Functional Metal Nanoparticles
by Intermatrix Synthesis Technique**

Julio Bastos Arrieta
Doctoral Thesis

Doctoral Studies in Chemistry

Supervisors:

Maria Muñoz Tapia &
Dmitri Muraviev

Department of Chemistry

Faculty of Science

2014

Report submitted to aspire for the Doctor Degree

Julio Bastos Arrieta

Supervisors' Approval;

Dra. Maria Muñoz Tapia

Dr. Dmitri Muraviev

Bellaterra (Cerdanyola del Vallès), September 16th, 2014

*Con, por y para mi
familia*

This work presented here has been possible thanks to the personal grant awarded from Universitat Autònoma de Barcelona in the *Personal Investigador en Formació* Fellowship Program. Financial support was obtained from the project *Nuevo material nanocomposite para el tratamiento combinado de aguas*. (ACCIÓ, *Departament d'Innovació, Universitats i Empresa de la Generalitat de Catalunya*, Spain) (VALTEC-09-2-0056), developed under the supervision of Dr. Dmitri Muraviev and Dr. Maria Muñoz Tapia executed within *Grup de Tècniques de Separació* and *Grup de Sensors i Biosensors* from the *Departament de Química* (Universitat Autònoma de Barcelona, Barcelona, Spain) to whom I have more than gratitude, since they both guided me through all these years.

I acknowledge the scientific and personal support offered by Dr. Yurii Gun'ko, Dr. Valerie Gerard and Ms. Raquel Serrano (Trinity College Dublin, Ireland) and Dr. Prof. Larisa Tarkova and Ms. Anja Stenbock (DWI Leibniz-Institut für Interaktive Materialien Aachen, Germany) during the both three-month research stays which helped me to enhance my scientific expertise and research included in this PhD Thesis.

Table of Contents

Table of Contents

Table of Contents	II
Figure Index.....	V
Table Index.....	X
Acronym List.....	XI
Graphical Abstract.....	XIII
Summary.....	XIV
Resum.....	XV
Resumen	XVI
1. Introduction.....	1
1.1. General Introduction	1
1.2. Nanotechnology, Nanomaterials and Nanocomposites: historical background, properties and applications.	2
1.2.1. Nanoparticle Stabilization	6
1.3. Stabilization of NPs with Polymers: Preparation and Synthesis of Polymer – Metal Nanocomposites by Intermatrix Synthesis Technique (IMS).....	7
1.3.1 The role of ion exchange in IMS.....	11
1.3.2 IMS of BFNCs with favourable distribution due to Donnan Exclusion Effect	15
1.3.3 IMS – precipitation stages for the preparation of BFNCs.....	20
1.3.4 IMS – galvanic displacement stages for preparation of BFNCs.	21
1.4. Characterization techniques for metal – polymer nanocomposites (PMNCs). 22	
1.4.1 Scanning electron microscopy(SEM) and Transmission electron Microscopy (TEM).....	23
1.4.2 Scanning Transmission Microscopy ((S)-TEM)	24
1.4.3 Laser Confocal Scanning Microscopy (LCSM)	24
1.4.4 Spectroscopic Ellipsometry	25
1.4.5 Brunauer – Emmet – Teller (BET) surface analysis: gas adsorption – desorption technique.	25
1.4.6 Inductively Coupled Plasma (ICP-MS).....	25
1.4.7 Thermogravimetric analysis (TGA)	26
1.5. Current and future applications of BFNCs prepared by IMS.	26
1.5.1 Heterogeneous Catalysis.....	28
1.5.2 Electrochemical Sensors:.....	30

1.5.3	Bactericide Activity.....	33
1.5.4	BFNCs for energy storage systems:	34
1.6.	Concluding Remarks:	35
	References.....	36
2.	Motivation, Aims and Publication Compendium.....	45
2.1	Motivation, perspectives and research innovation.....	45
2.2	General Aims	45
2.3	Specific Aims.....	46
2.4	Publication compendium	46
3.	Donnan Exclusion Effect Intermatrix Synthesis Technique: distribution and shape control technique for the environmentally friendly preparation of bifunctional nanocomposites.	53
3.1	Preparation of CdS-QDs on cationic gel type polymeric matrix by DEEIMS-precipitation technique.....	55
3.2	DEEIMS of Ag-FMNPs on gel-type cationic polymeric matrix with formaldehyde as neutral reducing agent.	57
3.3	DEEIMS of Au and Ag-FMNPs on gel-type anionic polymer using ascorbic acid (AA) and sodium borohydride (NaBH ₄) as ionic reducing agents.....	59
3.3.1	Symmetrical version of classical DEEIMS applied for anionic matrices.	59
3.3.2	DEEIMS of Au-FMNPs using anionic NPs-precursor.	61
3.4	DEEIMS of Ag-FMNPs on gel-type cationic polymer using AA and NaBH ₄ as reducing agents.	64
3.4.1	Enhanced DEEIMS of Ag nano- and microstructures on cationic gel type polymers.....	68
3.4.2	Preparation of AgAu microstructures by DEEIMS-galvanic replacement technique.	73
3.5	Concluding Remarks:	77
	References:.....	77
4.	Evaluation of ion exchange properties and morphology changes due to IMS of Ag-FMNPs on gel –type polymeric matrices.	84
4.1	Morphological changes on gel-type cationic polymer due to IMS of Ag-FMNPs:.....	84
4.2	Evaluation of ion exchange properties of cationic and anionic gel – type polymers before and after modification with Ag-FMNPs.	92
4.3	Concluding Remarks.....	97
	References.....	97

5. Applications of Bifunctional Nanocomposites prepared by Intermatrix Synthesis Technique.....	102
5.1 Heterogeneous Catalysis:.....	102
5.1.1 Synthesis and Characterization of Pd-MCNPs.....	103
5.1.2 Evaluation of Catalytic Activity for Catalysis of Suzuki Cross Coupling Reaction(SCCR).....	108
5.1.3 Concluding Remarks	110
5.2 Further feasible approaches of IMS for novel reactive surfaces:	110
5.2.1 Intermatrix Synthesis of FMNPs on multiwall CNTs (MWCNTs).....	111
5.2.2 Intermatrix Synthesis of CdS-QDs on SPEEK/PTFs (CdS-QDs@SPEEK/PTFs).....	119
5.2.3 Intermatrix Synthesis of CdS-QDs on Nanodiamonds (CdS-QDs@NDs)	123
5.2.4 Concluding Remarks:	125
References:.....	125
6. Conclusions	130
ANNEX 1	137
ANNEX 2	143
ANNEX 3	148
ANNEX 4	160

Figure Index

Figure 1.1. examples of relevant discoveries and inventions dealing with development of materials technology.	1
Figure 1.2. Basic principles for the design of Nanomaterials	2
Figure 1.3: Range of plasmonic resonance for gold nanoparticles in function of their morphology ²⁵	4
Figure 1.4: Green principles scheme for the preparation of NMs.	5
Figure 1.5 Ostwald ripening mechanism for the uncontrollable growth of NPs in solution.	6
Figure 1.6 Different routes for the incorporation of FMNPs in a composite material a) In situ: using synthesis of FMNPs. b) Ex situ: FMNPs synthesis in solution and incorporation by impregnation to the matrix support.....	7
Figure 1.7 A) In red the number of publication per year introducing the term “nano” and in blue the publications per year introducing the term “Nanocomposite”. . B) Shows the trending topics of the overall publications related to “nano” in 2013.	8
Figure 1.8 FMNPs stabilized in polymeric matrix (A) by IMS that offers mechanical resistance(B) to reduce the risk of NMs release.	9
Figure 1.9 breakthrough profile scheme for ion exchange.	13
Figure 1.10 different breakthrough profiles in function of polymer selectivity kinetics. Reversible process (black), non-favourable process (red dash curve) and favourable process (blue dash curve).	14
Figure 1.11: Scheme of ion exchange processes during stage 1 IMS in A) cationic exchanger, B) anionic exchanger and the final FMNPs favourable distribution on the surface of the BFNCs C) proved by cross section SEM images in which white zone show FMNPs layer.	16
Figure 1.12: Increase of FMNPs layer thickness due to consecutive IMS cycles.....	17
Figure 1.13 Different FMNPs structures achievable by different IMS alternative routes: a) monometallic b,c) bi-metallic Core-Shell structure in function of the order of IMS stages and d) Alloy FMNP.	19
Figure 1.14: Confocal Laser microscopy of smooth gel –type cationic a) smooth surface and b) surface roughness increase due to IMS of Ag-FMNPs.	19
Figure 1.15: A) Ag micro cube obtained by IMS on gel type cation exchanger and B) EDS spectra identifying the silver content in micro cube structure.	21

Figure 1.16: Galvanic displacement of Ag to Au to prepare a) AgAu micro cubes on gel type cationic exchange and b) EDS spectra identifying the presence of silver and gold with profile distribution (Au over Ag).	22
Figure 1.17: Advantages of heterogeneous nanocatalysis.....	28
Figure 1.18: Scheme of feasible separation methods for BFNCs materials for catalytic applications.....	29
Figure 1.19: Scheme of the enhanced electronic transfer of modified electrodes with FMNPs.....	32
Figure 1.20: Calibration curves of electrochemical detection of H ₂ O ₂ concentration with Pt@Cu, Pt- and Cu-FMNP composite SPEEK membranes Experimental conditions: potential: -250 mV; 0.1 M acetate buffer(Adapted from Muraviev <i>et.al</i> ⁹⁸)	33
Figure 1.21: Bactericide activity of hybrid AgAu –cubic microstructures containing NCs	34
Figure 3.1: Schematic representation of the DEE during ion exchange showing repulsion, attachment and diffusion through DEE layer depending on the charge of species and layer.....	54
Figure 3.2: Schematic representation of FMNPs distribution due to IMS A) Raw ion exchanger surface B) FMNPs with favourable distribution mainly on the ion exchanger surface because of DEE interaction with metal precursors and reducing agents and C) FMNPs distribution	55
Figure 3.3: A) Cross section SEM image of CdS-QDs containing nanocomposite. B) EDS – LineScan Analysis of cross section showing the distribution of CdS-QDs	56
Figure 3.4: A) Cross section of Ag-FMNPs containing nanocomposite with B) Element Mapping and C) EDS -LineScan analysis showing the interior distribution of Ag-FMNPs due to IMS with formaldehyde as reducing agent	58
Figure 3.5 Schematic representation of chemical structures AA and [AA] _{ox}	60
Figure 3.6: Ag-FMNPs distribution mainly on the surface on gel-type anionic exchanger due to IMS. A, B) Cross section and LineScan using NaBH ₄ as reducing agent. C,D) Cross section and EDS LineScan using AA as reducing agent.....	61
Figure 3.7: HR-SEM image and size distribution histogram of Au FMNPs on anionic gel – type polymer A, B) IMS using NaBH ₄ as reducing agent. C,D) IMS using AA as reducing agent. Non evidence of agglomeration is observed in neither case.....	63
Figure 3.8: Ag-FMNPs distribution mainly on surface on gel-type cation-exchanger due to IMS. A,B) Cross section and LineScan using NaBH ₄ as reducing agent C,D) Cross section and EDS LineScan using AA as reducing agent.....	65
Figure 3.9: HR-SEM image and size distribution histogram of Au FMNPs on cationic gel – type polymer A, B) IMS using NaBH ₄ as reducing agent. C, D) IMS using AA as reducing agent. No agglomeration is observed in both cases.....	66

Figure 3.10: HR-SEM images of surface morphology changes on cationic gel-type ion-exchanger due to IMS of IMS of Ag-FMNPs. Magnification of D>>C>>B>>A.....	67
Figure 3.11: HR-SEM images of Ag-FMNPs on gel-type cationic polymer showing appearance of micro-cubic structures. Magnification of B>>A.....	67
Figure 3.12: Schematic representation of formation of Ag –cubic structures on surface of gel-type cationic polymer by DEEIMS.....	69
Figure 3.13: HR-SEM images of different stages of the formation of Ag-cubic structures on gel-type cationic polymer using 0.01M NaBH ₄ as reducing agent during DEEIMS:70	
Figure 3.14: HR-SEM images showing favourable distribution and homogenous size of optimized IMS of Ag-cubic structures with 0.05M NaBH ₄ as reducing agent. Magnification C>>B>>A.	70
Figure 3.15: HR-SEM images of different stages of the formation of Ag-cubic structures on gel-type cationic polymer using AA as reducing agent during DEEIMS:	71
Figure 3.16: HR-SEM images and size distribution histograms of Ag-cub structures synthesized by optimized IMS A, B) with NaBH ₄ as reducing agent. C, D) with AA as reducing agent. No agglomeration evidence is observed in neither case.	72
Figure 3.17: A) HR-SEM image and B) EDS-LineScan of Ag-cubic structure showing distribution profile for Ag.	72
Figure 3.18: Schematic representation of galvanic replacement of Ag to Au for DEEIMS of AgAu-cubic structures.....	74
Figure 3.19: HR-SEM images of Ag-cubic structures (A, B) and consequent evidence of hollowed AgAu structures due to galvanic replacement of Ag to Au (C, D).	75
Figure 3.20: Schematic representation of consecutive stages of Kirkendall Effect during the galvanic effect of Ag (grey colour) to Au (gold colour) for the preparation of hollowed NPs.....	75
Figure 3.21: HR-SEM images (A, B, C) and EDS-LineScan (D) for AgAu-cubic structures synthesized by DEEIMS.	76
Figure 4.1: (A) High resolution SEM image of NC bead cross section and (B, C) Line Scan EDS spectra showing distribution of Ag-FMNPs (red) in sulfonic gel type cation-exchange resin modified with Ag-FMNPs.	85
Figure 4.2: Schematic diagram of interaction of FMNPs synthesized inside polymer matrix (B) and SEM images of cationic gel type polymer surface before (A) and after (C) IMS of Ag-FMNPs.....	86
Figure 4.3: High-resolution SEM images of: a) NPs free granulated polymer. b, c, d, e, f): Ag-FMNPs containing polymer with clearly seen as worm-like structure of NC surface and nanopores. Magnification a = b < c < d < e < f.....	87

Figure 4.4: High-Resolution SEM images of Ag-FMNPs with an average diameter of 33 ± 1 nm on gel type polymer, show distribution of the FMNPs with non-evident agglomerates after surface modification Magnification of $b \gg a$.	89
Figure 4.5: SEM images of cross sections of Ag-FMNPs-gel-type sulfonic polymer PMNC granules at different times of metal loading stage and thicknesses (Δl) of final FMNPs layer (time of $a < b$).	90
Figure 4.6: Thickness of FMNPs layer versus metal loading time.	90
Figure 4.7: Breakthrough curves of displacement of Na^+ with Ca^{2+} from FMNPs-free sulfonic cation-exchange resin and NCs obtained after different times of metal loading stage. Area marked by dotted lines corresponds to ion exchange capacity of resin and NC samples.	94
Figure 4.8: Breakthrough curves of displacement of OH^- with Cl^- ions from FMNPs-free quaternary amine anion-exchange resin (grey) and NC (dark grey) obtained by DEEIMS technique with metal loading time of 1 minute.	95
Figure 5.1: SEM images of granule cross-sections and respective LineScan EDS spectra showing distribution of Pd-MNPs inside nanocomposites obtained by (A) classic and (B,C) novel version of IMS technique by using cation (A) and anion exchange resins (B,C).	106
Figure 5.2: SEM images of Purolite A520E resin (sample MNCP E in Table 5.1) before (A) and after (B and C) DEDIMS of Pd-PSMNCs.	107
Figure 5.3: TEM images (A, B) and size distribution histogram (C) of MCNP A (sample MNCP 3, see Table 5.1).	108
Figure 5.4: SCCR yield per catalytic run due to the application of the Pd-MCNPs.	109
Figure 5.5: Lineal increase of SCCR yield as function of palladium content in Pd-PSMNCs containing nanocomposite.	109
Figure 5.6: Schematic representation of catalytic performance of Pd-PSMNCs containing nanocomposite for SCCR.	110
Figure 5.7: HR-TEM images of A) raw MWCNTs; B) Ag-; C) Au-; D) Cu-; E) Pd- and F) Pt-FMNPs@MWCNTs.	113
Figure 5.8: HR-TEM images of A) raw MWCNTs; B) Pd-FMNPs@MWCNTs C) Pd-FMNPs@MWCNTs amplification and D) the corresponding EDS spectra from C.	114
Figure 5.9: A) HR-TEM raw MWCNT B) HR-(S)TEM CdS-QDs on MWCNTs after one IMS cycle. C) and d) HR-(S)TEM images of CdS-QDs on MWCNTs after two sequential IMS cycles. Magnification of $D \gg C$.	115
Figure 5.10: A) (S)TEM image and B) size distribution histogram for CdS-QDs on MWCNTs with an average diameter of 2.3 ± 0.4 nm.	116
Figure 5.11: EDS spectra of A) MWNCTs Catalyst showing high Ni content. B) CdS-QDs showing the presence of Cd and S.	116

Figure 5.12: Scheme of analytical procedure for determination of MWCNTs in water. A) addition of Cd(NO ₃) ₂ aqueous solution to blank and water sample under analysis, B) precipitation of CdS(s) and formation of CdS-QDs on MWCNTs surface, C) centrifugation and D) aliquot from liquid phases of blank and analyte is analysed on spectrophotometer for detection of MWCNTs due to presence of CdS-QDs.	118
Figure 5.13: Dependence of intensity of fluorescence emission at wavelength of $\lambda=405\text{nm}$ on relative concentration of MWCNTs decorated with CdS-QDs. Zero point corresponds to emission of blank (see text).	119
Figure 5.14: Schematic representation of SC of SPEEK over silicon wafers: dropping of SPEEK (A) followed by spin – up of SPEEK (B). Actual picture of SPEEK dissolved polymer in DMF interacting with Silicon wafer as product of spin-off stage (C, D). PTF formation after evaporation stage (E, F).	121
Figure 5.15: A) Schematic representation of IMS of CdS-QDs on SPEEK PTFs. B) (S)TEM picture of CdS-QDs with their corresponding EDS on C. D) HR-TEM image and size distribution histogram of QDs (E).	122
Figure 5.16: HR-TEM images of NDs (A,B magnification $B \gg \gg A$) and raw NDs size distribution histogram(C).	123
Figure 5.17: A) Schematic representation of IMS CdS-QDS on NDs. B) HR-TEM image of raw NDs and EDS spectra on D. C) (S)TEM image of CdS-QDs modified NDs and corresponding EDS spectra on E.	124

Table Index

Table 1.1: Atoms exposed in Au-NPs surface as function of NP diameter.14.....	3
Table 1.2: Reactive matrices used for IMS of FMNPs.....	18
Table 1.3: main characterization techniques commonly used for BFNCs.	23
Table 4.1: Increase of pore diameters in Ag-MNPs-containing Purolite C100E resin samples	87
Table 4.2: Thickness values of Ag-FMNPs layer at low metal loading times determined from cross section measurements	91
Table 5.1: Metal content in Pd-PSMNCs nanocomposites synthesized by applying different metal loading-reduction cycles.	105
Table 5.2: TGA analysis of FMNPs@ MWCNTs/expoxy composites.....	114

Acronym List

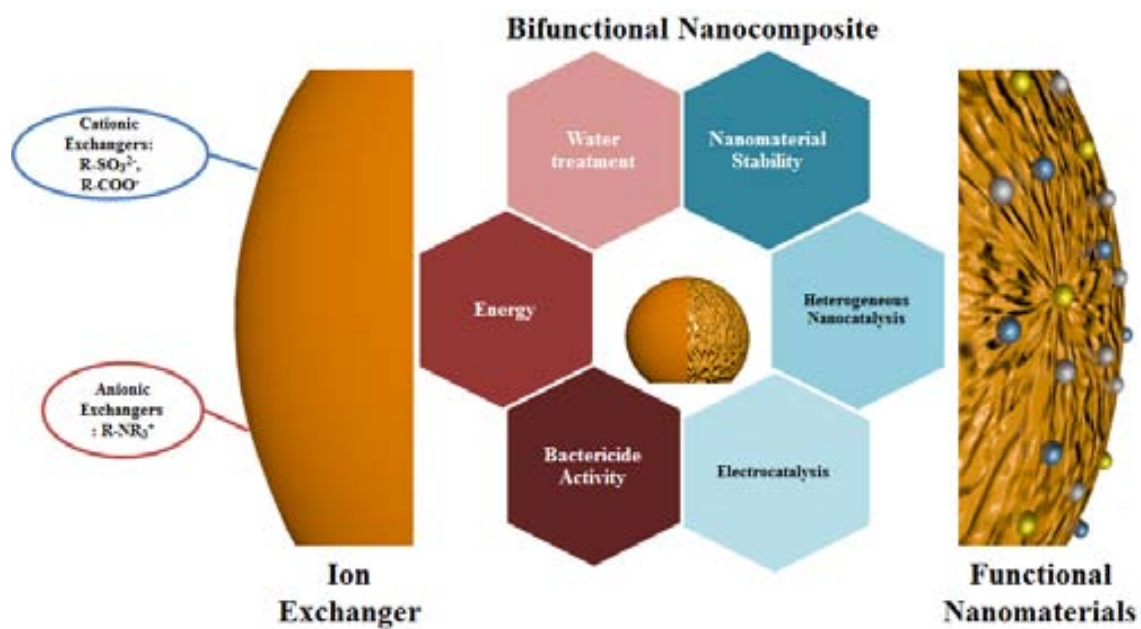
Acronym	Meaning
AA	Ascorbic Acid
BET	Brunauer – Emmet – Teller
BFNCs	Bifunctional Nanocomposites
CNTs	Carbon Nanotubes
DEE	Donnan Exclusion Effect
DEEIMS	Intermatrix Synthesis coupled with Donnan Exclusion Effect
DMF	Dimethylformamide
EDS	Energy dispersive X-Ray Spectroscopy
FMNPs	Functional Metal Nanoparticles
FNMs	Functional Nanomaterials
ICP	Inductively Coupled Plasma
IEC	Ion Exchange Capacity
IMS	Intermatrix Synthesis
LCSM	Laser Confocal Scanning Microscopy
MNPs	Metal Nanoparticles
MWCNTs	Multiwall Carbon Nanotubes
NCs	Nanocomposites
NDs	Nanodiamonds
NMs	Nanomaterials
NPs	Nanoparticles
PMNCs	Polymer Metal Nanocomposites
PTFs	Polymeric Thin Films
QDs	Quantum Dots
SEM	Scanning Electron Microscopy
SPEEK	Sulfonated Poly(etherether)ketone
STEM	Scanning Transmission Electron Microscopy
TEM	Transmission Electron Microscopy
TGA	Thermogravimetric Analysis

*“Ama no lo que eres; sino aquello en
lo que te puedes llegar a convertir”*

-DQ-

Summary

Graphical Abstract



Summary

In this Doctoral Thesis, the Intermatrix Synthesis (IMS) technique has been described as a feasible methodology for the modification of reactive matrices with Nanoparticles (NPs), which is based on the ion exchange properties of the NPs supporting surface, such as ion exchange resins and the innovation of the application of IMS on polymeric nanofilms, carbon nanotubes (CNTs) and nanodiamonds (NDs).

The effects of nanostructured materials on the environment are one of the most important issues of technology in recent years. Given their high level of development, production, dissemination and application, the main concerns associated with nanomaterials (NMs) include: a) the high reactivity and toxicity of many NMs compared to their macroscopic analogues, b) the lack of appropriate analytical techniques for their determination in environment and c) the absence of effective legislation to regularize the convenient levels of various NMs in soil, water and air. Therefore, it is a must to ensure the security and stability of NMs through its incorporation into the Bifunctional Nanocomposites (BFNCs)

The bifunctionality of BFNCs is determined by the specific properties of the matrix in which the metal NPs (MNPs) are synthesized (for example by ion exchange polymers) and by their respective properties of the MNPs (magnetism, bactericidal, nanocatalyzadores). Surface modification of reactive matrices with MNPs is conducted through the IMS coupled to Donnan exclusion effect (DEE). Thus, the added value BFNCs prepared are characterized, their properties are evaluated and stability and the favourable distribution of the MNPs mainly on the surface of BFNCs is verified.

The IMS includes different possibilities for the preparation of MNPs on BFNCs. In the first stage ion exchange is performed on the matrix to attach the NPs precursors. Subsequently, the IMS includes: a) Reduction of ions by using a reducing agent such as NaBH_4 or b) precipitation of NMs as quantum dots (QDs) or metal oxides by adding the respective counterion. Whichever route is followed, the ion exchange functional groups of the matrix are regenerated; so IMS cycles can be repeated to increase the thickness of the MNPs or to produce bimetallic core-shell type MNPs. An extended version of the IMS is presented as using galvanic replacement for the preparation of Au- MNPs and AgAu-MNPs in cationic matrices using MNPs initially synthesized as nano-templates for crystallization of new mono or bimetallic MNPs.

An important advantage provided by the IMS technique is its versatility, allowing the synthesis of BFNCs with the desired properties for different applications: bactericidal activity, magnetism, electrochemistry and heterogeneous catalysis, among others.

Resum

En aquesta Tesi Doctoral s'ha desenvolupat la tècnica de Síntesi intermatricial (IMS), com a una metodologia factible per la modificació de matrius reactives amb nanopartícules (NPs) basada en les propietats d'intercanvi iònic de la superfície que es vol modificar; com a raó: resines intercanviadores iòniques i la innovació en la modificació de nanofilms polimèrics funcionalitzats, nanotubs de carboni (CNTs) i nanodiamants (NDs).

L'efecte dels materials nanoestructurats sobre el medi ambient és un dels temes més importants a la tecnologia en els darrers anys. A causa del seu alt grau de desenvolupament, producció, difusió i aplicació, les majors preocupacions socials als Nanomaterials (NMs) inclouen: a) l'elevada reactivitat i toxicitat de molts NMs en comparació dels seus anàlegs macroscòpics, b) l'absència de tècniques analítiques òptimes per a la seva determinació en el medi ambient i c) l'absència d'una legislació efectiva que regularitzi els nivells permesos de diversos NMs en sòl, aigua i aire. Per això és primordial la seguretat i estabilitat dels NMs a través de la seva incorporació en els Nanocomposites bifuncionals (BFNCs)

La bifuncionalitat dels BFNCs és determinada per les propietats pròpies de la matriu en la qual les NPs metàl·liques (MNPs) són sintetitzades (per exemple polímers d'intercanvi iònic) i per les propietats respectives de les MNPs (magnetisme, activitat bactericida, nanocatlizadores). La modificació superficial de les matrius reactives amb MNPs es porta a terme a través de la IMS a cobrada a l'Efecte d'exclusió de Donnan (DEE). D'aquesta manera, els BFNCs preparats amb valor afegit són caracteritzats, les seves propietats són avaluades i es comprova l'estabilitat i la distribució favorable de les MNPs principalment en la superfície dels BFNCs.

La IMS inclou diferents possibilitats per a la preparació de MNPs i BFNCs. En una primera etapa es realitza un intercanvi iònic sobre la matriu per fixar els precursors de les NPs. Posteriorment la IMS pot incloure: a) Reducció dels ions a l'utilitzar un agent reductor com NaBH_4 o b) precipitació de NMs com quantum dots (QDs) o òxids metàl·lics a l'afegir el contraió respectiu. Sigui quina sigui la ruta que s'empri, els grups funcionals d'intercanvi iònic propis de la matriu són regenerats; de manera que els cicles de IMS poden repetir-se per augmentar el gruix de les MNPs o bé per produir MNPs bimetal·liques tipus core-shell. Una versió estesa de la IMS és presentada a l'utilitzar el desplaçament galvànic com a precursor per Au-MNPs i Ag-Au-MNPs a matrius catióniques, utilitzant MNPs sintetitzades inicialment com nanoplantilles per a la cristallització de les noves MNPs mono- o bi-metàl·liques.

Un avantatge molt important que aporta la tècnica IMS és la seva gran versatilitat, possibilitant la síntesi de BFNCs amb les propietats desitjades per a les diferents aplicacions: activitat bactericida, magnetisme, catàlisi heterogènia i electroquímica, entre d'altres.

Resumen

En esta Tesis Doctoral se ha desarrollado la técnica de Síntesis Intermatricular (IMS), como una metodología factible para la modificación de matrices reactivas con Nanopartículas (NPs) basada en las propiedades de intercambio iónico de la superficie que se desea modificar; tales como: como resinas intercambiadoras iónicas y la innovación en la modificación de nanofilms poliméricos funcionalizados, nanotubos de carbono (CNTs) y nanodiamantes (NDs).

El efecto de los materiales nanoestructurados sobre el medio ambiente es uno de los temas más importantes de la tecnología en los últimos años. Dado su alto grado de desarrollo, producción, difusión y aplicación, las mayores preocupaciones asociadas a los Nanomateriales (NMs) incluyen: a) la elevada reactividad y toxicidad de muchos NMs en comparación con sus análogos macroscópicos, b) la ausencia de técnicas analíticas adecuadas para su determinación en el medio ambiente y c) la ausencia de una legislación efectiva que regularice los niveles permitidos de varios NMs en suelo, agua y aire. Por ello es primordial la seguridad y estabilidad de los NMs a través de su incorporación en los Nanocomposites Bifuncionales (BFNCs)

La bifuncionalidad de los BFNCs es determinada por las propiedades propias de la matriz en la que las NPs metálicas (MNPs) son sintetizadas (por ejemplo polímeros de intercambio iónicos) y por las propiedades respectivas de las MNPs (magnetismo, actividad bactericida, nocoaguladores). La modificación superficial de las matrices reactivas con las MNPs se lleva a cabo a través de la IMS aplicada al Efecto de Exclusión de Donnan (DEE). De esta manera, los BFNCs preparados con valor añadido son caracterizados, sus propiedades son evaluadas y se comprueba la estabilidad y la distribución favorable de las MNPs principalmente en la superficie de los BFNCs.

La IMS incluye diferentes posibilidades para la preparación de MNPs en BFNCs. En una primera etapa se realiza un intercambio iónico sobre la matriz para fijar los precursores de las NPs. Posteriormente la IMS puede incluir: a) Reducción de los iones al utilizar un agente reductor como NaBH_4 o b) precipitación de NMs como quantum dots (QDs) u óxidos metálicos al agregar el contraión respectivo. Sea cual sea la ruta que se siga, los grupos funcionales de intercambio iónico propios de la matriz son regenerados; por lo que los ciclos de IMS pueden repetirse para aumentar el grosor de las MNPs o bien para producir MNPs bimetalicas tipo core-shell. Una versión extendida de la IMS es presentada al utilizar el desplazamiento galvánico como precursor para Au- MNPs y Ag Au-MNPs en matrices catiónicas, utilizando MNPs sintetizadas inicialmente como nanoplantillas para la cristalización de las nuevas MNPs mono o bimetalicas.

Una ventaja muy importante que aporta la técnica IMS es su gran versatilidad, posibilitando la síntesis de BFNCs con las propiedades deseadas para las diferentes aplicaciones: actividad bactericida, magnetismo, catálisis heterogénea y electroquímica, entre otras.

*“There is nothing to be scared of,
just everything to be explained”*

-Marie Curie-

Introduction

1. Introduction

1.1. General Introduction

Everyday humans interact with a great amount of different materials and with the imminent need to control matter. Since the very beginning of their existence, humans have design materials to change and take advantage of the surrounding elements to improve their life quality. Figure 1.1 presents some relevant inventions through the history of humanity.

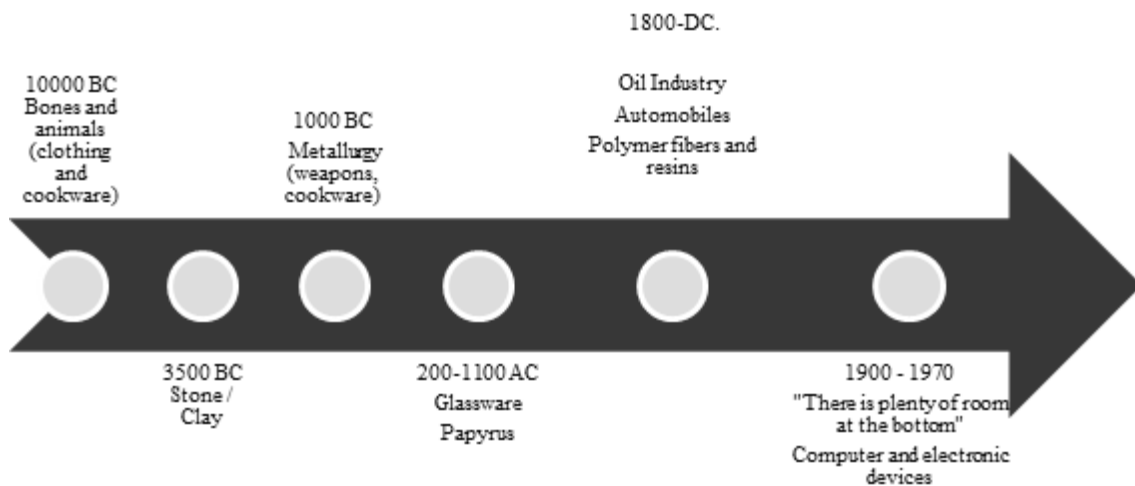


Figure 1.1. Examples of relevant discoveries and inventions dealing with development of materials technology.

Life in the twenty-first century is ever dependent on an unlimited variety of advanced materials. The term material may be broadly defined as any solid-state component or device that may be used to address a current or future societal need. For instance, simple building materials such as nails, wood, coatings, etc. address our need of shelter.

Material Science is focused on the understanding of the order of atoms, ions or molecules, that all joint turn out as a material¹. Bulk materials usually present different physical and chemical properties different from their nano-sized components.

The broad field of study of Material Science includes structures/properties of existing materials, synthesizing and characterizing novel, efficient and greener

materials. Furthermore, in perspective, material science pursues to estimate feasible properties of materials that has not yet been realized or invented.²⁻⁷

The design of materials depends on the current necessities of the society, the availability of resources and the investment required for an appropriate scale up production.

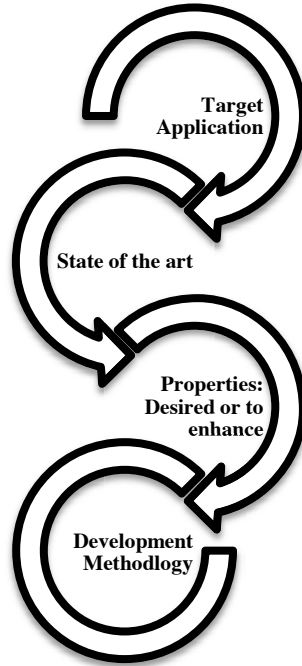


Figure 1.2. Basic principles for the design of Nanomaterials

1.2. Nanotechnology, Nanomaterials and Nanocomposites: historical background, properties and applications.

The main aim of material scientist is to overcome with new efficient and low cost methodologies for the preparation of novel materials. Taking that into account, the incorporation of Nanomaterials (NMs) into bulk components has become a priority.⁸⁻¹¹

NMs represent an alternative to conventional materials and have repercussion in fields like electronics, biochemical sensors, catalysis and energy. The nanoscale particles (from 1-10 0nm) increase the exposed surface area of the active component of the nanoparticles (NPs), enhancing properties as charge transfer and catalytic activity.^{12,13} Table 1.1 presents the data related to the ratio

between the diameter in nanometres of Au-NPs, the number of atoms contents and the percentage of surface atoms¹⁴.

Table 1.1: Atoms exposed in Au-NPs surface as function of NP diameter.¹⁴

Particle Diameter(nm)	Total number of atoms	Percentage of surface atoms
0.65	79	76
0.87	201	64
1.50	976	40
2.00	2406	31
2.80	6266	23

As seen in table 1, when approaching dimensions around the nanometre scales, the amount of surface atoms of the NPs increases significantly. This could explain the great reactivity of the NPs and the difference in properties from them analogous in bulk material,¹⁵ such as: optical response (colour), magnetic and electronic behaviour, melting points, redox potential, conductivity and others as shown in Figure 1.3.^{10,16-18}

In the antiquities, NPs were used by the Damascans to create swords with exceptionally sharp edges and the Romans to craft iridescent glassware. The manipulation of material at the atomic and molecular scale to create new functions and properties sounds like it should be a profoundly modern concept. But artisans from the past also controlled matter at the tiniest scales. The oldest object related to nanotechnology and therefore to nanocomposites is believed to be the Lycurgus cup, the manufacture of which dates back to the late fourth century B.C. It is a Roman cup is now in the British Museum, made of a glass type dichroic colour sample different depending on the interaction with the light still red when it is exteriorly illuminated from within and green when illuminated from outside. Chemical analysis revealed that the glass leading to the special feature of colour change is due to the content of a small amount of NMs of Ag and Au, in particular, metallic particles with a diameter of 70 nm.¹⁹⁻²¹ By

modern-day standards, they were dealing with nanocomposites (NCs), hybrid complex materials which at least one of their components remains in nanoscale.

Nanostructured materials including nanoparticles, nanowires, nanobands and carbon nanotubes (CNTs) have been intensively investigated due to their size related features, special chemical and physical properties²²

The size dependence of their properties has been focus of many studies like the one of Plieth et al, who studied the variation of the reduction potential.²³

Due to surface to volume ratio of NPs, there is a high percentage of surface atoms which introduces many size-dependent properties. The finite size of the particle confines the spatial distribution of electrons, leading to quantized energy levels product to size scale. This fact is very important for semiconductor materials and optics. This effect is specially seen in nanocrystal, leading to major discoveries in solid state physics. The relevance of nanotechnology is because special properties caused by the nanoscale, in which materials have new phenomena and properties (physical and chemical), different from the analogous at the macroscopic scale.²⁴

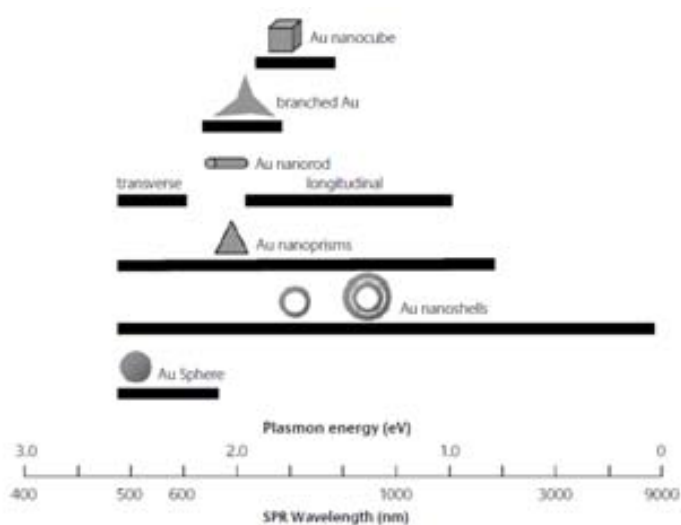


Figure 1.3: Range of plasmonic resonance for gold nanoparticles in function of their morphology²⁵

In recent years, the development of efficient green chemistry methods for synthesis of metal NPs (MNPs) has become a major focus of researchers. They have investigated in order to find an eco-friendly technique for production of well-characterized nanoparticles.^{12,26-28}

The use of engineered NPs as a consequence of the emerging field of materials science and mainly of nanotechnology is a concern of environmental scientists worldwide. However, a few studies have already demonstrated the toxic effects of NPs on various organisms. In spite of the extensive publications and studies involving Nanotechnology, it is still in discovery phase in which novel materials are first synthesized in small scale in order to identify new properties and further applications²⁹⁻³¹.

Some aspects can be taken into account referring to NPs release and effects:

1. NPs effects are scale dependent and not the same in larger scale or agglomerates. This means that effects may be quite different to adopt specific and more appropriate regulations.
2. These differences are based on size, surface chemistry and other specific interactions depending on the scale. Thus, the same material may have different regulations through the different sizes presented.
3. Effects must be conclusive to those products which commercialization is imminent. So, the NPs presented in the final product may be the ones, which the studies should focus on.

Figure 1.4 presents an overview of some green principles that could be applied for the preparation of novel NMs^{26,32,33}.

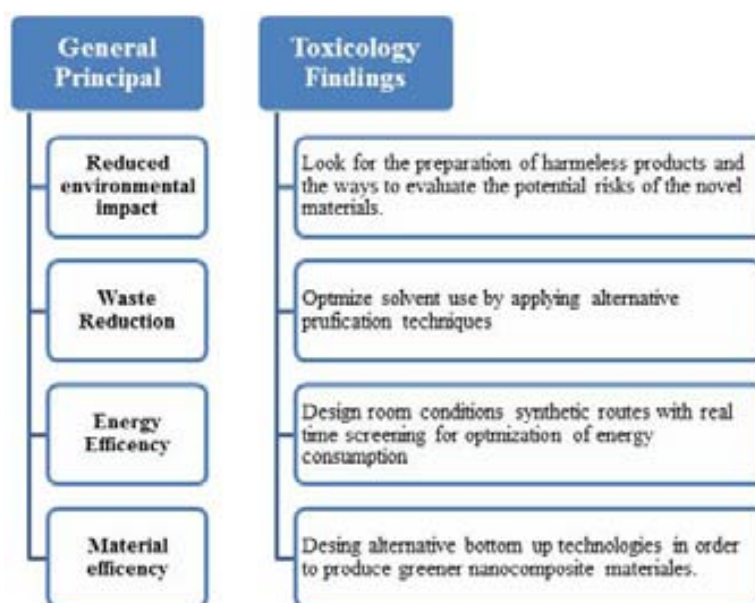


Figure 1.4: Green principles scheme for the preparation of NMs.

The environmental safety of nanocomposites, which consist of or contain nanoscale components, is one of the most important emerging topics of the Material Science and Nanotechnology fields. The main concerns dealing with the rapid development and commercialization of various nanomaterials are associated with:^{34–36}

1. the approved higher toxicity of many NMs in comparison with their larger counterparts.
2. the absence of the adequate analytical techniques for detection of NMs in the environment
3. the absence of the legislation normative for permitted levels of various NMs in water and air.

1.2.1. Nanoparticle Stabilization

It is noteworthy that NPs can aggregate not only as a result of a further manipulation but also during their growth. Figure 1.5 presents a typical mechanism of aggregation is the Ostwald ripening which is a growth mechanism where small particles dissolve and are consumed by larger particles.^{5,37–39} Then the average nanoparticle size increases with time, the particle concentration decreases and their solubility diminishes.

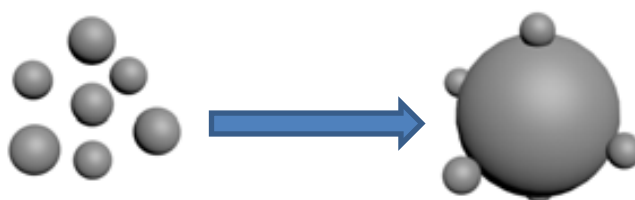


Figure 1.5 Ostwald ripening mechanism for the uncontrollable growth of NPs in solution.

Therefore, the stabilization of FMNPs is specifically required to prevent the agglomeration of the MNPs and non-controllable shape or size changes. The use of polymeric supports for the preparation of FMNPs is one of the most common and efficient way to avoid the issue of the MNPs stability^{12,20,40–43}. The

appropriate preparation methodology of hybrid Nanocomposite materials can be established depending on how are the FMNPs incorporated to the supporting matrix^{5,44}: a) in situ synthesis or b) ex situ synthesis with posterior incorporation of FMNP as shown in Figure 1.6

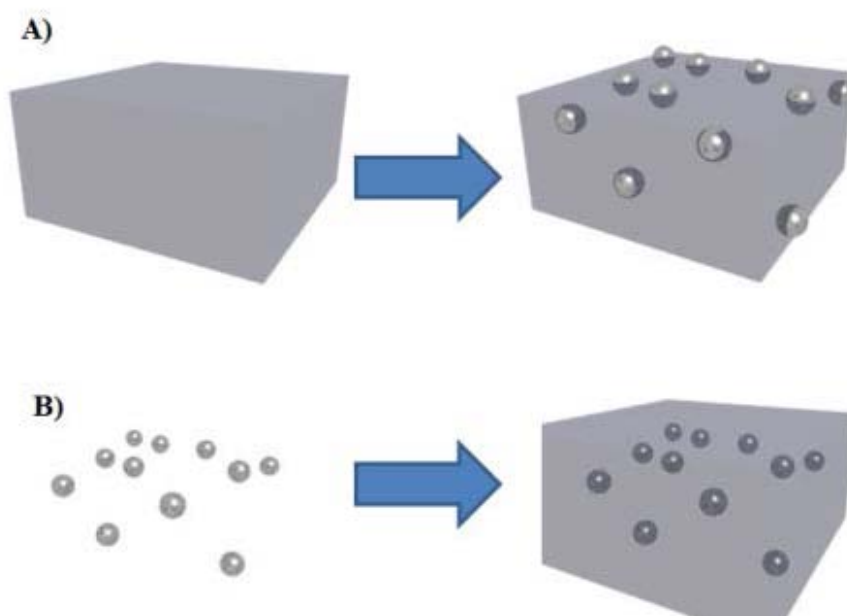


Figure 1.6 Different routes for the incorporation of FMNPs in a composite material a) In situ: using synthesis of FMNPs. b) Ex situ: FMNPs synthesis in solution and incorporation by impregnation to the matrix support

1.3. Stabilization of NPs with Polymers: Preparation and Synthesis of Polymer – Metal Nanocomposites by Intermatrix Synthesis Technique (IMS)

In this regard the increase of the safety of NMs is of particular importance. One way to prevent risk is the development of the environmentally-safe polymer-metal nanocomposite materials that consist in a functional polymer with immobilized functional MNPs (FMNPs) distributed mainly by the surface of the polymer with a higher stability to prevent release of the FMNPs.⁴⁵

The increase in the application of Nanocomposites (NCs) as shown in Figure 1.7; for example for bactericide assays, the polymeric matrix represents what makes the FMNPs (Ag-FMNPs) maximally accessible for the bacteria to be

eliminated. Another possibility of FMNPs synthesis is the Core-shell structure, which contains a superparamagnetic core coated with the functional metal shell, which provides, for example, the maximal bactericide activity^{51,52}. The MNPs are strongly captured inside the polymer matrix that prevents their escape into the medium under treatment. The superparamagnetic nature of FMNPs provides an additional level of the material safety as FMNPs leached from the polymer matrix can be easily captured by the magnetic traps to completely prevent any post-contamination of the treated medium.

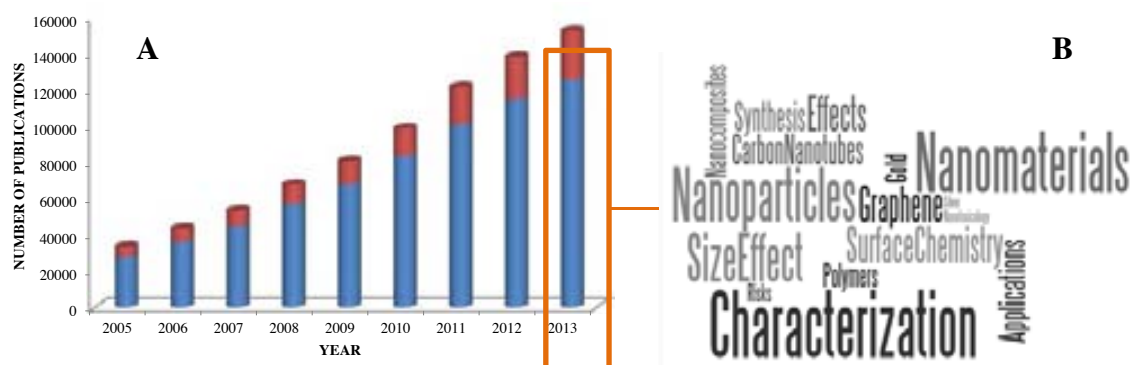


Figure 1.7 A) In read the number of publication per year introducing the term “nano” and in blue the publications per year introducing the term “Nanocomposite”. . B) Shows the trending topics of the overall publications related to “nano” in 2013.

MNPs can be obtained by various synthetic routes⁵, such as electrochemical methods, decomposition of organometallic precursors, reduction of metal salts in the presence of suitable (monomeric or polymeric) stabilizers, or vapour deposition methods. Sometimes, the presence of stabilizers is required to prevent the agglomeration of nanoclusters by providing a steric or electrostatic barrier between particles and, in addition, the stabilizers play a crucial role in controlling both the size and shape of nanoparticles.^{53–55}

FMNPs synthesized by in situ approaches; as IMS; exhibit long time stability against aggregation and oxidation. In addition, another advantage offered by IMS is the most favourable distribution of the FMNPs on the surface of the support. In the ex-situ synthesis approach, MNPS are dispersed after their synthesis in a solid or liquid medium by using different methodologies. The stabilization is limited by the re-aggregation of the MNPs along the time by the Oswald ripening mechanism. Moreover; the final distribution of the MNPs in the support is not

entirely controlled and homogenous. In terms of feasible applications such as catalysis, the presence of the FMNPs in a more accessible location to interact with the reagents is an important fact to consider.^{42,45,46,51,56}

The system FMNPs-Support shows a series of interactions that leads to the increase of the stability of the NMs and reduce the possibility of release, reducing as well the environmental impact of NMs when present in hybrid Nanocomposite materials. This can be explained by the increase of viscosity of the immobilizing support matrix (see Equation 1.1), and the decrease of the energy of particle-particle interaction in FMNPs systems regarding the MNPs prepared in solution. Figure 1.8 presents the stability offered by the host polymer matrix to the FMNPs to reduce the risk of release.⁵⁷

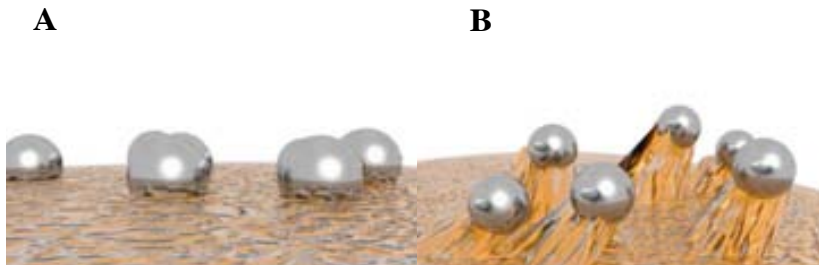


Figure 1.8 FMNPs stabilized in polymeric matrix (A) by IMS that offers mechanical resistance(B) to reduce the risk of NMs release.

$$k_c = \frac{8K_B T}{\eta} \quad [1.1]$$

η is the viscosity of the media, k_c is the rate constant of particle coagulation, K_B stands for the Boltzman constant, T is the absolute temperature. As the value of viscosity increases due to the presence for instance of a polymeric support, the rate of particle aggregation is decreased.

The modification polymeric matrices such as ion exchangers with FMNPs can be carried out by using the Intermatrix Synthesis (IMS) technique coupled with the Donnan exclusion effect (DEE). Such combination allows for production of polymer-metal nanocomposites with the distribution of FMNPs near the surface

of the polymer what appears to be the most favourable in their practical applications.⁴⁵⁻⁵⁰

The first communication about IMS of FM NPs in ion exchange polymeric materials dates back to 1949, in which Mills and Dickinson described the preparation of a weakly basic anion exchange resin containing Copper Metal Nanoparticles (Cu-MNPs or “colloidal copper”) and the use of this polymer-metal nanocomposite to remove oxygen from water based on its interaction with Cu-MNPs.⁵⁸ Since then, many studies of the modification of ion exchange resins with MNPs (mainly Cu-MNPs) resulted in the development of a new class of bifunctional ion exchange materials combining both the ion exchange properties determined by the presence of functional groups in the matrix, and the redox properties due to the presence of “colloidal metal” or MNPs in the matrix. They are also known as redoxites and electron exchangers.⁵⁹ Redoxites have found wide application in the complex water treatment processes at power stations for the removal of hardness ions by ion exchange and dissolved oxygen by redox reactions with MNPs. However, essentially no information about the sizes and the structures of MNPs in redoxite matrices and the features of their distribution inside polymers can be found in the literature

As described before, IMS technique is an efficient and simple methodology for the “in-situ” preparation of metal-polymer bifunctional nanocomposites (BFNCs). The general principles of IMS apply to all types of matrices (polymeric or not) with ion exchange functionality and for different types of FMNPs.

The main requirements for an ion exchange matrix to be used as a support for the IMS technique include:^{42,45}

- The matrix must be chemically compatible with the FMNPs surface.
- It bears a charge due to the presence of well-dissociated functional ion exchange groups. This requires a preconditioning acid–base and NaCl treatment of the supporting matrix before IMS technique that usually results in the Na^+ -form for cationic exchangers and the Cl^- -form for anionic
- The functional groups act as nanoreactors.

- Appropriate distances between the functional groups, in order to avoid agglomeration of FMNPs due to steric effects on the surface.
- Sufficient flexibility of the polymer chain segments to facilitate movements of ionic carriers.
- Appropriate swelling ratio of the matrix.
- Adequate hydrophilicity: as IMS is an environmentally friendly methodology that is carried out in aqueous media.

Regarding these points, the matrix acts as nanoreactors for the FMNPs and provide a confined medium for the synthesis controlling particle size and distribution. Moreover stabilizes and isolates the generated FMNPs, preventing their aggregation

1.3.1 The role of ion exchange in IMS

The Ion exchange functional groups of a matrix can immobilize metal ions and metal ion complexes can be considered as the key points for IMS because they are homogeneously distributed in the ion exchange matrix and be have as combinations of single isolated nanoreactors generating homogeneous nanocomposites.^{60,61} Ion Exchange polymeric matrices can be classified in four main groups:³⁵

- Cation exchangers (with anionic functionalities)
 - a) strong acid exchangers (e.g., containing sulfonic acid groups)
 - b) weak acid exchangers (e.g., containing carboxylic acid groups)
- Anion exchangers (with cationic functionalities)
 - a) strong base exchangers (e.g., containing quaternary ammonium groups)
 - b) weak base exchangers (e.g., containing amine groups)

The Ion exchange capacity (IEC) is the main features of ion exchange materials., it is expressed as counterion content in a given amount of material (e.g. grams of exchanger) is defined essentially by the amount of fixed charges that must be compensated through the exchange process to maintain the

electrostatic neutrality. All this taking into account that an ion exchanger can be considered as a “reservoir” containing certain amount exchangeable counterions

Research focused on polymeric matrices containing negative charged functional groups (i.e. cationic exchangers as sulfonic and carboxylic groups). Then the stages of IMS are as follows^{42,45,47,52,62}.

- a) Loading of the matrix with the desired FM NPs precursor cations and achieve their immobilization (sorption) onto the functional groups.
- b) Chemical reduction to zero-valent FMNPs with the appropriate reducing agent.

Ion exchange process is similar to a desorption process. Even though during ion exchange the species are ions that are not removed from the solution but are replaced by ions bound by the solid phase via electrostatic interactions to achieve electroneutrality. Accordingly, there are two ionic fluxes, one into the ion exchange particles and the other in the opposite direction out of the polymeric matrix.

In fact, upon the exchange of ionic compounds, a desorption also occurs onto the polymeric matrix due to hydrophobic interactions, making the evaluation of ion-exchange data much more complex. Accordingly, differentiation between a pure ion exchange process and a sorption process results to be almost impossible, without further analytical investigations, such as the quantification of ions released during the exchange or by the elaboration of breakthrough experiments to determine the ion exchange capacity of the host matrix.

Considering an ion exchange matrix in form RA and placed in a column. Then an electrolyte solution BY is passed through such that ion exchange takes place as shown in Equation 1.2.



The concentration of BY decreases meanwhile the concentration of AY increases. Moreover, the ionic form of the ion exchange matrix change from a decreasing amount of initial for RA for an increasing amount of RB form.

The overall process has its own kinetics, in which in the top of the column the top of the column the matrix becomes progressively totally converted to the B ionic form owing to the continual displacement of AY.

The end result is that at the top layers of Matrix are exhausted followed by an exchange zone across which the initial equivalent concentration C_0 , of ion B is reduced to zero whilst the concentration of ion A increases to C_0 . Below the exchange zone (breakthrough) ideally, the ion exchange matrix is entirely in the A form and in equilibrium with the effluent AY (no exchange takes place) as shown in Figure 1.9.

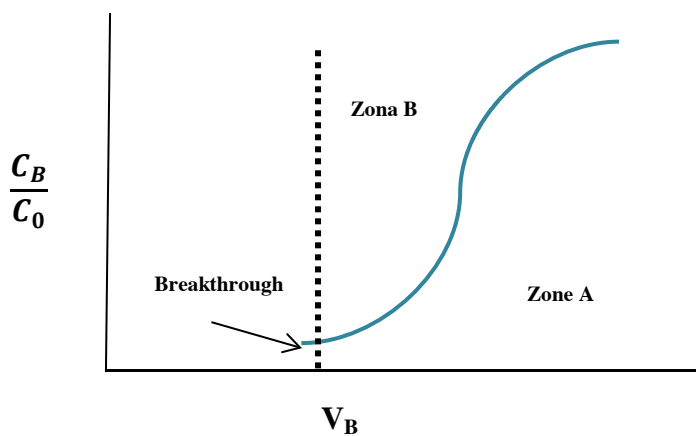


Figure 1.9 breakthrough profile scheme for ion exchange.

The area above the breakthrough curve up to the breakthrough point $V_B C_0$ is the matrix loading of the absorbed ion B. Thus, taking into account the total amount of B ions exchanged can be calculated and the IEC in miliequivalents per gram (meq/g) of the matrix can be calculated as the weight of matrix placed in the column and the concentrations are known values.

The breakthrough curve is little affected by the equilibrium and, all other considerations. Under conditions of constant column geometry and on presentation rate, the profile of the exchange zone and therefore the breakthrough curve remains unchanged with time or column length and is said to show a constant pattern as show in Figure 1.10.

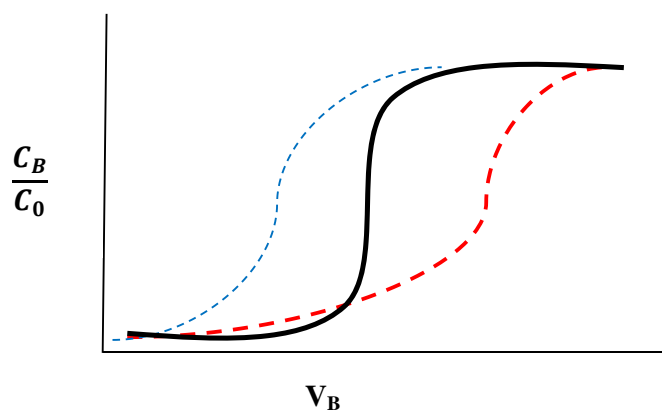


Figure 1.10 different breakthrough profiles in function of polymer selectivity kinetics. Reversible process (black), non-favourable process (red dash curve) and favourable process (blue dash curve).

Taking into account the value of the equilibrium constant of the Ion exchange process (K_{IE}) the following three main case scenarios can be considered:

$K_{IE} = 1$ totally reversible displacement process.



$K_{IE} \llll 1$ non favourable displacement process (equilibrium is displaced to the left): more V_B is required for the complete displacement of initial ionic form of matrix, then the breakthrough profile is not as sharpen defined.



$K_{IE} \gggg 1$ favourable displacement process (equilibrium is displaced to the right) : less V_B is needed for the displacement of initial ionic form of matrix, the breakthrough is faster.



Regarding this fact, comparing the breakthrough profiles for a supporting matrix before and after been modified with FMNPS by IMS is a conclusive proof of the effect of the presence of FMNPs on the matrix.

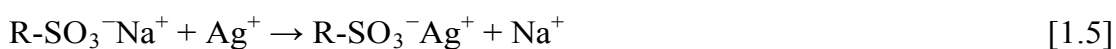
1.3.2 IMS of BFNCs with favourable distribution due to Donnan Exclusion Effect

DEE refers to the impossibility to penetrate deeply in a matrix when there is a coincidence between the charge of the outside ions (e.g. from the reducing agent) and the ones of the functional groups on the polymer surface. Thus, an equilibrium between ion concentration (either functional groups or from metal or reducing agent solution) and electrostatic repulsion takes place.

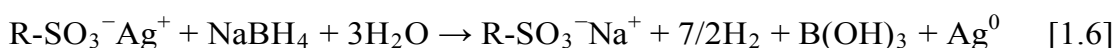
When IMS is coupled with Donnan Exclusion Effect (DEE)^{39,63,64} predicts that the use of negatively charged reducing agents such as NaBH_4 , leads to the location of the FMNPs mainly on the surface of the supporting matrix due to the electrostatic repulsion between the BH_4^- and the functional groups of the matrix (negatively charged as well).

Equations 1.5 and 1.6 show the example of IMS stages for the synthesis of Ag-FMNPs on a sulfonic cationic exchanger.

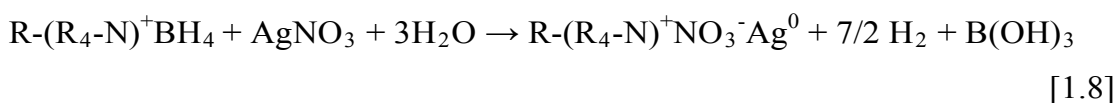
Metal loading stage:



Metal reduction stage



Considering the case of anion exchange matrices and the IMS of Ag-FMNPs, the first stage of IMS coupled with DEE is the sorption of the reducer anions on the positively charged functional groups^{40,51,62} of the matrix (Equation 1.7). The second stage (Equation 1.8) is the treatment of the polymer with solution of positively charged metal ions. Their rejection by the matrix bearing the charge of the same sign does not allow them to deeply penetrate into the polymer and their interaction with reducing agent proceeds (as in the previous case) near the surface of the support.



It seems important to emphasize that both versions of IMS technique lead to the most favourable distribution of FMNPs near the surface of BFNCs as seen in Figure 1.11, what is particularly important in practical application of such materials for complex water treatment. Note that similar procedure has been also applied for the synthesis of metal oxide nanoparticles inside ion exchange resins for removal of arsenic from water⁶⁵ and for the preparation of heterogeneous catalysts.⁶²

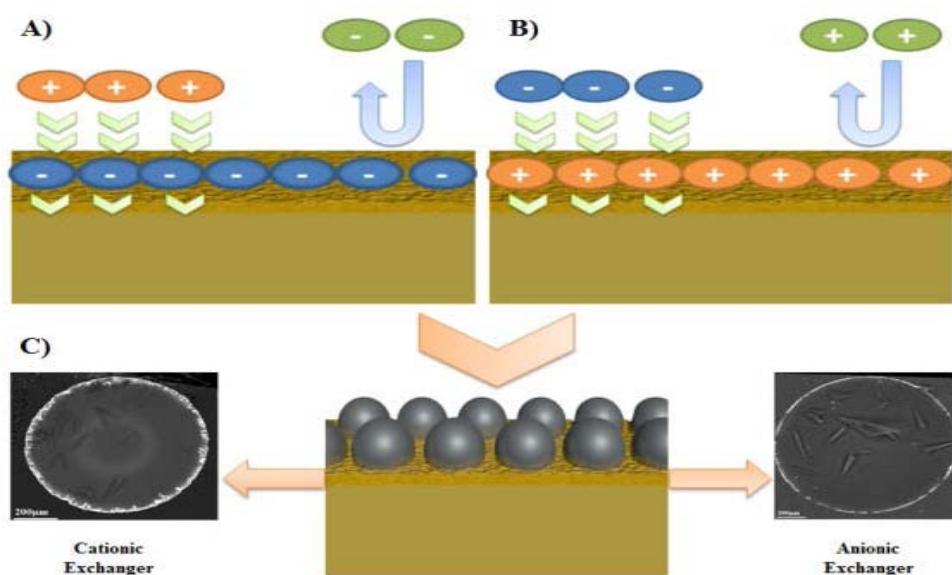


Figure 1.11: Scheme of ion exchange processes during stage 1 IMS in A) cationic exchanger, B) anionic exchanger and the final FMNPs favourable distribution on the surface of the BFNCs C) proved by cross section SEM images in which white zone show FMNPs layer.

After finishing the metal reduction the functional groups of the supporting matrix appear to be converted back into the initial ionic form (Na-form in the first and NO_3 -form and further treatment to obtain Cl-form for the anionic exchanger). This means that in both cases IMS reactions can be repeated without any additional pretreatment of the ion exchanger^{52,56,62}. This could result in the accumulation of a higher amount or increase of the thickness of the FMNPs when the same metal precursor is used as indicated in Figure 1.12.

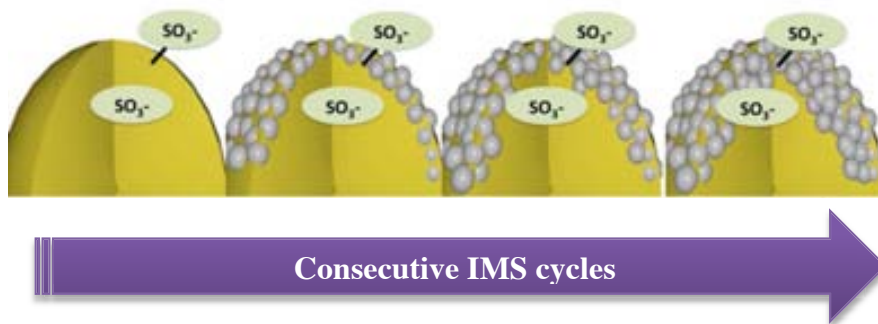


Figure 1.12: Increase of FMNPs layer thickness due to consecutive IMS cycles.

The main difference between these two versions of IMS method consists in the type of the matrix-immobilized reagent, which is the desired metal ion (FMNPs precursor) in on or other version.

The IMS technique is characterized by the following important features:

- 1) The formation of FMNPs on stabilizing matrix does not influence the IEC, what is confirmed by the results of determination of this value before and after IMS of FMNPs. This means that the functional groups are not blocked by the formed nanoparticles and can participate in the ion-exchange reactions (offering bifunctionality to the novel added value material)
- 2) After carrying out the IMS of FMNPs the functional groups of the matrix in both versions of IMS technique appear to be simultaneously regenerated (i.e., converted back into the initial ionic form). This means that metal-loading-reduction cycles can be repeated to accumulate the desired amount of FMNPs in the supporting polymer.

All above features can be considered as definite advantages of the developed in our studies IMS coupled with DEE. Technique as it appears to be applicable for the synthesis of FMNPs supported on any type of functional ion exchange reactive matrices. The reactive matrices presented in this PhD Thesis are listed in Table 1.2:

Table 1.2: Reactive matrices used for IMS of FMNPs.







Reactive Matrix	Functional Group	Picture	Ion Exchange Capacity(meq/g)
Purolite C100E: Gel – type polystyrene crosslinked with divinylbenzene resin	Sulfonic ($-\text{SO}_3^-$)		2.1
Sulfonated Poly(etherether)ketone Membrane(SPEEK)	Sulfonic ($-\text{SO}_3^-$)		2.2
SES® Multiwall carbon nanotubes (MWCNTs)	Carboxylic ($-\text{COO}^-$)		-
Purolite A520E Macroporous Styrene-Divinylbenzene Resin	Quaternary Amine ($\text{R}_4\text{-N}^+$)		1.9
Lewatit® K6387 gel+-type polystyrene crosslinked Resin	Quaternary Amine ($\text{R}_4\text{-N}^+$)		2.1
Nanodiamonds (NDs)	Carboxylic ($-\text{COO}^-$)		-

Figure 1.13 presents how when is IMS coupled with DEE and taking advantage of the ion exchange properties of the supporting matrix, the overall methodology turns into a valid synthetic route for the synthesis of different kind of FMNPs :

monometallic(increasing thickness), bi-metallic (Core-Shell structure) alloys and others.^{42,46,51,52,66}

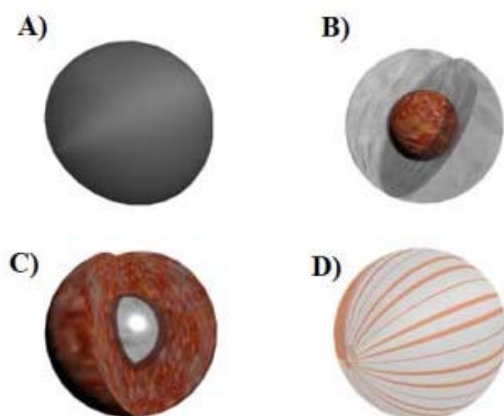


Figure 1.13 Different FMNPs structures achievable by different IMS alternative routes: a) monometallic b,c) bi-metallic Core-Shell structure in function of the order of IMS stages and d) Alloy FMNP.

Through the preparation of BFNCs, IMS of FMNPs could be accompanied by a strong change of the matrix morphology(see Figure 1.14) and the appearance of typical worm-like structure and nanoporosity on the surface of gel –type exchange polymers.⁶⁷

After carrying out the metal-loading-reduction IMS stages, the initially smooth polymer surface changes its morphology due to the appearance of the worm-like structure similar to that observed in the case of non-cross-linked polymers.⁶⁷

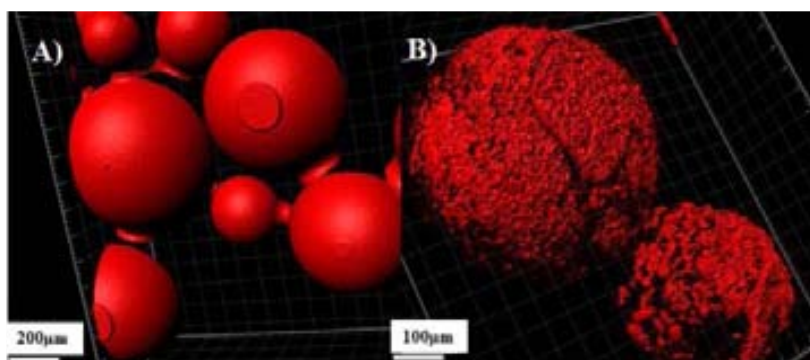


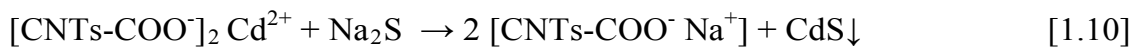
Figure 1.14: Confocal Laser microscopy of smooth gel –type cationic a) smooth surface and b) surface roughness increase due to IMS of Ag-FMNPs.

1.3.3 IMS – precipitation stages for the preparation of BFNCs.

IMS second stage can be customized in order to obtain different and reliable NMs as metal oxide FMNPs or quantum dots(QDs) by achieving the precipitation of the desired NMs instead of adding a reducing agent (usually used for direct reduction of monometallic NPs). QDs are known to present quantum confinement effects during light excitation, which gives them interesting optical and semi-conducting properties. Tuning these features and coupled them with its surface modification or using them for the surface modification of carbon nanotubes(CNTs) as supporting matrix, lead to explore the application of these nanocrystals to the field of preparation of BFNCs applied for sensor technology (fluorescent and biosensors) and to bioassays.⁶⁸⁻⁷¹

In this sense, surface modification of multiwall CNTs with CdS-QDs can be carried out using the following two sequential stages^{45,49} Stage 1: Loading (sorption) of Cd^{2+} ions (QDs precursors) onto the ion exchange groups (carboxylic) of CNTs (Equation 1.9)

Stage 2: Precipitation of CdS-QDs on the MWCNTs surface by adding Na_2S solution (Equation 1.10):



As it is clearly seen from Equation 10, after carrying out the QDs formation reaction (precipitation of CdS with Na_2S) on the surface of CNTs, the functional groups of the later appear to be regenerated, i.e. are converted back into the Na-form. This means that the QDs formation cycle can be repeated again by using the same reactions 9 and 10 without any additional pre-treatment of CNTs. This allows for accumulation of the desired amount of QDs on the surface of CNTs.

1.3.4 IMS – galvanic displacement stages for preparation of BFNCs.

Au FMNPs have made them focus of interested in the recent years due to their optical features. Their feasible applications are in fields as: biological microscopy, medicine and (bio) sensors. Therefore is a fact the importance to develop an efficient approach for their synthesis for their different possible morphologies (nanoprisms, nanocubes). Regarding this, IMS coupled with DEE and posterior galvanic displacement reaction, allows the preparation of BFNCs with such FMNPs (eg. AgAu-FMNPs).^{19,37,72–76}

The driving force for the galvanic displacement reaction arises from the difference in half-cell potentials between the metal ions to be reduced and the substrate to be oxidized.^{76,77} To achieve the deposition of metal nanoparticles, the half-cell potential of the reduced species must be higher than the one of the oxidized substrate. This is the case for Ag and Au. Then, the synthesis of AgAu-FMNPs is possible by IMS-galvanic displacement route, bringing the possibility an easy way to synthesize Au-FMNPs on cationic exchangers using Ag-FMNPs as “sacrifice” NPs. Considering the tuned IMS of Ag-FMNPs to obtain certain defined nano and microstructures^{78–80} as nano-micro cubes, as shown in Figure 1.15

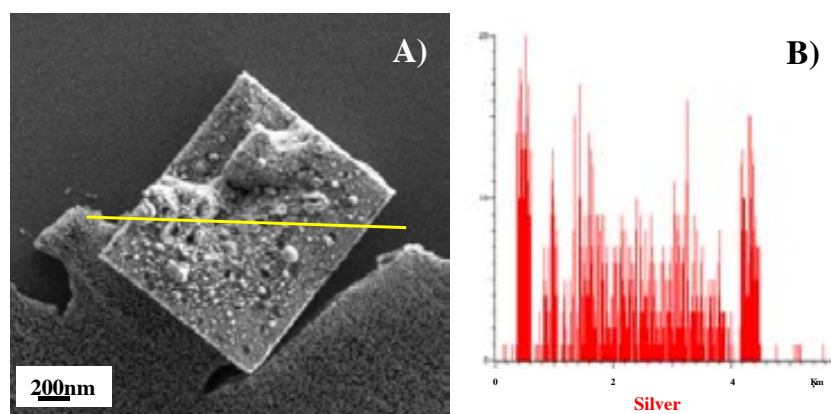


Figure 1.15: A) Ag micro cube obtained by IMS on gel type cation exchanger and B) EDS spectra identifying the silver content in micro cube structure.

The hybrid AgAu- FMNPs can combine in one only BFNC the electrocatalitcal activity of Au-FMNPs and the bactericide activity of Ag-FMNPs. In addition, during the galvanic displacement, the Au-FMNPs deposition

over previous Ag-FMNPs produces the activation of the template structure, enhancing the initial features. The displacement takes place from the outer zone of the Ag-FMNPs to the inner zone, which controlling the amount of Au added (as HAuCl_4) the final AgAu – FMNPs structure could be tuned to a Core-Shell structure or event to Au-FMNPs with hollow core. This can be seen in EDS spectra in Figure 1.16.

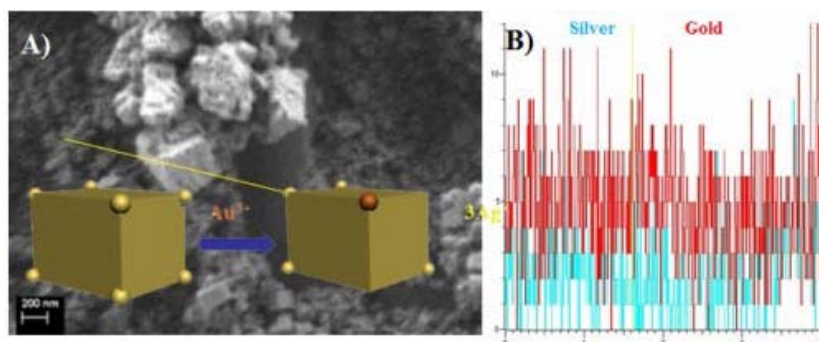


Figure 1.16: Galvanic displacement of Ag to Au to prepare a) AgAu micro cubes on gel type cationic exchange and b) EDS spectra identifying the presence of silver and gold with profile distribution (Au over Ag).

1.4. Characterization techniques for metal – polymer nanocomposites (PMNCs)

The advances of Materials Science is have involved the improvement of such characterization techniques. For instance, initial scientific observations were realized only by optical microscopy. Later on the resolution and the scope of interest lead to the apparition of electron microscopy. Currently, the need to arrive to atomic resolution (or beyond) allows the use of the term nanoscopy. This evolution joins the necessity of a better understanding of the structure – properties relation in novel materials. An important case is the development of ultrafast microscopy in which images can be taken in nanoseconds time interval, which opens new ways to study the dynamics of different processes.

After the design and synthesis of a nanocomposite material, the next step is the fully characterization of its principal features; such as: FMNPs size and distribution, chemical composition, morphology and special properties offered by the FMNPs. A complete and appropriate characterization is a most for the deeper understanding of the

behaviour of the Nanocomposite material; and therefore its further synthesis optimization or possible commercialization of the final added value material. Some characterization techniques on this PhD thesis are listed in table 3:

Table 1.3: main characterization techniques commonly used for BFNCs.

Technique	Property
Electron Microscopy: Scanning Electron Microscopy Transmission Electron Microscopy Scanning Transmission Microscopy (STEM)	Morphology, size and distribution of FMNPs
Laser Confocal Microscopy	Fluorescent properties and Surface characterization .
Atomic Force Microscopy (AFM)	Topographic surface analysis of thin layers.
Elipsometry	Thickness measurements for nanofilms
BET surface analysis: gas adsorption – desorption technique.	Surface area determination and average pore diameter.
Inductively Coupled Plasma (ICP-MS)	Quantitative metal content of nanocomposites
Energy Dispersive X-Ray Spectroscopy (EDS or EDX)	Qualitative distribution profile of metal species.
X-Ray Powder Diffraction (XRD)	Crystalline structure
Thermogravimetric analysis (TGA)	Metal content in simple

1.4.1 Scanning electron microscopy(SEM) and Transmission electron Microscopy (TEM)

Scanning Electron Microscopes (SEM) coupled with an Energy-Dispersive Spectrometer (EDS) Zeiss EVO MA 10 and Zeiss MERLIN FE-SEM and Transmission Electron Microscope (TEM) studies were carried out using JEOL 2011 and JEOL 1400. SEM and TEM techniques were used to obtain the metal concentration profiles across the cross-section of the FMNPs containing materials, to characterize the morphology of the polymer surface and for determination of FMNPs diameters. Samples were prepared by embedding several granules in the epoxy resin followed by cutting with a ultramicrotome (Leica EM UC6) using a 35° diamond knife (Diatome) at liquid nitrogen temperature (-160°C).

1.4.2 Scanning Transmission Microscopy ((S)-TEM)

(S)-TEM images were obtained using FEI Tecnai F20 S/TEM from the Electron Microscopy Facilities of Institut Català de Nanociència i Nanotecnologia (ICN2). This device offers high-resolution imaging, down to atomic scale, of the structure and morphology of samples in TEM and STEM modes up to 200kV operating voltage. Moreover the chemical analysis at nanometer level and chemical mapping via Energy Dispersive X-ray Spectroscopy can be achieved.

1.4.3 Laser Confocal Scanning Microscopy (LCSM)

Real time Intermatrix Synthesis (IMS) of Ag functional metal nanoparticles (FMNPs): surface modification of gel-type polymer: 4-D time-lapse imaging showing the IMS of Ag-FMNPs on a gel-type cationic exchange resin. Note an increase of FMNPs layer thickness in time and the different roughness of the surface of polymer. At $t = 0$ min, there is a free Ag-FMNPs with a homogeneous and smooth surface. At $t = 7$ min, the modified Ag-FMNPs gel-type polymer showed a heterogeneous surface area as worm-like structures.

Confocal measurements for morphology changes in a gel-type polymer. Samples were mounted on bottom-glass culture dishes (MatTek Corp., Ashland) and were examined using a TCS-SP5 (Leica Microsystems, Heidelberg, Germany) confocal laser scanning microscope. Images were taken using a 10x/0.4 Plan Achromat objective. Both free Ag-FMNPs and modified Ag-FMNPs gel-type polymer were excited with an Argon laser (488 nm). To determine the 3D structure, stacks of 50 to 100 sections were collected every 3 μm along the material's thickness. Three-dimensional models were generated from the xyz series using the Imaris X64 v. 6.2.0 software (Bitplane; Zürich, Switzerland).

The increase of FMNPs metal layer thickness with time was evaluated using 4D time-lapse. Projections were obtained from 40 sections (z -step = 4 μm). The stack of images was acquired every 7 s for 8 min. To determine the FMNPs layer localization different projections were generated from the xyz series vs. time using Imaris X64 v. 6.2.0 software (Bitplane, Zürich, Switzerland).

1.4.4 Spectroscopic Ellipsometry

It is an optical technique used for the determination of dielectric properties (complex refractive index or dielectric function), roughness and thickness of thin films. This is achieved by detecting the variation of angle of an incident known radiation source on the sample. The main drawback of this technique is the need of modelling the data obtained to fully understand the change of polarization of the incident beam of light to the sample and consequently to explain the influence in sample features involved in this process.

1.4.5 Brunauer – Emmet – Teller (BET) surface analysis: gas adsorption – desorption technique.

This technique is widely used for the characterization of porous materials because of the direct proportion of the adsorbed gas and the surface area of the material. BET theory predicts the amount of gas adsorbed in certain surface. The specific surface area and the porosity measurements were carried out by using BET technique on Micromeritics ASAP-2000 equipment from Institut de Ciències de ls Materials de Barcelona (ICMAB). Nanocomposite samples were heated and degassed with N₂ to remove previous absorbed gas molecules. After that, samples were introduced to a N₂ flow to detect the adsorption and desorption isotherms at 293K.

1.4.6 Inductively Coupled Plasma (ICP-MS)

A sample of about 10mg of FMNPs-containing material was immersed in aqua regia (1 mL) to completely dissolve the palladium by oxidation. The solution was filtered through a 0.22 μm Millipore filter and diluted for metal content quantification by Inductively Coupled Plasma Optical Emission Spectrometry, ICP–OES (Iris Intrepid II XSP spectrometer Thermo Electron Co) and ICP-MS (Agilent 7500). The average uncertainty of metal ions determination was less than 2% in all cases.

1.4.7 Thermogravimetric analysis (TGA)

In TGA the weight of a sample is measured as a function of sample temperature (scanning mode) or as a function of time (isothermal mode). It is based on the decomposition and thermal stability of a material under different temperatures. The mass change is detected and leads to the identification of components of the sample.

Thermogravimetric analysis was performed on a Netzsch instrument, model STA 449 F1 Jupiter®, with a flow of air. A ~20 mg sample was heated to 1000 °C at 10 °C/min, using a flow of air. The mass of the sample was continuously measured as a function of temperature and the rate of weight loss (d.t.g.) was automatically recorded.

1.5. Current and future applications of BFNCs prepared by IMS.

Recently, nanocomposite materials have been widely used for optical, electrical and magnetic applications. The preparation of novel and efficient nanocomposites is a big challenge, and so it is the central aspect for research for scientists. On one hand the preparation methodology is essential to obtain FMNPs with a favourable distribution over a polymeric support. This supports offer the stability for the FMNPs to avoid problems as agglomeration and release to the media.^{45–48,52,62,67,81,82} The feasible applications of bifunctional nanocomposites, such as the ones composed by FMNPs and an ion exchange matrix (resins, fibres, membranes) cover a broad range because of the dual features of the final hybrid material; combining ion exchange properties with the ones of the FMNPs synthesized on the polymer matrix.

The time has come to the application of these materials on innovative fields and industrial processes. Some new applications gaining interest in recent years are in terms of biomedical, catalytic, separation, sensor, microfabrication and fuel technologies.

The suitability of the BFNCs for a certain use depends on the FMNPs and the capability of the reagents to access them. Then, the physical chemistry

parameters of the support must allow the mass transfer and diffusion of reagents through it. This fact is particularly important in sensor and biosensor field, the preparation of novel materials for complex water treatments and bactericide assays, as well for heterogeneous Nanocatalysis.

For bactericide assays, the bacteria interact mainly with the FMNPs located at or near the BFNCs surface. In the case of catalytic processes, the kinetics of the catalytic reaction strongly depends on the accessibility of catalytic FMNPs for reactants. For this reason the surface distribution of catalytically active MNPs has to substantially enhance their properties.^{51,52}

One more aspect to be considered besides the FMNPs distribution when designing the modification of ion exchange materials for the preparation of BFNCs is that although MNPs in the final nanocomposite are strongly captured by the polymer, some of them could escape into the medium under treatment (water or reaction mixture).

IMS of FMNPs with a core-shell structure consisting of a superparamagnetic core coated with the functional metal shell of the minimal thickness, which provides the maximal bactericide or catalytic activity. The superparamagnetic nature of FMNPs provides an additional level of the material safety as MNPs leached from the polymer matrix can be easily captured by the magnetic traps to completely prevent any post-treatment contamination of the treated water. In the case of catalytic applications of polymer-metal nanocomposites this feature of MNPs allows for their easy recovery for reuse or recycling what is particularly important in case of noble MNPs. The presence of MNPs does not block the functional groups of the so that the BFNCs can be also used for the removal of some undesired ions (e. g., hardness ions, iron, nitrates, etc.) from the water what is particularly important in the case of complex water treatment.^{62,83}

1.5.1 Heterogeneous Catalysis

BFNCs have emerged as sustainable alternatives to conventional catalysts. Their nano-sized components increase the exposed surface area of the active component of the catalyst, thereby enhancing the contact between reactants and catalyst.

Some key points to consider are the capability to separate the catalyst from the reaction media once the catalytic process is over and the efficient selectivity of the catalyst for the desired reaction. These features can be tuned up by customizing the chemical composition and morphology of FM NPS in hybrid BFNCs materials.

Some relevant aspects and challenges of heterogeneous Nanocatalysis are presented in Figure 1.17.

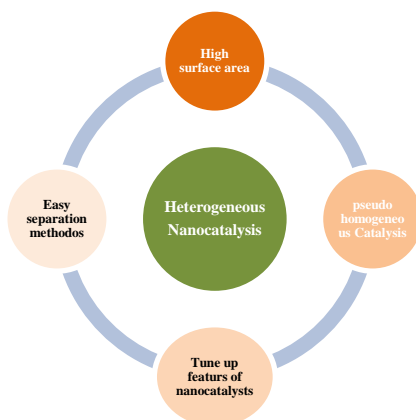


Figure 1.17: Advantages of heterogeneous nanocatalysis.

Regarding the fact that the final Nanocomposite material presents both properties of the NMs and the polymeric matrix, its application for catalysis is favoured by the feasibility to separate the catalyst from reaction media by a simple physical filtration step. In addition; the synthesis of FMNPs with magnetic core and a catalytic shell, makes possible as well to separate the BFNCs by applying a magnetic trap; as indicated in Figure 1.18.

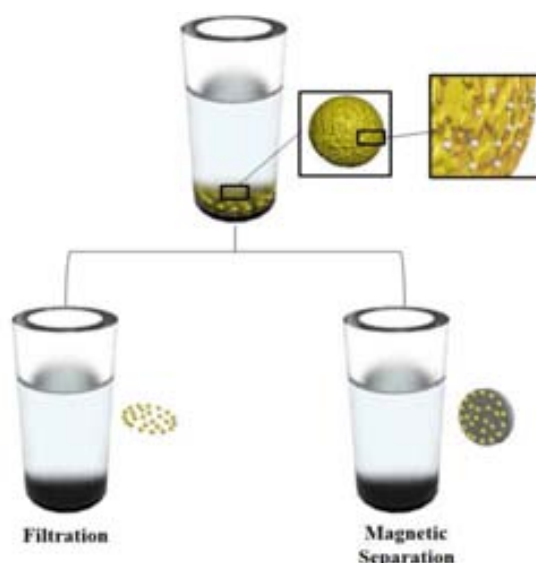


Figure 1.18: Scheme of feasible separation methods for BFNCs materials for catalytic applications.

Due to the potential application of Pd, Pt, Rh, and Au-FMNPs to be efficient and selective catalysts for several types of catalytic reactions, including olefinhydrogenation and C-C coupling such as Heck, Suzuki and Sonogashira reactions.^{5,12,48,84,85}

The catalytic activity of NCs prepared by IMS technique was tested for heterogeneous catalysis. This represents one the fields of the modern science and technology where the application of ultrafine catalyst particles dates back to the beginning of the last century.

Current application of heterogeneous catalysis encourages the development of novel nanocatalysts contained in hybrid materials such as nanocomposites. Regarding this fact, an appropriate support for the catalytic NPs is a mandatory in order to simplify their applications in reactions such as Pd-NPs to Suzuki Cross Coupling Reaction (SCCR), Pd catalysts are known to be suitable catalysts for this reaction, with applicability to the synthesis of fine chemicals.^{5,12,48,84,85}

1.5.2 Electrochemical Sensors:

A chemical sensor is an analytical device used to obtain chemical information from a sample. These are widely used for the detection and quantification of organic and inorganic compounds for clinical, biomedical and environmental purposes.⁸⁶⁻⁹⁰

Some basic requirements for a sensor include stability, selectivity, and high response rate for the analyte signal, long life cycle, low energy and analyte consumption.

Specifically, amperometric sensors are based on the application of an external potential that causes an electron transfer between the working electrode and the species in the solution under study. The current is proportional to the concentration of the analyte, it goes through an electrochemical cell that contains electroactive species. Thus, the quantitative detection of the analyte is achievable even at low concentrations like parts per billion (ppb). A suitable analyte for a certain electrode is the one that can be electrochemically oxidized or reduced on the electrode surface.

One drawback of amperometric sensors is their selectivity and their relatively long time response. The dependence between current intensity and analyte concentration is described by the following Equation 1.11:⁹¹⁻⁹³

$$i = \frac{nFAD_a C_a}{\delta} = k_A C_A \quad [11]$$

i represents the intensity, A represents the surface area, n is the number of electron moles per analyte mole involved in the redox process, F is Faraday's constant, D is the diffusion coefficient, C_a is concentration of electroactive species, δ is the thickness of diffusion layer and k_A is the equivalent of $nFAD_a/\delta$.

The use of FM NPs for the modification of amperometric sensors offers great advantages as the enhancement of mass transference rate through the polymer matrix and the increase in the surface area of the nanoelectrocatalyst.⁹¹

One simple way for the electrode modification using BFNCs is the incorporation of FMNPs nanocomposites containing noble metal NPs such as Pd, Au or Pt. Despite of the precursor reagent price, the great stability and oxidation resistance of these metals make them more than a good alternative for the preparation of amperometric sensors. and their electroactive features and catalytic behaviour for some chemical reactions.⁹²⁻⁹⁴

In addition to these advantages, the modification of sensors with nanocrystals as FMNPs could imply thermal evaporation, electroless deposition by galvanic replacement, MNPs hydrosol absorption or electrochemical deposition.⁹⁵⁻⁹⁷

The possible aggregation of the FM NPs limits their application in electrochemical systems. Due to this fact, the preparation of FMNPs must provide an extra level of stability and a favourable distribution in the final NC electrode material⁴⁵. Regarding this, the IMS technique becomes a valid FMNPs preparation methodology. IMS takes advantage of the ion exchange properties of the support matrix (e. g. sulfonic resins or membranes, carbon nanotubes) for consecutive loading and reduction processes during the synthesis of FMNPs with a favourable distribution in the final composite material..

For instance, taking advantage of the solubility of some polymeric membranes in organic solvents, the electrode modification can be carried out by the preparation of NPs ink. The ink is dropped on the surface of the sensor and let dry due to the volatility of the solvent, where the FMNPs stay attached on sensor surface.

By incorporating FMNPs, the electrochemical system substantially improves its the electron transfer⁴⁷. Among transfer mechanisms involved in sensors, some others)

Moreover, the, the insertion of FMNPs within a matrix containing immobilized enzymes, allows increasing substantially the conductivity of the matrix and therefore the transfer between the enzyme molecules to the surface of the electrode. The same effect takes place by decreasing the distance electrons hop(see Figure 1.19)

Furthermore, it should be noted that the incorporation of enzymes into the biosensors makes them a highly selective devices, which is owned one of the main drawbacks of amperometric sensors.

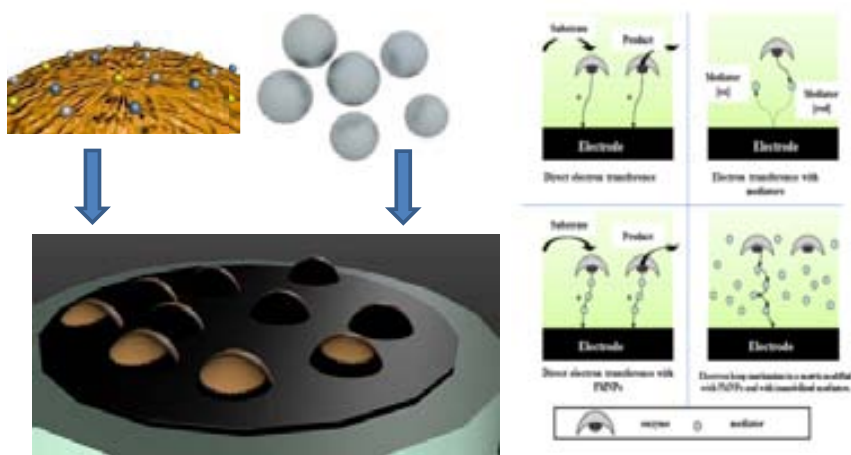


Figure 1.19: Scheme of the enhanced electronic transfer of modified electrodes with FMNPs.

An example of the feasibility of IMS prepared NCs for sensor applications is a glucose biosensor prepared by using the layer-by-layer deposition technique.

The modification of Graphite-epoxy composite electrodes (GECs) with Core-Shell Pt@Cu-MNPs on Sulfonated polyetheretherketone (SPEEK) membrane which was sequentially treated with polyethylenimine (PEI) and Glucose oxidase (GOx) solutions.^{98,99}

The sensitivity of biosensor at the same enzyme content (PEI-GOx layers) appears to strongly depend on the thickness of Pt-shell. This means that the

thickness of the catalytically active shell of MNPs can be used as an additional parameter for enhancing the biosensor performance. This conclusion follows from a high sensitivity of Pt@Cu toward hydrogen peroxide, which is one of the by-products of the enzymatic reaction proceeding in the course of glucose detection. The amperometric sensors prepared by modification of GECE with FMNPs demonstrate a high sensitivity toward hydrogen peroxide as can be seen in Figure 1.20.

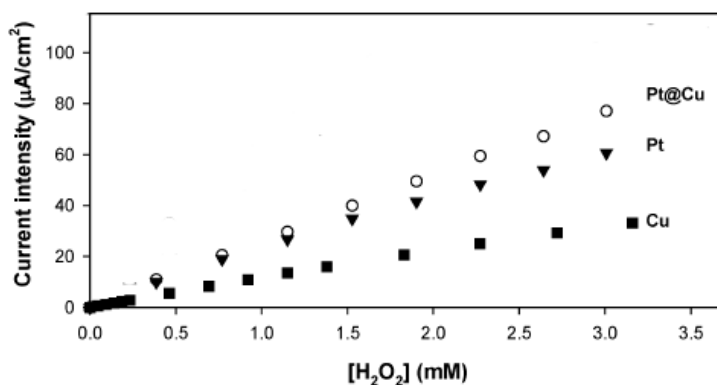


Figure 1.20: Calibration curves of electrochemical detection of H₂O₂ concentration with Pt@Cu, Pt- and Cu-FMNP composite S PEEK membranes. Experimental conditions: potential: -250 mV; 0.1 M acetate buffer (Adapted from Muraviev *et.al*⁹⁸)

1.5.3 Bactericide Activity

There are about 800 million people in the world which do not have access to clean and potable water. Therefore, the importance of potable water for people in some countries dictates the need for the development of innovative technologies and materials for the production of safe potable water. This type of application can be a perfect for the NCs for water treatment and bactericide assays.

Furthermore, the use of NCs can also help to solve one of the major operational problems associated with water treatment technology: the biofouling. With the coating of polymeric membranes with Ag-NPs, the accumulation of microorganism and their further multiplication in the material is impeded, thus the operational properties of the NCs are kept. Thus, the bactericide activity of AgAu-cubic microstructure containing composite materials is tested as a novel bactericidal NC. An increasing amount of AgAu-NCs (102 mgAg x g⁻¹ BFNC

and 59 mg Au x g⁻¹ NC) beads was added to individual wells containing 105 CFU/mL of *E. coli* suspension in LB medium. After overnight incubation, bacterial proliferation was evaluated by measuring the optical density of each well at 550 nm as this wavelength is indicative of bacterial proliferation. Raw materials were used as control.^{48,51,52,56}

Figure 1.21 shows the bactericide activity determined for both systems. There is the evidence of the feasible application of these AgAu – NCs as bactericide materials, since the performance obtained is very high (almost total killing effect with small amount of beads).

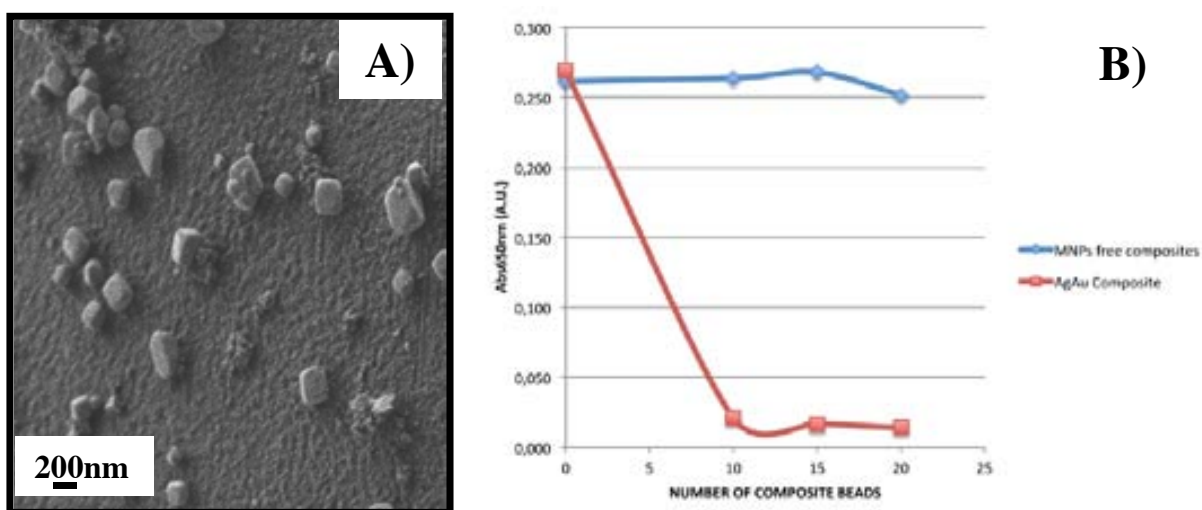


Figure 1.21: Bactericide activity of hybrid AgAu –cubic microstructures containing NCs

These results verify the suitability of IMS for the preparation of novel materials for the common applications of water treatment.

1.5.4 BFNCs for energy storage systems:

BFNCs are advantageous materials that offer huge surface to volume ratios, favourable transport properties, altered physical properties, and confinement effects resulting from the nanoscale dimensions, and have been extensively

studied for energy-related applications such as solar cells, catalysts, thermoelectrics, lithium ion batteries, supercapacitors, and hydrogen storage systems with high solar energy conversion efficiencies at low fabrication cost.

These materials can be tailored to harvest sunlight over a broad range of the spectrum, while plasmonic structures offer effective ways to reduce the thickness of light-absorbing layers. Multiple exciton generation, singlet exciton fission, photon down-conversion, and photon up-conversion realized in nanostructures, create significant interest for harvesting underutilized ultraviolet and currently unutilized infrared photons.^{100 101}

1.6. Concluding Remarks:

BFNCs demonstrate to have interesting features consisting in the mutual influence of components (supporting matrix and NPs) on each other. For example, the matrix provides stabilization of FMNPs, preventing their aggregation and uncontrollable growth. On the other hand, FMNPs can react with polymer chains serving as a sort of cross-linking agents, what results in the appearance of nanoporosity in gel type polymers. Their bifunctionality represents another interesting feature of these materials. On one hand it is determined by the functionality of the hosting polymer (e.g., ion exchanger), while on the other it is also determined by the properties of FMNPs (e.g., bactericide or catalytic activity). From this viewpoint the structural features of the BFNCs material start to play the key role in the field of functional materials for current and future applications. Therefore, the most favourable spatial and size distribution of FMNPs in NCs should be near the surface is one of the advantages of IMS as a green preparation methodology of NPs and BFNCs. Consequently, studying how IMS provides the most favourable distribution of the NPs in the BFNCs, the role of DEE, the possible effects on the initial ion exchange properties of the support matrix and further approaches of IMS; are described and discussed in the following sections.

References

- (1) Fhalman, B. *Materials Chemistry*; Second Edi.; Springer: New York, 2011.
- (2) Zang, J.; Wang, Y.; Bian, L.; Zhang, J.; Meng, F.; Zhao, Y.; Ren, S.; Qu, X. Surface Modification and Electrochemical Behaviour of Undoped Nanodiamonds. *Electrochim. Acta* **2012**, *72*, 68–73.
- (3) Saha, K.; Agasti, S. S.; Kim, C.; Li, X.; Rotello, V. M. Gold Nanoparticles in Chemical and Biological Sensing. *Chem. Rev.* **2012**, *112*, 2739–2779.
- (4) Binder, W. H.; Sachsenhofer, R. “Click” Chemistry in Polymer and Materials Science. *Macromol. Rapid Commun.* **2007**, *28*, 15–54.
- (5) Domènech, B.; Bastos-Arrieta, J.; Alonso, A. Bifunctional Polymer-Metal Nanocomposite Ion Exchange Materials. In *Ion Exchange Technologies*; Kilislioglu, A., Ed.; InTech, 2012; pp. 35–72.
- (6) Plieth, W. *Electrochemistry for Materials Science*; First Edit.; Elsevier: The Netherlands, 2008.
- (7) Sanchez, C.; Shea, K. J.; Kitagawa, S. Applications of Advanced Hybrid Organic–inorganic Nanomaterials: From Laboratory to Market. *Chem. Soc. Rev.* **2011**, *40*, 696–753.
- (8) Van Hove, M. a. From Surface Science to Nanotechnology. *Catal. Today* **2006**, *113*, 133–140.
- (9) Serrano, E.; Rus, G.; García-Martínez, J. Nanotechnology for Sustainable Energy. *Renew. Sustain. Energy Rev.* **2009**, *13*, 2373–2384.
- (10) Sanchez, F.; Sobolev, K. Nanotechnology in Concrete – A Review. *Constr. Build. Mater.* **2010**, *24*, 2060–2071.
- (11) Misra, P. *Metallic Nanoparticles*; Blackman, J. A., Ed.; First Edit.; Elsevier: Amsterdam, The Netherlands, 2009.
- (12) Campelo, J. M.; Luna, D.; Luque, R.; Marinas, J. M.; Romero, A. a. Sustainable Preparation of Supported Metal Nanoparticles and Their Applications in Catalysis. *ChemSusChem* **2009**, *2*, 18–45.
- (13) Savage, N.; Diallo, M. S.; Duncan, J.; Street, A.; Sustich, R. *Nanotechnology Applications for Clean Water*; First.; William Andrew Inc: Nueva York, 2009.
- (14) Hostetler, M. J.; Wingate, J. E.; Zhong, C.; Harris, J. E.; Vachet, R. W.; Clark, M. R.; Londono, J. D.; Green, S. J.; Stokes, J. J.; Wignall, G. D.; et al. Alkanethiolate Gold Cluster Molecules with Core Diameters from 1 . 5 to 5 . 2 Nm : Core and Monolayer Properties as a Function of Core Size. **2008**, *7463*, 17–30.

- (15) Zhang, Q.; Huang, J.-Q.; Qian, W.-Z.; Zhang, Y.-Y.; Wei, F. The Road for Nanomaterials Industry: A Review of Carbon Nanotube Production, Post-Treatment, and Bulk Applications for Composites and Energy Storage. *Small* **2013**, *9*, 1237–1265.
- (16) Akamatsu, K.; Adachi, S.; Tsuruoka, T.; Ikeda, S.; Tomita, S.; Nawafune, H. Nanoparticles with Controlled Microstructures. **2008**, 3042–3047.
- (17) Murray, R. W. Nanoelectrochemistry: Metal Nanoparticles, Nanoelectrodes, and Nanopores. *Chem. Rev.* **2008**, *108*, 2688–2720.
- (18) Luo, X.; Morrin, A.; Killard, A. J.; Smyth, M. R. Application of Nanoparticles in Electrochemical Sensors and Biosensors. *Electroanalysis* **2006**, *18*, 319–326.
- (19) Cortie, M. B.; McDonagh, A. M. Synthesis and Optical Properties of Hybrid and Alloy Plasmonic Nanoparticles. *Chem. Rev.* **2011**.
- (20) Ramesh, G. V.; Porel, S.; Radhakrishnan, T. P. Polymer Thin Films Embedded with in Situ Grown Metal Nanoparticles. *Chem. Soc. Rev.* **2009**, *38*, 2646–2656.
- (21) Ghosh, S. K.; Pal, T. Interparticle Coupling Effect on the Surface Plasmon Resonance of Gold Nanoparticles: From Theory to Applications. *Chem. Rev.* **2007**, *107*, 4797–4862.
- (22) Xiao, Y.; Li, C. M. Nanocomposites: From Fabrications to Electrochemical Bioapplications. *Electroanalysis* **2008**, *20*, 648–662.
- (23) Role, T.; Scattering, E. R. Electrochemical Properties of Small Clusters of Metal Atoms and Their Role in Surface Enhanced Raman Scattering. **1982**, *460*, 3166–3170.
- (24) Wang, Z. L. 1 Nanomaterials for Nanoscience and Nanotechnology. **2000**, *1*.
- (25) Tréguer-Delapierre, M.; Majimel, J.; Mornet, S.; Duguet, E.; Ravaine, S. Synthesis of Non-Spherical Gold Nanoparticles. *Gold Bulletin*, 2008, *41*, 195–207.
- (26) Polshettiwar, V.; Varma, R. S. Green Chemistry by Nano-Catalysis. *Green Chem.* **2010**, *12*, 743.
- (27) Elizondo, N.; Segovia, P.; Coello, V. Green Synthesis and Characterizations of Silver and Gold Nanoparticles. In *Green Chemistry - Environmentally Benign Approaches*; Kidwai, M., Ed.; InTech, 2012.
- (28) Iravani, S. Green Synthesis of Metal Nanoparticles Using Plants. *Green Chem.* **2011**, *13*, 2638.
- (29) Sharifi, S.; Behzadi, S.; Laurent, S.; Forrest, M. L.; Stroeve, P.; Mahmoudi, M. Toxicity of Nanomaterials. *Chem. Soc. Rev.* **2012**, *41*, 2323–2343.

- (30) Chan, V. S. W. Nanomedicine: An Unresolved Regulatory Issue. *Regul. Toxicol. Pharmacol.* **2006**, *46*, 218–224.
- (31) Franco, A.; Hansen, S. F.; Olsen, S. I.; Butti, L. Limits and Prospects of the “Incremental Approach” and the European Legislation on the Management of Risks Related to Nanomaterials. *Regul. Toxicol. Pharmacol.* **2007**, *48*, 171–183.
- (32) Fahmy, T. Y. a; Mobarak, F. Green Nanotechnology: A Short Cut to Beneficiation of Natural Fibers. *Int. J. Biol. Macromol.* **2011**, *48*, 134–136.
- (33) Wong, S.; Karn, B. Ensuring Sustainability with Green Nanotechnology. *Nanotechnology* **2012**, *23*, 290201.
- (34) Devadasu, V. R.; Bhardwaj, V.; Kumar, M. N. V. R. Can Controversial Nanotechnology Promise Drug Delivery? *Chem. Rev.* **2013**, *113*, 1686–1735.
- (35) Alonso, A.; Bastos-Arrieta, J.; Davies, G. Ecologically Friendly Polymer-Metal and Polymer-Metal Oxide Nanocomposites for Complex Water Treatment. In *Nanocomposites - New Trends and Developments*; Ebrahimi, F., Ed.; InTech, 2012; pp. 187–213.
- (36) Dahl, J. a; Maddux, B. L. S.; Hutchison, J. E. Toward Greener Nanosynthesis. *Chem. Rev.* **2007**, *107*, 2228–2269.
- (37) Tiano, A. L.; Koenigsmann, C.; Santulli, A. C.; Wong, S. S. Solution-Based Synthetic Strategies for One-Dimensional Metal-Containing Nanostructures. *Chem. Commun. (Camb)*. **2010**, *46*, 8093–8130.
- (38) Muñoz-Rojas, D.; Oró-Solé, J.; Ayyad, O.; Gómez-Romero, P. Facile One-Pot Synthesis of Self-Assembled Silver@polypyrrole Core/shell Nanosnakes. *Small* **2008**, *4*, 1301–1306.
- (39) Donnan, F. G. Theory of Membrane Equilibria and Membrane Potentials in the Presence of Non-Dialysing Electrolytes. A Contribution to Physical-Chemical Physiology. *J. Memb. Sci.* **1995**, *100*, 45–55.
- (40) Cumbal, L.; Sengupta, A. K. Arsenic Removal Using Polymer-Supported Hydrated iron(III) Oxide Nanoparticles: Role of Donnan Membrane Effect. *Environ. Sci. Technol.* **2005**, *39*, 6508–6515.
- (41) Burato, C.; Centomo, P.; Pace, G.; Favaro, M.; Prati, L.; Corain, B. Generation of Size-Controlled palladium(0) and gold(0) Nanoclusters inside the Nanoporous Domains of Gel-Type Functional Resins. *J. Mol. Catal. A Chem.* **2005**, *238*, 26–34.
- (42) Ruiz, P.; Muñoz, M.; Macanás, J.; Muraviev, D. N. Intermatrix Synthesis of Polymer–Copper Nanocomposites with Tunable Parameters by Using Copper Comproportionation Reaction. *Chem. Mater.* **2010**, *22*, 6616–6623.

- (43) Ruckenstein, E.; Park, J. S. Preparation of Polymer Composites. A Colloidal Pathway. *Chem. Mater.* **1989**, *1*, 343–348.
- (44) Sarkar, S.; Guibal, E.; Quignard, F.; SenGupta, a. K. Polymer-Supported Metals and Metal Oxide Nanoparticles: Synthesis, Characterization, and Applications. *J. Nanoparticle Res.* **2012**, *14*, 715.
- (45) Muraviev, D. N. Inter-Matrix Synthesis of Polymer Stabilised Metal Nanoparticles for Sensor Applications. *Contrib. to Sci.* **2005**, *3*, 19–32.
- (46) Bastos-Arrieta, J.; Muñoz, M.; Ruiz, P.; Muraviev, D. N. Morphological Changes of Gel-Type Functional Polymers after Intermatrix Synthesis of Polymer Stabilized Silver Nanoparticles. *Nanoscale Res. Lett.* **2013**, *8*, 255.
- (47) Ruiz, P.; Muñoz, M.; Macanás, J.; Turta, C.; Prodius, D.; Muraviev, D. N. Intermatrix Synthesis of Polymer Stabilized Inorganic Nanocatalyst with Maximum Accessibility for Reactants. *Dalton Trans.* **2010**, *39*, 1751–1757.
- (48) Alonso, A.; Macanás, J.; Shafir, A.; Muñoz, M.; Vallribera, A.; Prodius, D.; Melnic, S.; Turta, C.; Muraviev, D. N. Donnan-Exclusion-Driven Distribution of Catalytic Ferromagnetic Nanoparticles Synthesized in Polymeric Fibers. *Dalton Trans.* **2010**, *39*, 2579–2586.
- (49) Ruiz, P.; Macanás, J.; Muñoz, M.; Muraviev, D. N. Intermatrix Synthesis: Easy Technique Permitting Preparation of Polymer-Stabilized Nanoparticles with Desired Composition and Structure. *Nanoscale Res. Lett.* **2011**, *6*, 343.
- (50) Konev, D. V.; Fertikov, V. V.; Kravchenko, T. a.; Kalinichev, a. I. The Inverse Problem of the Kinetics of Redox Sorption Taking into Account the Size of Ultradisperse Metal Particles in an Electron-Ion Exchanger. *Russ. J. Phys. Chem. A* **2008**, *82*, 1363–1367.
- (51) Alonso, A.; Muñoz-Berbel, X.; Vigués, N.; Rodríguez-Rodríguez, R.; Macanás, J.; Mas, J.; Muñoz, M.; Muraviev, D. N. Intermatrix Synthesis of Monometallic and Magnetic Metal/metal Oxide Nanoparticles with Bactericidal Activity on Anionic Exchange Polymers. *RSC Adv.* **2012**, *2*, 4596–4599.
- (52) Alonso, A.; Vigués, N.; Muñoz-Berbel, X.; Macanás, J.; Muñoz, M.; Mas, J.; Muraviev, D. N. Environmentally-Safe Bimetallic Ag@Co Magnetic Nanocomposites with Antimicrobial Activity. *Chem. Commun. (Camb).* **2011**, *47*, 10464–10466.
- (53) Nagarajan, R.; Hatton, T. *Nanoparticles: Synthesis, Stabilization, Passivation, and Functionalization*; Nagarajan, R.; Alan Hatton, T., Eds.; First Edit.; ACS Publications: United States of America, 2008.
- (54) Yang, M.; Yang, Y.; Liu, Y.; Shen, G.; Yu, R. Platinum Nanoparticles-Doped Sol-Gel/carbon Nanotubes Composite Electrochemical Sensors and Biosensors. *Biosens. Bioelectron.* **2006**, *21*, 1125–1131.

- (55) Reddy, L. H.; Arias, J. L.; Nicolas, J.; Couvreur, P. Magnetic Nanoparticles: Design and Characterization, Toxicity and Biocompatibility, Pharmaceutical and Biomedical Applications. *Chem. Rev.* **2012**, *112*, 5818–5878.
- (56) Alonso, A.; Muñoz-Berbel, X.; Vigués, N.; Macanás, J.; Muñoz, M.; Mas, J.; Muraviev, D. N. Characterization of Fibrous Polymer Silver/cobalt Nanocomposite with Enhanced Bactericide Activity. *Langmuir* **2012**, *28*, 783–790.
- (57) Domènech, B.; Muñoz, M.; Muraviev, D. N.; Macanás, J. Uncommon Patterns in Nafion Films Loaded with Silver Nanoparticles. *Chem. Commun. (Camb)*. **2014**, *50*, 4693–4695.
- (58) Xu, P.; Han, X.; Zhang, B.; Du, Y.; Wang, H.-L. Multifunctional Polymer-Metal Nanocomposites via Direct Chemical Reduction by Conjugated Polymers. *Chem. Soc. Rev.* **2014**, *43*, 1349–1360.
- (59) Zolotukhina, E. V.; Kravchenko, T. a. Synthesis and Kinetics of Growth of Metal Nanoparticles inside Ion-Exchange Polymers. *Electrochim. Acta* **2011**, *56*, 3597–3604.
- (60) Barbaro, P.; Liguori, F. Ion Exchange Resins: Catalyst Recovery and Recycle. *Chem. Rev.* **2009**, *109*, 515–529.
- (61) Alexandratos, S. D. Ion-Exchange Resins: A Retrospective from Industrial and Engineering Chemistry Research. *Ind. Eng. Chem. Res.* **2009**, *48*, 388–398.
- (62) Bastos-Arrieta, J.; Shafir, A.; Alonso, A.; Muñoz, M.; Macanás, J.; Muraviev, D. N. Donnan Exclusion Driven Intermatrix Synthesis of Reusable Polymer Stabilized Palladium Nanocatalysts. *Catal. Today* **2012**, *193*, 207–212.
- (63) Levenstein, R.; Hasson, D.; Semiat, R. Utilization of the Donnan Effect for Improving Electrolyte Separation with Nanofiltration Membranes. **1996**, *116*, 77–92.
- (64) Mijangos, F.; Tikhonov, N.; Ortueta, M.; Dautov, A. Modeling Ion-Exchange Kinetics in Bimetallic Systems. *Ind. Eng. Chem. Res.* **2002**, *41*, 1357–1363.
- (65) Greenleaf, J. E.; Lin, J.; Sengupta, A. K. Two Novel Applications of Ion Exchange Fibers: Arsenic Removal and Chemical-Free Softening of Hard Water. *Environ. Prog.* **2006**, *25*, 300–311.
- (66) Domènech, B.; Muñoz, M.; Muraviev, D. N.; Macanás, J. Polymer-Stabilized Palladium Nanoparticles for Catalytic Membranes: Ad Hoc Polymer Fabrication. *Nanoscale Res. Lett.* **2011**, *6*, 406.
- (67) Muraviev, D.; Macanas, J.; Farre, M.; Munoz, M.; Alegret, S. Novel Routes for Inter-Matrix Synthesis and Characterization of Polymer Stabilized Metal Nanoparticles for Molecular Recognition Devices. *Sensors Actuators B Chem.* **2006**, *118*, 408–417.

- (68) Elliott, S. D.; Moloney, M. P.; Gun'ko, Y. K. Chiral Shells and Achiral Cores in CdS Quantum Dots. *Nano Lett.* **2008**, *8*, 2452–2457.
- (69) Petryayeva, E.; Algar, W. R.; Medintz, I. L. Quantum Dots in Bioanalysis: A Review of Applications across Various Platforms for Fluorescence Spectroscopy and Imaging. *Appl. Spectrosc.* **2013**, *67*, 215–252.
- (70) Moloney, M. P.; Gun'ko, Y. K.; Kelly, J. M. Chiral Highly Luminescent CdS Quantum Dots. *Chem. Commun. (Camb)*. **2007**, 7345, 3900–3902.
- (71) Bera, D.; Qian, L.; Tseng, T.-K.; Holloway, P. H. Quantum Dots and Their Multimodal Applications: A Review. *Materials (Basel)*. **2010**, *3*, 2260–2345.
- (72) Yang, J.; Yang, J.; Ying, J.; Way, B.; Nanos, T.; Engineering, P.; Academy, C. Morphology and Lateral Strain Control of Pt Nanoparticles via Core À Shell Toward Oxygen Reduction Reaction. **2012**, 9373–9382.
- (73) Astruc, D. *Nanoparticles and Catalysis*; Astruc, D., Ed.; First Editi.; Wiley-VCH: Weinheim, Germany, 2008.
- (74) Kao, J.; Thorkelsson, K.; Bai, P.; Rancatore, B. J.; Xu, T. Toward Functional Nanocomposites: Taking the Best of Nanoparticles, Polymers, and Small Molecules. *Chem. Soc. Rev.* **2013**, *42*, 2654–2678.
- (75) Njoki, P. N.; Wu, W.; Lutz, P.; Maye, M. M. Growth Characteristics and Optical Properties of Core/Alloy Nanoparticles Fabricated via the Layer-by-Layer Hydrothermal Route. *Chem. Mater.* **2013**, *25*, 3105–3113.
- (76) Sieb, N. R.; Wu, N.; Majidi, E.; Kukreja, R.; Branda, N. R.; Gates, B. D. Hollow Metal Nanorods with Tunable. **2009**, *3*, 1365–1372.
- (77) Sau, T. K.; Rogach, A. L. Nonspherical Noble Metal Nanoparticles: Colloid-Chemical Synthesis and Morphology Control. *Adv. Mater.* **2010**, *22*, 1781–1804.
- (78) Zhou, Y.; Zhou, X.; Park, D. J.; Torabi, K.; Brown, K. a; Jones, M. R.; Zhang, C.; Schatz, G. C.; Mirkin, C. a. Shape-Selective Deposition and Assembly of Anisotropic Nanoparticles. *Nano Lett.* **2014**, *14*, 2157–2161.
- (79) Personick, M. L.; Langille, M. R.; Zhang, J.; Mirkin, C. a. Shape Control of Gold Nanoparticles by Silver Underpotential Deposition. *Nano Lett.* **2011**, *11*, 3394–3398.
- (80) Burda, C.; Chen, X.; Narayanan, R.; El-Sayed, M. a. Chemistry and Properties of Nanocrystals of Different Shapes. *Chem. Rev.* **2005**, *105*, 1025–1102.
- (81) Ruiz, P.; Muñoz, M.; Macanás, J.; Muraviev, D. N. Reactive & Functional Polymers Intermatrix Synthesis of Polymer-Stabilized PGM @ Cu Core – Shell Nanoparticles with Enhanced Electrocatalytic Properties. *React. Funct. Polym.* **2011**, *71*, 916–924.

- (82) Alonso, A.; Bastos-arrieta, J.; Davies, G. L.; Gun, Y. K.; Vigués, N.; Muñoz-berbel, X.; Macanás, J.; Mas, J.; Muñoz, M.; Muraviev, D. N. Ecologically Friendly Polymer-Metal and Polymer- Metal Oxide Nanocomposites for Complex Water Treatment.
- (83) Alonso, a.; Shafir, a.; Macanás, J.; Vallribera, a.; Muñoz, M.; Muraviev, D. N. Recyclable Polymer-Stabilized Nanocatalysts with Enhanced Accessibility for Reactants. *Catal. Today* **2012**.
- (84) Zhang, Y.; Cui, X.; Shi, F.; Deng, Y. Nano-Gold Catalysis in Fine Chemical Synthesis. *Chem. Rev.* **2012**, *112*, 2467–2505.
- (85) Wu, Y.; Wang, D.; Li, Y. Nanocrystals from Solutions: Catalysts. *Chem. Soc. Rev.* **2013**.
- (86) Sarkar, S.; Chatterjee, P. K.; Cumbal, L. H.; Sengupta, A. K. Hybrid Ion Exchanger Supported Nanocomposites : Sorption and Sensing for Environmental Applications. *Chem. Eng. J.* **2011**, *166*, 923–931.
- (87) Shipway, a N.; Katz, E.; Willner, I. Nanoparticle Arrays on Surfaces for Electronic, Optical, and Sensor Applications. *Chemphyschem* **2000**, *1*, 18–52.
- (88) Redel, E.; Mirtchev, P.; Huai, C.; Petrov, S.; Ozin, G. a. Nanoparticle Films and Photonic Crystal Multilayers from Colloidally Stable, Size-Controllable Zinc and Iron Oxide Nanoparticles. *ACS Nano* **2011**, *5*, 2861–2869.
- (89) Personick, M. L.; Mirkin, C. a. Making Sense of the Mayhem behind Shape Control in the Synthesis of Gold Nanoparticles. *J. Am. Chem. Soc.* **2013**, *135*, 18238–18247.
- (90) Moon, J. H.; Yang, S. Chemical Aspects of Three-Dimensional Photonic Crystals. *Chem. Rev.* **2010**, *110*, 547–574.
- (91) Shenhar, R.; Norsten, T. B.; Rotello, V. M. Polymer-Mediated Nanoparticle Assembly: Structural Control and Applications. *Adv. Mater.* **2005**, *17*, 657–669.
- (92) Campbell, F. W.; Compton, R. G. The Use of Nanoparticles in Electroanalysis: An Updated Review. *Anal. Bioanal. Chem.* **2010**, *396*, 241–259.
- (93) Welch, C. M.; Compton, R. G. The Use of Nanoparticles in Electroanalysis: A Review. *Anal. Bioanal. Chem.* **2006**, *384*, 601–619.
- (94) Hrapovic, S.; Liu, Y.; Male, K. B.; Luong, J. H. T. Platinum Nanoparticles and Carbon Nanotubes Interactions with Pt Nanoparticles to Form a Network That Connected Pt Nanoparticles to the Electrode Surface . TEM Nanoparticles on Carbon Nanotubes Whereas Cyclic Volta-. **2004**, *76*, 1083–1088.
- (95) Lee, K. Y.; Kim, M.; Hahn, J.; Suh, J. S.; Lee, I.; Kim, K.; Han, S. W. Assembly of Metal Nanoparticle-Carbon Nanotube Composite Materials at the Liquid/liquid Interface. *Langmuir* **2006**, *22*, 1817–1821.

- (96) Choi, H. C.; Shim, M.; Bangsaruntip, S.; Dai, H. Spontaneous Reduction of Metal Ions on the Sidewalls of Carbon Nanotubes. *J. Am. Chem. Soc.* **2002**, *124*, 9058–9059.
- (97) Qu, L.; Dai, L.; Osawa, E. Shape/size-Controlled Syntheses of Metal Nanoparticles for Site-Selective Modification of Carbon Nanotubes. *J. Am. Chem. Soc.* **2006**, *128*, 5523–5532.
- (98) Muraviev, D. N.; Ruiz, P.; Muñoz, M.; Macanás, J. Novel Strategies for Preparation and Characterization of Functional Polymer-Metal Nanocomposites for Electrochemical Applications. *Pure Appl. Chem.* **2008**, *80*, 2425–2437.
- (99) Muraviev, D. N.; Macanás, J.; Ruiz, P.; Muñoz, M. Synthesis, Stability and Electrocatalytic Activity of Polymer-Stabilized Monometallic Pt and Bimetallic Pt/Cu Core-Shell Nanoparticles. *Phys. Status Solidi* **2008**, *205*, 1460–1464.
- (100) Chen, G.; Seo, J.; Yang, C.; Prasad, P. N. Nanochemistry and Nanomaterials for Photovoltaics. *Chem. Soc. Rev.* **2013**, *42*, 8304–8338.
- (101) Zhang, Q.; Uchaker, E.; Candelaria, S. L.; Cao, G. Nanomaterials for Energy Conversion and Storage. *Chem. Soc. Rev.* **2013**, *42*, 3127–3171.
- (102) Mochalin, V. N.; Shenderova, O.; Ho, D.; Gogotsi, Y. The Properties and Applications of Nanodiamonds. *Nat. Nanotechnol.* **2012**, *7*, 11–23.

Motivation, Aims &
Publication
Compendium

2. Motivation, Aims and Publication Compendium

2.1 Motivation, perspectives and research innovation

Being part of a research group with such as the one supervised by Dr. Dmitri Muraviev and Dr. Maria Muñoz has offered me the opportunity get involved into the “Nano World” in an innovative and different way. In addition to the large number of publications related to nanomaterials, the great results obtained by former companions as Dr. Ruiz, Dr. Alonso and Dr. Domènech; increase the challenge to contribute significantly within the group itself.

By the time I enrolled the group, its scientific background includes in my group research includes the use of ion exchange polymeric supports (membranes and resins) to for the application of IMS technique for the application of the final bifunctional nanocomposite materials including heterogeneous catalysis, bactericide assays and electrochemical analysis.

Therefore, part of the contributions obtained through the development of this PhD thesis is the optimization and application of three IMS routes for the preparation of the nanocomposites; based on: a) ion exchange properties of matrix support and reduction stage. b) Precipitation of nanomaterial of interest c) galvanic replacement between nano templates and nanomaterials of interest. All of them offer the advantages of: stability, favourable distribution in final nanocomposite and they are not expensive.^{45,46,102}

Consequently, new types of nanomaterials were synthesized (quantum dots, bimetallic alloys) on novel reactive surfaces (carbon nanotubes, nanodiamonds, nanofilms) and therefore going beyond the traditional IMS scope. Regarding this, new characterization techniques were added as well to the overall expertise of the group.

2.2 General Aims

The general aim of this research work was focused on the design and optimization of the environmentally friendly surface modification of reactive matrices with FMNPs by different IMS routes; depending on the initial features of the chosen support for the NPs and the feasible application of the final novel nanocomposite material.

2.3 Specific Aims

In order to accomplish the general aim presented above, some specific aims and studies were carried out:

- 1) Development and enhancement of the IMS technique for both cationic and anionic ion exchangers
- 2) Synthesis, characterization and applications as heterogeneous nanocatalysts of Pd-FMNPs by the reflection version of IMS for anionic exchangers.
- 3) Analysis of the morphological changes on gel-type polymer due to the IMS of Ag-FMNPs.
- 4) Study of the role of the reducing agent used in IMS technique coupled with DEE on the
- 5) Synthesis and evaluation of Ag nano and microstructures on gel-type polymer matrices by classical IMS technique.
- 6) Synthesis, characterization and feature evaluation of AgAu microstructures on gel-type polymer matrix prepared by the extension method of IMS coupled with galvanic replacement.
- 7) Evaluation of the ion exchange properties of polymeric matrices before and after IMS of FMNPs by breakthrough curve profile.
- 8) Expanding the application of the different version of IMS technique to novel surfaces as nanofilms, CNTs and NDs.
- 9) Synthesis and evaluation of CdS- QDs on CNTs by extension method of IMS – precipitation technique.
- 10) Preparation, characterization and modification with FMNPs of S PEEK nanolayers by IMS technique coupled with DEE.

2.4 Publication compendium

The main results content in this thesis have been presented in several international conferences and events:

- a) 10th International Conference on Catalysis in Membrane Reactors (ICCMR 10), Moscow, Russia, June 2011
- b) 13th Trends in Nanotechnology 2012 (TNT'12) Madrid, Spain. September, 2012

- c) Society of Chemical Industry SCI Ion Exchange Conference 2012(IEX'12) Cambridge, UK. September 2012. First place Award)
- d) Institut Català de Nanotecnologia: Rethinking Nano Conference 2012. Barcelona, Spain. November, 2012. (First place Award)
- e) 3er. Jornades Doctorals del Departament de Química de la UAB. Barcelona, Spain. May, 2013. (First place Award)
- f) 3rd Frontiers in Polymer Science Conference 2013. Sitges, Spain. May, 2013. (First place Award)
- g) 11th International Conference on Catalysis in Membrane Reactors (ICCMR 11), Oporto, Portugal. July 2013. (First place Award)
- h) 14th Trends in Nanotechnology 2013 (TNT'13) Seville, Spain. September, 2013. (First place Award)
- i) 6th International Workshop on Polymer / Metal Nanocomposites. Toulouse, France. September, 2013

The research done was completed with two research stays abroad of three months each, indicated as follows:

- a) School of Chemistry of Trinity College Dublin, Ireland: under the supervision of Dr. Yurii Gun'ko. Dates: December 27th, 2012 to March 27th, 2013.
- b) Interactive Material Institute DWI at Aachen University, Germany. (Currently Leibniz Institute) under the supervision of Prof. Dr. Larisa Tsarkova. Dates: November 15th, 2013 to February 15th, 2014.

The content of “Results and Discussion” section includes a compilation of the following publications as first author.

- a) Bastos-Arrieta, J.; Shafir, A.; Alonso, A.; Muñoz, M.; Macanás, J.; Muraviev, D. N. Donnan Exclusion Driven Intermatrix Synthesis of Reusable Polymer Stabilized Palladium Nanocatalysts. *Catal. Today* **2012**, 10–13.
- b) Bastos-Arrieta, J.; Muñoz, M.; Ruiz, P.; Muraviev, D. N. Morphological Changes of Gel-Type Functional Polymers after Intermatrix Synthesis of Polymer Stabilized Silver Nanoparticles. *Nanoscale Res. Lett.* **2013**, 8, 255.
- c) Bastos-Arrieta, J.; Muñoz, M. and Muraviev, D. N. Surface modification of gel-type ion exchange polymers by the Intermatrix Synthesis of silver Nanoparticles. *Reactive and Functional Polymers*; May, 2014. (Submitted).
- d) Bastos-Arrieta, J., Muñoz, J., Baeza, M., Céspedes, F., Muñoz, M. and Muraviev, D. N: Simple synthesis of CdS Quantum Dots on multiwall carbon nanotubes: to make CNTs visible. *RSC Advances*; June, 2014. (Submitted)

Currently, some new manuscripts are under preparation and are going to be submitted in the near future, dealing with the role of reducing agents during IMS for the preparation of microstructures.

Moreover, the author of this thesis has participated as a co-author in the following publications:

- a) Alonso, A.; Bastos-Arrieta, J.; Davies, G. Ecologically Friendly Polymer-Metal and Polymer-Metal Oxide Nanocomposites for Complex Water Treatment. In *Nanocomposites - New Trends and Developments*; Ebrahimi, F., Ed.; InTech, 2012; pp. 187–213.
- b) Domènech, B.; Bastos-Arrieta, J.; Alonso, A. Bifunctional Polymer-Metal Nanocomposite Ion Exchange Materials. In *Ion Exchange Technologies*; Kilislioglu, A., Ed.; InTech, 2012; pp. 35–72.
- c) Muñoz, J., Bastos-Arrieta, J., Muñoz, M., Céspedes, F., Muraviev, D. N. and Baeza, M. Simple green routes for the customized preparation of sensitive carbon nanotubes/epoxy nanocomposite electrodes with functional Metal Nanoparticles. *RSC Advances*, (Accepted Article). doi:10.1039/C4RA07294D

*“Ever tried, ever failed. No Matter
Try again, fail again. Fail better...”*

-Samuel Beckett-

Results & Discussion

Chapter 3



Intermatrix Synthesis technique (IMS) has proven to be an environmentally friendly methodology for the preparation of functional nanomaterials (FNMs) on different reactive matrices. The distribution of these FMNs is an important feature to control depending on the final application of the hybrid Nanocomposite;: bactericide assays, electroanalytical analysis, water treatment, heterogeneous catalysis and others. IMS coupled with the Donnan Exclusion Effect (DEE), offers the feasibility to control the FMNs distribution, taking into account the adequacy of the ion exchange form of the reactive matrix and the chemical nature of the reducing agent used during the synthesis. In addition, slightly modified IMS stages (precipitation, galvanic replacement) coupled with DEE are shape control synthetic routes on solid phase for the preparation of Ag and AgAu nano- and microstructures with favourable distribution.

3. Donnan Exclusion Effect Intermatrix Synthesis Technique: distribution and shape control technique for the environmentally friendly preparation of bifunctional nanocomposites.

The progress in polymeric materials could be expected in the design and development of Bifunctional Nanocomposite (BFNCs) materials have implied the combination of the nanoparticles (NPs) properties and the ones from the support matrix; increasing their structural and functionality complexity.^{1,2} Therefore, it is expected that these new hybrid materials to be used for drug delivery, protein purification, electrochemical sensors, catalysis, water treatment and others.^{2,3}

In addition to these progress, there is the challenge to include to this approach an understanding of the properties of nanomaterials (NMs) such as toxicity and ecotoxicity from the point of view of green chemistry.⁴ The possibility of using reactive matrices containing ion exchange functional groups support matrices for NPs stabilization is a growing field to achieve this aim.⁵

BFNCs containing inorganic FMNPs have become important due to their potential application for novel electronic, optical, and magnetic devices. The size of the FMNPs is one of the key features that determine the properties of the BFNCs. Since the physical interactions depend on both the particle size and interparticle spacing, precise control over the spacing under a fixed particle size is an important challenge for understanding the physical interactions in the BFNCs field.⁶

One major concern for these added value materials is the functional metal nanoparticles (FMNPs) distribution in terms of size and matrix location, space, physical and chemical properties of the matrix formed, and the understanding of the kinetics of the BFNCs formation. Moreover, it is important to take into account the FMNPs affinity and adhesion to the matrix and the possible consequent changes of the matrix due to the FMNPs (porosity, ion exchange capacity)^{2,7}

FMNPs distribution in the BFNCs materials is of great importance as it allows for maximally tuning their properties for further applications. For example, in catalytic applications,⁸ the best situation is when the catalyst MNPs are located near the

polymer surface what provides the maximum accessibility of the reactants to the catalytic centres. In electrochemical or electroanalytical applications (e.g., in sensors and biosensors), a homogeneous distribution of FMNPs has been considered to be preferable as it enhances the electron conductivity of the system.^{9,10}

The Intermatrix Synthesis (IMS) is an *in situ* methodology for the preparation of BFNCs that offers the advantage of FMNPs distribution customization.¹¹⁻¹⁴ The major advantages of the *in situ* methods are that they usually yield a homogeneous distribution of NPs in the support matrix.¹⁵ NPs distribution in BFNCs can be characterised by different analytical and microscopic techniques such as TEM, SEM and EDS,

Regarding IMS, the feasibility to tune FMNPs distribution is related to the chemical reduction stage or the reducing agent selection. In both cases, the driven force of the final NPs distribution is due to the coupling of IMS with Donnan Exclusion Effect (DEE). Figure 3.1 shows a schematic representation of DEE involved during the ion exchange process of IMS

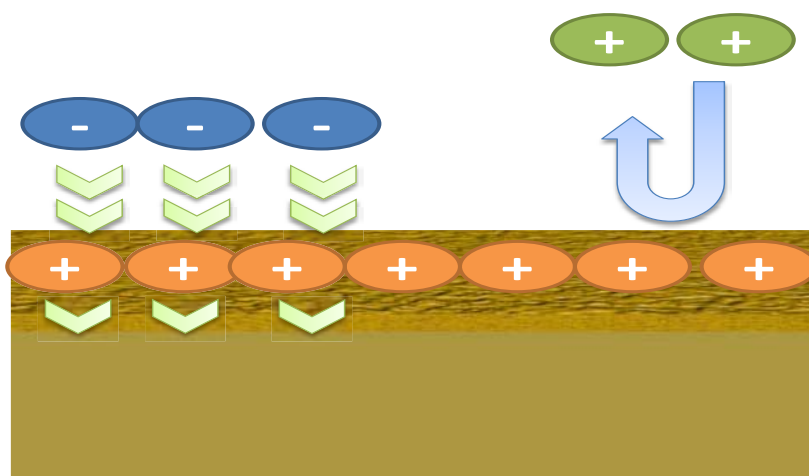


Figure 3.1: Schematic representation of the DEE during ion exchange showing repulsion, attachment and diffusion through DEE layer depending on the charge of species and layer.

DEE is based on the inability of ions to diffuse outward from one phase in a heterogeneous system^{16,17,18,19} (such as ions in aqueous solution to the interior of supporting matrix). This happens when the sign of the charge of this specie is the same of the one present on the ion exchange functional groups of the support reactive matrix. The result of this interaction during reduction stays allows the formation of the MNPs with tuned distribution. Depending on the selection of charged reducing agent, DEE for both cation exchange and anion exchange matrices results in their formation mainly

near the surface of the polymer. If a neutral reducing agent is chosen, the NPs distribution in the BFNCs is distributed in the interior and exterior zone of the matrix; as shown in Figure 3.2.

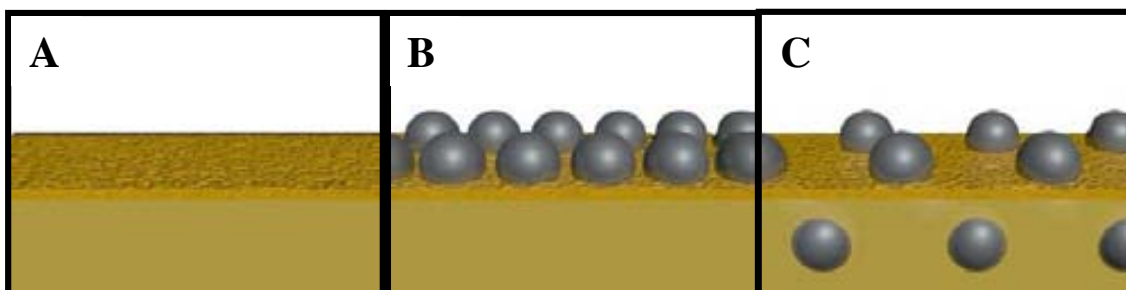


Figure 3.2: Schematic representation of FMNPs distribution due to IMS A) Raw ion exchanger surface B) FMNPs with favourable distribution mainly on the ion exchanger surface because of DEE interaction with metal precursors and reducing agents and C) FMNPs distribution

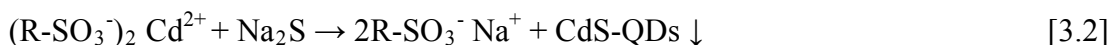
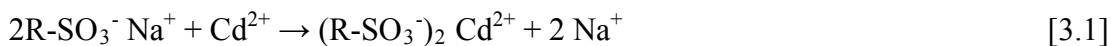
This chapter evaluates and proves the DEE coupled with the IMS (DEEIMS) on the FMNPs distribution and the role of reducing agent on the preparation of different NMs.

3.1 Preparation of CdS-QDs on cationic gel type polymeric matrix by DEEIMS-precipitation technique.

QDs are special kind of nanomaterials because of optical and semi-conducting properties.²⁰⁻²³ Specifically, CdS-QDs are feasible NMs to be prepared by DEEIMS-precipitation technique. This method is inexpensive, versatile, and technologically simple to produce different kind of NPs as well as BFNCs of a wide range of materials such as metal oxide NPs and QDs.^{24,25,26} The synthetic procedure requires the control over reaction conditions: pH, temperature and NPs - precursors.

As every NPs synthetic route, it lies in control of the particle size and thus achieving a narrow particle size and special distribution. Regarding this fact, DEEIMS becomes a valid methodology for the preparation, for example, of CdS-QDs containing BFNCs with favourable distribution on a gel-type cationic polymeric matrix. In addition, the *in situ* preparation gives an extra level of stability to of these QDs – BFNCs.

Equations 3.1 and 3.2 describe the DEEIMS of CdS-QDs on a gel-type cationic polymeric matrix.



As it is shown in Equation 3.1, the initial Na^+ form of the supporting matrix allows a better ion exchange – precursor loading stage of Cd^{2+} ions on the sulfonic groups. Equation 3.2 shows the QDs formation. In this case, the use of an ionic reducing agent is not necessary due to the addition of the precipitation precursor (sulphide ion). The cadmium content in the final composite is $110 \text{ mg Cd} \times \text{g}^{-1} \text{ BFNC}$, corresponding to a 93% of effective cadmium loading during stage 1 of DEEIMS.

The distribution of the CdS-QDs obtained by DEEIMS is similar to that predictable and obtained for zero-valent MNPs.^{10,27,28} QDs are mainly located near the NC surface (see Figure 3.3). The following important conclusion follows from the results obtained: in the course of DEEIMS of QDs when using ionic reduction or precipitation reagents, the DEE appears to be the driving force responsible for the surface distribution of the CdS-QDs. The necessary condition in this case is the coincidence of the charge sign of ionic reagent that causes the precipitation, with that of the functional groups of the hosting polymer.

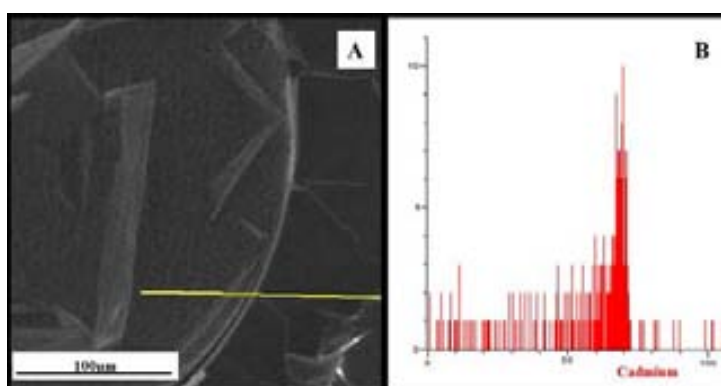


Figure 3.3: A) Cross section SEM image of CdS-QDs containing nanocomposite. B) EDS – LineScan Analysis of cross section showing the distribution of CdS-QDs

3.1.1 DEEIMS of Ag-FMNPs on gel-type cationic polymeric matrix with formaldehyde as neutral reducing agent.

The understanding of the fundamental origins of the physical properties of BFNCs through systematic studies of the controlled FMNPs distribution (size and interparticle distance) makes valid the idea of incorporating these NPs in the interior of a stabilizer matrix. In order to achieve this, some researchers have used a methodology very similar to DEEIMS but for the selection of the reducing agent and the principles their studies are based on.

Thus, the preparation of NC microspheres containing Ni-NPs is accomplished via chemical surface modification.^{29,30} This method takes advantage of the hydrolysis ability of the certain polymeric host, and subsequent ion exchange and annealing in hydrogen atmosphere induces both reduction of the doped metallic ions and reformation of the initial polymeric structures via dehydration. As DEEIMS, the particle size and homogenous distribution of the embedded Ni-NPs can be controlled. This procedure can be extended to the preparation of other types of NPs in order to obtain photonic or magnetic BFNCs materials.

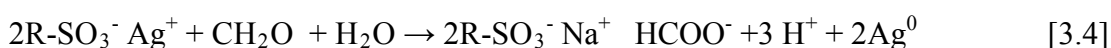
Regarding the feasible applications of BFNCs with interior distributed FMNPs; it is necessary to introduce new alternative preparation procedures. DEEIMS seems to be a suitable to obtain this distribution by a more environmentally friendly methodology; as the use of high temperature, organic solvents or even the use of hydrogen fluxes are not needed.

As discussed before, DEE affects the diffusion of ionic species through a charged matrix. In order to obtain an interior distribution of FMNPs by DEEIMS on a cationic exchanger matrix; its second stage must include a non-ionic reducing agent such as formaldehyde. The loading of silver ions into the matrix is represented by Equation 3.3. As the negatively charged sulfonic groups of the gel-type cationic polymer are redistributed through the entire matrix; so will be the Ag^+ ions due to diffusion and electrostatic interaction with them.

Regarding formaldehyde reduction rate it would be too slow at room temperature due to low or neutral pH. Therefore, the second stage of DEEIMS included 2M of

formaldehyde in a aqueous alkaline solution. These conditions make formaldehyde a suitable reducing agent for silver.^{31,32}

DEEIMS of Ag⁺-FMNPs on a gel-type cationic polymeric resin using formaldehyde as neutral reducing agent is presented in equations 3.3 and 3.4



Equation 3.3 shows the typical DEEIMS NPs – precursor loading stage, in this case of silver ions due to the exchange of Na⁺ to Ag⁺. Consequently, Equation 3.4 presents the formation of Ag-FMNPs. The silver content in the final BFNCs was around 159mg Ag x g⁻¹ BFNC, which corresponds to 70% efficiency of silver loading during DEEIMS stage 1.

In order to confirm the Ag-NPs intern distribution in the gel-type polymer, SEM characterization and EDS analysis were performed to the samples. As it can be seen in Figure 3.4, the element mapping and the LineScan EDS analysis verify this. Moreover, distribution is consistent and conclusive of DEE influence during the appearance of the FMNPs in the second stage of DEEIMS.

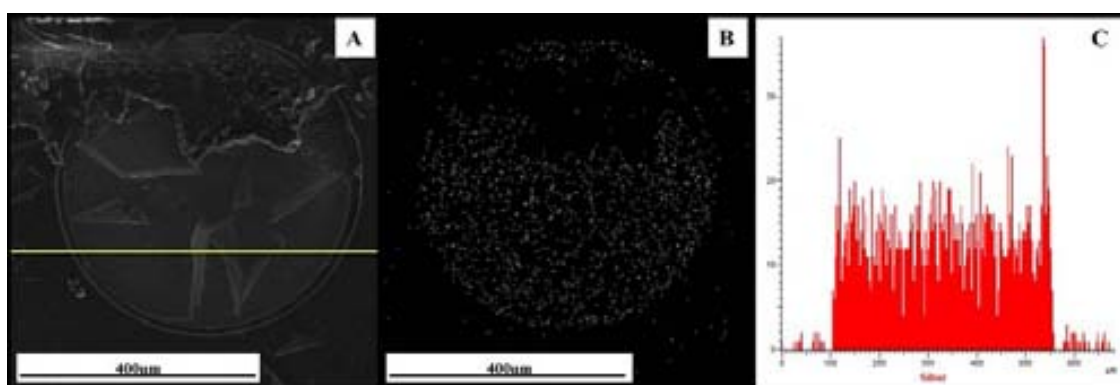


Figure 3.4: A) Cross section of Ag-FMNPs containing nanocomposite with B) Element Mapping and C) EDS - LineScan analysis showing the interior distribution of Ag-FMNPs due to IMS with formaldehyde as reducing agent

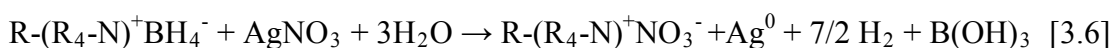
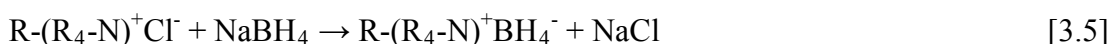
3.2 DEEIMS of Au and Ag-FMNPs on gel-type anionic polymer using ascorbic acid (AA) and sodium borohydride (NaBH₄) as ionic reducing agents.

The development of DEEIMS in our research group has been done mostly on cationic polymeric exchangers.^{11,12,25,33-35} Nevertheless, as one of the principles of DEEIMS is the feasibility to load the FMNPs precursors by an ion exchange stage to a suitable form of the exchanger support; this technique is a suitable for the surface modification of anionic exchanger matrices with FMNPs.^{10,25}

As it has been shown in reactions 3.1 and 3.3; usually the initial stage of DEEIMS involves the loading of the metal ion (NPs precursor) to the cationic exchanger matrix. As for anionic exchangers, DEE disables the diffusion of cations through this type of matrices. Therefore; two DEEIMS alternative procedures could be carried out. The first one consists in a symmetrical version of DEEIMS for cationic exchangers, in which the first stage is the loading of the ionic reducing agent (usually anions) and consequent loading of the metal cation (NPs precursor) at the reduction stage. The second procedure consists in the use of an anionic NPs – precursor (such as HAuCl₄) followed by the reducing stage.

3.2.1 Symmetrical version of classical DEEIMS applied for anionic matrices.

Thus, regarding the symmetrical DEEIMS procedure for anionic exchangers; the first stage would consist in the loading of an anionic reducing agent as NaBH₄. Then, from a more favourable ionic form for anionic exchange (Cl⁻-form), the stages for DEEIMS of Ag-FMNPs are presented as follows in Equations 3.5 and 3.6



The negative charge present in BH_4^- makes it to get attached to the quaternary amine groups of the support matrix due to DEE. The opposite effect occurs to the silver ions which bear positive charge and it results that the reduction process appears to be “localized” mainly near the surface of this polymer. The Ag-NPs distribution can be observed in Figures 3.6A and 3.6B. Moreover the Ag content for the BFNCs prepared by this methodology corresponds to an average $180 \text{ mg Ag} \times \text{g}^{-1}$ BFNC for a metal loading efficiency of 77%.

As it can be seen in Equation 3.6, the oxidation of BH_4^- ion leads to the release of hydrogen. As discussed before, hydrogen has been used as neutral reducing agent for the preparation of BFNCs with internal distribution of Ni microrstructures.^{29,30} Thus, ascorbic acid ($\text{C}_6\text{H}_8\text{O}_6 = \text{AA}$) was used as neutral reducing agent for DEEIMS of Ag-FMNP. To verify that the reduction of Ag ions, and consequently the Ag-NPs distribution in this NC, is due to the DEE for BH_4^- and not because of the release of H_2 . Considering $[\text{AA}]_{\text{ox}} = \text{C}_6\text{H}_6\text{O}_6$, the oxidation of AA is presented in Equation 3.7 and the reduction of Ag^+ ions with AA is presented in Equation 3.8. Chemical structures of AA and $[\text{AA}]_{\text{ox}}$ are presented in Figure 3.5.

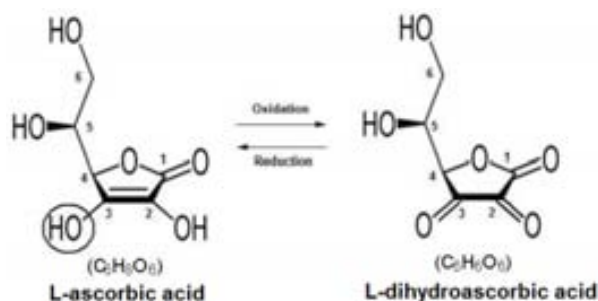
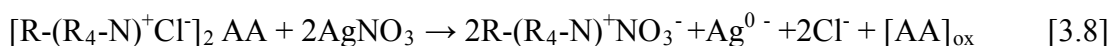


Figure 3.5 Schematic representation of chemical structures AA and $[\text{AA}]_{\text{ox}}$



AA is used as the reducing agent because it is weaker than NaBH_4 , and also because the reducing ability of ascorbic acid can be easily tuned through adjustment of the solution pH.³⁶ For our purposes, it is a suitable redox agent for silver ions with no associated release of H_2 (see Equation 3.7). The Ag-NPs distribution can be observed in

Figures 3.6C and 3.6D. The Ag content for the BFNCs prepared by this methodology corresponds to an average $174\text{mg Ag} \times \text{g}^{-1}$ BFNC for a metal loading efficiency of 75%.

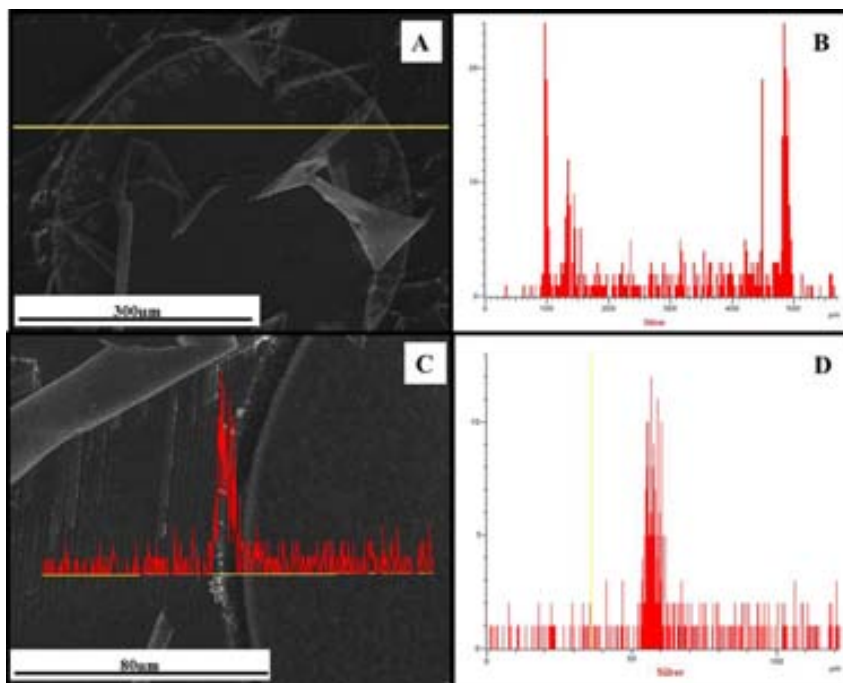


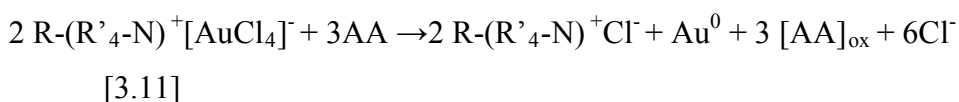
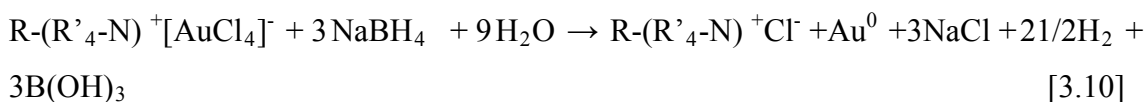
Figure 3.6: Ag-FMNPs distribution mainly on the surface on gel-type anionic exchanger due to IMS. A, B) Cross section and LineScan using NaBH_4 as reducing agent. C,D) Cross section and EDS LineScan using AA as reducing agent.

As seen in EDS spectra from Figures 3.5B and 3.5D; despite the methodology use for the preparation of Ag-FMNPs, most of them seem to be located on the surface of the polymeric matrix. This is conclusive evidence of the role of DEE for the final distribution of the NPs prepared by DEEIMS and that H_2 is not responsible for the reduction metal ions when NaBH_4 is used as reducing agent.

3.2.2 DEEIMS of Au-FMNPs using anionic NPs-precursor.

MNPs precursors are usually found in cationic form. The feasibility of anionic MNPs precursors depends on finding the corresponding stable chemical form, which are commonly found as chloride anionic complexes (e.g. PdCl_4^- , AuCl_4^-) Using AuCl_4^- as Au-NPs precursor, the loading stage of DEEIMS is presented in Equation 3.9 The

reducing stage using NaBH_4 is presented in Equation 3.10 and when using AA as reducing agent in Equation 3.11.



The effectiveness of loading stage is evidenced by the results of Au content in the BFNCs. For both reducing agents, the average Au content value is $113\text{mgAu} \times \text{g}^{-1}$ BFNC corresponding to 82% of efficiency of the loading stage. Macroscopic observation of these Au containing BFNCs showed colour difference: reddish for the ones prepared with NaBH_4 and blue for the ones prepared with AA.

This observation is a clear example of the effect of changes caused by nanometre scale of materials. Bulk gold presents yellow colour; but when gold is subdivided into smaller and smaller particles, the ratio of the radius to the wavelength becomes important, and when the particle is smaller than the wavelength, the different light wavelengths absorbed by the particle; the different colours they present. When Au-NPs are small their colour is red, due to their strong absorption of green light at about 520 nm, corresponding to the frequency at which a plasmon resonance occurs. As the size increases, the plasmon resonance changes causing the variation of the visible colour of the Au-NPs. (from red to blue and purple)^{37,38} Figure 3.7 presents HR-SEM images and size distribution histograms for Au-NPs synthesized by DEEIMS using both NaBH_4 (Figures 3.7A and 3.7B) and AA (Figures 3.7C and 3.7D) as reducing agents.

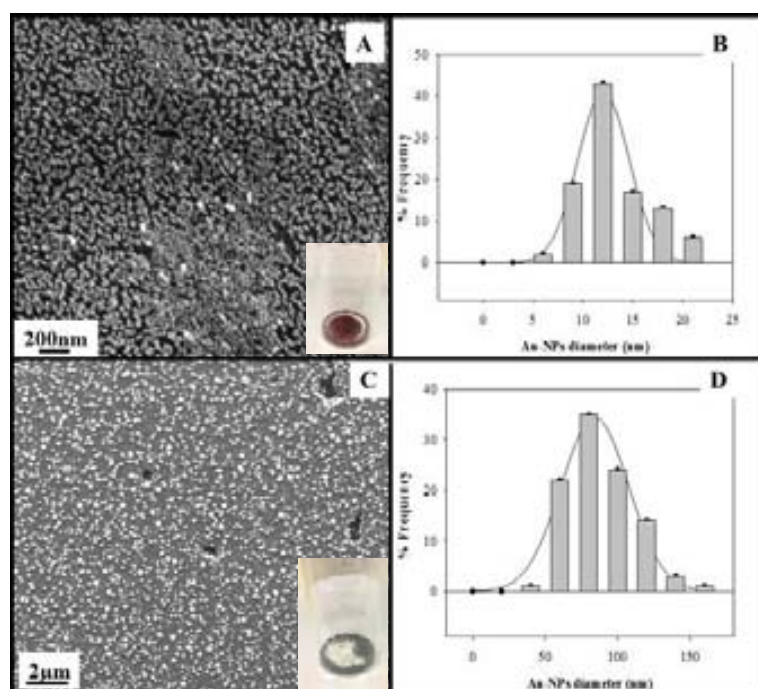


Figure 3.7: HR-SEM image and size distribution histogram of Au FMNPs on anionic gel – type polymer A, B) IMS using NaBH_4 as reducing agent. C,D) IMS using AA as reducing agent. Non evidence of agglomeration is observed in neither case.

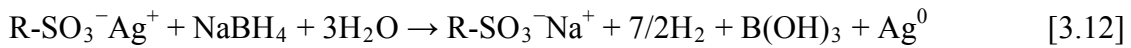
The size distribution histograms show that Au-NPs synthesized with NaBH_4 have an average diameter of 12.0 ± 0.8 nm; meanwhile the Au-NPs synthesized with AA have an average diameter of 79 ± 3 nm. These sizes explain the difference of macroscopic colour of the Au-NPs containing BFNCs.

The size difference between alternative routes of DEIMS depends on the strength of the reducing agent used in the NPs formation stage, summed to the stabilization offered by the supporting matrix. A strong reducing agent ensures that the particles obtained are smaller and monodisperse than the ones obtained when using a weaker reducing agent.³⁶ The reduction rate of NaBH_4 is so much faster than the one from AA. That faster rate produces a large number of NPs and may inhibit aggregation mechanisms (this added to the stability offered by polymeric matrix). In order to produce larger particles, the number of NPs nuclei should be low; thus the NPs growth is related at the expense of the remaining metal ions in solutions that could be reduced.^{39,40}

3.3 DEEIMS of Ag-FMNP s on gel-type cationic polymer using AA and NaBH₄ as reducing agents.

As discussed before, DEEIMS for cationic exchangers is based on the initial loading stage of cationic MNPs precursors (Equation 3.3), followed by the use of a negatively charged reducing agent during the second stage. Thus, the reducing agent bears the same charge of the functional groups of the cationic exchanger (e.g. sulfonic).

The borohydride anions also bear negative charges and therefore, cannot deeply penetrate inside the matrix due to the action of electrostatic repulsion (DEE). The depth of their penetration inside the matrix is balanced by the sum of two driving forces acting in the opposite directions: 1) the gradient of borohydride concentration and 2) the DEE¹⁹. The action of the second force limits deep penetration of borohydride anions into the matrix so that Equation 3.12 proceeds in the surface zone of the polymer what results in the formation of MNPs mainly near the surface of the matrix. The Ag-NPs distribution obtained by this synthetic route is shown in Figures 3.8A and 3.8B. The Ag content obtained by this procedure is 200mg Ag x g⁻¹ BFNC corresponding to 88% of effective loading stage.



Consequently with the results obtained for anionic DEEIMS with NaBH₄; the effective role of the reduction due to BH₄⁻ and not because of the released H₂ should be proved. Therefore the second stage of DEEIMS was carried out using AA as reducing agent as shown in Equation 3.13. Figures 3.8C and 3.8D present the Ag-NPs distribution obtained by this methodology. Moreover, the Ag content obtained by this route is 190 mg Ag x g⁻¹ BFNC for 84% of effective loading stage.



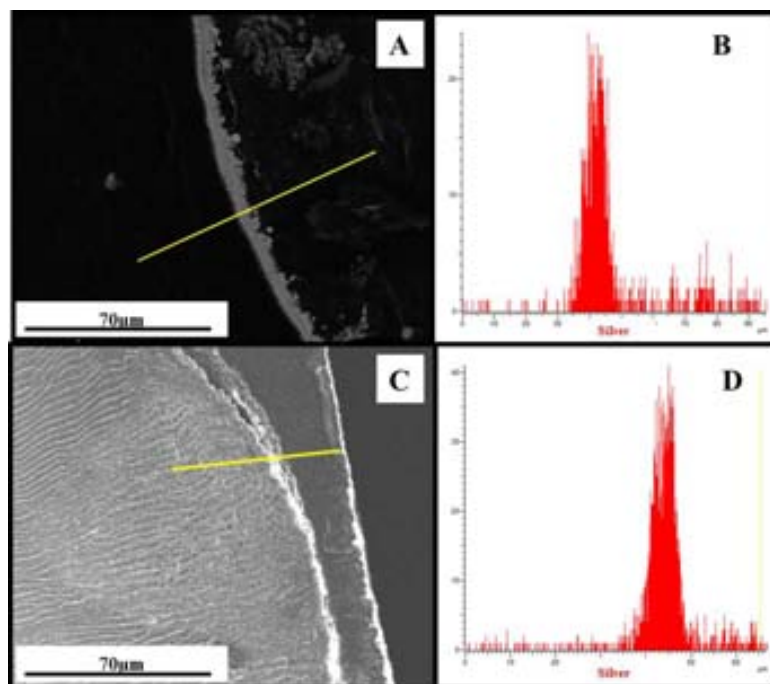


Figure 3.8: Ag-FMNPs distribution mainly on surface on gel-type cation-exchanger due to IMS. A,B) Cross section and LineScan using NaBH_4 as reducing agent C,D) Cross section and EDS LineScan using AA as reducing agent

As it could be seen from Figure 3.8, it is clear that this version of DEEIMS results on the situation of FMNPs on the surface of the obtained NC materials, providing the most favourable distribution that substantially enhances their practical applications such as bactericide assays and water treatment.^{11,25,41,42}

Size distribution histograms present in Figure 3.9, were calculated in order to prove if the in cationic matrices is evident as well the difference in Ag-NPs diameter because of the reducing agent used to prepared them.

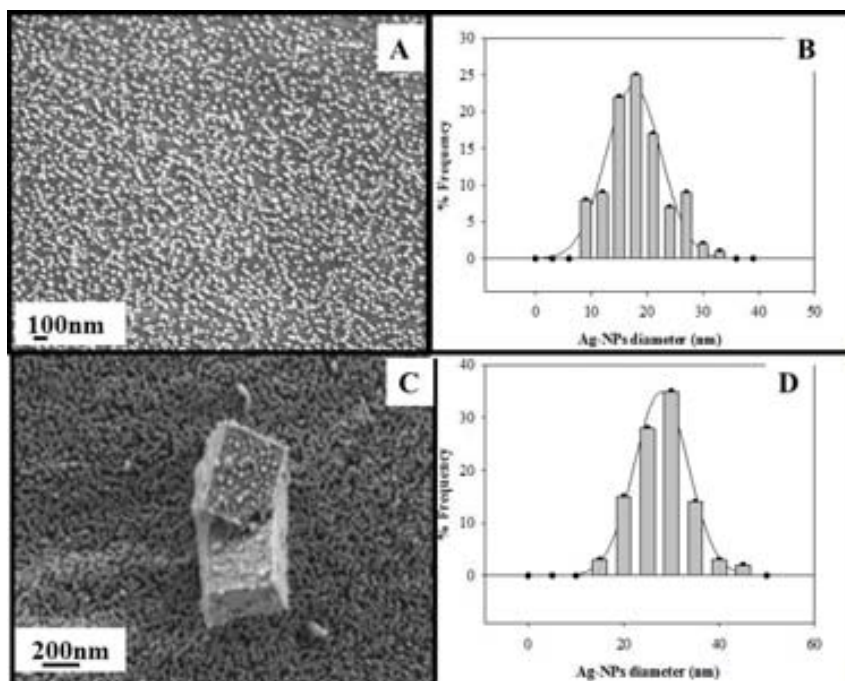


Figure 3.9: HR-SEM image and size distribution histogram of Au FMNPs on cationic gel – type polymer A, B) IMS using NaBH_4 as reducing agent. C, D) IMS using AA as reducing agent. No agglomeration is observed in both cases.

The average diameter obtained for the Ag-NPs prepared with NaBH_4 is 16.8 ± 0.9 nm. For the Ag-NPs prepared with AA the average value is 28.1 ± 0.9 nm. Even though the difference is not as big as the one observed in the analogous anionic system; these values are conclusive to say that the use of AA leads to obtain BFNCs with larger Ag-NPs, due to the slow rate redox process.

In despite of the reducing agent used, surface SEM analysis of these Ag-NPs containing BFNCs showed clear morphological changes (see Figure 3.10). The changes in morphology of the polymer surface are caused by a strong interaction of Ag-NPs with the polymer matrix. These morphological changes are associated with the inter-polymer mechanical stress, resulting from a strong interaction between Ag-NPs and the gel-type polymer chains.¹¹

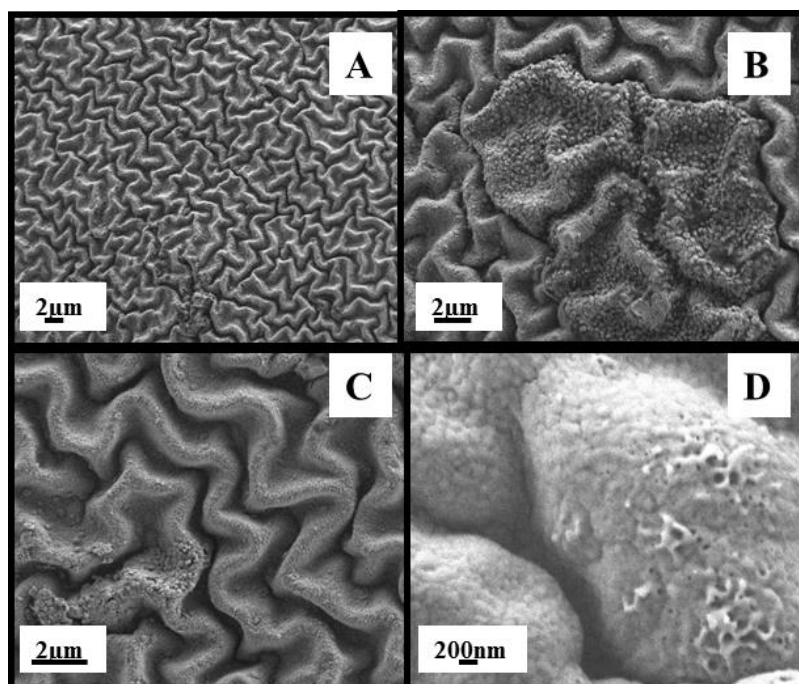


Figure 3.10: HR-SEM images of surface morphology changes on cationic gel-type ion-exchanger due to IMS of Ag-FMNPs. Magnification of D>>C>>B>>A.

In addition to the appearance of nanoporosity on the surface of this gel-type polymers; some regular shape defined silver nano and microstructures were found with further SEM characterization. DEEIMS on this cationic gel – type polymer produces well distributed Ag-NPs with no evident agglomerates. This fact summed to the morphological surface changes and the stabilization offered by the matrix itself; may explain the feasibility of this technique to obtain well defined silver structures; shown in Figure 3.11

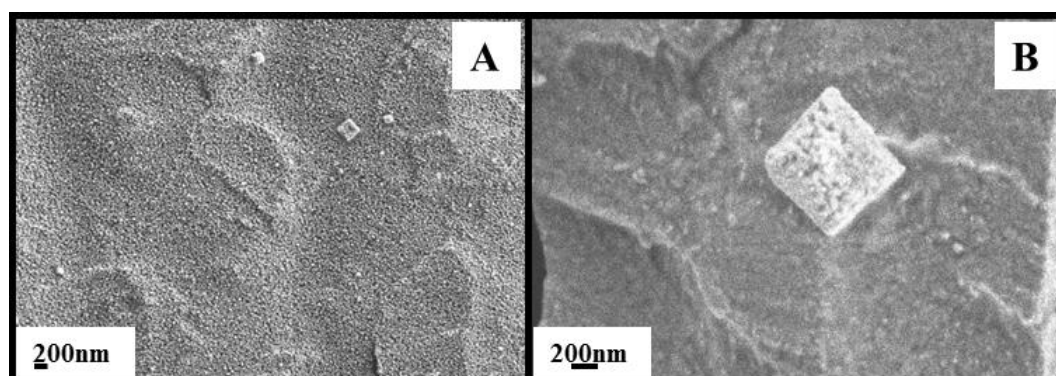


Figure 3.11: HR-SEM images of Ag-FMNPs on gel-type cationic polymer showing appearance of micro-cubic structures. Magnification of B>>A.

3.3.1 Enhanced DEEIMS of Ag nano- and microstructures on cationic gel type polymers.

More recently, the importance of well-defined particles and structures (from nanometres to several micrometres), has been recognized in numerous applications, including ceramics, pigments, catalysts, electronics biological labelling, and catalysis.^{40,43} Common methods for size control employ capping agents such as surfactants, ligands, polymers, or dendrimers, to confine the growth in the nanometer scale.⁴⁴

There are no accepted mechanisms to explain how shape control works, but much of the efforts are currently devoted to the controlled growth of metal nanoparticles of different morphologies and the chemical mechanisms behind the generation of particle shapes.⁴⁵ Despite this, the morphology control of NP formation can be achieved by changing experimental parameters, which include the concentration of reactants, temperature, pH and the addition of crystal seeds, stabilizers, oxidation/reduction agents, stirring rate, polymeric supports and others.

NP shape control is a complex process requiring a fundamental understanding of the interactions between solid state chemistry, interfacial reactions and kinetics in which crystal growth must be balanced. For the case of BFNCs prepared by DEEIMS, it seems that the stability product to the polymer matrix (steric stabilization), the electrostatic stability due to the ion exchange groups and the oxidized form of the reducing agents binding to the particle surface; prevent aggregation.³⁶

Part of the challenge is the environmentally friendly particle morphological controlled by DEEIMS in solid phase. BFNCs with directional properties are opening new horizons in material science. Structural, optical, and electrical properties can be greatly augmented by the fabrication of composite materials with anisotropic microstructures or with anisotropic particles uniformly dispersed in an isotropic matrix. Dispersion can be seen as a favourable distribution over the support surface, and this is one of the advantages of DEEIMS^{46,47}

The growth of nanocrystals could be controlled by the diffusion of particles as well as the reaction at the surface.⁴⁸ For DEEIMS for cationic exchangers, the NP precursor loading stage is a fixed step which depends on the ion exchange properties of

the matrix. Therefore, the step that can be tuned is the NPs appearance during stage 2 of DEEIMS when the reaction with the reducing agent takes place. Thus; stage 2 of DEEIMS of Ag-NPs was slightly modified in terms of reducing agent concentration and stirring rates in order to optimize the preparation of Ag nano- and microstructures.

Figure 3.12 presents a schematic representation of structure growing through DEEIMS on cationic gel-type polymer.

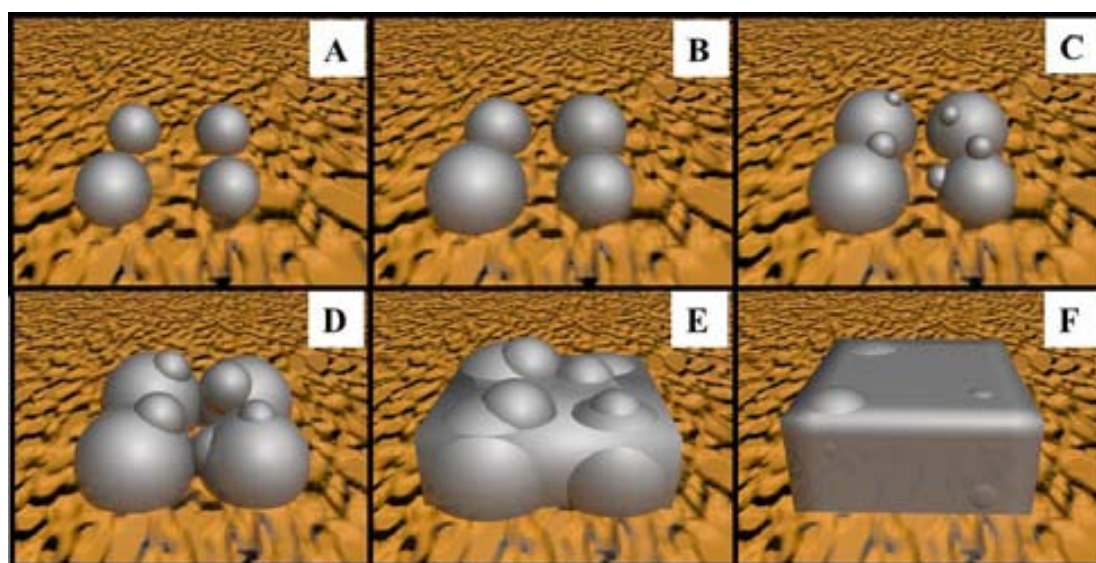


Figure 3.12: Schematic representation of formation of Ag-cubic structures on surface of gel-type cationic polymer by DEEIMS.

Seed-Mediated Growth Approach is on proposed methodology to be customized for Shape-Controlled DEEIMS. It consists in the reduction of cations by a strong reducing agent (e.g. NaBH_4) at room temperature and aqueous solution.⁴⁴ The adapted key steps for nano- and microstructure preparation by DEEIMS would be⁴⁹: 1) Control of nucleation and size into nanometric scale (role of reducing agent). 2) Stirring rate during reduction stage and 3) presence of determined stabilizers (supporting matrix). Regarding this, the optimization of DEEIMS of what seem to be cubic structures; the concentration of NaBH_4 and AA were changed in parallel experiments (0.01M, 0.05M and 0.1M) in order to screen the Ag structure formation. Thus, stirring and addition rate ($2 \text{ mL} \times \text{min}^{-1}$) were kept constant in all experiments.

Considering the strong reducing power of NaBH_4 , samples corresponding to different redox time were characterized by SEM (Figure 3.13). As it can be seen, the morphological changes summed to the effect of stability of the supporting matrix, the small nuclei formation trend of NaBH_4 evidence different stages of the formation of Ag structures.

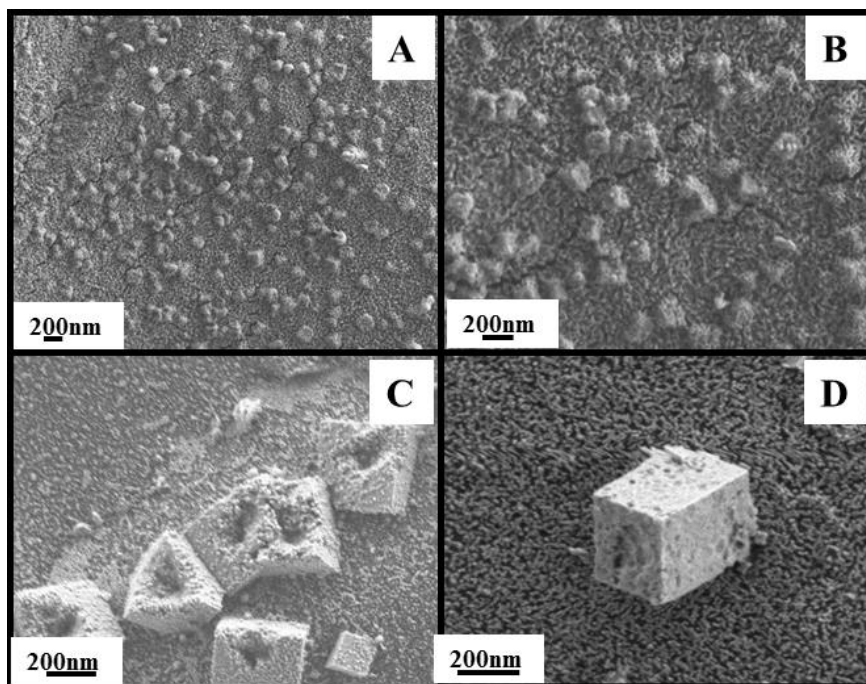


Figure 3.13: HR-SEM images of different stages of the formation of Ag-cubic structures on gel-type cationic polymer using 0.01M NaBH_4 as reducing agent during DEEIMS:

More shape – defined Ag structures with more favourable distribution were obtained when changing the NaBH_4 concentration to 0.05M as can be seen in Figure 3.14

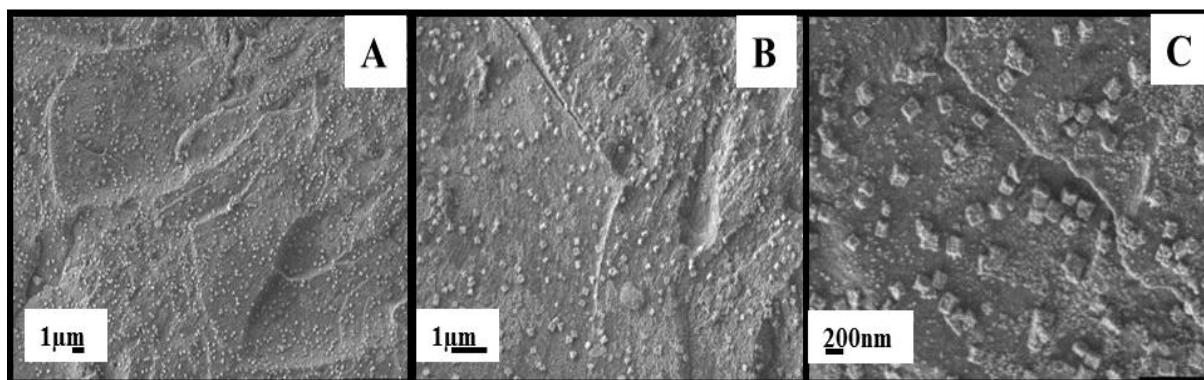


Figure 3.14: HR-SEM images showing favourable distribution and homogenous size of optimized IMS of Ag-cubic structures with 0.05M NaBH_4 as reducing agent. Magnification $C \gg B \gg A$.

Considering the previous results dealing the size difference of Ag-NPs obtained with AA; it was expectable to obtain larger structures when this weaker reducing agent was used. Figure 3.15 shows different stages in the growing of Ag microstructures prepared by DEEIMS with AA.

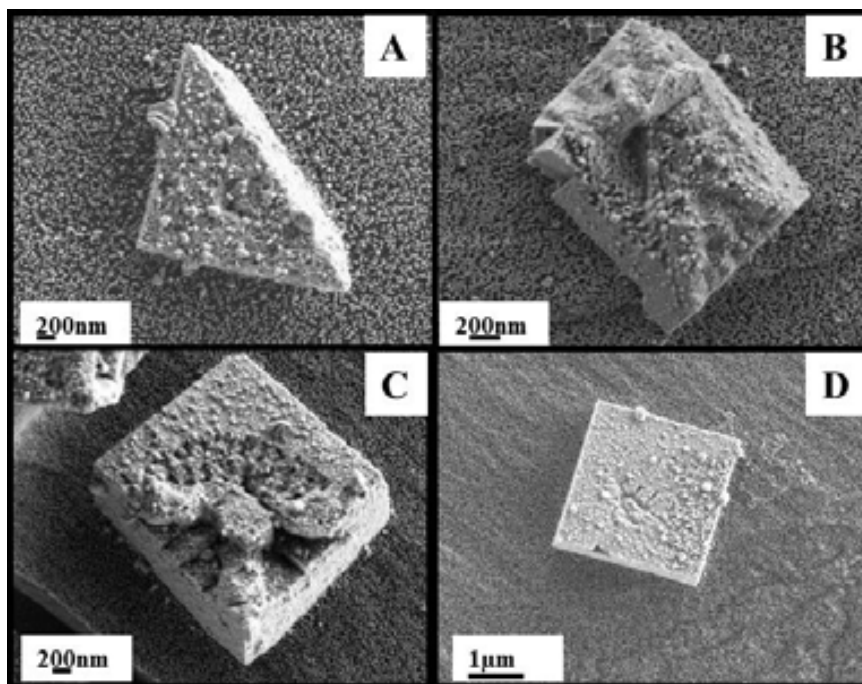


Figure 3.15: HR-SEM images of different stages of the formation of Ag-cubic structures on gel-type cationic polymer using AA as reducing agent during DEEIMS:

SEM images showed wide different size values of the Ag structures obtained by both procedures. Size distribution histograms presented in Figure 3.16 confirm once again that NaBH_4 strong reducing power is enough driven force to prepare so much smaller shape-defined Ag structures ($149 \pm 4 \text{ nm}$) than the ones that were prepared using AA under the same experimental conditions. ($1261 \pm 9 \text{ nm}$)

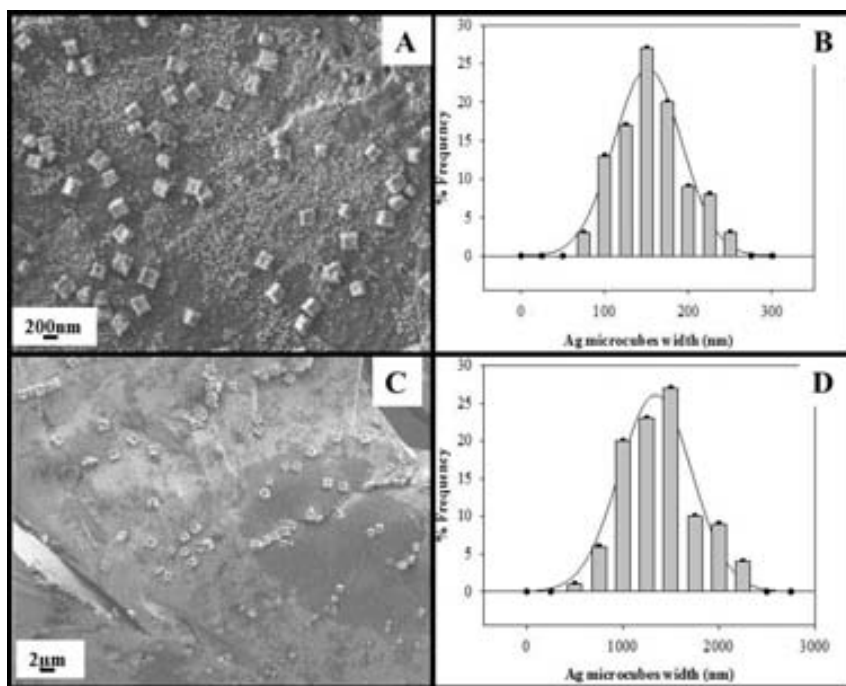


Figure 3.16: HR-SEM images and size distribution histograms of Ag-cub structures synthesized by optimized IMS A, B) with NaBH_4 as reducing agent. C, D) with AA as reducing agent. No agglomeration evidence is observed in neither case.

In order to verify the chemical identity of the structures obtained, EDS analysis were performed in several samples. Figure 3.17 shows the concluding silver presence in the cubic structures obtained by shape – controlled DEEIMS.

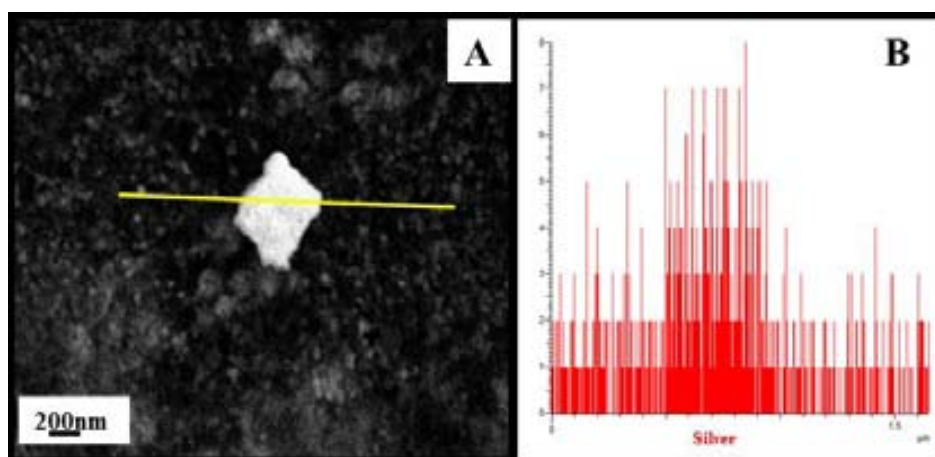


Figure 3.17: A) HR-SEM image and B) EDS-LineScan of Ag-cubic structure showing distribution profile for Ag.

3.3.2 Preparation of AgAu microstructures by DEEIMS-galvanic replacement technique.

DEEIMS has proved to be a suitable methodology for the shape-controlled preparation of nano- and microstructures in BFNCs. Further approach of DEEIMS would be the preparation of hybrid bimetallic microstructures with controlled hollow interior and shell thickness by taking advantage of the different chemical activities of components of the hybrid structures.^{50,51}

Due to their large surface area and low density, hollow structures research has special interest to the potential application of these materials for fabrication of lightweight structural materials and in promising applications for nanoreactors, drug delivery, and catalysis.⁵¹ Regarding this fact, the synthesis of these hybrid hollow structures could be achieved by extending DEEIMS with a galvanic replacement stage.

Galvanic replacement consists in the deposition of a metal of higher redox potential onto a template NP or structure of a material with a lower redox potential without the need of a reducing agent. A suitable galvanic replacement pair would be Au ($E_{\text{Au}^{3+}/\text{Au}} = 1.31\text{V}$) and Ag ($E_{\text{Ag}^+/\text{Ag}} = 0.80\text{V}$). The difference in redox potentials drives the oxidation of the template material by the metal salt precursor of the metal being reduced. This process has been used to prepare hollow bimetallic nanostructures of a range of shapes and compositions.^{52,53} This methodology makes possible to obtain metallic selective films with high purity and its reaction rate increases with temperature.⁵⁴

As it was previously discussed, DEEIMS of Ag-cubic nano- and microstructures was optimized in terms of size homogeneity and distribution. Therefore, these shaped-controlled structures can be used as sacrificial templates for the preparation of AgAu bimetallic structures; as Ag and Au are suitable for galvanic replacement.^{53,55}

The feasible features of the hybrid structures can be customized by tailoring the diffusion of ions (seen as accessibility of atoms), and the process can be followed *in situ* by monitoring the plasmonic behaviour. This can be done by handling the reagent addition and stirring rates, these two aspects seem to be beneficial to the characteristics of the coating, by improving uniformity and roughness which both depend on the templates.⁵⁴

Thus, the optimized DEEIMS of Ag-cubic nano- and microstructures makes feasible to use them as templates for the preparation of shaped-controlled AgAu structures. Galvanic replacement of Ag to Au arises to almost 100% effectivity. As for our interest is the preparation of bi-metallic AgAu structures, the amount of Au added should be the right to keep Ag⁰ from the original structure. Figure 3.18 and Equation 3.14 describe the galvanic replacement of Ag to Au for the preparation of AgAu microstructures.

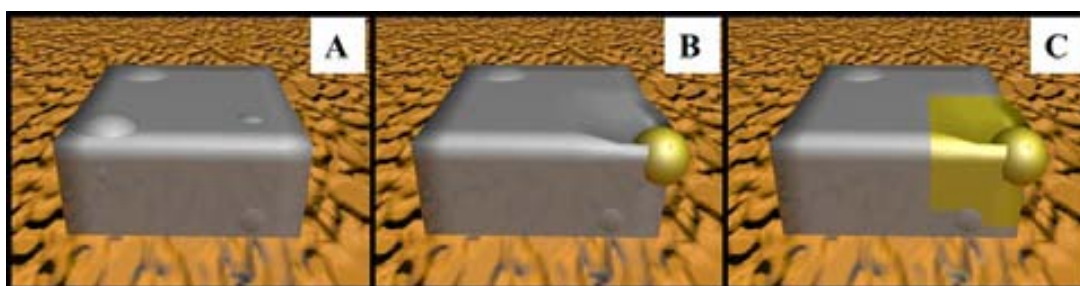


Figure 3.18: Schematic representation of galvanic replacement of Ag to Au for DEEIMS of AgAu-cubic structures.



The screening of the process can be seen in Figure 3.19. It seems that galvanic replacement of Ag to Au acts on the Ag-cubic structures causing the appearance of holes and sort of channels in them; due to the deposition of Au and the oxidation of Ag from the initial template.

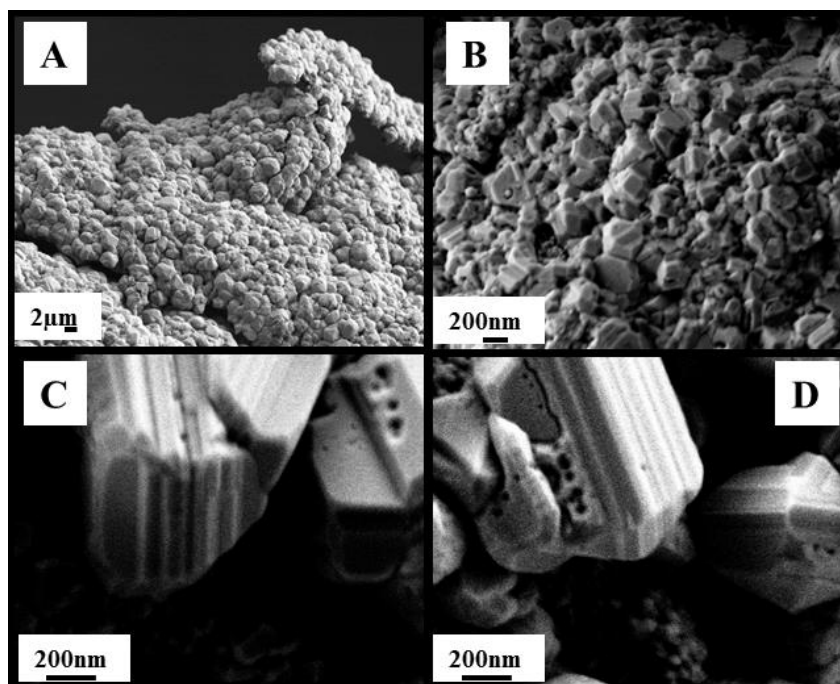


Figure 3.19: HR-SEM images of Ag-cubic structures (A, B) and consequent evidence of hollowed AgAu structures due to galvanic replacement of Ag to Au (C, D).

The appearance of these holes can be explained by the Kirkendall effect, which in this case refers to the phenomenon of a drift of interface between a diffusion of the reduced Au and the oxidized Ag; as shown schematically in Figure 3.20. The confined space of the nano- and microstructures enabled the collapse of vacancies to generate homogeneous cavities inside the templates and mostly retained the monodispersity of the original Ag-cubic structures.⁵⁰

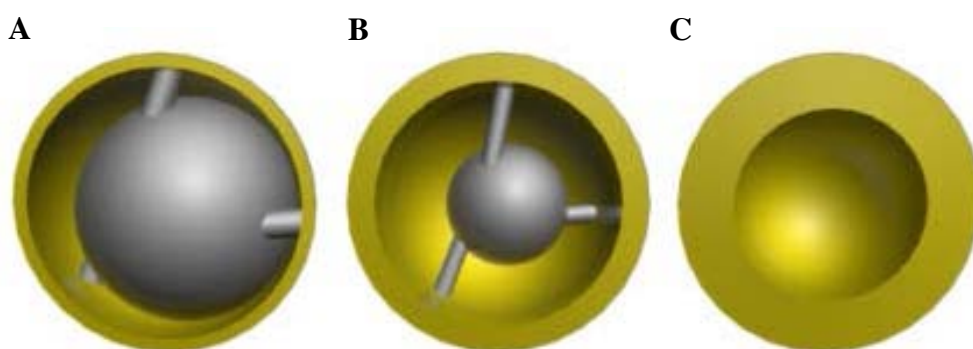


Figure 3.20: Schematic representation of consecutive stages of Kirkendall Effect during the galvanic effect of Ag (grey colour) to Au (gold colour) for the preparation of hollowed NPs.

Therefore, combining the galvanic replacement of Ag to Au with the subsequent Kirkendall Effect, the overall process involves two steps: deposition of the Au on the Ag template and interdiffusion of atomic species of both components into the new hybrid hollowed material. During the galvanic replacement, the outward diffusion of Ag is much faster through the layer than the inward Au diffusion leading to the formation of a nanoscale void in the centre of the structure.⁵¹ EDS analysis of AgAu hybrid structures showed the distribution profile of Ag and Au, verifying the location of Au in the upper zone of structure. Moreover, SEM characterization shows favourable space distribution of the AgAu –cubic structures, which metal content analysis is 102 mgAg x g⁻¹ BFNC and 59 mg Au x g⁻¹ BFNC. These metal content results show decrease in Ag content in the NC and an effective Au loading by galvanic replacement reaching 95% of yield.

It is important to highlight that DEEIMS-galvanic replacement procedure is a suitable way to synthesize Au-NPs on cationic matrices, using low cost “sacrificial” NPs (e.g. Cu-NPs).

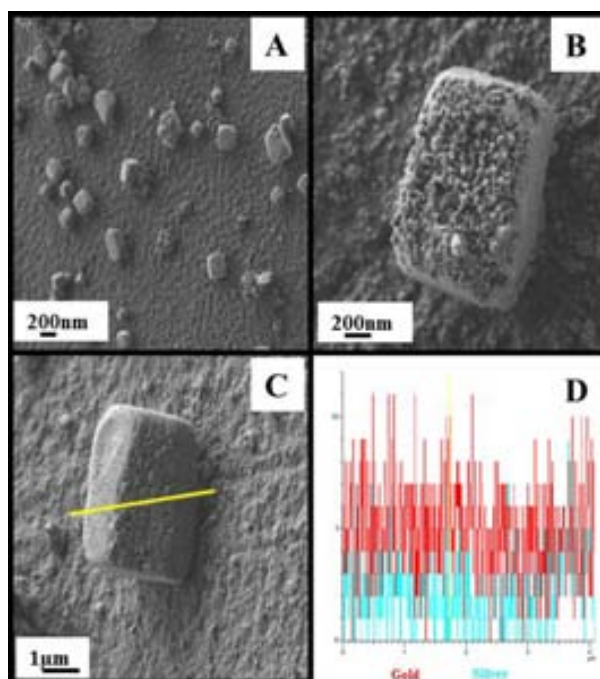


Figure 3.21: HR-SEM images (A, B, C) and EDS-LineScan (D) for AgAu-cubic structures synthesized by DEEIMS.

3.4 Concluding Remarks:

DEEIMS has proved to be a suitable synthetic methodology for the preparation of BFNCs with tuned NPs distribution depending on the reducing agent used; proving that DEE has a determinant role during the NPs appearance. Moreover, controlling the rate of reduction stage, shaped – controlled DEEIMS of Ag – cubic nano- and microstructures is achieved. These Ag-cubic structures are used as templates for the preparation of AgAu – cubic microstructures by the extension of DEEIMS with a galvanic replacement stage.

References:

- (1) Yao, J.; Yang, M.; Duan, Y. Chemistry, Biology, and Medicine of Fluorescent Nanomaterials and Related Systems: New Insights into Biosensing, Bioimaging, Genomics, Diagnostics, and Therapy. *Chem. Rev.* **2014**.
- (2) Savage, N.; Diallo, M. S.; Duncan, J.; Street, A.; Sustich, R. *Nanotechnology Applications for Clean Water*; First.; William Andrew Inc: Nueva York, 2009.
- (3) Morose, G. The 5 Principles of “Design for Safer Nanotechnology.” *J. Clean. Prod.* **2010**, *18*, 285–289.
- (4) Dahl, J. a; Maddux, B. L. S.; Hutchison, J. E. Toward Greener Nanosynthesis. *Chem. Rev.* **2007**, *107*, 2228–2269.
- (5) Gubin, S. P. Magnetic Nanoparticles. **2009**.
- (6) Akamatsu, K.; Shinkai, H.; Ikeda, S.; Adachi, S.; Nawafune, H.; Tomita, S. Controlling Interparticle Spacing among Metal Nanoparticles through Metal-Catalyzed Decomposition of Surrounding Polymer Matrix. *J. Am. Chem. Soc.* **2005**, *127*, 7980–7981.
- (7) Nicolais, L.; Carotenuto, G. *Metal-Polymer Nanocomposites*; A JOHN WILEY & SONS, INC: New Jersey, 2005.
- (8) Ozkan, U. *Design of Heterogeneous Catalysts*; Wiley-VCH Verlag GmbH & Co. KGaA, 2009.
- (9) Ruiz, P.; Muñoz, M.; Macanás, J.; Muraviev, D. N. Intermatrix Synthesis of Polymer–Copper Nanocomposites with Tunable Parameters by Using Copper Comproportionation Reaction. *Chem. Mater.* **2010**, *22*, 6616–6623.

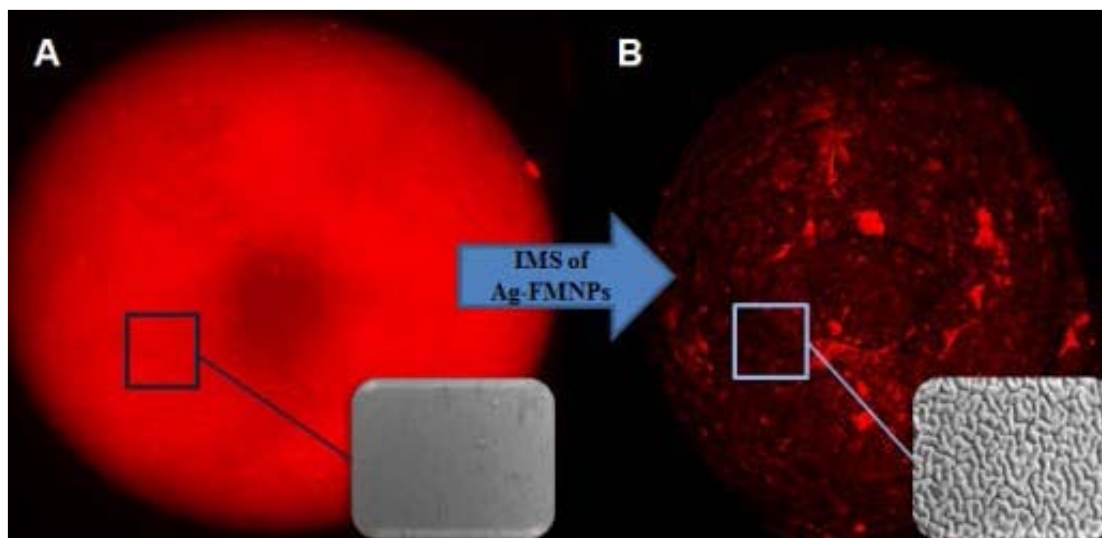
- (10) Bastos-Arrieta, J.; Shafir, A.; Alonso, A.; Muñoz, M.; Macanás, J.; Muraviev, D. N. Donnan Exclusion Driven Intermatrix Synthesis of Reusable Polymer Stabilized Palladium Nanocatalysts. *Catal. Today* **2012**, *193*, 207–212.
- (11) Bastos-Arrieta, J.; Muñoz, M.; Ruiz, P.; Muraviev, D. N. Morphological Changes of Gel-Type Functional Polymers after Intermatrix Synthesis of Polymer Stabilized Silver Nanoparticles. *Nanoscale Res. Lett.* **2013**, *8*, 255.
- (12) Ruiz, P.; Macanás, J.; Muñoz, M.; Muraviev, D. N. Intermatrix Synthesis: Easy Technique Permitting Preparation of Polymer-Stabilized Nanoparticles with Desired Composition and Structure. *Nanoscale Res. Lett.* **2011**, *6*, 343.
- (13) Ruiz, P.; Muñoz, M.; Macanás, J.; Turta, C.; Prodius, D.; Muraviev, D. N. Intermatrix Synthesis of Polymer Stabilized Inorganic Nanocatalyst with Maximum Accessibility for Reactants. *Dalton Trans.* **2010**, *39*, 1751–1757.
- (14) Domènech, B.; Muñoz, M.; Muraviev, D. N.; Macanás, J. Polymer-Stabilized Palladium Nanoparticles for Catalytic Membranes: Ad Hoc Polymer Fabrication. *Nanoscale Res. Lett.* **2011**, *6*, 406.
- (15) Kao, J.; Thorkelsson, K.; Bai, P.; Rancatore, B. J.; Xu, T. Toward Functional Nanocomposites: Taking the Best of Nanoparticles, Polymers, and Small Molecules. *Chem. Soc. Rev.* **2013**, *42*, 2654–2678.
- (16) Puttamraju, P.; SenGupta, A. K. Evidence of Tunable On–Off Sorption Behaviors of Metal Oxide Nanoparticles: Role of Ion Exchanger Support. *Ind. Eng. Chem. Res.* **2006**, *45*, 7737–7742.
- (17) Levenstein, R.; Hasson, D.; Semiat, R. Utilization of the Donnan Effect for Improving Electrolyte Separation with Nanofiltration Membranes. **1996**, *116*, 77–92.
- (18) Cumbal, L.; SenGupta, A. K. Arsenic Removal Using Polymer-Supported Hydrated Iron(III) Oxide Nanoparticles: Role of Donnan Membrane Effect. *Environ. Sci. Technol.* **2005**, *39*, 6508–6515.
- (19) Donnan, F. G. Theory of Membrane Equilibria and Membrane Potentials in the Presence of Non-Dialysing Electrolytes. A Contribution to Physical-Chemical Physiology. *J. Memb. Sci.* **1995**, *100*, 45–55.
- (20) Elliott, S. D.; Moloney, M. P.; Gun'ko, Y. K. Chiral Shells and Achiral Cores in CdS Quantum Dots. *Nano Lett.* **2008**, *8*, 2452–2457.
- (21) Petryayeva, E.; Algar, W. R.; Medintz, I. L. Quantum Dots in Bioanalysis: A Review of Applications across Various Platforms for Fluorescence Spectroscopy and Imaging. *Appl. Spectrosc.* **2013**, *67*, 215–252.
- (22) Moloney, M. P.; Gun'ko, Y. K.; Kelly, J. M. Chiral Highly Luminescent CdS Quantum Dots. *Chem. Commun. (Camb)*. **2007**, 7345, 3900–3902.

- (23) Bera, D.; Qian, L.; T seng, T.-K.; Holloway, P. H. Quantum Dots and Their Multimodal Applications: A Review. *Materials (Basel)*. **2010**, *3*, 2260–2345.
- (24) Lu, A.-H.; Salabas, E. L.; Schüth, F. Magnetic Nanoparticles: Synthesis, Protection, Functionalization, and Application. *Angew. Chem. Int. Ed. Engl.* **2007**, *46*, 1222–1244.
- (25) Alonso, A.; Muñoz-Berbel, X.; Vigués, N.; Rodríguez-Rodríguez, R.; Macanás, J.; Mas, J.; Muñoz, M.; Muraviev, D. N. Intermatrix Synthesis of Monometallic and Magnetic Metal/metal Oxide Nanoparticles with Bactericidal Activity on Anionic Exchange Polymers. *RSC Adv.* **2012**, *2*, 4596–4599.
- (26) Sau, T. K.; Rogach, A. L. Nonspherical Noble Metal Nanoparticles: Colloid-Chemical Synthesis and Morphology Control. *Adv. Mater.* **2010**, *22*, 1781–1804.
- (27) Alonso, A.; Macanás, J.; Safir, A.; Muñoz, M.; Vallibera, A.; Prodius, D.; Melnic, S.; Turta, C.; Muraviev, D. N. Donnan-Exclusion-Driven Distribution of Catalytic Ferromagnetic Nanoparticles Synthesized in Polymeric Fibers. *Dalton Trans.* **2010**, *39*, 2579–2586.
- (28) Alonso, A.; Muñoz-Berbel, X.; Vigués, N.; Macanás, J.; Muñoz, M.; Mas, J.; Muraviev, D. N. Characterization of Fibrous Polymer Silver/cobalt Nanocomposite with Enhanced Bactericide Activity. *Langmuir* **2012**, *28*, 783–790.
- (29) Akamatsu, K.; Adachi, S.; Tsuruoka, T.; Ikeda, S.; Tomita, S.; Nawafune, H. Nanoparticles with Controlled Microstructures. **2008**, 3042–3047.
- (30) Akamatsu, K.; Fujii, M.; Tsuruoka, T.; Nakano, S.; Murashima, T.; Nawafune, H. Mechanistic Study on Microstructural Tuning of Metal Nanoparticle/Polymer Composite Thin Layers: Hydrogenation and Decomposition of Polyimide Matrices Catalyzed by Embedded Nickel Nanoparticles. *J. Phys. Chem. C* **2012**, *116*, 17947–17954.
- (31) Chou, K.-S.; Lu, Y.-C.; Lee, H.-H. Effect of Alkaline Ion on the Mechanism and Kinetics of Chemical Reduction of Silver. *Mater. Chem. Phys.* **2005**, *94*, 429–433.
- (32) Songping, W.; Shuyuan, M. Preparation of Ultrafine Silver Powder Using Ascorbic Acid as Reducing Agent and Its Application in MLCI. *Mater. Chem. Phys.* **2005**, *89*, 423–427.
- (33) Domènech, B.; Muñoz, M.; Muraviev, D. N.; Macanás, J. Uncommon Patterns in Nafion Films Loaded with Silver Nanoparticles. *Chem. Commun. (Camb)*. **2014**, *50*, 4693–4695.
- (34) Muraviev, D.; Macanas, J.; Farre, M.; Munoz, M.; Alegret, S. Novel Routes for Inter-Matrix Synthesis and Characterization of Polymer Stabilized Metal Nanoparticles for Molecular Recognition Devices. *Sensors Actuators B Chem.* **2006**, *118*, 408–417.

- (35) Domènech, B.; Muñoz, M.; Muraviev, D. N.; Macanás, J. Catalytic Membranes with Palladium Nanoparticles: From Tailored Polymer to Catalytic Applications. *Catal. Today* **2012**, *193*, 158–164.
- (36) Personick, M. L.; Mirkin, C. a. Making Sense of the Mayhem behind Shape Control in the Synthesis of Gold Nanoparticles. *J. Am. Chem. Soc.* **2013**, *135*, 18238–18247.
- (37) Ghosh, S. K.; Pal, T. Interparticle Coupling Effect on the Surface Plasmon Resonance of Gold Nanoparticles: From Theory to Applications. *Chem. Rev.* **2007**, *107*, 4797–4862.
- (38) An, C. J.; Yoo, H.-W.; Cho, C.; Park, J.-M.; Choi, J. K.; Jin, M. L.; Lee, J.-Y.; Jung, H.-T. Surface Plasmon Assisted High Performance Top-Illuminated Polymer Solar Cells with Nanostructured Ag Rear Electrodes. *J. Mater. Chem. A* **2014**, *2*, 2915.
- (39) Suber, L.; Sondi, I.; Matijević, E.; Goia, D. V. Preparation and the Mechanisms of Formation of Silver Particles of Different Morphologies in Homogeneous Solutions. *J. Colloid Interface Sci.* **2005**, *288*, 489–495.
- (40) Goia, D. V.; Matijević, E. Preparation of Monodispersed Metal Particles. **1998**, 1203–1215.
- (41) Alonso, A.; Vigués, N.; Muñoz-Berbel, X.; Macanás, J.; Muñoz, M.; Mas, J.; Muraviev, D. N. Environmentally-Safe Bimetallic Ag@Co Magnetic Nanocomposites with Antimicrobial Activity. *Chem. Commun. (Camb)*. **2011**, *47*, 10464–10466.
- (42) Alonso, a.; Shafir, a.; Macanás, J.; Vallribera, a.; Muñoz, M.; Muraviev, D. N. Recyclable Polymer-Stabilized Nanocatalysts with Enhanced Accessibility for Reactants. *Catal. Today* **2012**.
- (43) Personick, M. L.; Langille, M. R.; Zhang, J.; Mirkin, C. a. Shape Control of Gold Nanoparticles by Silver Underpotential Deposition. *Nano Lett.* **2011**, *11*, 3394–3398.
- (44) Jana, N. R.; Gearheart, L.; Murphy, C. J. Seed-Mediated Growth Approach for Shape-Controlled Synthesis of Spheroidal and Rod-like Gold Nanoparticles Using a Surfactant Template. *Adv. Mater.* **2001**, *13*, 1389–1393.
- (45) Luque, R.; Balu, A. M.; Campelo, J. M.; Gonzalez-Arellano, C.; Gracia, M. J.; Luna, D.; Marinas, J. M.; Romero, A. A. Tunable Shapes in Supported Metal Nanoparticles: From Nanoflowers to Nanocubes. *Mater. Chem. Phys.* **2009**, *117*, 408–413.
- (46) Adair, J. H.; Suvaci, E. Morphological Control of Particles. *Curr. Opin. Colloid Interface Sci.* **2000**, *5*, 160–167.

- (47) Anastas, P.; Eghbali, N. Green Chemistry: Principles and Practice. *Chem. Soc. Rev.* **2010**, *39*, 301–312.
- (48) Biswas, K.; Varghese, N.; Rao, C. N. R. Growth Kinetics of Gold Nanocrystals: A Combined Small-Angle X-Ray Scattering and Calorimetric Study. *Small* **2008**, *4*, 649–655.
- (49) Jana, N. R. Gram-Scale Synthesis of Soluble, near-Monodisperse Gold Nanorods and Other Anisotropic Nanoparticles. *Small* **2005**, *1*, 875–882.
- (50) Liu, Y.; Goebel, J.; Yin, Y. Templated Synthesis of Nanostructured Materials. *Chem. Soc. Rev.* **2013**, *42*, 2610–2653.
- (51) Wang, W.; Dahl, M.; Yin, Y. Hollow Nanocrystals through the Nanoscale Kirkendall Effect. **2013**.
- (52) Odom, T. W.; Schatz, G. C. Introduction to Plasmonics. *Chem. Rev.* **2011**, *111*, 3667–3668.
- (53) Aherne, D.; Gara, M.; Kelly, J. M.; Gun'ko, Y. K. From Ag Nanoprisms to Triangular AuAg Nanoboxes. *Adv. Funct. Mater.* **2010**, *20*, 1329–1338.
- (54) Carraro, C.; Maboudian, R.; Magagnin, L. Metallization and Nanostructuring of Semiconductor Surfaces by Galvanic Displacement Processes. *Surf. Sci. Rep.* **2007**, *62*, 499–525.
- (55) Njoki, P. N.; Wu, W.; Lutz, P.; Maye, M. M. Growth Characteristics and Optical Properties of Core/Alloy Nanoparticles Fabricated via the Layer-by-Layer Hydrothermal Route. *Chem. Mater.* **2013**, *25*, 3105–3113.

Chapter 4



The modification of gel –type polymers can be carried out with Intermatrix Synthesis technique(IMS) coupled with Donnan Exclusion Effect(DEE) what results in the most favourable distribution of silver nanoparticles near the surface of nanocomposite material. The surface of the cationic polymer-metal nanocomposite is characterised by the worm-like structure due to the interaction of metal nanoparticles with polymer chains. This interaction leads to the formation of nanoporosity in the matrix what enhances its mass-transfer characteristics. Moreover, it has been shown that modification of gel-type ion exchangers with silver nanoparticles essentially does not change the ion exchange properties of the initial polymeric matrix.

4. Evaluation of ion exchange properties and morphology changes due to IMS of Ag-FMNPs on gel -type polymeric matrices.

Intermatrix Synthesis (IMS) technique coupled with the Donnan Exclusion Effect (DEE) provides a n environmentally friendly route for the modification of reactive polymer surfaces with functional metal nanoparticles (FMNPs).¹ Previous reports on the application of IMS for the preparation of polymer-metal Nanocomposites (NCs) proof the most favourable distribution of the FMNPs near the surface of the host polymeric matrix with no evident agglomerates. The results of the modification of gel-type ion exchange polymeric matrices (cationic and anionic) with Ag-FMNPs are presented in this section. As the aim of the application of IMS is obtaining an added value NC material; the initial ion exchange features of the polymeric support are re-evaluated to proof the bifunctionality of these novel polymer-metal NCs (PMNCs).

4.1 Morphological changes on gel-type cationic polymer due to IMS of Ag-FMNPs:

Depending on the final application of interest for these NCs catalytic or bactericide activity, and with the goal to obtain the most favourable distribution of NPs in the polymer, IMS methodology has been coupled with the DEE (DEEIMS). The distribution of FMNPs near the surface of the NC material may be considered as really the most favourable for practical application of NCs of this type as it provides an enhanced access of the substrates (in catalytic applications) or bacteria (in water disinfection) to the FMNPs layer of the NC.

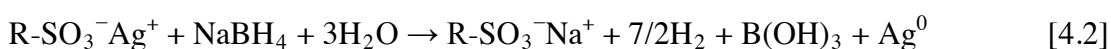
The general DEEIMS of Ag-FMNPs was carried out by loading of the functional groups of 400mg the gel-type sulfonic polymer with Ag^+ by using $0.1 \text{ mol} \times \text{L}^{-1}$ aqueous AgNO_3 solution (20mL) followed by reduction with $0.1 \text{ mol} \times \text{L}^{-1}$ aqueous NaBH_4 . Some kinetic studies were developed by changing metal loading time at stage 1 of IMS. Figure 4.1 shows distribution of Ag-FMNPs in the NC where a desirable metal content

is observed mainly on the polymeric surface; this due to DEEIMS methodology as indicated in the following Equations:

Metal loading stage:



Metal reduction stage



As it is seen from Equation (4.2), the negatively charged borohydride anions (the actual reducing agent) cannot deeply penetrate into the polymeric matrix bearing the charge of the same sign due to the action of DEE. As the result, the reduction of Ag ions leading to the formation of Ag-FMNPs proceeds near the surface of the polymer. As it also follows from the same Equation, the functional groups of the polymer appear to be regenerated in the course of metal reduction, i.e. are converted back into the initial Na-form (see Equation (4.1)). This means that the metal loading reduction cycle can be repeated without any additional pre-treatment of the polymer what has been shown to lead to the increase of FMNPs layer thickness in the NC and consequently an increase in the FMNPs content.^{1,2} The thickness of Ag-FMNPs layer (I.E., FMNPs content) can be also tuned by changing the time of the metal loading stage.

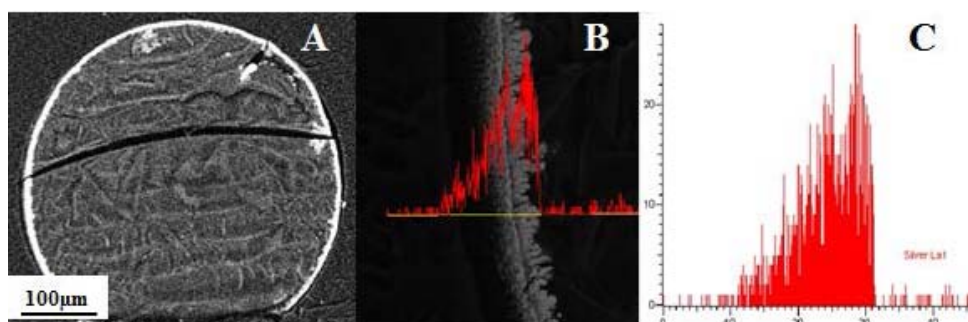


Figure 4.1: (A) High resolution SEM image of NC bead cross section and (B, C) Line Scan EDS spectra showing distribution of Ag-FMNPs (red) in sulfonic gel type cation-exchange resin modified with Ag-FMNPs.

The system FMNPs-Polymer shows a series of interactions that leads to the increase of the stability of the NPs and reduces the possibility of release, reducing as well the environmental impact of these PMNCs. This can be explained by the increase of viscosity of the immobilizing media which in this case is the support matrix (see Equation), and the decrease of the energy of particle-particle interaction in FMNPs systems regarding the MNPs prepared in solution.³

As it is clearly seen in SEM images shown in Figure 4.2, the initially smooth polymer surface (see Figure 4.2A) dramatically changes after IMS of Ag-MNPs (Figure 4.2B and 4.2C) due to appearance of “worm-like” morphology. Note that similar effects were observed by the authors in IMS of Cu-MNPs in other functional gel-type polymers.⁴

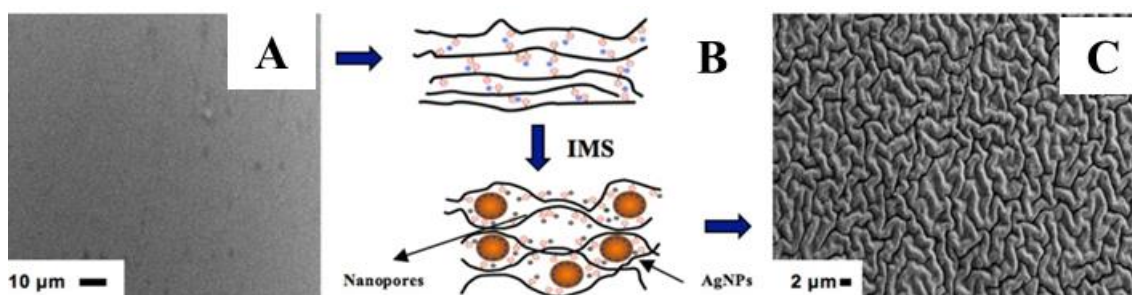


Figure 4.2: Schematic diagram of interaction of FMNPs synthesized inside polymer matrix (B) and SEM images of cationic gel type polymer surface before (A) and after (C) IMS of Ag-FMNPs

A more detailed structure of the PMNC surface is shown on the high-resolution SEM images presented in Figure 4.3. Although the rigidity of cross-linked polymer matrix is far higher than that of their non-cross-linked analogues, one can also expect the appearance of similar morphological changes in the case of DEEIMS of MNPs in the matrices of cross-linked polymers.⁴ As it is seen in Figures 4.3A and 4.3B, after carrying out the metal-loading-reduction cycle (DEEIMS of MNPs) the initially smooth polymer surface changes its morphology due to the appearance of the worm-like structure similar to that observed in the case of non-cross-linked polymers product of IMS of Cu-FMNPs.⁴ As it is also seen in Figures 4.3E and 4.3F, the morphological changes result also in the appearance of nanopores in the gel-type polymer.

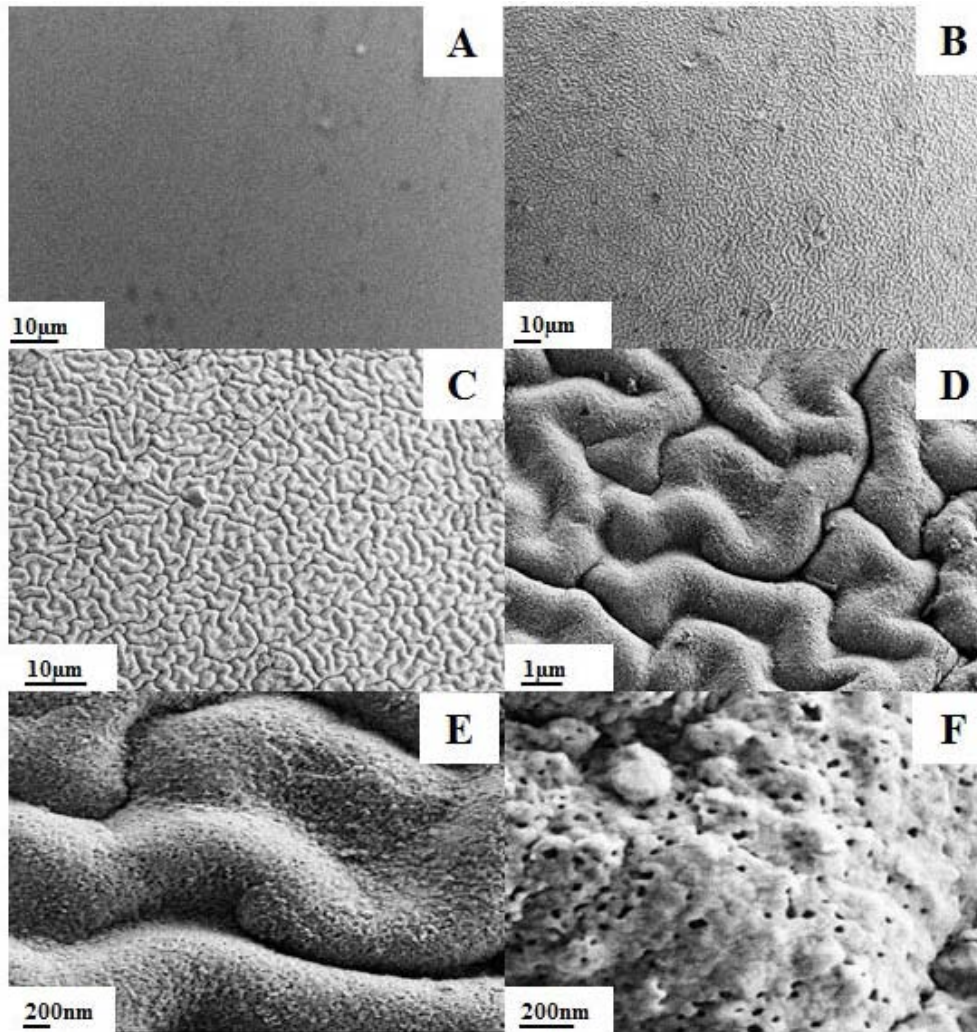


Figure 4.3: High-resolution SEM images of: a) NPs free granulated polymer. b, c, d, e, f): Ag-FMNPs containing polymer with clearly seen as worm-like structure of NC surface and nanopores. Magnification $a = b < c < d < e < f$

As it is clearly seen in Figures 4.1C the majority of Ag-MNPs are located on the polymer surface what results in the appearance of numerous bumps on the initially smooth polymer surface. Moreover, as can be observed in Figure 4.3(C,D,E,F) IMS of Ag-FMNPs on the gel-type polymer results in the appearance of numerous “nanoholes” (nanopores) on the surface of polymer what can be considered as a qualitative confirmation of the results obtained by BET analysis and shown in Table 4.1.

Table 4.1: Increase of pore diameters in Ag-MNPs-containing Purolite C100E resin samples

Sample	Ag-MNPs content, mg/g	BET Average pore diameter, (\bar{I} 0.2 nm)

Raw Gel Type Polyer	0	1.9
Ag- PMNC (5*)	112.7 ± 0.5	2.3
Ag-PMNC (10*)	143.5 ± 0.5	4.4

(*) numbers show the time in minutes of metal-loading cycle carried out.

The appearance of nanoporosity results in turn in increase of the internal surface area what can be one of the factors explaining the excellent performance of these NCs in bactericide as says.^{2,5} The bactericide activity of Ag-FMNPs-cation-exchange polymer NCs with different thickness of Ag-FMNPs layer was tested previously and after 60 minutes contact time the E. Coli activity decreased to zero. Moreover, it has been also shown that the bactericide activity of these NCs does not depend on the thickness of the Ag-FMNPs layer. Therefore, the preparation the layer with the minimum quantity of FMNPs and with the most favourable distribution provides the same bactericide results at lower production cost and time.⁵

The increase of FMNPs content near the surface of the matrix can be considered as an additional diffusional barrier for the ions to be removed by the NC material. However, the formation of FMNPs layer is accompanied by formation of nanopores and increase of the surface area by up to 20% in comparison with the initial.⁶

The thickness of the FMNPs layer on cation exchangers can be tuned and optimized within the metal loading stage of the IMS process. As the performance of these NCs for bactericide water treatment does not depend on the thickness of Ag-FMNPs layer the increase of the amount of silver content in NC appears to be undesirable. An additional argument in favour of this point deals with the better accessibility of the functional groups of the polymer for ions to be removed within a complex water treatment cycle at a minimal FMNPs content.

As it is seen in Figure 4.4, the polymer provides an effective stabilization effect towards Ag-FMNPs so that no visible agglomeration of silver NPs can be observed. This fine distribution of the nanomaterial is a very important feature for the bactericide (and catalytic) applications of NC material.

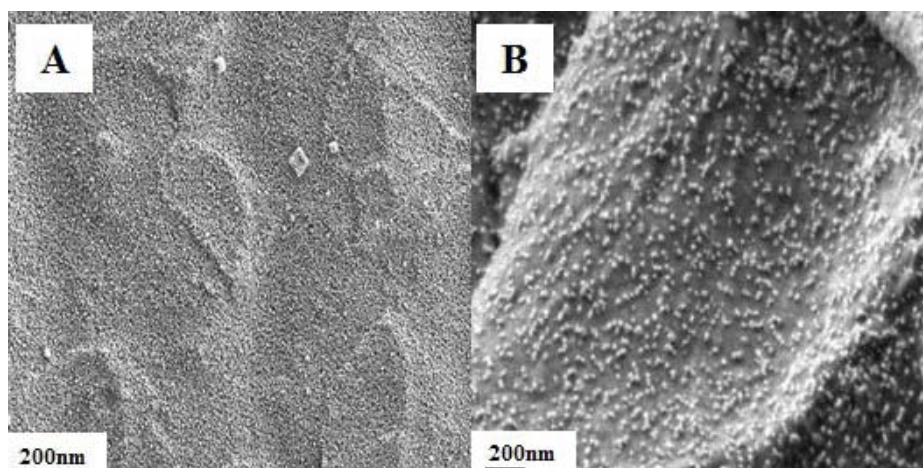


Figure 4.4: High-Resolution SEM images of Ag-FMNPs with an average diameter of 33±1nm on gel type polymer, show distribution of the FMNPs with non-evident agglomerates after surface modification Magnification of b>>>a.

Therefore, optimization of the Ag-FMNPs content by minimizing the thickness of FMNPs layer combined with an appropriate distribution is a mandatory for the preparation of novel polymer-metal bactericide composite materials. Figure 4.5 presents SEM images of cross sections of Ag-FMNPs-gel-type sulfonic polymer PMNCs granules at different times of metal loading stage and, as the result, different thickness of Ag-FMNPs layer. The amount of Ag present is between the range of 88 to 200 mg Ag per gram of polymeric matrix; depending on the loading time stage. The metal loading efficiency is around 85% for the 20min loading time, considering the initial amount of silver solution used for stage 1 of DEEIMS and the ion exchange capacity of the polymeric matrix.

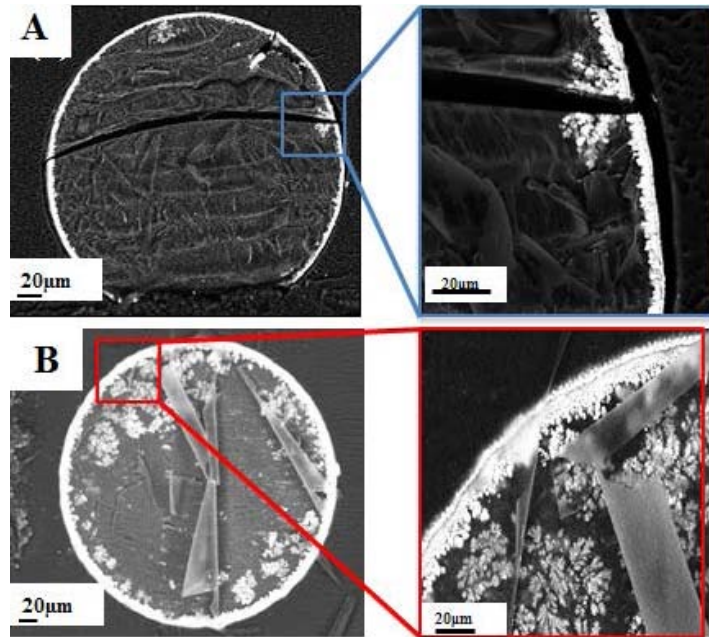


Figure 4.5: SEM images of cross sections of Ag-FMNPs-gel-type sulfonic polymer PMNC granules at different times of metal loading stage and thicknesses (Δl) of final FMNPs layer (time of a<b).

The values of FMNPs layer thickness obtained from the SEM images of cross-sections of PMNCs granules (see Figure 4.5) demonstrate a linear dependence on the metal loading time as it shows in Figure 4.6. This linear dependence can be used as a sort of calibration curve to determine the thickness of FMNPs layer at any time within the given time interval. The results of this estimation are shown in Table 4.2.

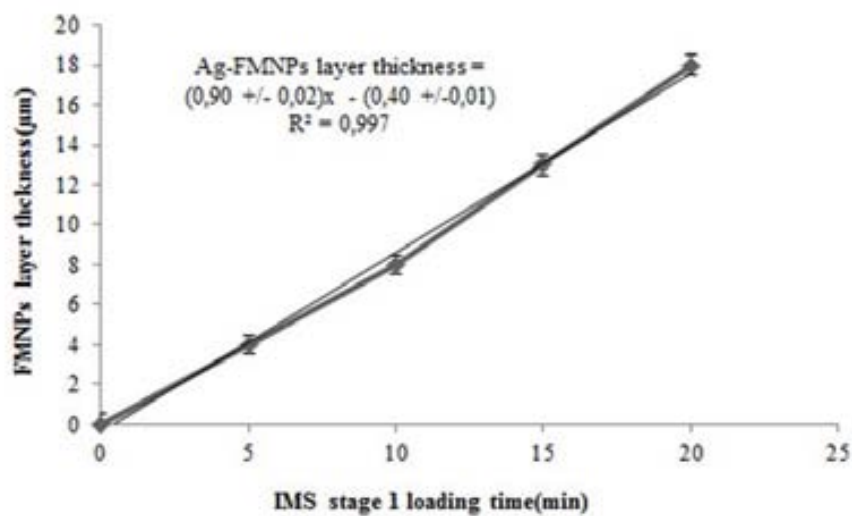


Figure 4.6: Thickness of FMNPs layer versus metal loading time.

Table 4.2: Thickness values of Ag-FMNPs layer at low metal loading times determined from cross section measurements

IMS stage 1 loading time (min)	Ag-FMNPs layer thickness μm (± 0.02μm)
1	0.50
3	2.30
7	5.90

The results shown in Figure 4.5 and Table 4.2 can also be used for estimation of the diffusion coefficient of Ag⁺ ions in the polymer phase and compare it with the value reported by Matuzuru and Wadachi for gel-type sulfonated cation-exchanger of a, which equals $1,3 \times 10^{-7} \text{ cm}^2/\text{s}^{20}$.

Under the conditions of experiments carried out in this research, the intra-particle diffusion (in the resin phase) is considered to control the kinetics of ion exchange. The diffusion coefficient of silver ions in this case can be calculated from the models first described by Boyd, Adamson and Mayers⁸ and Helfferich⁹ and developed by other researchers^{10,11} by using for example, the following Equation:

$$t = \frac{q^* F r^2}{6 D C_i}, \quad [4.3]$$

where q^* is the ion-exchange capacity of the resin (mequiv/g), F is the degree of exchange at certain time (s), r is the diffusion distance of the ions into the matrix (cm), D is the diffusion coefficient of Ag⁺ ions (cm^2/s) in the resin phase and t is the time of diffusion (in our case it is the metal loading time) and C_i is the concentration of the metal salt solution (mequiv/l).

The F value standing in Equation (4.3) can be calculated by taking into account the thickness of the Ag-FMNPs layer (Δl , see Figure 4.5 b, right) as follows:

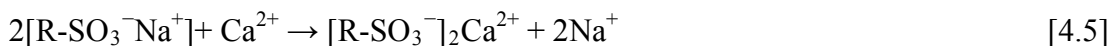
$$F = \frac{r^3 - (r - \Delta l)^3}{r^3} \quad [4.4]$$

The D_{Ag^+} value calculated by using Equations (4.3) and (4.4) equals to $3.5 \times 10^{-7} \text{ cm}^2/\text{s}$, what is sufficiently close to that reported by Matuzuru and Wadachi (see above). The difference between the calculated and the reported D values can be mainly attributed to the appearance of Ag-FMNPs layer near the surface of the resin beads (see Figure 4.5) and also by possible differences in the cross linking degree of the polymer matrices and in the other experimental conditions. In other words the resistance of the PMNC material towards mass-transfer does not change dramatically in comparison with the initial FMNPs-free polymer.

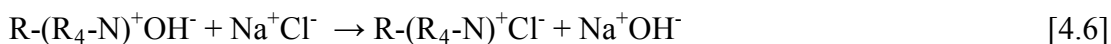
4.2 Evaluation of ion exchange properties of cationic and anionic gel – type polymers before and after modification with Ag-FMNPs.

The ion exchange capacity for the anionic exchanger gel-type polymer (quaternary ammine) and for the cationic exchanger gel-type (sulfonic) were calculated by volumetric titration were $2.1 \text{ meq} \times \text{g}^{-1}$ in both cases.

For both anionic and cationic breakthrough experiments a column with internal diameter of 0.025m was used for an average bed particle diameter of $500 \mu\text{m}$. For the breakthrough curve profile for cationic gel –type polymer modified and unmodified with Ag-FMNPs a fixed bed of the resin was placed in the column. A Ca^{2+} solution was introduced with a pump and made go through the fixed bed particles with a flux rate of $1 \text{ mL}/\text{min}$. Then, each 2 mL of effluent were collected separated samples for the determination of displacement of Na^+ to Ca^{2+} as described in Equation (3).



Similar procedure was followed for anionic breakthrough curve profile. Modified and unmodified with Ag-FMNPs quaternary gel-type amine anion exchanger were used as fixed bed in the column. Cl^- solution was introduced with pump and made go through the fixed bed particles with a flux rate of 1 mL/min. Then, each 2 mL of effluent were collected separated samples for the determination of displacement of OH^- to Cl^- as described in Equation (4).



On Figure 4.7 are shown the breakthrough curves obtained within a series of experiments on displacement Na^+ with Ca^{2+} ions from the initial polymer (FMNPs-free) and NC samples containing different amounts of FMNPs are presented. The slope of the curves shown in Figure 4.7 qualitatively reflects the kinetic properties of the corresponding material so that the closer it to 90° the faster is the mass transfer process inside the polymer matrix. This means that after DEDIMS of FMNPs the functional groups of the ion exchanger remain almost equally accessible for ions to be removed from the water under treatment. At the same time what it also follows from the results shown in Figure 6, the slowing down of the ions diffusion can be decreased by minimizing the thickness of FMNPs layer moreover the negative impact of this layer is partially compensated by the appearance of nanoporosity in NC material (see above).

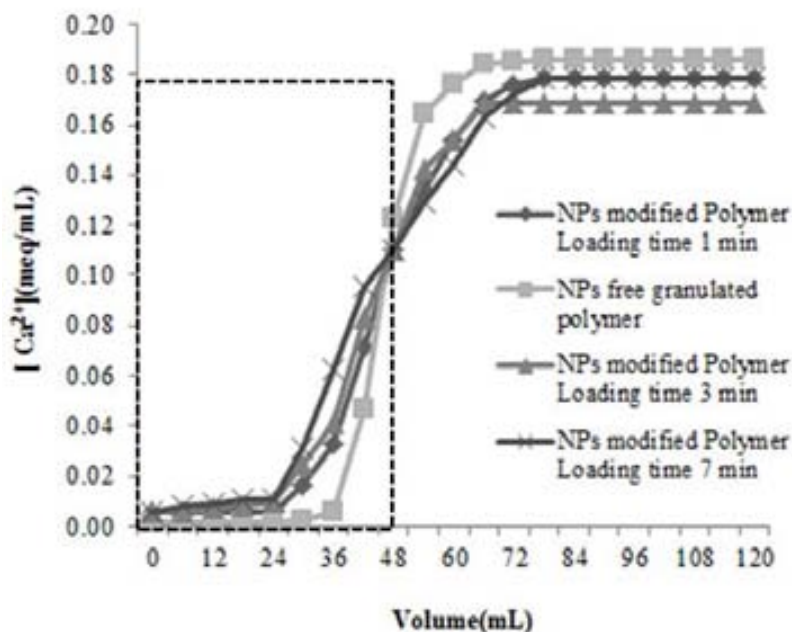
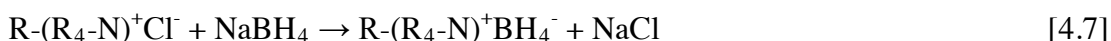


Figure 4.7: Breakthrough curves of displacement of Na^+ with Ca^{2+} from FMNPs-free sulfonic cation-exchange resin and NCs obtained after different times of metal loading stage. Area marked by dotted lines corresponds to ion exchange capacity of resin and NC samples.

The area marked by the horizontal and vertical dotted lines in Figure 4.7 corresponds to the ion exchange capacity, q^* (see eq.4.3) of the initial polymer and PMNC samples. The vertical dotted line has to pass through the inflection point of each breakthrough curve and as it is seen these points for all curves essentially coincide with each other. This means that q^* values of all NC samples coincide with that of the initial polymer. The q^* value estimated from Figure 4.7 appears to equal to $2.0 \text{ meq} \cdot \text{g}^{-1}$ what is very close the value of $2.1 \text{ meq} \cdot \text{g}^{-1}$ obtained by the quantitative titration of a certain mass of the initial polymer in the H^+ -form with alkali solution.

Figure 4.8 presents the breakthrough curve profiles obtained with modified and unmodified Ag- FMNPs anion-exchange resin of gel type. The modification was carried out by DEEIMS of Ag - FMNPs by using the following reactions:



As it clearly follows from the breakthrough curve profiles shown in Figure 7, the displacement of OH^- with Cl^- ions from the FMNPs free anion exchanger and Ag-FMNPs-containing NC coincide essentially in all points. This means that the kinetics of OH^- - Cl^- exchange is the same in both cases. In other words the Ag-FMNPs layer does not create any additional diffusional barrier for exchanging ions. Another conclusion which follows from the breakthrough curves shown in Figure 4.8, concerns the equality of ion exchange capacity values of FMNPs free and Ag-FMNPs-containing anion exchanger. The capacity of both samples estimated from the data of Figure 4.8 appears to be equal to 2.1 meq g^{-1} what coincides with the value obtained by titration of a certain mass of the initial polymer in the OH^- -form with acid solution.

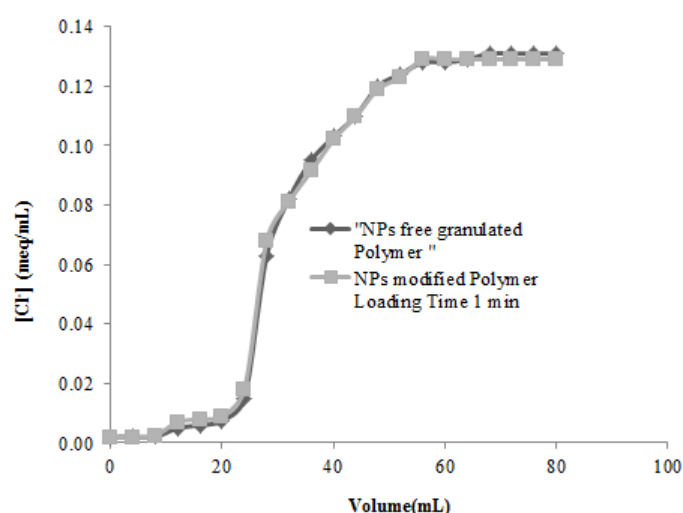


Figure 4.8: Breakthrough curves of displacement of OH^- with Cl^- ions from FMNPs-free quaternary amine anion-exchange resin (grey) and NC (dark grey) obtained by DEEIMS technique with metal loading time of 1 minute.

Comparison of the data shown in Figures 4.7 and 4.8 allows to conclude that minimization of the metal loading time allows to decrease the thickness of Ag-FMNPs layer what in turn permits to maintain the ion exchange properties of the ion exchange material unchanged. This is particularly true in the case of anion exchange polymer.

The comparison of DEEIMS versions used for modification of cation exchangers (see Equations 5 and 6) and anion exchangers (see Equations (4.7) and (4.8)) polymeric matrices leads to a quite logic conclusion: both versions of DEEIMS procedure are in fact the specular reflection of each other. Indeed, in the first case after

the loading of the functional groups with metal ions (Equation (4.1)) the polymer is treated with reducing agent (Equation (4.2)), anions of which (the actual reducer) bear the same charge (negative) as the functional groups of the polymer. Due to the action of DEE they cannot deeply penetrate inside the matrix and the reduction of metal ions leading to formation of FMNPs proceeds near the polymer surface (see Figure 4.1C).

In the case of anion exchange polymer, the first stage of DEEIMS is the sorption of the reducer anions on the positively charged functional groups of the polymer (Equation (4.7)). The second stage (Equation (4.8)) is the treatment of the polymer with solution of positively charged metal ions. Their rejection by the matrix bearing the charge of the same sign does not allow them to deeply penetrate into the polymer and their interaction with reducing agent proceeds (as in the previous case) near the surface of the polymer. It seems important to emphasize that both versions of DEEIMS technique lead to the most favourable distribution of FMNPs near the surface of PMNC material, what is particularly important in practical application of such materials for complex water treatment. Note that similar procedure has been also applied for the synthesis of metal oxide nanoparticles inside ion exchange resins for removal of arsenic from water¹² and for the preparation of heterogeneous catalysts.¹³

4.3 Concluding Remarks

The surface modification of ion exchange materials with FMNPs by DEEIMS technique has shown to provide the most favourable distribution of FMNPs in the final NC materials enhancing their feasible applications such as complex water treatment and heterogeneous catalysis. This technique has demonstrated to be an efficient synthetic methodology applicable for the preparation of bifunctional polymer-metal NCs from polymers of either functionality, i.e. bearing either negatively (e.g., cation exchangers) or positively (e.g., anion exchangers) charged functional groups. Regarding this fact, the modification of polymers with negatively charged functional groups with FMNPs by using DEEIMS technique showed to be accompanied by the regeneration of the functional groups, i.e. their conversion into the initial Na⁺-form. This permit to easily increase the thickness of FMNPs layer (if required) by carrying out consecutive metal-loading-reduction DEEIMS cycles.

In addition, the ion exchange capacity of the FMNPs modified polymers is not essentially changed after DEEIMS as it can be deduced from the breakthrough curve profiles obtained on the unmodified and modified matrices with FMNPs. As it also follows from these data, the resistance of the matrix towards ions diffusion can be minimized by varying the thickness of FMNPs layer and can reach the same value as that of the unmodified polymer.

Particularly, the modification of cation-exchange gel-type cation exchange polymer of with Ag-FMNPs has shown to cause strong modification of the polymer morphology due to the appearance of the worm-like structure on the polymer surface and the nanoporosity, which enhances the rate of mass transfer in the final NC material.

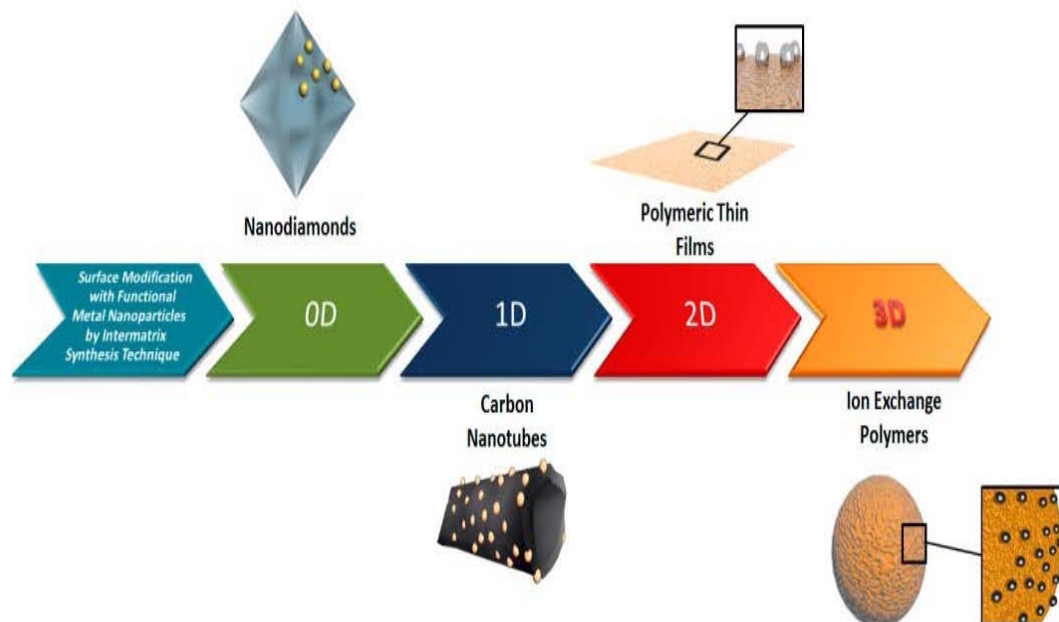
References:

- (1) Muraviev, D. N. Inter-Matrix Synthesis of Polymer Stabilised Metal Nanoparticles for Sensor Applications. *Contrib. to Sci.* **2005**, 3, 19–32.

- (2) Alonso, A.; Vigués, N.; Muñoz-Berbel, X.; Macanás, J.; Muñoz, M.; Mas, J.; Muraviev, D. N. Environmentally-Safe Bimetallic Ag@Co Magnetic Nanocomposites with Antimicrobial Activity. *Chem. Commun. (Camb)*. **2011**, *47*, 10464–10466.
- (3) Domènech, B.; Muñoz, M.; Muraviev, D. N.; Macanás, J. Uncommon Patterns in Nafion Films Loaded with Silver Nanoparticles. *Chem. Commun. (Camb)*. **2014**, *50*, 4693–4695.
- (4) Muraviev, D.; Macanas, J.; Farre, M.; Munoz, M.; Alegret, S. Novel Routes for Inter-Matrix Synthesis and Characterization of Polymer Stabilized Metal Nanoparticles for Molecular Recognition Devices. *Sensors Actuators B Chem*. **2006**, *118*, 408–417.
- (5) Alonso, A.; Muñoz-Berbel, X.; Vigués, N.; Macanás, J.; Muñoz, M.; Mas, J.; Muraviev, D. N. Characterization of Fibrous Polymer Silver/cobalt Nanocomposite with Enhanced Bactericide Activity. *Langmuir* **2012**, *28*, 783–790.
- (6) Bastos-Arrieta, J.; Muñoz, M.; Ruiz, P.; Muraviev, D. N. Morphological Changes of Gel-Type Functional Polymers after Intermatrix Synthesis of Polymer Stabilized Silver Nanoparticles. *Nanoscale Res. Lett.* **2013**, *8*, 255.
- (7) Taylor, P.; Matsuzuru, H.; Wadachi, Y. Journal of Nuclear Science and Influence of Differences in Resin-Matrix Structure on Ion-Exchange Adsorption of Trace Amounts of Ag (I), Co (II) and Cr (III) Influence of Differences in Resin-Matrix Structure on Ion-Exchange Adsorption of Trace Amount. *J. Nucl. Sci. Technol.* **1975**, *12*, 344–349.
- (8) Boyd, G.; Adamson, A. W.; Myers, L. S. The Exchange Adsorption of Ions from Aqueous Solutions by Organic Zeolites. II. Kinetics. *J. Am. Chem. Soc.* **1947**, *69*, 2836–2848.
- (9) Helfferich, F. *Ion Exchange*; McGraw-Hill Book Co. Inc.: New York, 1962; p. Chapter 6.

- (10) Helfferich, F. Ion-Exchange Kinetics. V. Ion Exchange Accompanied by reactions Ion Exchange Kinetics. *J. Phys. Chem.* **1965**, *69*, 1178–1187.
- (11) Helfferich, F. ION-EXCHANGE KINETICS. 1 III. EXPERIMENTAL TEST OF THE THEORY OF PARTICLE-DIFFUSION CONTROLLED ION EXCHANGE. *J. Phys. Chem.* **1962**, *66*, 39–44.
- (12) Greenleaf, J. E.; Lin, J.; Sengupta, A. K. Two Novel Applications of Ion Exchange Fibers: Arsenic Removal and Chemical-Free Softening of Hard Water. *Environ. Prog.* **2006**, *25*, 300–311.
- (13) Bastos-Arrieta, J.; Shafir, A.; Alonso, A.; Muñoz, M.; Macanás, J.; Muraviev, D. N. Donnan Exclusion Driven Intermatrix Synthesis of Reusable Polymer Stabilized Palladium Nanocatalysts. *Catal. Today* **2012**.

Chapter 5



Intermatrix synthesis technique (IMS) has proven to be a valid methodology for the preparation of bifunctional Metal-Polymer Nanocomposites (MPNCs) containing Functional Metal Nanoparticles (FMNPs) with bactericide, magnetic, catalytical and electrocatalytical properties. In this section we report the recent advances in the application of IMS for the preparation of multi-dimensional Nanocomposite materials (from 0 D such as nanodiamonds (NDs) to 3 D as granulated exchange polymers) by the modification of different types of reactive surfaces with FMNPs.

5. Applications of Bifunctional Nanocomposites prepared by Intermatrix Synthesis Technique.

5.1 Heterogeneous Catalysis:

Heterogeneous catalysis represents one of the fields of the modern science and technology where the application of ultrafine catalyst particles dates back to the beginning of the last century^{1,2}. Application of the heterogeneous catalysis within the last decades has been strongly stimulated by the development of the new generation of catalysts with nanometer dimensions. The development of the catalysts of this type requires in many instances the search of appropriate supports to simplify their practical applications.^{3,4}

On the other hand, the development of novel synthesis approach requires in many instances the catalysts with high quality active sites, which are characterized by good structure - performance relationships. This refers for example, to Carbon – Carbon bond formation reactions, which represent a fundamental tool for organic synthesis, as it can be used in the preparation of fine chemicals. Most frequently used reactions of this type are palladium catalyzed C-C coupling reactions, such as for instance, Suzuki Cross Coupling Reaction (SCCR), widely known for its applicability to the synthesis of fine chemicals.⁵⁻⁷

Polymeric supports play in this regard a very important role for several reasons such as, for example the ease of their preparation in the most appropriate physical form (e.g., granulated, fibrous, membranes, etc.), the possibility to produce the macroporous matrices with highly developed surface areas and so on. However, the immobilization of the catalyst nanoparticles on the appropriate polymeric support represents a separate task, which in some instances is not so simple.^{8,9}

The use of the bifunctional polymers as supports for the heterogeneous nanocatalysts has in this sense, one more important advantage dealing with the possibility to synthesize the catalyst nanoparticles directly at the “point of use”, i.e.

inside the supporting polymer. In the case of the metal catalyst nanoparticles (MCNPs) this results in the formation of the catalytically-active polymer-metal nanocomposites.¹⁰

5.1.1 Synthesis and Characterization of Pd-MCNPs

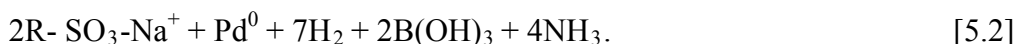
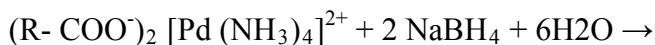
The difference between the “classical” and the novel version of the IMS technique developed in this study become clear after comparison of their respective reaction schemes, which can be written for the case of formation of Pd-MCNPs in the strong acid (a) and the strong base (b) functional polymers as follows:

a) IMS in cation exchange polymers (classical version):

1) Metal-loading stage

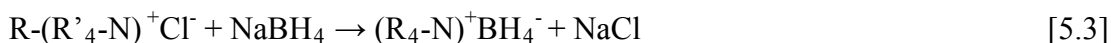


2) Metal-reduction stage

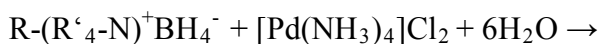


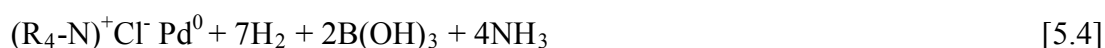
b) IMS in anion exchange polymers (novel version):

1) Reducer-loading stage



2) Metal-loading-reduction stage





As it is seen from the above reaction schemes, the main difference between (a) and (b) versions of IMS consists in the first stage of the process. In the first case the functional groups of the polymer are loaded with the desired metal ions, while in the second case the loading is carried out with desired reducer ions. The second stage in the first case consists in the reduction of metal ions with ionic reducer, located in the external solution. As far as the charge sign of reducer anions coincide with that of the polymer matrix, they cannot deeply penetrate inside the polymer due to the action of the Donnan exclusion effect (DEE) and as the result, the reduction process appears to be “localized” near the surface of the polymer.

Unlike version (a), version (b) of IMS starts with the loading of the functional groups of the polymer with the reducer anions (see first stage, reaction 3). As the result, the second stage of this version permits to couple the metal-loading and the metal-reduction processes in one step. The metal loading is carried out by using external solution containing metal ions bearing the charge of the same sign as that of the functional groups of the polymer, what does not allow them to deeply diffuse inside the polymer matrix (DEE). Again, the reduction of metal ions and therefore, the formation of MCNPs have to proceed near the surface of the polymer. For obvious reasons the second version of IMS technique (version b) can be classified as a sort of the symmetrical reflection of version (a).

In both versions of IMS technique DEE plays a very important role as it appears to be responsible for the desired nonhomogeneous distribution of MCNPs inside the polymer-metal nanocomposite. The action of this effect is observed in both cases within the second stage of IMS process (see Equations 5.2 and 5.4). The following two “driving forces” acting in the opposite directions are responsible for the DEE: 1) the electric field determined by the charge of the polymer matrix¹¹⁻¹⁴ and 2) the concentration of the ionic component in the external solution (in fact the concentration gradient of this component). The first force rejects the ions of the same charge as that of the functional groups of the polymer while the second one drives these ions to move into the polymer matrix. The first force can be hardly varied as it has a constant value

determined by the ion exchange capacity of the polymer and the degree of dissociation of its functional groups. The second force can be easily varied by changing the concentration of respective component in the external solution, what has to result in the changes in the composition of the final nanocomposite (NCs) content.

The variation of the MNPs content inside the polymer can be also achieved by using the following two additional approaches: 1) incomplete loading of the functional groups of the polymer with respective component (metal ions in the version “a” or reducing agent ions in the version “b” of IMS) prior to carrying out the final stage, and 2) the use of repetitive metal-loading-reduction cycles. The first approach allows for the obtaining of nanocomposites with low MNPs content while the second one permits to substantially increase this value. The results collected in Table 5.1 confirm the validity of the first (see samples MNCP A, B and C) approach

Table 5.1: Metal content in Pd-PSMNCs nanocomposites synthesized by applying different metal loading-reduction cycles.

Sample	[NaBH ₄](M)	mg Pd/g _{matrix} (± 0.2)	Loading-reduction cycles
MCNP A	0.1	30.8	1
MCNP B	0.05	12.8	1
MNCP C	0.025	4.0	1
MNCP D	0.1	30.4	1
MNCP E		57.9	2
MNCP F		61.4	2
MNCP G		89.9	3

The possibility to use the second approach follows from the above reaction schemes (see reactions 5.2 and 5.4). Indeed, after finishing the metal reduction (IMS

version a) or the metal-loading-reduction stages (IMS version b) the functional groups of the polymer appear to be converted back into the initial ionic form (Na-form in the first and Cl-form in the second case). This means that in both cases IMS of MNP cycles can be repeated without any additional pretreatment of the ion exchanger. This has to result in the accumulation of a higher amount of the metal (or MNPs) inside the polymer. This supposition is confirmed by the results obtained when using the novel version of IMS technique (see above version b), which are also presented in Table 5.1 (see samples D, E, F and G). As it is seen, the dependence of the metal amount in the polymer versus the number of metal-loading-reduction cycles carried out follows a linear trend.

The results presented in Figure 5.1 confirm the validity of the proposed metal distribution. Indeed, as it is seen in SEM images of the cross-sections of the granules of respective polymer-metal NCs shown in this Figure, the distribution of Pd-MCNPs obtained by using both versions of IMS technique is quite similar. As it is seen in Figure 5.1, both synthetic methodologies lead to the formation of NPs distributed mainly on the surface of the polymer. It is important to emphasize that in both cases the NCs distribution of this type appears to be the result of the purposeful use of the Donnan Effect and does not depend on the functionality of the polymer. The last conclusion is of particular importance as it substantially widens the applicability of IMS technique for the synthesis of catalytically-active polymer-metal NCs with the enhanced accessibility of NCs for reactants.

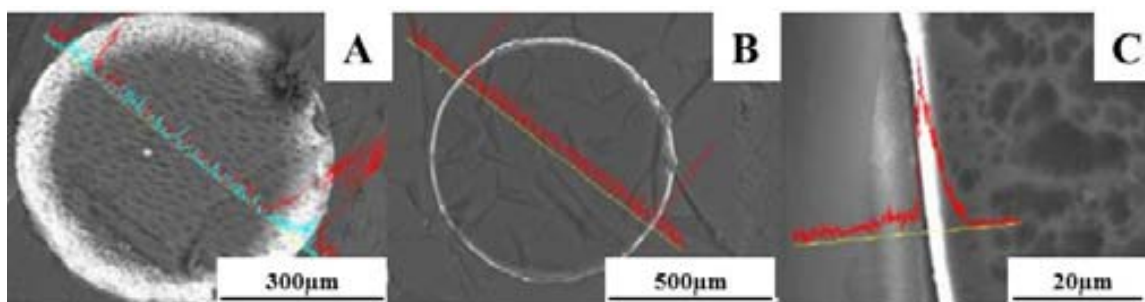


Figure 5.1: SEM images of granule cross-sections and respective LineScan EDS spectra showing distribution of Pd-MNPs inside nanocomposites obtained by (A) classic and (B,C) novel version of IMS technique by using cation (A) and anion exchange resins (B,C)

One more important conclusion follows from the detailed examination of SEM images of the surface of NCs granules, which are shown in Figure 5.2. As it is seen, the surface of the initial ion exchange material looks absolutely smooth (see Figure 5.2A). After IMS of Pd-MCNPs the morphology of the polymer surface changes due to the formation of fractal-like structures of partially aggregated Pd-MNPs (see Figures 5.2B and 5.2C). In this case the formation of MNP fractals on the surface of polymer can be explained by the action of Diffusion Limited Aggregation (DLA) mechanism.¹⁵ The efficiency of MNP fractals in the catalytic applications is known not to differ dramatically from that of MCNPs due to the insignificant difference of the surface area of the former and the latter.^{16–18}

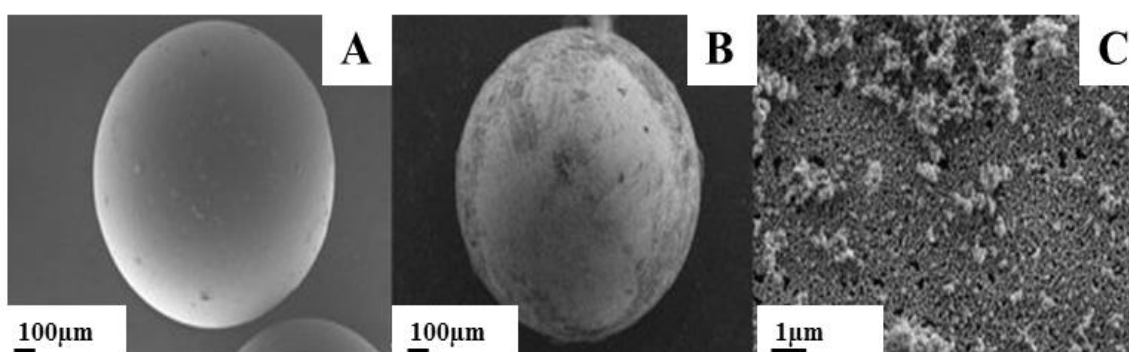


Figure 5.2: SEM images of Purolite A520E resin (sample MNCP E in Table 5.1) before (A) and after (B and C) DEDIMS of Pd-PSMNCs.

The formation of Pd-MNP fractals proceeds only on the surface of the polymer granules, while inside the polymer no MNPs aggregation is observed. This conclusion follows from the TEM images of nanocomposite cross-sections shown in Figure 5.3. As it can be seen in Figures 5.3A and 5.3B, Pd-MNPs are well separated from each other and do not form any visible aggregates. This testifies to the high stabilizing efficiency of the polymer. An average diameter of Pd-MCNPs (corresponding to the maximum on size distribution histogram, see Figure 5.3C) equals to 35 nm, what provides a sufficiently high surface area and multiple catalytic centers.

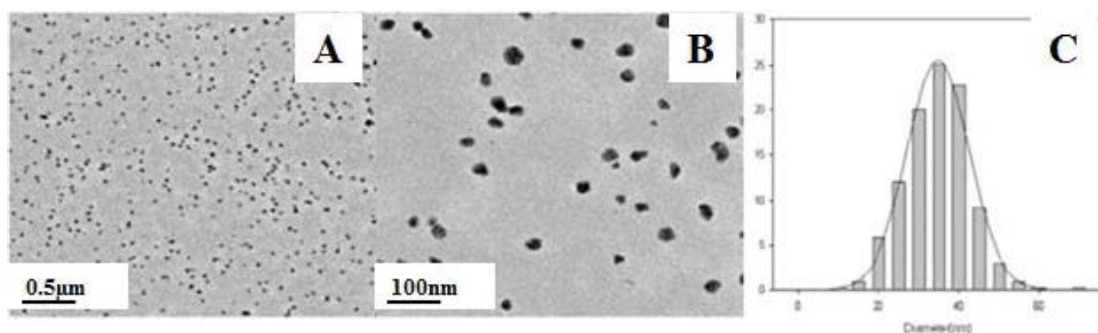


Figure 5.3: TEM images (A, B) and size distribution histogram (C) of MCNP A (sample MNCP 3, see Table 5.1)

5.1.2 Evaluation of Catalytic Activity for Catalysis of Suzuki Cross Coupling Reaction(SCCR)

A known quantity of Pd- MCNPss (corresponding to 1% molar rate of Pd to 4-bromoacetophenone) was mixed with 4-bromoacetophenone 98% (1 mmol), phenylboronic acid 98% (1 mmol), K_2CO_3 (1 mmol) dissolved in the mixture of dimethylformamide (DMF)– H_2O (80:20) and stirred at 80°C for 18 h as it was settle as optimal experimental conditions for this reaction in previous works by using the analogue cation exchanger as matrix.¹⁴ The conversion degree and the efficiency rate of the reaction were followed by monitoring by gas chromatography (7820A GC, Agilent Technology).

After finishing the first catalytic cycle the granulated nanocomposite was separated from the reaction mixture by simple filtration and then reused in sequential cycles. The results of this series of experiments for nanocomposite samples MNCP A, B and C (see Table 5.1) are shown in Figure 5.4. As it is seen, the nanocomposite with the maximum Pd content (sample A) demonstrates the higher catalytic activity in comparison with other samples. The first two cycles give approximately a 35% reaction yield, which then gradually decreases. The other two samples (B and C) give far lower yields and the results obtained with these samples are not as stable as those obtained with sample A., due to the Pd content achieved in each nanocomposite.

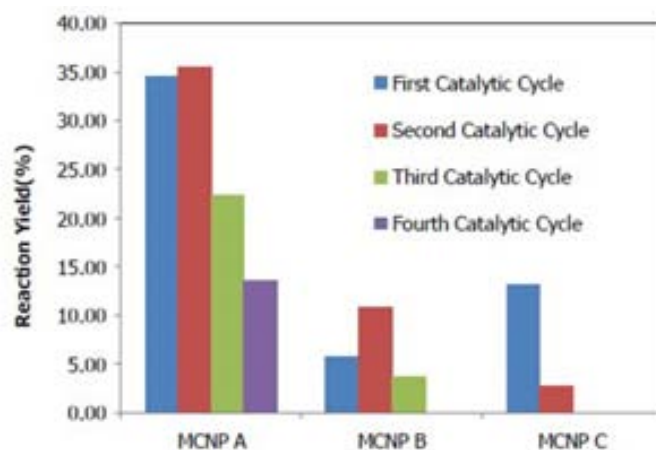


Figure 5.4: SCCR yield per catalytic run due to the application of the Pd-MCNPs

As shown in Figure 5.5, a substantial increase of the reaction yield was obtained when using the nanocomposite samples with higher Pd-PSMNCs content (samples MCNP E, F and G in Table 5.1). The dependence of the reaction yield obtained within the second catalytic cycle versus absolute Pd content in the nanocomposite (mg Pd/g nanocomposite) is shown in Figure 5.5 and Figure 5.6

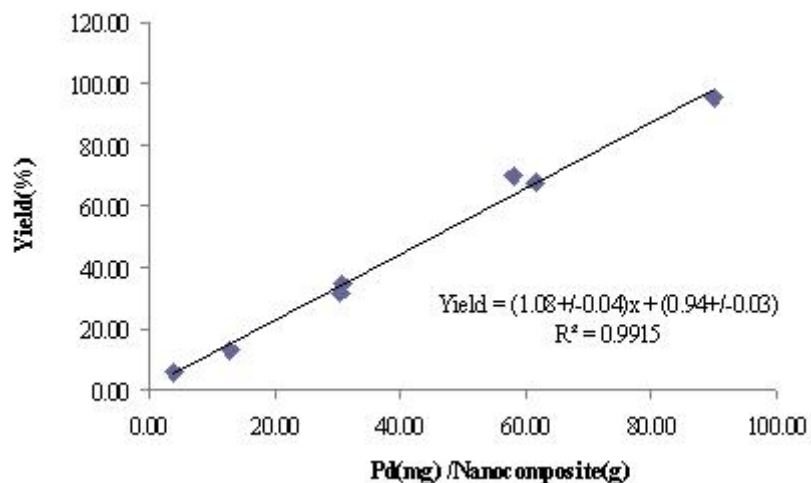


Figure 5.5: Lineal increase of SCCR yield as function of palladium content in Pd-PSMNCs containing nanocomposite.

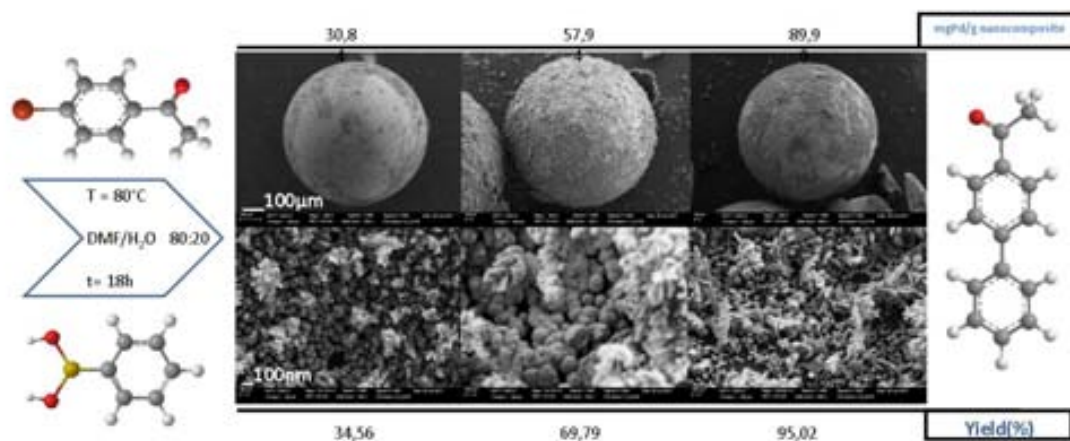


Figure 5.6: Schematic representation of catalytic performance of Pd-PSMNCs containing nanocomposite for SCCR.

5.1.3 Concluding Remarks

The main conclusion, which follows from the results obtained in this study concerns the extension of the IMS technique developed in our previous works to the polymers with anion exchange functionality. It has been demonstrated that an anionic exchange resin (Purolite A 520E) can be successfully used for the DEDIMS of Pd-MCNPs with the most favorable distribution of catalyst MNPs. The catalytic activity of nanocomposites obtained was checked in the SCCR and the yield of the reaction was shown to be directly proportional to the palladium content in the nanocomposite. It has been also shown that DEDIMS does not affect IEC of the polymeric support what gives a possibility for carrying out consecutive metal-loading reduction cycles. The catalytic activity of the palladium catalyst has been shown to be quite similar to both MNPs and MNP-fractals.

5.2 Further feasible approaches of IMS for novel reactive surfaces:

IMS has proved to be a valid procedure for the surface modification of polymeric ion exchange matrices such as resins, membranes and fibres with mono and bi-metallic functional metal nanoparticles (FMNPs). Depending on the chemical nature of these FMNPs, the produced polymer-metal nanocomposites (PMNCs) have different applications: bactericide assays, complex water treatment, heterogeneous catalysis and

electrocatalysis.^{11,19–24} In despite of the *in situ* formation of the FMNPs on the polymeric support, its initial ion exchange properties are not significantly changed, which represents another advantage of IMS.

This section presents the extended use of IMS as a simple and effective procedure for the preparation of FMNPs and more specifically CdS-Quantum Dots (QDs) on novel reactive surfaces such as carbon nanotubes (CNTs), nanodiamonds (NDs) and sulfonated polyether – etherketone (SPEEK) polymeric thin films (PTFs). This methodology includes two stages based on aqueous chemistry: 1) loading the functional groups with MNPs precursor (e.g., metal or metal complex ions) and 2) *in situ* formation of FMNPs in the supporting matrix after reduction of the precursor. Accordingly, the feasibility of the IMS of CdS-QDs on MWCNTs (CdS-QDs@MWCNTs) for the preparation of epoxy nanocomposite electrodes was evaluated in terms of electrochemical and electroanalytical features in our recent publication from J. Muñoz *et.al.*²⁵

QDs are known to present quantum confinement effects during light excitation, which gives them interesting optical and semi-conducting properties. Tuning these features and coupled them with its surface modification or using them for the surface modification of these reactive surfaces and led to explore the application of these hybrid material to the field of sensors (fluorescent and biosensors) and to bioassays.^{26–29}

5.2.1 Intermatrix Synthesis of FMNPs on multiwall CNTs (MWCNTs)

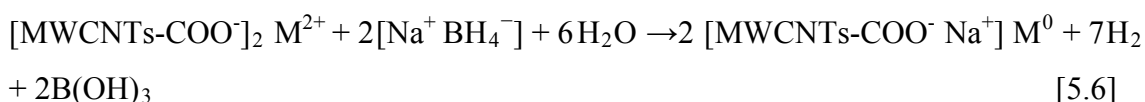
Carbon Nanotubes (CNTs) represent an important group of nanomaterials which are receiving different applications since their discovery, due to their remarkable electrical, chemical, mechanical, thermal and structural properties. FMNPs have been used extensively in the fields of physical, chemical and material sciences in the past few years due to their surface-volume ratio that gives them special properties different from the analogous bulk material. FMNPs have received considerable attention for their catalytic and electrochemical features for the preparation of amperometric sensors and biosensors leading an enhancement of the electron transfer between redox centers in the

analyte and the electrode, decreasing overpotentials of many analytically important electrochemical reactions.

IMS takes advantage of the ion exchange properties of the support matrix (e.g. sulfonic resins, CNTs) for consecutive loading and reduction processes during the synthesis of FMNPs with a favourable distribution in the final composite material. IMS is based on the following two sequential steps:

- a) Introduction of the FMNPs precursors into the polymer: by loading their functional groups with the desired metal ions or metal complex precursors of the nanoparticles.
- b) Their reduction to zero-valent state inside the support matrix: is carried out by using an appropriate reducing agent as NaBH₄ or ascorbic acid.

Equations (5.5) and (5.6) present the IMS on MWCNTs with carboxylic functionality:



During stage 2 of IMS, the ion exchange functionality of the MWCNTs is regenerated; what allows repeating sequential loading and reduction stages to increase the amount of FMNPs content and their thickness.

5.2.1.1 Characterization of FMNPs@MWCNTs

IMS technique provides a favorable distribution of the FMNPs on the MWCNTs surface as shown in the HR-TEM. Furthermore; the support provides their stability and simplifies their access for reagents in the catalytic or electrocatalytic applications of the final nanocomposite electrode material. In addition to the distribution of the FMNPs, it is observed a homogenous size distribution over the surface of the MWCNTs. No

agglomeration of different FMNPs@MWCNTs is detected by HR-TEM images shown in Figure 5.7.

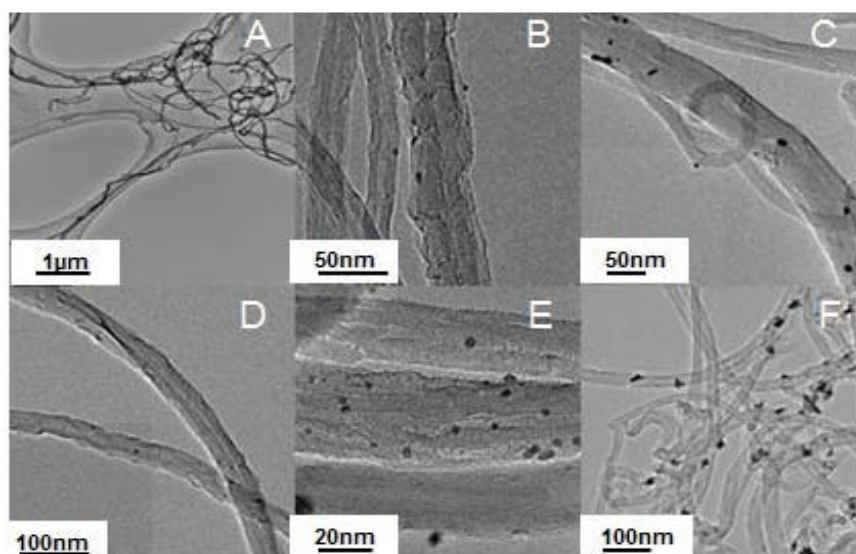


Figure 5.7: HR-TEM images of A) raw MWCNTs; B) Ag-; C) Au-; D) Cu-; E) Pd- and F) Pt-FMNPs@MWCNTs

The identification of the metal content for Ag-FMNPs@MWCNTs case is accomplished by EDS spectra (see Figure 5.8D) and TGA analysis (in Table 5.2) differentiating the FMNPs from the catalyst remaining from the industrial synthesis of the MWCNTs. The fact that the FMNPs are well distributed over the surface of the MWCNTs leads to the idea of increasing the electrochemical conductivity and an overall enhancement of the electrochemical features as proven in the corresponding electroanalytical characterization.²⁵

Table 5.2: TGA analysis of FMNPs@ MWCNTs/epoxy composites

FMNPs@ MWCNTs	TGA ($\pm 0.1\%$ in FMNPs)
Raw MWCNTs	98% in C
Pd-FMNPs@MWCNTs	1.7
Ag-FMNPs@MWCNTs	5.6
Au-FMNPs@MWCNTs	6.6
Cu-FMNPs@MWCNTs	7.0
Pt-FMNPs@MWCNTs	8.5?

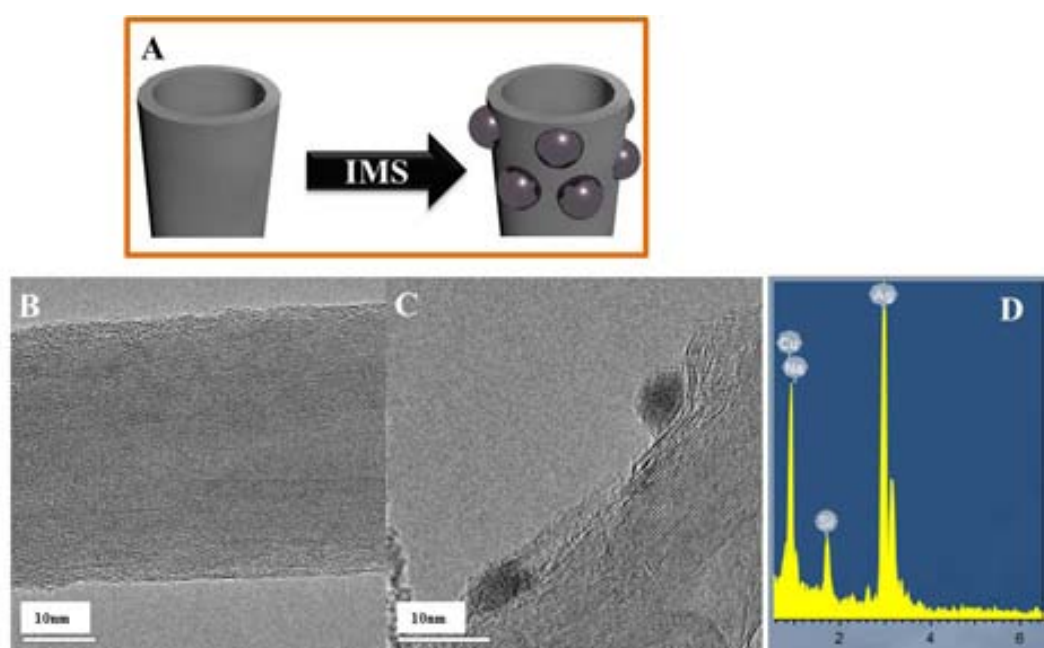


Figure 5.8: HR-TEM images of A) raw MWCNTs; B) Pd-FMNPs@MWCNTs C) Pd-FMNPs@MWCNTs amplification and D) the corresponding EDS spectra from C.

5.2.1.2 Intermatrix Synthesis of CdS-QDs@MWCNTs

The modification of MWCNTs with QDs can be carried out by taking advantage of their ion exchange functionality. In this case, the first stage remains absolutely the

same (loading the functional groups with NPs precursor), while the second one includes the formation of NPs (QDs) by precipitation reaction (instead of reduction). IMS can be described as follows: ^{12,30}

Stage 1: Loading of Cd^{2+} ions (QDs pr ecur sors) ont o t he carboxylic gr oups of MWCNTs, Equation (5.7), and

Stage 2: Precipitation of CdS-QDs on the MWCNTs surface by adding Na_2S , Equation (5.8):



Characterization of CdS-QDs@MWCNTs

As it is clearly seen from Equation (5.8), after carrying out the QDs formation reaction on t he MWCNTs surface, the functional groups appear to be r egenerated, as they are converted back into the Na^+ form. This means that the QDs formation cycle can be r epeated a gain b y u sing bot h Equations w ithout a ny additional pr e-treatment o f MWCNTs. This allows for accumulation of the desired amount of QDs on the surface of MWCNTs as seen in Figure 5.9.

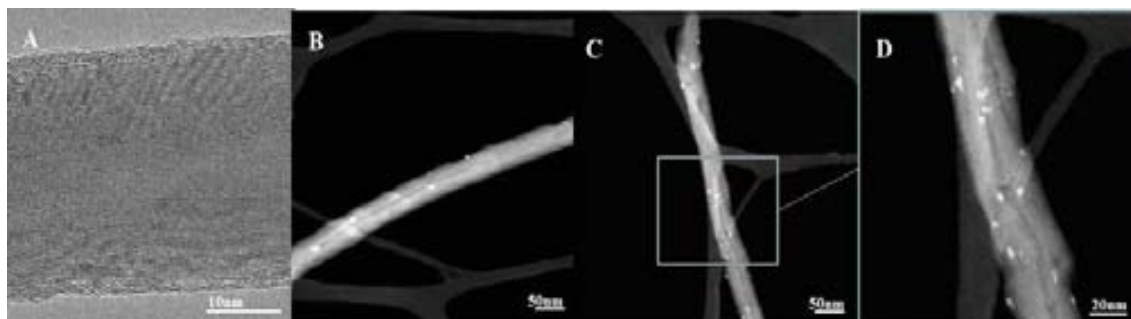


Figure 5.9: A) HR-TEM raw MWCNT B) HR-(S)TEM CdS-QDs on MWCNTs after one IMS cycle. C) and d) HR-(S)TEM images of CdS-QDs on MWCNTs after two sequential IMS cycles. Magnification of D>>C.

The microscopic characterization of QD-MWCNTs nanocomposites shows in Figure 5.9B confirms that the CdS-QDs are located mainly on the surface of MWCNTs. Moreover, QDs are well separated from each other and do not form any visible agglomerates. The raw MWCNTs also contain Fe and Ni catalyst particles used by the manufacturer to grow the CNTs. These catalysts are located inside of the MWCNTs walls. In order to differentiate the QDs from the catalyst particles, EDS analysis of CdS-QD@MWCNTs was also performed. Furthermore, the size distribution of the CdS-QDs is another parameter which can be used for their identification. An average diameter of CdS-QDs is 2.3 ± 0.4 nm as shown in Figure 5.10, while the one of the catalyst is higher (> 10 nm).

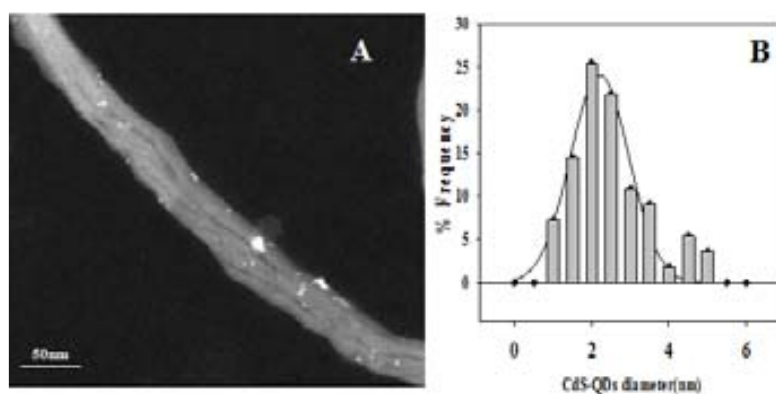


Figure 5.10: A) (S)TEM image and B) size distribution histogram for CdS-QDs on MWCNTs with an average diameter of 2.3 ± 0.4 nm.

The corresponding EDS spectra in Figure 5.11 confirm the presence of CdS-QDs and clearly differentiate QDs from Ni catalyst.

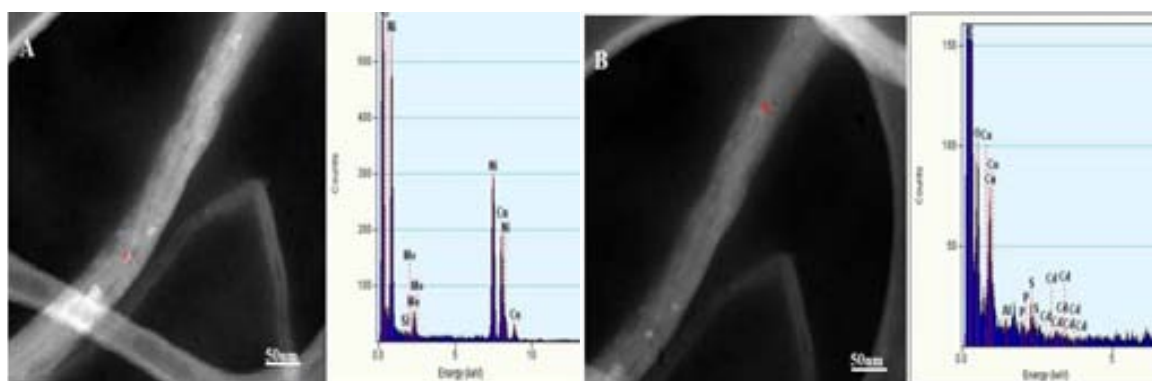


Figure 5.11: EDS spectra of A) MWNCTs Catalyst showing high Ni content. B) CdS-QDs showing the presence of Cd and S.

The QDs content after one step was evaluated by the thermogravimetric analysis (TGA) and appeared to be equal to 11.0% weight of CdS-QDs. As is also seen in Figure 5.9, despite of a larger amount of QDs accumulated on the MWCNT surface after two sequential loading-precipitation cycles, no evidence of QD agglomerates formation can be detected. Therefore, this fact can be considered as an additional advantage of IMS as synthetic route.

Application of CdS-QDs@MWCNTs for MWCNTs detection in water

After the modification of MWCNTs with CdS-QDs, they acquire optical properties,³¹ demonstrating fluorescence emission spectra and start to be visible. These spectra were determined for different concentrations of CdS-QDs@MWCNTs in aqueous solution. Figure 5.12 presents the schematic diagram of sample preparation procedure for proposed analytical methodology for detection of CNTs in water.

The procedure is based on the supposition that CdS-QDs can be formed only on the surface of supporting material, such as for example MWCNTs. The surface of this material serves as both QDs formation medium as it bears the QDs-precursors (Cd^{2+} ions fixed on the carboxylic groups of CNTs) and the QDs-stabilizing medium as it prevents their agglomeration and uncontrollable grows (see Figure 5.9). Based on this supposition, it was also assumed that QDs cannot be formed in the QDs-free aqueous phase (used as blank) as in this case only the formation of CdS macrocrystalline precipitate can occur.

Precipitation of CdS in blank was carried out by using the same reagent amount as for IMS of CdS-QDs on MWCNTs. Then, the solution obtained was centrifuged. The aliquot of the resulting upper liquid phase was used as blank solution. An analogous procedure was applied for the water samples containing MWCNTs. After centrifugation, aliquots from the samples containing different MWCNTs concentration (differing by factors 1x, 2x and 3x) were taken for spectrophotometric analysis.

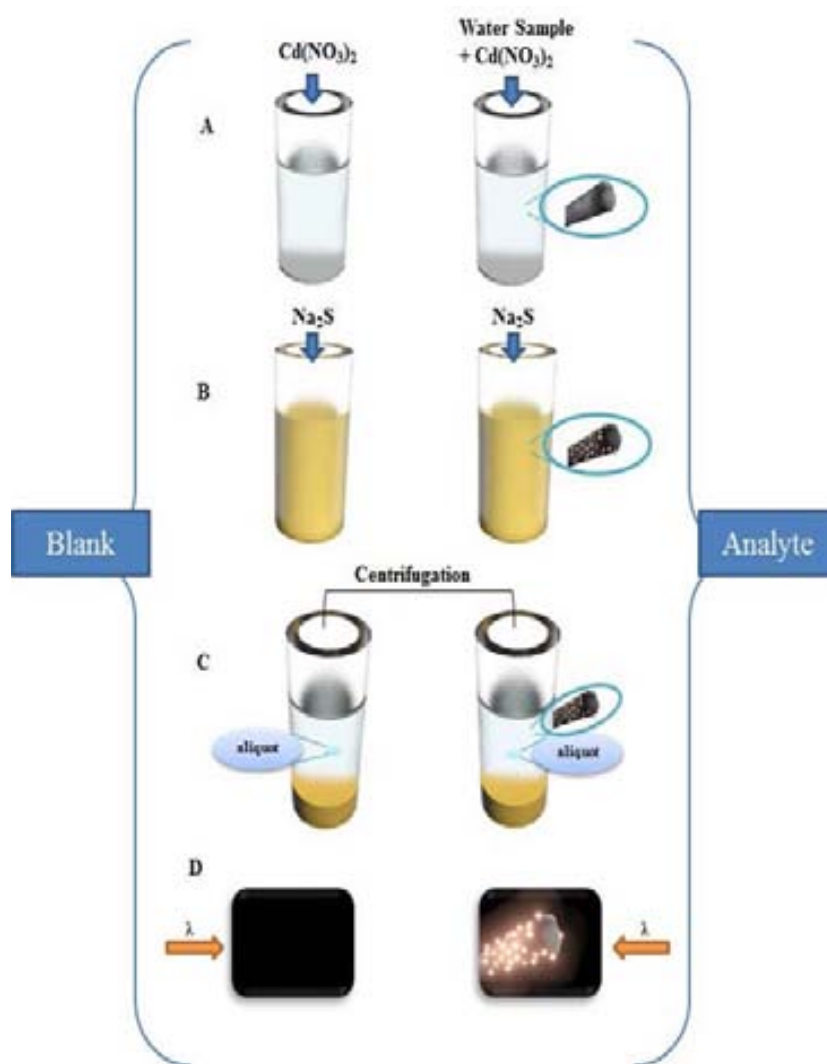


Figure 5.12: Scheme of analytical procedure for determination of MWCNTs in water. A) addition of $\text{Cd}(\text{NO}_3)_2$ aqueous solution to blank and water sample under analysis, B) precipitation of $\text{CdS}(\text{s})$ and formation of CdS -QDs on MWCNTs surface, C) centrifugation and D) aliquot from liquid phases of blank and analyte is analysed on spectrophotometer for detection of MWCNTs due to presence of CdS -QDs.

Figure 5.13 presents the values of fluorescent emission at the wavelength of $\lambda = 405\text{nm}$ for three different concentrations of CdS -QDs@MWCNTs (obtained after one QDs loading cycle) in aqueous phase. As it is seen in Figure 5.12, the fluorescent emission at this particular wavelength appears to be directly proportional to the concentration of analyte (MWCNTs) in the sample. This fact can be used for the quantitative detection of MWCNTs in water samples.

Consequently, it can be concluded that non-aggressive IMS technique proves to be applicable for the functionalization of MWCNTs with CdS -QDs what makes them spectrophotometrically detectable. IMS methodology is an environmentally friendly

technique as the amount of reagents used for IMS of QDs on MWCNTs surface can be minimized and only aqueous solutions are used in all cases. In addition, it seems important to emphasise that this methodology offers the possibility of detection of these NMs by using simple procedure shown in Figure 9, what makes detectable its presence in water.

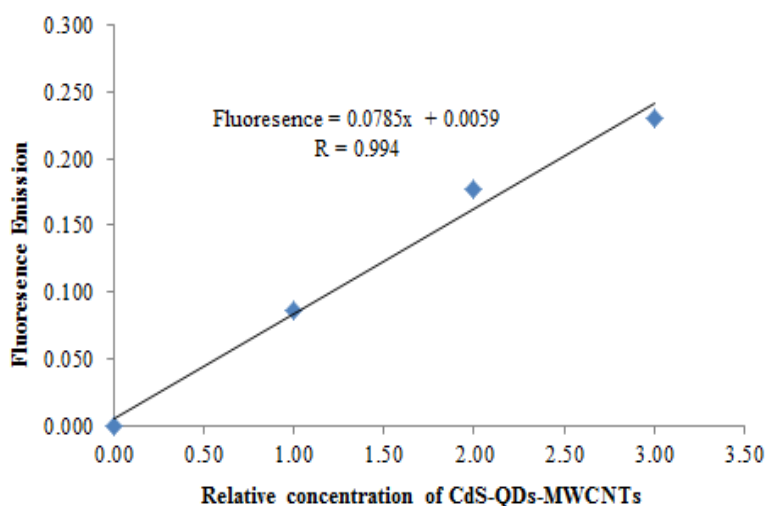


Figure 5.13: Dependence of intensity of fluorescence emission at wavelength of $\lambda = 405\text{nm}$ on relative concentration of MWCNTs decorated with CdS-QDs. Zero point corresponds to emission of blank (see text).

An increase of CdS-QDs load on MWCNTs surface combined with a more sensitive spectrophotometric equipment, will allow to substantially decrease the limit of detection of MWCNTs in water. Moreover; the proposed methodology seems to be easily adaptable for detection of other carbon NMs such fullerenes, nanodiamonds and some others. Moreover, the final distribution of the QDs on the support makes feasible the application of the obtained NMs also in catalysis or electrocatalysis.

5.2.2 Intermatrix Synthesis of CdS-QDs on SPEEK/PTFs (CdS-QDs@SPEEK/PTFs)

SPEEK membrane presents an IEC value of $2 \text{ meq}\cdot\text{g}^{-1}$ as product of a tuned sulfonation degree. This fact has made this polymeric membrane a suitable matrix for the implementation of IMS for the synthesis of different FMNPs with different applications.^{11,32,33}

Preparing PTFs of SPEEK membrane by spin coating (SC) involves the production of a material with optimal properties, which chemical properties are not changed. SC offers a novel type of polymeric support for IMS. SC is currently a predominant technique used to produce uniform thin films of organic materials with customized thicknesses of the order of micrometres and nanometers.^{34,35,36} Consequently, the re-assembly and disposition of the functionality of the initial material for IMS of Cd-QDs.

The formation of SPEEK/PTFs involves the equilibrium of several different species to produce the homogenous polymeric layer. The approach to achieve homogeneity in the layer thickness and distribution required several optimization cycles of SPEEK polymer dissolved and dropped on a silicon wafer. The viscosity and surface tension of dissolved SPEEK, could cause non-homogenous film distribution, therefore a plasma etching³⁷ procedure was carried out on the silicon wafers to improve affinity between the wafer and the substrate as SPEEK flow on a flat spinning substrate is one of the most important physical processes involved in SC.^{35,36}

SC of SPEEK involves different stages,³⁶ as can be seen in Figure 5.14: 1) deposition of SPEEK on silicon wafer, 2) spin-up due to centrifuge force in which the substrate is accelerated up to its final desired rotation speed, 3) spin-off in which gradual fluid thinning occurs and 4) evaporation in which spin-off stage ends the film drying stage begins.

Stages 1 to 3 are sequential. In addition, stages 3 and 4 usually overlap, being these two the more important for the final coating thickness

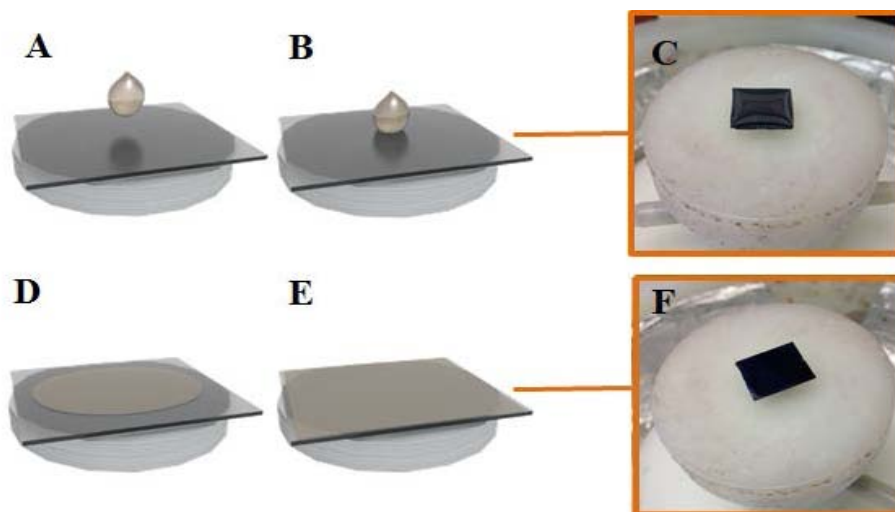
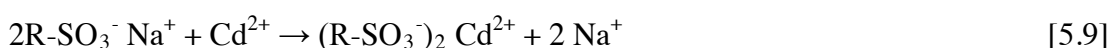
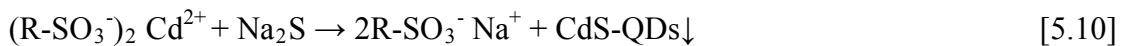


Figure 5.14: Schematic representation of SC of SPEEK over silicon wafers: dropping of SPEEK (A) followed by spin – up of SPEEK (B). Actual picture of SPEEK dissolved polymer in DMF interacting with Silicon wafer as product of spin-off stage (C, D). PTF formation after evaporation stage (E, F).

The election of the solvent is fundamental for homogenous coating. In this case, dimethylformamide was selected because of the solubility of SPEEK in it and its volatility, favouring stages 3 and 4 of overall SC process. Thickness control during SC is dependent on the viscosity of the polymer drop to be coated (SPEEK) and its surface tension interaction with the wafer. This factor could be tuned by changing the concentration of SPEEK during deposition (1% to 5% v/v in DMF) and keeping constant the SC parameters such as time, revolutions and acceleration rate.

After obtaining different SPEEK/PTFs with different thicknesses (from 50 to 250 nm as obtained from ellipsometry measurements³⁸) and considering that the ion exchange properties of SPEEK have not been significantly changed during SC, IMS of CdS-QDs can be carried out. The overall process can be described by Equations (5.9) and (5.10) Firstly, from Na⁺ form of SPEEK/PTF (which is the most favourable for the ion exchange) the PTF is loaded with Cd²⁺ ions by a simple ionic exchange between cadmium and sodium ions, Equation (5.9). Equation (5.10) corresponds to the second stage of IMS, where the precipitation of CdS-QDs on the SPEEK/PTF is due to the addition of Na₂S. The regeneration of the initial Na⁺ form of the support is also observed; which makes possible to repeat the overall cycle of IMS in order to increase the amount and thickness of the QDs synthesized.^{11,32,33}





The surface modification of SPEEK/PTF is shown in Figure 5.15. Figure 5.15B shows a (S)TEM picture of CdS-QDs (white dots) and the Energy Dispersive X-Ray (EDS) of Figure 5.15C is a qualitative proof of the presence of the Cd and S in the sample. The size distribution of the QDs on the SPEEK/PTF was determined of HR-TEM images (5.15D and 5.15E) from which a size distribution of $(3.4 \pm 0.3 \text{ nm})$ is obtained.

Electron microscopy images and EDS analysis evidence that IMS is a valid technique for the synthesis of CdS-QDs in 2D polymeric supports such as SPEEK/PTFs prepared by SC. In addition, QDs size distribution was similar to other FMNPs synthesized by IMS on SPEEK 3D films.²³

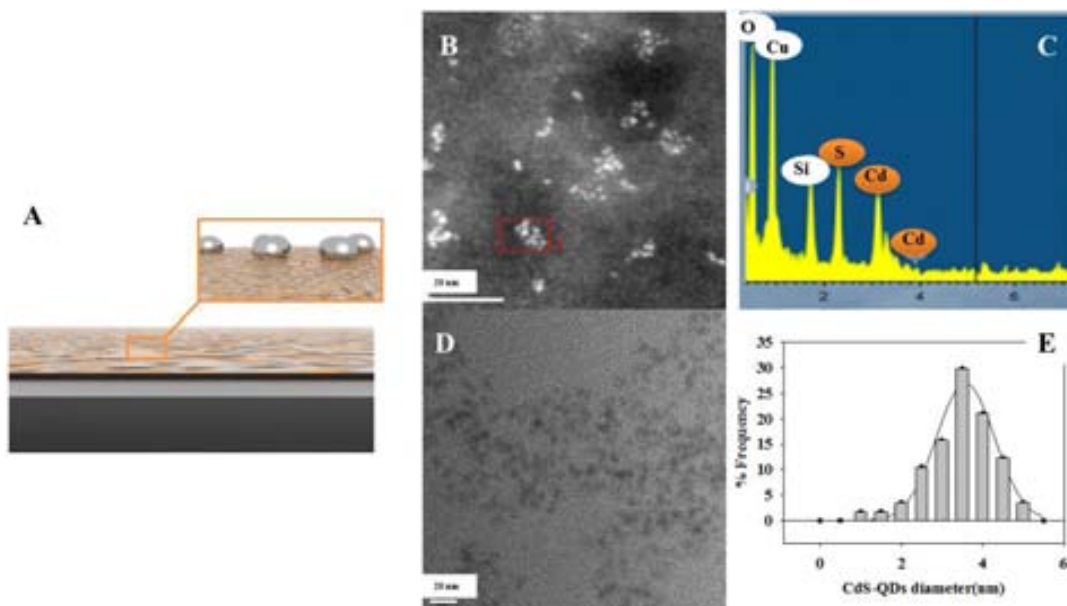


Figure 5.15: A) Schematic representation of IMS of CdS-QDs on SPEEK PTFs. B) (S)TEM picture of CdS-QDs with their corresponding EDS on C. D) HR-TEM image and size distribution histogram of QDs (E).

5.2.3 Intermatrix Synthesis of CdS-QDs on Nanodiamonds (CdS-QDs@NDs)

NDs are less toxic nano carbon forms compared with MWCNTs. Their feasibility of applications due to their biocompatibility and high temperature resistant, make them an interesting matrix for the development of new low-dimensional carbon nanomaterials.³⁹⁻⁴¹

NDs usually present diameters from 4 to 5 nm and tend to agglomerate³⁹ Experimental characterization of raw NDs showed a size distribution value of 3.5 ± 0.3 nm. Agglomerates can be avoided by ultrasonication of the sample before TEM analysis (see Figure 5.16).

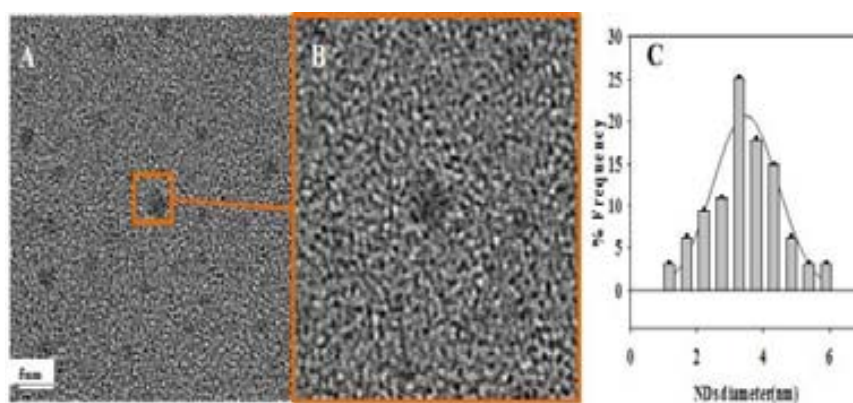
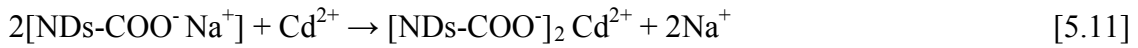


Figure 5.16: HR-TEM images of NDs (A,B magnification $B \gg A$) and raw NDs size distribution histogram(C).

The acidic treatment of the NDs leads to the appearance of carboxylic groups on their surface. Consequently, the activated NDs represent an analogous form of carboxylic polymers (eg. carboxylic resins and fibres) in which IMS was successfully applied for the preparation of FMNPs.^{14,42}

IMS has never been used before for the surface modification of 0 D supports as NDs. Even though; as it is based on the ion exchange functionality of the support; the IMS of CdS-QDs on NDs procedure proposed is described by Equations (5.11) and (5.12).



Equation (5.11) shows the Na^+ form of NDs. Sodium ion is exchanged by Cd^{2+} to complete the initial stage of IMS. Then, NDs sodium ion form is regenerated which makes feasible the repetition of IMS cycles, as can be seen in Equation (5.12). In spite of this fact, it is important to highlight the size limitation of the reactive surface support (average 3.5 nm). In addition, the expected size of the CdS-QDs on these NDs supports is even smaller than the ones obtained on SPEEK/PTHs.

The presence of CdS-QDs on the NDs was evaluated and proved by HR-TEM, (S)TEM pictures and EDS analysis (see Figure 5.17). The EDS spectra of raw NDs (Figure 5.17D) and modified-NDs with CdS-QDs (Figure 5.17E) were compared. The last spectrum verifies the presence of cadmium and sulphide.

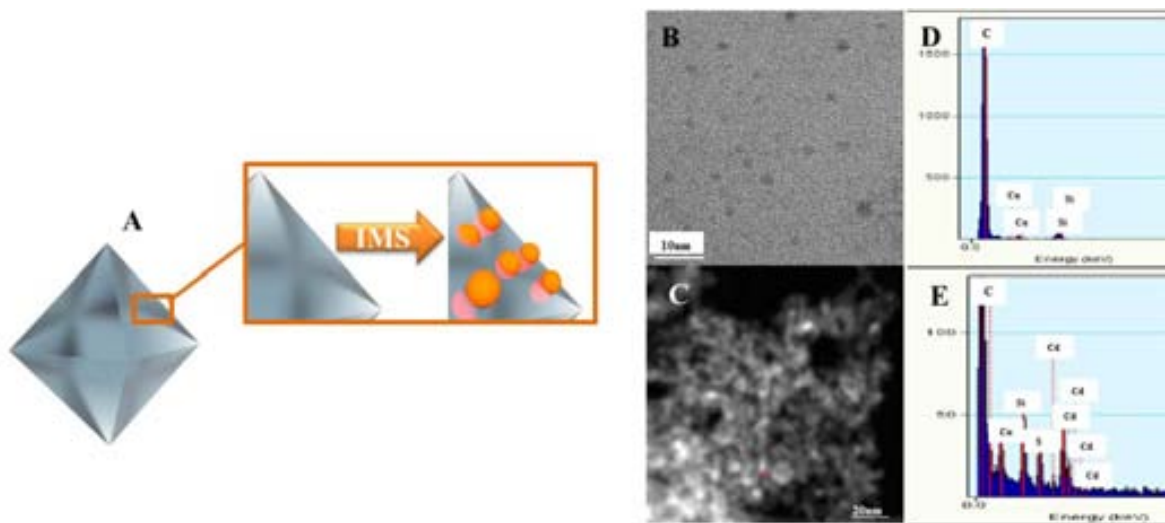


Figure 5.17: A) Schematic representation of IMS CdS-QDs on NDs. B) HR-TEM image of raw NDs and EDS spectra on D. C) (S)TEM image of CdS-QDs modified NDs and corresponding EDS spectra on E.

5.2.4 Concluding Remarks:

IMS demonstrates to be a valid route for the preparation of multi-dimensional Nanocomposite materials (from 0 Ds such as NDs to 3 D as granulated exchange polymers) by the modification of different types of reactive surfaces with FMNPs. It can be concluded that IMS is a non-aggressive and environmentally friendly technique, applicable for the functionalization of MWCNTs, NDs and PTFs with CdS-QDs with favourable distribution as shown in electron microscopy characterization.

References:

- (1) Adams, C. Applied Catalysis: A Predictive Socioeconomic History. *Top. Catal.* **2009**, *52*, 924–934.
- (2) Van Hove, M. a. From Surface Science to Nanotechnology. *Catal. Today* **2006**, *113*, 133–140.
- (3) Wang, Z.; Chen, G.; Ding, K. Self-Supported Catalysts. *Chem. Rev.* **2009**, *109*, 322–359.
- (4) Centi, G.; Perathoner, S. Novel Catalyst Design for Multiphase Reactions. *Catal. Today* **2003**, *79-80*, 3–13.
- (5) Biffis, A.; Zecca, M.; Basato, M. Palladium Metal Catalysts in Heck C–C Coupling Reactions. *J. Mol. Catal. A Chem.* **2001**, *173*, 249–274.
- (6) Sullivan, J. a.; Flanagan, K. a.; Hain, H. Suzuki Coupling Activity of an Aqueous Phase Pd Nanoparticle Dispersion and a Carbon nanotube/Pd Nanoparticle Composite. *Catal. Today* **2009**, *145*, 108–113.
- (7) Batail, N.; Genelot, M.; Dufaud, V.; Joucla, L.; Djakovitch, L. Palladium-Based Innovative Catalytic Procedures: Designing New Homogeneous and Heterogeneous Catalysts for the Synthesis and Functionalisation of N-Containing Heteroaromatic Compounds. *Catal. Today* **2011**.
- (8) Najar, H.; Saïd Zina, M.; Ghorbel, a. Catalytic Activity of Palladium Supported on Mesoporous Modified Y-Zeolite in Methane Combustion. *Kinet. Catal.* **2010**, *51*, 602–608.
- (9) Polshettiwar, V.; Luque, R.; Fihri, A.; Zhu, H.; Bouhrara, M.; Basset, J.-M. Magnetically Recoverable Nanocatalysts. *Chem. Rev.* **2011**.

- (10) Kung, H. H.; Kung, M. C. Nanotechnology: Applications and Potentials for Heterogeneous Catalysis. *Catal. Today* **2004**, *97*, 219–224.
- (11) Ruiz, P.; Muñoz, M.; Macanás, J.; Turta, C.; Prodius, D.; Muraviev, D. N. Intermatrix Synthesis of Polymer Stabilized Inorganic Nanocatalyst with Maximum Accessibility for Reactants. *Dalton Trans.* **2010**, *39*, 1751–1757.
- (12) Muraviev, D. N. Inter-Matrix Synthesis of Polymer Stabilized Metal Nanoparticles for Sensor Applications. *Contrib. to Sci.* **2005**, *3*, 19–32.
- (13) Muraviev, D. N.; Ruiz, P.; Muñoz, M.; Macanás, J. Novel Strategies for Preparation and Characterization of Functional Polymer-Metal Nanocomposites for Electrochemical Applications. *Pure Appl. Chem.* **2008**, *80*, 2425–2437.
- (14) Alonso, A.; Macanás, J.; Safir, A.; Muñoz, M.; Vallibera, A.; Prodius, D.; Melnic, S.; Turta, C.; Muraviev, D. N. Donnan-Exclusion-Driven Distribution of Catalytic Ferromagnetic Nanoparticles Synthesized in Polymeric Fibers. *Dalton Trans.* **2010**, *39*, 2579–2586.
- (15) Witten, T. A.; Sander, L. M. Diffusion-Limited Aggregation. *Phys. Rev. B* **1983**, *27*, 5686–5697.
- (16) ROTHSCILD, W. G. Fractals in Heterogeneous Catalysis. *Catal. Rev. Sci. Eng.* **33**, 71–107.
- (17) Romeu, D.; Gómez, A.; Ramírez, J.; Silva, R.; Pérez, O.; González, A.; Yacamán, M. Surface Fractal Dimension of Small Metallic Particles. *Phys. Rev. Lett.* **1986**, *57*, 2552–2555.
- (18) Sander, L.; Ghaisas, S. Fractals and Patterns in Catalysis. *Phys. A Stat. Mech. its Appl.* **1996**, *233*, 629–639.
- (19) Alonso, A.; Vigués, N.; Muñoz-Berbel, X.; Macanás, J.; Muñoz, M.; Mas, J.; Muraviev, D. N. Environmentally-Safe Bimetallic Ag@Co Magnetic Nanocomposites with Antimicrobial Activity. *Chem. Commun. (Camb)*. **2011**, *47*, 10464–10466.
- (20) Alonso, A.; Bastos-arrieta, J.; Davies, G. L.; Gun, Y. K.; Vigués, N.; Muñoz-berbel, X.; Macanás, J.; Mas, J.; Muñoz, M.; Muraviev, D. N. Ecologically Friendly Polymer-Metal and Polymer-Metal Oxide Nanocomposites for Complex Water Treatment.
- (21) Alonso, A.; Muñoz-Berbel, X.; Vigués, N.; Rodríguez-Rodríguez, R.; Macanás, J.; Mas, J.; Muñoz, M.; Muraviev, D. N. Intermatrix Synthesis of Monometallic and Magnetic Metal/metal Oxide Nanoparticles with Bactericidal Activity on Anionic Exchange Polymers. *RSC Adv.* **2012**, *2*, 4596–4599.
- (22) Domènech, B.; Muñoz, M.; Muraviev, D. N.; Macanás, J. Polymer-Stabilized Palladium Nanoparticles for Catalytic Membranes: A High Polymer Fabrication. *Nanoscale Res. Lett.* **2011**, *6*, 406.

- (23) Ruiz, P.; Muñoz, M.; Macanás, J.; Muraviev, D. N. Intermatrix Synthesis of Polymer–Copper Nanocomposites with Tunable Parameters by Using Copper Comproportionation Reaction. *Chem. Mater.* **2010**, *22*, 6616–6623.
- (24) Domènech, B.; Muñoz, M.; Muraviev, D. N.; Macanás, J. Uncommon Patterns in Nafion Films Loaded with Silver Nanoparticles. *Chem. Commun. (Camb)*. **2014**, *50*, 4693–4695.
- (25) Muñoz, J.; Bastos-Arrieta, J.; Munoz, M.; Muraviev, D. N.; Céspedes, F.; Baeza, M. Simple Green Routes for the Customized Preparation of Sensitive Carbon Nanotubes/epoxy Nanocomposite Electrodes with Functional Metal Nanoparticles. *RSC Adv.* **2014**.
- (26) Elliott, S. D.; Moloney, M. P.; Gun'ko, Y. K. Chiral Shells and Achiral Cores in CdS Quantum Dots. *Nano Lett.* **2008**, *8*, 2452–2457.
- (27) Petryayeva, E.; Algar, W. R.; Medintz, I. L. Quantum Dots in Bioanalysis: A Review of Applications across Various Platforms for Fluorescence Spectroscopy and Imaging. *Appl. Spectrosc.* **2013**, *67*, 215–252.
- (28) Moloney, M. P.; Gun'ko, Y. K.; Kelly, J. M. Chiral Highly Luminescent CdS Quantum Dots. *Chem. Commun. (Camb)*. **2007**, *7345*, 3900–3902.
- (29) Bera, D.; Qian, L.; Tseng, T.-K.; Holloway, P. H. Quantum Dots and Their Multimodal Applications: A Review. *Materials (Basel)*. **2010**, *3*, 2260–2345.
- (30) Ruiz, P.; Macanás, J.; Muñoz, M.; Muraviev, D. N. Intermatrix Synthesis: Easy Technique Permitting Preparation of Polymer-Stabilized Nanoparticles with Desired Composition and Structure. *Nanoscale Res. Lett.* **2011**, *6*, 343.
- (31) Son, J. S.; Park, K.; Kwon, S. G.; Yang, J.; Choi, M. K.; Kim, J.; Yu, J. H.; Joo, J.; Hyeon, T. Dimension-Controlled Synthesis of CdS Nanocrystals: From 0D Quantum Dots to 2D Nanoplates. *Small* **2012**, *8*, 2394–2402.
- (32) Muraviev, D. N.; Macanás, J.; Ruiz, P.; Muñoz, M. Synthesis, Stability and Electrocatalytic Activity of Polymer-Stabilized Monometallic Pt and Bimetallic Pt/Cu Core-Shell Nanoparticles. *Phys. Status Solidi* **2008**, *205*, 1460–1464.
- (33) Muraviev, D.; Macanas, J.; Farre, M.; Munoz, M.; Alegret, S. Novel Routes for Inter-Matrix Synthesis and Characterization of Polymer Stabilized Metal Nanoparticles for Molecular Recognition Devices. *Sensors Actuators B Chem.* **2006**, *118*, 408–417.
- (34) Chou, K.-S.; Huang, K.-C.; Lee, H.-H. Fabrication and Sintering Effect on the Morphologies and Conductivity of Nano-Ag Particle Films by the Spin Coating Method. *Nanotechnology* **2005**, *16*, 779–784.
- (35) Decher, G.; Schlenoff, J. B. Multilayer Thin Films. **2012**.
- (36) Sahu, N.; Parija, B.; Panigrahi, S. Fundamental Understanding and Modeling of Spin Coating Process: A Review. *Indian J. Phys.* **2009**, *83*, 493–502.

- (37) Höcker, H. Plasma Treatment of Textile Fibers. *Pure Appl. Chem.* **2002**, *74*, 423–427.
- (38) Redel, E.; Mirtchev, P.; Huai, C.; Petrov, S.; Ozin, G. a. Nanoparticle Films and Photonic Crystal Multilayers from Colloidally Stable, Size-Controllable Zinc and Iron Oxide Nanoparticles. *ACS Nano* **2011**, *5*, 2861–2869.
- (39) Mochalin, V. N.; Shtenderova, O.; Ho, D.; Gogotsi, Y. The Properties and Applications of Nanodiamonds. *Nat. Nanotechnol.* **2012**, *7*, 11–23.
- (40) Purto, K. V.; Petunin, A. I.; Burov, A. E.; Puzyr, A. P.; Bondar, V. S. Nanodiamonds as Carriers for Address Delivery of Biologically Active Substances. *Nanoscale Res. Lett.* **2010**, *5*, 631–636.
- (41) Fu, C.-C.; Lee, H.-Y.; Chen, K.; Lim, T.-S.; Wu, H.-Y.; Lin, P.-K.; Wei, P.-K.; Tsao, P.-H.; Chang, H.-C.; Fann, W. Characterization and Application of Single Fluorescent Nanodiamonds as Cellular Biomarkers. *Proc. Natl. Acad. Sci. U. S. A.* **2007**, *104*, 727–732.
- (42) Alonso, A.; Muñoz-Berbel, X.; Vigués, N.; Macanás, J.; Muñoz, M.; Mas, J.; Muraviev, D. N. Characterization of Fibrous Polymer Silver/cobalt Nanocomposite with Enhanced Bactericide Activity. *Langmuir* **2012**, *28*, 783–790.

“The journey is the reward”

-Steve Jobs-

Conclusions

6. Conclusions

This section summarizes the principal conclusive results obtained through the development of this PhD Thesis, focused on the application of the Intermatrix Synthesis Technique coupled with the Donnan Exclusion Effect (DEEIMS) as green methodology for the preparation of different bifunctional nanocomposites (BFNCs). The main aim of the PhD research included surface modification of reactive matrices with functional metal nanoparticles (FMNPs) by different DEEIMS routes, the evaluation of the properties of the BFNCs and looking for feasible applications for them

For the research based on BFNCs containing FMNPs, particular emphasis has been devoted to modifying nanoparticle surface chemistry, size, and shape to tailor the thermodynamic driving forces in the assembly process. Fundamental understanding of the role of the ion exchange, reducing agents, metal precursors and the matrix itself; have been taken into account and described as the characterization of BFNCs allows concluding information ,

In addition, recent developments in DEEIMS exposed in this thesis lead the preparation of different kind of nanocrystals such as quantum dots (QDs) and FMNPs; with a wide range of compositions and geometries, with future feasible approaches and applications, since it has been proved that the main requirement for the application of this environmentally friendly technique, is to find a reactive surface in terms of ion exchange functionality.

The generation of results presented in this Thesis, included some general stages through the design of the optimized preparation of BFNCs:

- a) Understanding and optimizing DEEIMS for customized preparation of BFNCs:
- b) Understanding the surface changes and the impact on ion exchange properties of the reactive surfaces due to DEEIMS.
- c) Enhancing the performance of the BFNCs for specific applications.
- d) Designing further approaches of DEEIMS: novel matrices.

Consequently, specific conclusions obtained are listed below

- 1) DEEIMS can be considered as a valid technique for modification of both anionic and cationic exchangers. Both primary ion exchange stages (loading the NPs precursors and reduction) can be applied in the “classical” or “symmetrical” version depending on the surface to be modified with NPS.
- 2) The loading stage of DEEIMS for both anionic and cationic exchangers proved to be efficient due to the previous adequacy of the reactive matrix with a more suitable ionic form: Na-form for cationic exchangers and Cl-form anionic exchangers. This means that the ion exchange process and incorporation of the FMNPs precursors is more favourable; obtaining loading exchange efficiencies up to 85% in average.
- 3) The driven force of the customized distribution of the FMNPs in the BFNCs was proved to be DEE. Depending of the charge of the functional groups of the reactive matrix and the ionic charge of the reducing agent, DEEIMS leads to the customized spatial distribution of FMNPs in the BFNCs. Therefore, ionic reducing agents (NaBH_4 and Ascorbic Acid) allow obtaining BFNCs with FMNPs mainly located on the surface of polymer for both anionic and cationic exchangers. On the contrary; when using neutral reducing agents (such as, e.g. formaldehyde) the distribution of FMNPs appears to be homogeneous throughout the volume of BFNC.
- 4) The size distribution of FMNPs has been shown to be the result of reducing reduction stage of DEEIMS, more specifically of the reduction agent strength. It has been verified that the use of a strong reducing agent such as NaBH_4 in DEEIMS leads to formation of smaller NPs than when a “softer” reducing agent such as AA is used, mainly due to change of the nucleation rate during the reduction stage for both ion-exchange systems.
- 5) The second stage of DEEIMS (NPs formation) can be modified by using the precipitation reaction instead of the reduction one by substituting the reduction agent with the precipitation one. By using this version of DEEIMS technique the synthesis of CdS-QDs on a gel-type cation-exchange polymer was achieved, with a favourable distribution of the QDs mainly on the surface of the matrix

and with high efficiency of the loading stage. This is the first time in our research group that QDs were prepared by using DEEIMS. Due to their interesting properties, simple green methodologies for the preparation of BFNCs containing QDs, can be considered as a new priority for their further applications.

- 6) By controlling the concentration of the reducing agent, its reduction power and the addition rate, DEEIMS becomes a suitable technique for the preparation of controlled-shape nanostructures, such as e.g. Ag-cubic nano- and microstructures. Electron microscopy characterization and metal content analysis verified the chemical identity of these structures. Accordingly with the spatial distribution advantage offered by DEEIMS for NPs, it is conserved when these Ag-cubic structures are prepared.
- 7) The galvanic displacement stage carried out after DEEIMS represents a new approach applicable for preparation of BFNCs. It is important to emphasize that by this extended approach, the DEEIMS of Au-NPs on cationic exchangers is possible when a suitable galvanic replacement pair is selected. This means, to use DEEIMS for the preparation of low cost “sacrificial” NPs (such as Cu) and then to carry out a galvanic replacement stage with a more valuable metal as Au. The efficiency of galvanic replacement coupled with DEEIMS has proved to be almost 100%.
- 8) Regarding the extension of DEEIMS with galvanic replacement, the preparation of AgAu bimetallic cubic structures can be prepared using previously synthesized Ag-cubic structures as templates. The spatial profile distribution of AgAu in the hybrid structures and the electron microscopy characterization have shown that these structures tend to be hollow. This can be explained by the Kirkendall Effect during the galvanic replacement stage; in which the diffusion of Au is slower than the Ag. The tuned preparation of these hollow hybrid structures opens a brand new research field due to this extension of DEEIMS.
- 9) iDEEIMS of Ag-MNPs on cationic gel-type polymers induces the appearance of nanoporosity in the BFNCs. This improves the mass-transfer characteristics of

the matrix what is particularly important for carrying out the ion exchange processes on these materials. These changes can be explained due to the localization of the Ag-NPs mainly in the surface of the matrix in which the interaction with the polymeric changes leads to the increase of the cross-linking degree and therefore the appearance of the “worm-like” structures on the polymer surface.

- 10) Evaluation of the ion exchange properties of BFNCs with surface morphological changes before and after DEEIMS, shows that the ion exchange capacity of the polymer is not essentially changed after its modification with FMNP and the morphological changes observed. It is verified by the breakthrough curve profiles obtained on the unmodified matrix and modified with Ag-FMNPs. As it also follows from these data, the resistance of the matrix towards ions diffusion can be minimized by varying the thickness of FMNPs layer and it can reach the same value as that of the unmodified polymer.
- 11) It is demonstrated that DEEIMS is also suitable for the preparation of heterogeneous nanocatalysts with the most favorable distribution of nanocatalyst NPs, such as Pd-NPs containing BFNCs. The catalytic activity of these BFNCs was checked in the Suzuki and proved to be effective and recyclable.
- 12) The application of DEEIMS does not depend on the scale of the supporting reactive surface but just on its ion exchange functionality. Considering this fact, it has been shown the feasibility of DEEIMS application for modification of other novel reactive matrices such as carbon nanotubes (CNTs) and nanodiamonds (NDs).
- 13) The classic version of DEEIMS was carried out on CNTs to obtain different noble metal NPs, due to the carboxylic functionality of this support. Moreover, the extension of DEEIMS with galvanic replacement was used as well for the preparation of Au-NPs on the CNTs. The final application of these BFNCs is for the enhancement of electrochemical sensors response to specific analytes. In addition, a DEEIMS-precipitation technique was carried out on CNTs to obtain CdS-QDs.

14) DEEIMS demonstrates to be a valid route for the preparation of multi-dimensional (from 0 D to 3 D) BFNCs (by the modification of different types of reactive surfaces with FMNPs). It can be concluded that DEEIMS is a non-aggressive and environmentally friendly technique, applicable for the functionalization of CNTs, Nanodiamonds (NDs) with QDs with favourable distribution.

The main conclusion of these PhD thesis, is that DEEIMS demonstrated to be an effective synthetic methodology suitable for the preparation BFNCs in reactive surfaces of either functionality, i.e. bearing either negatively (e.g., cation exchangers) or positively (e.g., anion exchangers) charged functional groups. It was proved the feasible application of DEEIMS for the modification of novel matrices such as nanodiamonds with FMNPs. In further research, the modification of novel interesting reactive surfaces such as graphene may be accomplished by the optimization of the process and adequacy of the matrix.

Annexes

ANNEX 1



Donnan exclusion driven intermatrix synthesis of reusable polymer stabilized palladium nanocatalysts

Julio Bastos-Arrieta^a, Alexandr Shafir^a, Amanda Alonso^a, Maria Muñoz^a, Jorge Macanás^b, Dmitri N. Muraviev^{a,*}

^a Analytical Chemistry Division, Chemistry Department, Autonomous University of Barcelona, 08193 Bellaterra, Barcelona, Spain

^b Department of Chemical Engineering, UPC, Terrassa 08222, Barcelona, Spain

ARTICLE INFO

Article history:

Received 14 September 2011

Received in revised form

16 December 2011

Accepted 11 January 2012

Available online 15 February 2012

Keywords:

Intermatrix synthesis

Donnan effect

Composite

Palladium

Nanocatalyst

Suzuki cross coupling reaction

ABSTRACT

This paper reports the Donnan exclusion driven intermatrix synthesis (DEDIMS) of Pd polymer-stabilized metal nanocatalysts (PSMNCs) in an anion exchange resin as a novel heterogeneous catalyst for Suzuki cross-coupling reaction (SCCR). An average diameter of the obtained PSMNCs was around 35 nm and the catalytic performance was found to be proportional to the Pd content in the nanocomposite. Stability of the catalyst was evaluated within several reaction cycles.

© 2012 Elsevier B.V. All rights reserved.

1. Introduction

Heterogeneous catalysis represents one of the fields of the modern science and technology where the application of ultrafine catalyst particles dates back to the beginning of the last century [1,2]. Application of the heterogeneous catalysis within the last decades has been strongly stimulated by the development of the new generation of catalysts with nanometer dimensions. The development of the catalysts of this type requires in many instances the search of appropriate supports to simplify their practical applications [3,4].

On the other hand, the development of novel synthesis approach requires in many instances the catalysts with high quality active sites, which are characterized by good structure–performance

relationships. This refers for example, to carbon–carbon bond formation reactions, which represent a fundamental tool for organic synthesis, as it can be used in the preparation of fine chemicals. Most frequently used reactions of this type are palladium catalyzed C–C coupling reactions, such as for instance, Suzuki cross-coupling reaction (SCCR), widely known for its applicability to the synthesis of fine chemicals [5–7].

Polymeric supports play in this regard a very important role for several reasons such as, for example the ease of their preparation in the most appropriate physical form (e.g., granulated, fibrous, membranes, etc.), the possibility to produce the macroporous matrices with highly developed surface area and some others. However, the immobilization of the catalyst nanoparticles on the appropriate polymeric support represents a separate task, which in some instances is not so simple [8,9].

The use of the functional polymers as supports for the heterogeneous nanocatalysts has in this sense, one more important advantage dealing with the possibility to synthesize the catalyst nanoparticles directly at the “point of use”, i.e. inside the supporting polymer. In the case of the metal catalyst nanoparticles (MCNPs) this results in the formation of the catalytically active polymer–metal nanocomposites [10].

The intermatrix synthesis (IMS) represents one of the most efficient and simple techniques, which can be used for this purpose [2,10–13]. The major part of the work in this field has been done

Abbreviations: MNPs, Metal nanoparticles; MNCs, Metal nanocatalysts; PSMNCs, Polymer-stabilized metal nanocatalysts; DEDIMS, Donnan exclusion driven intermatrix synthesis; SCCR, Suzuki cross-coupling reaction; IEC, Ion exchange capacity; MCNPs, Metal catalyst nanoparticles; ICP-OES, Inductively coupled plasma optical emission spectrometry; ICP-MS, Inductively coupled plasma mass spectrometry; DEE, Donnan exclusion effect; SEM, Scanning Electron Microscopy; TEM, Transmission Electron Microscopy; IMS, intermatrix synthesis.

* Corresponding author at: Grup de Sensors i Biosensors, Departament de Química, Universitat Autònoma de Barcelona, 08193 Bellaterra, Barcelona, Spain. Tel.: +34 935 814 860.

E-mail address: dimitri.muraviev@uab.es (D.N. Muraviev).

with the polymers bearing negatively charged functional groups (cation exchange membranes, resins or fibers), which first have to be loaded with the desired metal ions (MCNPs precursors) followed by their reduction to zero-valent state (MCNPs) by using an appropriate reducing agent [10–17]. Several recent publications by the authors describe the IMS of MCNPs with the most favorable distribution near the surface of nanocomposite for catalytic applications [3,10]. This version of IMS is based on the coupling of the “classic” version of IMS technique with the Donnan exclusion effect [8–11].

In general, the desired distribution of MCNPs is achieved by using the ionic reducing agents bearing the charge of the same sign as that of the polymeric matrix [18–26]. The action of Donnan exclusion does not allow for the deep penetration of the reducer ions inside the polymer loaded with metal ions. As the result, their reduction proceeds mainly in the surface part of the polymeric matrix [21].

This communication reports the results obtained by the further development of the Donnan effect driven intermatrix synthesis (DEDIMS) technique by its extension to the polymers, which matrices bear the positively charged functional groups (anion exchange polymers or resins). The version of DEDIMS technique, which is applied in this case, can be considered as the “symmetrical reflection” of the previously developed DEDIMS method.

2. Materials and methods

2.1. Reagents and materials

Metal salts as $\text{Pd}(\text{NH}_3)_4\text{Cl}_2 \cdot \text{H}_2\text{O}$, and NaBH_4 (all from Aldrich, Germany), mineral acids and organic compounds for SCCR and solvents (all from Panreac, S.A. Spain) of p.a. grade were used as received. Bidistilled water was used in all experiments.

A portion of granulated Purolite A520E resin of known weight and granule size (~ 0.5 mm in diameter) was washed by bidistilled water and then dried at 80°C for 24 h. The resin was then stirred in NaOH 1 M solution for 6 h to convert it from Cl^- to OH^- form. Finally the polymer was dried at 80°C for 24 h.

2.2. Intermatrix synthesis of Pd-PSMNCs

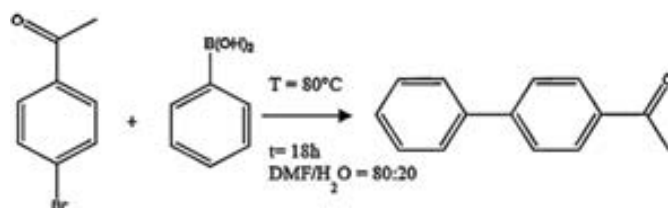
The IMS of Pd-PSMNCs was carried out by the loading of the functional groups of the polymer with reducing agent anions by using 20 mL of 0.1 M aqueous NaBH_4 solution followed by the treatment of the resin with 10 mL of 0.01 M $\text{Pd}(\text{NH}_3)_4\text{Cl}_2$ solution. The last stage resulted in the formation of polymer–metal nanocomposite containing Pd-PSMNCs. Some of the working parameters of the IMS procedure (such as Pd concentration and the experimental conditions) will be detailed in each experiment. This is the symmetric process of the usual performed in the group research.

2.3. Determination of ion exchange capacity (IEC) of resin

The IEC of the polymer was checked before and after IMS of Pd-PSMNCs by using the following procedure: several samples of around 200 mg of Purolite A520E resin with or without Pd-PSMNCs were immersed in aliquots of 25 mL of 0.0059 M Na_2CO_3 and stirred for 4 h. Then aliquots of 20 mL were taken from the resulting solution for titration with HCl 0.0477 M. The IEC values were calculated from the titration results and appeared to equal 1.22 ± 0.04 meq/ g_{resin} before and after IMS of Pd-PSMNCs.

2.4. Analysis of nanocomposite composition

A sample of around 10 mg of PSMNCs-containing material was immersed in 1 mL of *aqua regia* to completely dissolve palladium



Scheme 1. Schematic diagram of Suzuki cross-coupling reaction.

by oxidation. The obtained solution was filtrated through a $0.22 \mu\text{m}$ Millipore filter and adequately diluted for metal content quantification by Inductively Coupled Plasma Optical Emission Spectrometry, ICP–OES (Iris Intrepid II XSP spectrometer from Thermo Electron Co.) and Inductively Coupled Plasma Mass Spectroscopy, ICP–MS (Agilent 7500). An average uncertainty of metal ions determination was in all cases lower than 2%.

2.5. SEM and TEM characterization

Scanning Electron Microscopes (SEM) coupled with an Energy-Dispersive Spectrometer (EDS) Zeiss EVO MA 10 and Zeiss MERLIN FE-SEM and Transmission Electron Microscope (TEM) studies were carried out by using JEOL 2011 and JEOL 1400 microscopes (all from Servei de Microscòpia of Universitat Autònoma de Barcelona). SEM and TEM techniques were used to obtain the metal concentration profiles along the cross-section of the PSMNC-containing materials, morphology of the polymer surface and for determination of MNPs diameter distribution histograms. The nanocomposite samples were prepared by embedment of several granules in an epoxy resin followed by cutting and cross-sectioning with Leica EM UC6 ultramicrotome using a 35° diamond knife (Diatome) at the temperature of liquid nitrogen (-196°C).

2.6. Catalysis of Suzuki cross-coupling reaction

A known quantity of Pd-PSMNCs (corresponding to 1% molar rate of Pd to 4-bromoacetophenone) was mixed with 4-bromoacetophenone 98% (1 mmol), phenylboronic acid 98% (1 mmol), K_2CO_3 (1 mmol) dissolved in the mixture of $\text{DMF}-\text{H}_2\text{O}$ (80:20) and stirred at 80°C for 18 h as it was settle as optimal experimental conditions for this reaction in previous works by using the analogue cation exchanger as a matrix [15]. The conversion degree and the efficiency rate of the reaction were followed by monitoring by gas chromatography (7820A GC, Agilent Technologies) (Scheme 1).

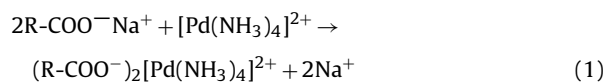
3. Results

3.1. Traditional (classic) and novel versions of IMS technique

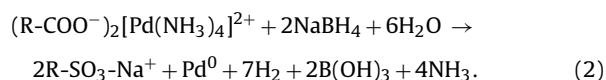
The difference between the “classical” and the novel version of the IMS technique developed in this study become clear after comparison of the respective reaction schemes, which can be written for the case of formation of Pd-MCNPs in the strong acid (a) and the strong base (b) functional polymers as follows:

(a) IMS in cation exchange polymers (classical version):

(1) Metal-loading stage

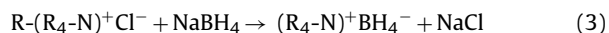


(2) Metal-reduction stage

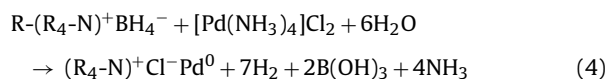


(b) IMS in anion exchange polymers (novel version):

(3) Reducer-loading stage



(4) Metal-loading-reduction stage



As it is seen from the above reaction schemes, the main difference between (a) and (b) versions of IMS consists in the first stage of the process. In the first case the functional groups of the polymer are loaded with the desired metal ions, while in the second case the loading is carried out with desired reducer ions. The second stage in the first case consists in the reduction of metal ions with ionic reducer, located in the external solution. As far as the charge sign of reducer anions coincide with that of the polymer matrix, they cannot deeply penetrate inside the polymer due to the action of the Donnan exclusion effect (DEE) and as the result, the reduction process appears to be “localized” near the surface of the polymer.

Unlike version (a), version (b) of IMS starts with the loading of the functional groups of the polymer with the reducer anions (see first stage, reaction (3)). As the result, the second stage of this version permits to couple the metal-loading and the metal-reduction processes in one step. The metal loading is carried out by using external solution containing metal ions bearing the charge of the same sign as that of the functional groups of the polymer, what does not allow them to deeply diffuse inside the polymer matrix (because of DEE). Again, the reduction of metal ions and therefore, the formation of MCNPs have to proceed near the surface of the polymer. For obvious reasons the second version of IMS technique (version b) can be classified as a sort of the symmetrical reflection of version (a).

In both versions of IMS technique, DEE plays a very important role as it appears to be responsible for the desired nonhomogeneous distribution of MCNPs inside the polymer–metal nanocomposite. The action of this effect is observed in both cases within the second stage of IMS process (see Eqs. (2) and (4)). The following two “driving forces” acting in the opposite directions are responsible for the DEE: (1) the electric field determined by the charge of the polymer matrix [14,15,19,21,22] and (2) the concentration of the ionic component in the external solution (in fact the concentration gradient of this component). The first force rejects the ions of the same charge as that of the functional groups of the polymer while the second one drives these ions to move into the polymer matrix. The first force can be hardly varied as it has a constant value determined by the ion exchange capacity of the polymer and the degree of dissociation of its functional groups. The second force can be easily varied by changing the concentration of respective component

Table 1

Metal content in Pd-PSMNCs nanocomposites synthesized by applying different metal loading-reduction cycles.

Sample	[NaBH ₄](M)	mg _{Pd} /g _{matrix} (+/0.2)	Loading-reduction cycles
MCNP A	0.1	30.8	1
MCNP B	0.05	12.8	1
MNCP C	0.025	4.0	1
MNCP D	0.1	30.4	1
MNCP E	0.1	57.9	2
MNCP F	0.1	61.4	2
MNCP G	0.1	89.9	3

in the external solution, what has to result in the changes in the composition of the final nanocomposite (MNPs content).

The variation of the MNPs content inside the polymer can be also achieved by using the following two additional approaches: (1) incomplete loading of the functional groups of the polymer with respective component (metal ions in the version “a” or reducing agent ions in the version “b” of IMS) prior to carrying out the final stage, and (2) the use of repetitive metal-loading-reduction cycles. The first approach allows for the obtaining of nanocomposites with low MNPs content while the second one permits to substantially increase this value. The results collected in Table 1 confirm the validity of the first (see samples MNCP A–C) approach.

The possibility to use the second approach follows from the above reaction schemes (see reactions (2) and (4)). Indeed, after finishing the metal reduction (IMS version a) or the metal-loading-reduction stages (IMS version b) the functional groups of the polymer appear to be converted back into the initial ionic form (Na-form in the first and Cl-form in the second case). This means that in both cases IMS of MNP cycles can be repeated without any additional pretreatment of the ion exchanger. This has to result in the accumulation of a higher amount of the metal (or MNPs) inside the polymer. This supposition is confirmed by the results obtained when using the novel version of IMS technique (see above version b), which are also presented in Table 1 (see samples D–G). As it is seen, the dependence of the metal amount in the polymer versus the number of metal-loading-reduction cycles carried out follows a linear trend.

3.2. Microscopic characterization of polymer–metal nanocomposites

The results presented in Fig. 1 confirm the validity of the proposed metal distribution. Indeed, as it is seen in SEM images of the cross-sections of the granules of respective polymer–metal nanocomposites shown in this figure, the distribution of Pd-MCNPs obtained by using both versions of IMS technique is quite similar. As it clearly follows from the images shown in Fig. 1, both synthetic methodologies lead to the formation of MCNPs distributed mainly by the surface of the polymer. It is important to emphasize

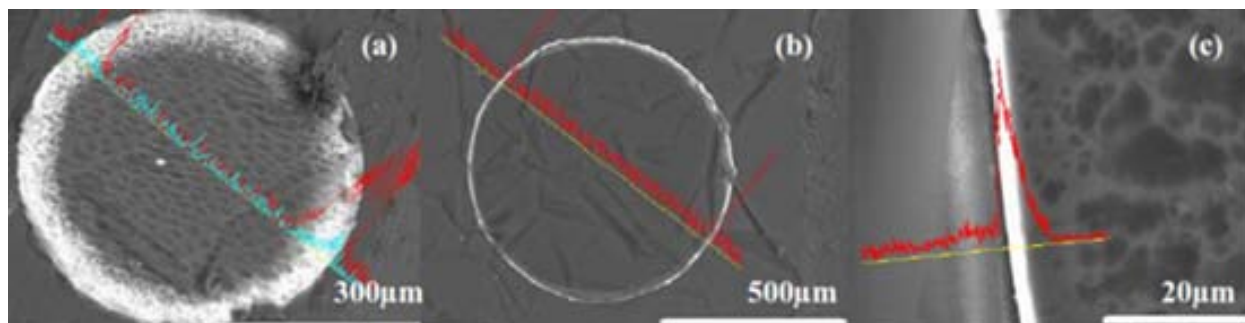


Fig. 1. SEM images of granule cross-sections and respective LineScan EDS spectra showing distribution of Pd-MNPs inside nanocomposites obtained by (a) classic and (b, c) novel version of IMS technique by using cation (a) and anion exchange resins (b,c).

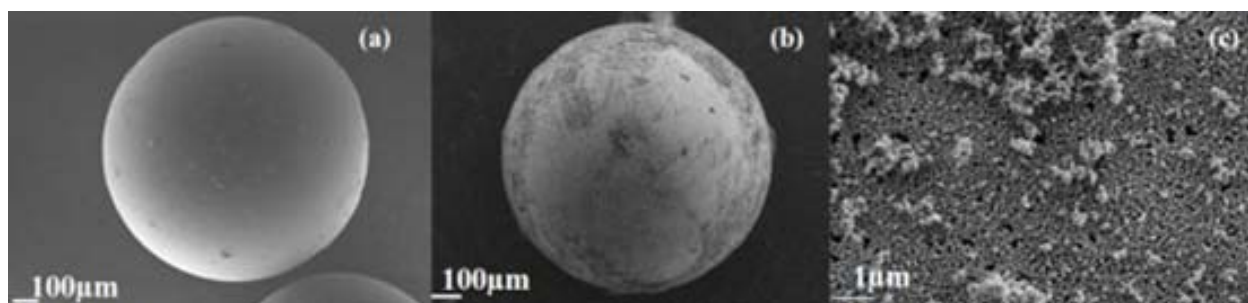


Fig. 2. SEM images of Purolite A520E resin (sample MNCP E as seen in Table 1) before (a) and after (b and c) DEDIMS of Pd-PSMNCS.

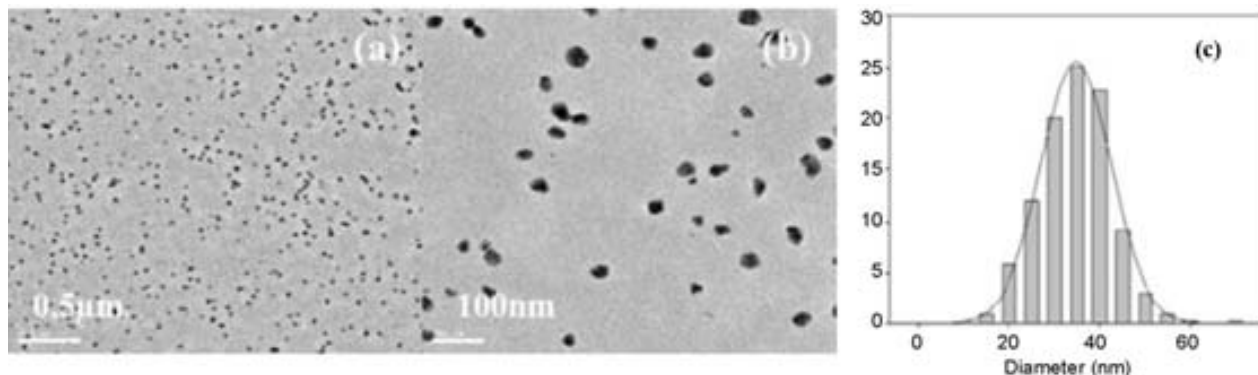


Fig. 3. TEM images (a,b) and size distribution histogram (c) of MCNP A (sample MNCP 3, see Table 1).

that in both cases the MCNPs distribution of this type appears to be the result of the purposeful use of the Donnan effect and does not depend on the functionality of the polymer. The last conclusion is of particular importance as it substantially widens the applicability of IMS technique for the synthesis of catalytically active polymer–metal nanocomposites with the enhanced accessibility of MCNPs for reactants.

One more important conclusion follows from the detailed examination of SEM images of the surface of nanocomposite granules, which are shown in Fig. 2. As it is seen, the surface of the initial ion exchange material looks absolutely smooth and clean (see Fig. 2a). After IMS of Pd-MCNPs the morphology of the polymer surface changes due to the formation of fractal-like structures of partially aggregated Pd-MNPs (see Fig. 2b and c). In this case the formation of MNP fractals on the surface of polymer can be explained by the action of diffusion limited aggregation mechanism. The efficiency of MNP fractals in the catalytic applications is known not to differ dramatically from that of MCNPs due to the insignificant difference of the surface area of the former and the latter [27–29].

The formation of Pd-MNP fractals proceeds only on the surface of the polymer granules, while inside the polymer no MNPs aggregation is observed. This conclusion follows from the TEM images of nanocomposite cross-sections shown in Fig. 3. As it is seen in Fig. 3a and b, Pd-MNPs are well separated from each other and do not form any visible aggregates. This testifies to the high stabilizing efficiency of the polymer. An average diameter of Pd-PSMNCS (corresponding to the maximum on size distribution histogram, see Fig. 3c) equals to 35 nm, what provides a sufficiently high surface area and multiple catalytic centers.

3.3. Catalytic applications of Pd-PSMNCS

Catalytic activity of nanocomposites was tested in the model Suzuki cross-coupling reaction (SCCR) by following the procedure described in Section 2. After finishing the first catalytic cycle

the granulated nanocomposite was separated from the reaction mixture by simple filtration and then reused in sequential cycles. The results of this series of experiments for nanocomposite samples MNCP A–C (see Table 1) are shown in Fig. 4. As it is seen, the nanocomposite with the maximum Pd content (sample A) demonstrates the higher catalytic activity in comparison with other samples. The first two cycles give approximately a 35% reaction yield, which then gradually decreases. The other two samples (B and C) give far lower yields and the results obtained with these samples are not as stable as those obtained with sample A, due to the Pd content achieved in each nanocomposite.

As shown in Fig. 5, a substantial increase of the reaction yield was obtained when using the nanocomposite samples with higher Pd-PSMNCS content (samples MNCP E–G in Table 1). The dependence of the reaction yield obtained within the second catalytic

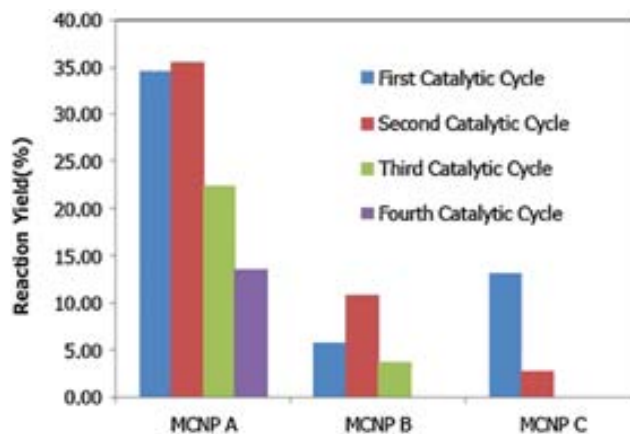


Fig. 4. SCCR yield per catalytic run due to the application of the Pd-PSMNCS.

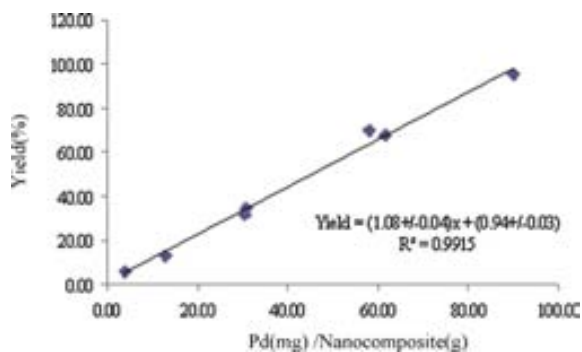


Fig. 5. Lineal increase of SCCR yield as function of palladium content in Pd-PSMNCs containing nanocomposite.

cycle versus absolute Pd content in the nanocomposite (mg Pd/g nanocomposite) is shown in Fig. 5.

As it is seen, the dependence presented in this figure follows the linear trend.

4. Discussion

The novel version of IMS technique developed in this study is focused on the modification of polymers with anion exchange functional groups with catalytically active MNPs (Pd-PSMNCs). The comparison of this novel version of IMS technique with that developed in our previous work permits to classify it as a sort of symmetrical reflection of the previously developed one [14–16,18,19,21]. The main difference between these two versions of IMS method consists in the type of the polymer-immobilized reagent, which is the desired metal ion (MNPs precursor) in version “a” and the reducer ion in version “b”. A similar approach was also used by Sen Gupta et al. to modify anion exchange resins with iron oxide nanoparticles and the posterior application of these nanocomposite materials for large-scale effective removal of arsenic from potable water [30,31]. However, no results obtained by studying the distribution of nanoparticles in the polymer matrix were reported by the authors in their publications.

The polymeric matrices used in all versions (both a and b) of the IMS technique serve both as a sort of nanoreactor for the synthesis of MNPs and also as the stabilizing agent preventing their aggregation and coalescence after formation inside the polymer. The IMS technique is characterized by the following important features:

- (1) The formation of MNPs inside stabilizing polymeric matrix does not influence the IEC of the polymer, what is confirmed by the results of determination of this value before and after IMS of MNPs. This means that the functional groups of the polymer after formation of the nanocomposite are not blocked by the formed nanoparticles and can participate in the ion-exchange reactions.
- (2) After carrying out the IMS of MNPs the functional groups of the polymer in both versions of IMS technique appear to be simultaneously regenerated (i.e., converted back into the initial ionic form). This means that metal-loading-reduction cycles can be repeated to accumulate the desired amount of PSMNCs in the supporting polymer.
- (3) The use of the ionic reducing agents, the ions of which bear the charge of the same sign as that of the functional groups of the polymer, permits to couple IMS technique with Donnan Exclusion Effect (DEE). The DEDIMS version of IMS technique allows for achieving the distribution of PSMNCs being the most favorable for the heterogeneous catalysis applications.
- (4) Immobilization of PSMNCs in the granulated polymer substantially simplifies their catalytic applications and also allows for

an easy recovery of the catalyst from the reaction mixture for reuse by using a simple filtration procedure.

All above features can be considered as definite advantages of the developed in our studies DEDIMS technique as it appears to be applicable for the synthesis of PSMNCs supported on any type of functional polymers.

The absolute amount of PSMNC immobilized on the polymer appears to be connected with the physical form of the catalyst MNPs. At low Pd-PSMNC loading palladium forms MNPs well separated from each other (see Fig. 3). At the higher palladium loading values Pd-MNPs also form the fractal structures, which are partially located on the surface of supporting polymer (see Fig. 2c). However, as it is clearly seen in Fig. 5, both forms of Pd-MNCs (MNPs and fractals) demonstrate quite similar catalytic activity what results in the linear dependence of this parameter on the palladium content in the nanocomposite. In conclusion we would like to emphasize that this publication reports the results of the first successful IMS of catalytically active MNPs in the polymer with anion exchange functionality.

5. Conclusions

The main conclusion, which follows from the results obtained in this study concerns the extension of the IMS technique developed in our previous works to the polymers with anion exchange functionality. Here we demonstrate that an anionic exchange resin (Purolite A520E) can be successfully used for the DEDIMS of Pd-PSMNCs with the most favorable distribution of catalyst MNPs. The catalytic activity of nanocomposites obtained was checked in the Suzuki CCR and the yield of the reaction was shown to be directly proportional to the palladium content in the nanocomposite. It has been also shown that DEDIMS does not affect IEC of the polymeric support what gives a possibility for carrying out consecutive metal-loading reduction cycles. The catalytic activity of the palladium catalyst has been shown to be quite similar to both MNPs and MNP-fractals.

Acknowledgements

Programa Operatiu de Catalunya (FEDER) is acknowledged for the financial support within the project VALTEC09-02-0058. JB also thanks the Autonomous University of Barcelona for the personal grant and Servei de Microscòpia of Universitat Autònoma de Barcelona for the SEM and TEM images.

References

- [1] C. Adams, *Top. Catal.* 52 (2009) 924.
- [2] M. a Van Hove, *Catal. Today* 113 (2006) 133.
- [3] Z. Wang, G. Chen, K. Ding, *Chem. Rev.* 109 (2009) 322.
- [4] G. Centi, S. Perathoner, *Catal. Today* 79–80 (2003) 3.
- [5] A. Biffis, M. Zecca, M. Basato, *J. Mol. Catal.* 173 (2001) 249.
- [6] J. Sullivan, K. Flanagan, H. Hain, *Catal. Today* 145 (2009) 108.
- [7] N. Batail, M. Genelot, V. Dufaud, L. Joucla, Djakovitch, *Catal. Today* (2011).
- [8] H. Najjar, M. Saïd Zina, Ghorbel, *Kinet. Catal.* 51 (2010) 602.
- [9] V. Polshettiwar, R. Luque, A. Fihri, H. Zhu, M. Bouhrara, J.M. Basset, *Chem. Rev.* (2011).
- [10] H.H. Kung, M.C. Kung, *Catal. Today* 97 (2004) 219.
- [11] P. Gómez-Romero, C. Sanchez, *New J. Chem.* 29 (2005) 57.
- [12] J.A. Asensio, S. Borrás, P. Gómez-Romero, *J. Polym. Sci. A: Polym. Chem.* 40 (2002) 3703.
- [13] B. Corain, K. Jerabek, P. Centomo, P. Canton, *Angew. Chem.* 116 (2004) 977.
- [14] P. Ruiz, M. Muñoz, J. Macanás, C. Turta, D. Prodius, D.N. Muraviev, *Dalton Trans.* 39 (2010) 1751.
- [15] A. Alonso, M. Muñoz, J. Macanás, D.N. Muraviev, *Dalton Trans.* 39 (2010) 2579.
- [16] P. Ruiz, M. Muñoz, J. Macanás, D.N. Muraviev, *Chem. Mater.* 22 (2010) 6616.
- [17] D. Prodius, F. Macaev, V. Mereacre, S. Shova, Y. Lutsenco, E. Styngach, et al., *Inorg. Chem. Commun.* 12 (2009) 642.
- [18] D.N. Muraviev, J. Macanás, P. Ruiz, M. Muñoz, *Phys. Status Solidi (A)* 205 (2008) 1460.
- [19] D.N. Muraviev, P. Ruiz, M. Muñoz, J. Macanás, *Pure Appl. Chem.* 80 (2008) 2425.

- [20] P. Barbaro, F. Liguori, *Chem. Rev.* 109 (2009) 515.
- [21] D.N. Muraviev, *Contrib. Sci.* 3 (2005) 19.
- [22] F.G. Donnan, *J. Membr. Sci.* 100 (1995) 45.
- [23] J.D.S. Newman, G.J. Blanchard, *Langmuir ACS J. Surf. Colloid* 22 (2006) 5882.
- [24] C. Yang, J. Xing, Y. Guan, J. Liu, H. Liu, *J. Alloy Compds.* 385 (2004) 283.
- [25] C. Liu, X. Wu, T. Klemmer, N. Shukla, X. Yang, D. Weller, et al., *J. Phys. Chem. B* 108 (2004) 6121.
- [26] W.G. Rothschild, *Catal. Rev.* 33 (2007) 71–107.
- [27] D. Romeu, J. Ramírez, R. Silva, O. Pérez, A. González, M. Yacamán, *Phys. Rev. Lett.* 57 (1986) 2552.
- [28] L. Sander, S. Ghaisas, *Phys. Chem. A* 233 (1996) 629.
- [29] S. Sarkar, P. Chatterjee, L.H. Cumbal, A. Sen Gupta, *Chem. Eng. J.* 166 (2010) 1923.
- [30] S. Sarkar, L. Blaney, A. Gupta, D. Ghosh, A. Sen Gupta, *React. Funct. Polym.* 67 (2007) 1599.
- [31] P. Puttamraju, A. Sen Gupta, *Ind. Eng. Chem. Res.* 45 (2006) 7737.

ANNEX 2

NANO EXPRESS

Open Access

Morphological changes of gel-type functional polymers after intermatrix synthesis of polymer stabilized silver nanoparticles

Julio Bastos-Arrieta¹, Maria Muñoz¹, Patricia Ruiz² and Dmitri N Muraviev^{1*}

Abstract

This paper reports the results of intermatrix synthesis (IMS) of silver metal nanoparticles (Ag-MNPs) in Purolite C100E sulfonic ion exchange polymer of the gel-type structure. It has been shown that the surface morphology of the initial MNP-free polymer is absolutely smooth, but it dramatically changes after the kinetic loading of Ag on the polymer and then IMS of Ag-MNPs. These morphological changes can be explained by the interaction of Ag-NPs with the polymer chains, leading to a sort of additional cross-linking of the polymer. As a result, the modification of the gel-type matrix with Ag-MNPs leads to the increase of the matrix cross-linking, which results in the increase of its surface area and the appearance of nanoporosity in the polymer gel. Ag-MNPs are located near the polymer surface and do not form any visible agglomerations. All these features of the nanocomposites obtained are important for their practical applications in catalysis, sensor applications, and bactericide water treatment.

Keywords: Ion exchange, Metal nanoparticles, Nanocomposite, Intermatrix synthesis, Surface modification, Nanoporosity

Background

Ion exchange materials find numerous large-scale industrial applications in various fields, such as water treatment processes, catalysis, and some others. The efficiency of the use of ion exchangers in some instances can be substantially improved by tailored modification of commercially available ion exchange materials with, for example, functional metal nanoparticles (FMNPs) [1].

The modification of ion exchangers with FMNPs can be carried out by using the intermatrix synthesis (IMS) technique coupled with the Donnan exclusion effect. Such combination allows for production of polymer-metal nanocomposites with the distribution of FMNPs near the surface of the polymer on what appears to be the most favorable in their practical applications. This technique has been used to modify the polymers with cation exchange functionality with FMNPs by using the procedure described by the following sequential stages: (1) immobilization (sorption) of metal or metal complex

ions (FMNP precursors) onto the functional groups of the polymer and (2) their chemical or electrochemical reduction inside the polymer matrix (IMS stage) [2-7].

The use of the functional polymers as supports for the metal nanoparticles (MNPs) and metal oxide nanoparticles has, in this sense, one more important advantage dealing with the possibility to synthesize the FMNPs directly at the 'point of use', i.e., inside the supporting polymer, which results in turn in the formation of the polymer-metal nanocomposites (PMNCs) with desired functionality [8-11].

Ag, due to its antibacterial features, represents one of the hot topics of investigation in the noble metal research. The unusual properties of nanometric scale materials in comparison with those of their macro counterparts give in many instances a number of advantages in their practical applications [12-14]. In fact, Ag-MNPs are widely used due to their more efficient antimicrobial activity in comparison with bulk silver [15]. Some of our previous studies were dealt with the IMS of Ag-NPs in different polymer matrices and application of resulting PMNCs for bactericide water treatment [2,3]. Essentially, in all publications dedicated to the synthesis and application of Ag-MNPs in

* Correspondence: Dimitri.Muraviev@uab.cat

¹Department of Chemistry, Universitat Autònoma de Barcelona, Barcelona 08193, Spain

Full list of author information is available at the end of the article

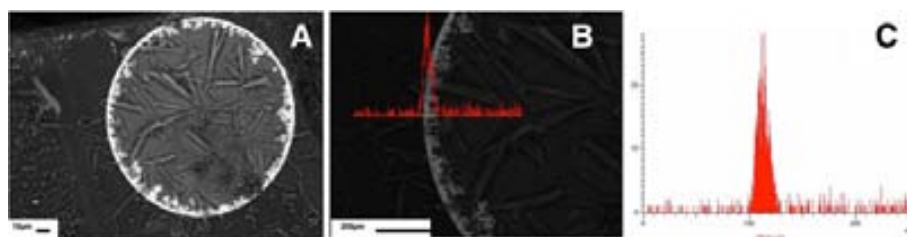


Figure 1 SEM image and line scan EDS spectra. (A) High-resolution SEM image of the cross section of Purolite C100E resin modified with Ag-MNPs. (B, C) Line Scan EDS spectra showing distribution of Ag-MNPs in PMNC.

various supporting polymers, the main attention was paid to the properties of MNPs, i.e., to the properties of just one component of PMNCs, which are determined by PMNC components: the polymer matrix, the NPs, as well as the interaction between them.

In this communication, we report the results obtained by studying the properties of the polymer component of FMNPs composed of Ag-MNPs and Purolite C100E resin of the gel type. It has been shown that IMS of Ag-MNPs in a gel-type polymer results in the dramatic changes of its morphology.

Methods

Reagents and materials

All chemicals, such as AgNO_3 , NaOH (Panreac, S.A., Barcelona, Spain), NaBH_4 (Aldrich, Munich, Germany), mineral acids, and others, were of p.a. grade and were used as received. Bidistilled water was used in all experiments. The ion exchange capacity of C100E resin (Purolite, Bala Cynwyd, PA, USA) was determined by acid-base titration to equal to 2.1 meq g^{-1} .

Synthesis and characterization of PMNCs

The IMS of Ag-NPs in Purolite C100E resin was carried by following the standard procedure which included the loading of the functional groups of the polymer in the initial Na form with Ag^+ ions by using 0.1 M AgNO_3 solution followed by their reduction with NaBH_4 solution.

A sample of approximately 10 mg of PMNC was immersed in aqua regia (1 mL) to completely dissolve Ag-MNPs. The final solution was filtered through a $0.22 \mu\text{m}$ Millipore filter (Millipore Co., Billerica, MA, USA) and diluted for quantification of metal content by using induced coupled plasma optical emission spectrometry (Iris Intrepid II XSP spectrometer, Thermo Electron Co., Waltham, MA, USA) and ICP-MS (Agilent 7500, Agilent Technologies, Inc., Santa Clara, CA, USA). The average uncertainty of metal ion determination was less than 2% in all cases. The specific surface area and the porosity measurements were carried out by using BET technique on Micromeritics ASAP-2000 equipment (Micromeritics Instrument Co., Norcross, GA, USA).

Scanning electron microscope (SEM) coupled with an energy-dispersive spectrometer (EDS) (Zeiss EVO MA 10 and Zeiss MERLIN FE-SEM, Carl Zeiss AG, Oberkochen, Germany) and transmission electron microscope (TEM) studies were carried out using JEOL 2011 and JEOL 1400 (JEOL Ltd., Akishima, Tokyo, Japan). SEM and TEM techniques were used to obtain the metal concentration profiles across the cross section of the FMNP-containing materials, to characterize the morphology of the polymer surface, and for determination of MNP diameters. The PMNC samples were prepared by embedding several granules in the epoxy resin followed by cutting with an ultramicrotome (Leica EM UC6, Leica Microsystems Ltd., Milton Keynes, UK) using a 35° diamond knife (Diatome, Hatfield, PA, USA) at liquid nitrogen temperature (-160°C).

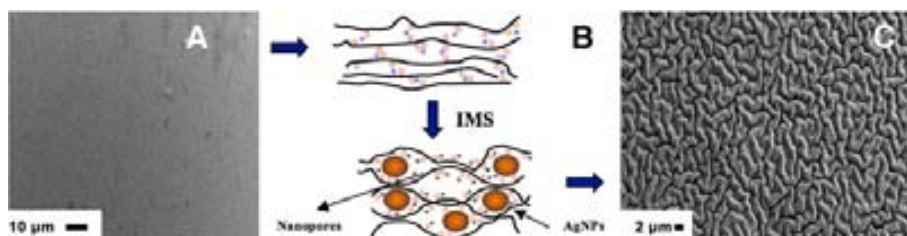


Figure 2 Schematic diagram and SEM images. Schematic diagram of the interaction of MNPs synthesized inside (B) the polymer matrix and SEM images of Purolite C100E resin surface (A) before and (C) after IMS of Ag-MNPs.

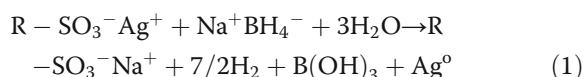
Table 1 Increase of pore diameters in Ag-MNP-containing Purolite C100E resin samples

Sample	Ag-MNP content (mg/g)	BET average pore diameter (nm)
C100E	0	1.9
Ag-C100E PMNC (5 ^a)	112.7 ± 0.5	2.3 ± 0.2
Ag-C100E PMNC (10 ^a)	143.5 ± 0.5	4.4 ± 0.2

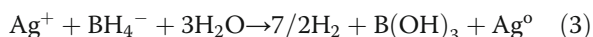
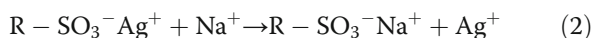
^aNumbers show the time of metal loading cycle carried out.

Results and discussion

The efficiency of the final application of PMNCs (e.g., in catalysis [4,5,16] or in complex water treatment [3,15]) strongly depends on the distribution of FMNPs in the polymer. The IMS technique coupled with the Donnan exclusion effect (DEE-IMS) was shown to allow for achieving the desired distribution of FMNPs near the surface of the hosting polymer [2-4,17,18]. The metal reduction stage of IMS in our case is described by the following equation:



Equation 1 is in fact the sum of the following two equations:



The use of an ionic reducing agent (BH_4^-) bearing the same charge as the functional groups of the polymer is the key point DEE-IMS. Indeed, the polymer matrix bears negative charges due to the presence of well-dissociated functional groups (sulfonic). The borohydride anions also bear negative charges and therefore cannot deeply penetrate inside the matrix due to the action of electrostatic repulsion. The depth of their penetration inside the matrix is balanced by the sum of two driving forces acting in the opposite directions: (1)

the gradient of borohydride concentration and (2) the DEE [19]. The action of the second force limits deep penetration of borohydride anions into the matrix so that reaction (3) proceeds in the surface zone of the polymer which results in the formation of MNPs mainly near the surface of the matrix. The reduction of metal ions with sodium borohydride results in the conversion of functional groups into the initial Na form which permits repetition of the metal loading-reduction cycle (without special resin pretreatment) for increasing the MNP content in FMNPs mainly on the polymer surface (Figure 1).

The appearance of Ag-MNPs in the gel-type polymer is accompanied by their interaction with polymer chains (see Figure 2C) which results in the dramatic changes of polymer surface morphology and appearance of nanopores, wherein the diameter appears to depend on the MNP content in FMNPs (see Table 1).

As it is clearly seen in the SEM images shown in Figure 2, the initially smooth polymer surface (see Figure 2A) dramatically changes after IMS of Ag-MNPs (Figure 2B,C) due to the appearance of a 'worm-like' morphology. Note that similar effects were observed by the authors in IMS of Cu-MNPs in other functional polymers of the gel type [20]. A more detailed structure of the PMNC surface is shown on the high-resolution SEM images presented in Figure 3. As it is clearly seen in Figure 3B,C, the majority of Ag-MNPs are located under the polymer surface which results in the appearance of numerous bumps on the initially smooth polymer surface. Moreover, as one can see in Figure 3C, IMS of Ag-MNPs inside the gel-type polymer results in the appearance of numerous 'nanoholes' (nanopores) on the surface of the polymer which can be considered as a qualitative confirmation of the results obtained by BET analysis and shown in Table 1.

The dramatic changes in morphology of the polymer surface are caused by a strong interaction of Ag-MNPs with the polymer matrix. These morphological changes are associated with the inter-polymer mechanical stress, resulting from a strong interaction between Ag-MNPs and the polymer chains. The changes observed must substantially improve the mass transfer properties of the Purolite®

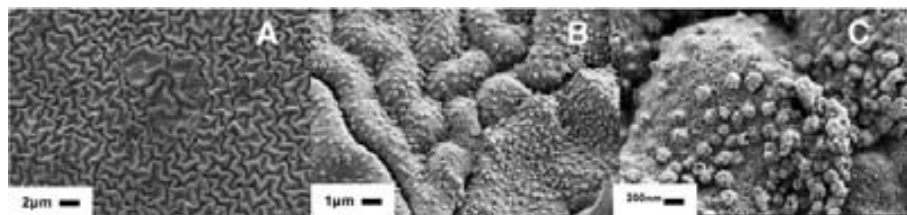


Figure 3 High-resolution SEM images of the surface of Purolite C100E modified with Ag-NPs. Magnification A < B < C. (A) High-resolution SEM image of the increase of cross-linking degree of Purolite C100E resin modified with Ag-MNPs (B,C).

C100E resin in comparison with the initial (MNP-free) polymer due to the appearance of nanoporosity (see Figure 3 and Table 1).

Conclusions

IMS technique coupled with the DEE can be successfully applied for the modification of polymers with FMNPs. This version of IMS results in the situation of FMNPs onto the surface of the obtained nanocomposite materials, providing the most favorable distribution that substantially enhances their practical applications. In addition, the DEE-IMS of Ag-MNPs inside the polymeric matrix results in dramatic changes of their morphology, where the most remarkable changes are observed in the case of gel-type polymers (such as Purolite C100E).

The appearance of Ag-MNP-induced porosity results in the formation of a nanoporous nanocomposite material with enhanced mass transfer characteristics, which in turn, must improve the performance of corresponding sensors and biosensors based upon these novel materials as well as the bactericide assays. It seems important to emphasize that the nanoporosity simultaneously appears in C100E resin in the course of the polymer loading with Ag-MNPs.

Competing interests

The authors declare that they have no competing interests.

Authors' contributions

JB carried out the experimental design and procedure, and material characterization and drafted the manuscript. PR and MM participated with the writing and correction of the manuscript. DNM conceived the study and participated in its design and coordination. All authors read and approved the final manuscript.

Acknowledgments

The authors are sincerely grateful to all their associates cited throughout the text for making this publication possible. Part of this work was supported by the research grant MAT2006-03745, 2006-2009 from the Ministry of Science and Technology of Spain, which is also acknowledged for the financial support of DNM. JB also thanks the Autonomous University of Barcelona for the personal grant.

Author details

¹Department of Chemistry, Universitat Autònoma de Barcelona, Barcelona 08193, Spain. ²MATGAS Research Center, Campus de la UAB, Bellaterra, Barcelona 08193, Spain.

Received: 15 November 2012 Accepted: 20 April 2013

Published: 29 May 2013

References

1. Barbaro P, Liguori F: Ion exchange resins: catalyst recovery and recycle. *Chem Rev* 2009, **109**(2):515–529.
2. Ruiz P, Muñoz M, Macanás J, Muraviev DN: Intermatrix synthesis of polymer–copper nanocomposites with tunable parameters by using copper comproportionation reaction. *Chem Mater* 2010, **22**(24):6616–6623.
3. Alonso A, Muñoz-Berbel X, Vigués N, Rodríguez-Rodríguez R, Macanás J, Mas J, Muñoz M, Muraviev DN: Intermatrix synthesis of monometallic and magnetic metal/metal oxide nanoparticles with bactericidal activity on anionic exchange polymers. *RSC Advances* 2012, **2**(11):4596.
4. Bastos-Arrieta J, Shafir A, Alonso A, Muñoz M, Macanás J, Muraviev DN: Donnan exclusion driven intermatrix synthesis of reusable polymer stabilized palladium nanocatalysts. *Catal Today* 2012, **193**(1):207–212.
5. Domènech B, Muñoz M, Muraviev DN, Macanás J: Catalytic membranes with palladium nanoparticles: from tailored polymer to catalytic applications. *Catal Today* 2012, **193**(1):158–164.
6. Muraviev DN, Ruiz P, Muñoz M, Macanás J: Novel strategies for preparation and characterization of functional polymer-metal nanocomposites for electrochemical applications. *Pure Appl Chem* 2008, **80**(11):2425–2437.
7. Ruiz P, Muñoz M, Macanás J, Turta C, Prodius D, Muraviev DN: Intermatrix synthesis of polymer stabilized inorganic nanocatalyst with maximum accessibility for reactants. *Dalton Trans* 2010, **39**(7):1751–1757.
8. Kudinov A, Solodyannikova YV, Tsabilev OV, Obukhov DV: Deoxygenation of chemically purified water at thermal power plants. *Power Tech Eng* 2009, **43**(2):131–134.
9. Zolotukhina EV, Kravchenko TA: Synthesis and kinetics of growth of metal nanoparticles inside ion-exchange polymers. *Electrochim Acta* 2011, **56**(10):3597–3604.
10. Das B, Sengupta AK: Industrial workstation design: a systematic ergonomics approach. *Appl Ergon* 1996, **27**(3):157–163.
11. Gomez-Romero P, Clément S: Hybrid materials. Functional properties. From Maya Blue to 21st century materials. *New J Chem* 2005, **29**(1):57.
12. Cumbal L: Polymer supported inorganic nanoparticles: characterization and environmental applications. *React Funct Polym* 2003, **54**(1):167–180.
13. Cuentas-Gallegos AK, Lira-Cantú M, Casañ-Pastor N, Gómez-Romero P: Nanocomposite hybrid molecular materials for application in solid-state electrochemical supercapacitors. *Adv Funct Mater* 2005, **15**(7):1125–1133.
14. Ayyad O, Muñoz-Rojas D, Oró-Solé J, Gómez-Romero P: From silver nanoparticles to nanostructures through matrix chemistry. *Journal of Nanoparticle Research* 2009, **12**(1):337–345.
15. Alonso A, Vigués N, Muñoz-Berbel X, Macanás J, Muñoz M, Mas J, Muraviev DN: Environmentally-safe bimetallic Ag@Co magnetic nanocomposites with antimicrobial activity. *Chem Commun* 2011, **47**(37):10464–10466.
16. Alonso A, Shafir A, Macanás J, Vallribera A, Muñoz M, Muraviev DN: Recyclable polymer-stabilized nanocatalysts with enhanced accessibility for reactants. *Catal Today* 2012, **193**(1):200–206.
17. Domènech B, Muñoz M, Muraviev DN, Macanás J: Polymer-stabilized palladium nanoparticles for catalytic membranes: ad hoc polymer fabrication. *Nanoscale Res Lett* 2011, **6**(1):p406.
18. Muraviev DN: Inter-matrix synthesis of polymer stabilised metal nanoparticles for sensor applications. *Contrib Sci* 2005, **3**(1):19–32.
19. Donnan FG: Theory of membrane equilibria and membrane potentials in the presence of non-dialysing electrolytes: a contribution to physical-chemical physiology. *J Membr Sci* 1995, **100**(1):45–55.
20. Muraviev D, Macanas J, Farre M, Munoz M, Alegret S: Novel routes for inter-matrix synthesis and characterization of polymer stabilized metal nanoparticles for molecular recognition devices. *Sensor Actuator B Chem* 2006, **118**(1):408–417.

doi:10.1186/1556-276X-8-255

Cite this article as: Bastos-Arrieta et al.: Morphological changes of gel-type functional polymers after intermatrix synthesis of polymer stabilized silver nanoparticles. *Nanoscale Research Letters* 2013 **8**:255.

Submit your manuscript to a SpringerOpen® journal and benefit from:

- Convenient online submission
- Rigorous peer review
- Immediate publication on acceptance
- Open access: articles freely available online
- High visibility within the field
- Retaining the copyright to your article

Submit your next manuscript at ► springeropen.com

ANNEX 3



Simple synthesis of CdS Quantum Dots on multiwall carbon nanotubes: to make CNTs visible.

Journal:	<i>ChemComm</i>
Manuscript ID:	CC-COM-06-2014-004210
Article Type:	Communication
Date Submitted by the Author:	02-Jun-2014
Complete List of Authors:	Bastos Arrieta, Julio; Universitat Autònoma de Barcelona, Chemistry Muñoz, Jose Maria; Universitat Autònoma de Barcelona, Baeza, Mireia; Universitat Autònoma de Barcelona, Céspedes, Francisco; Universitat Autònoma de Barcelona, Dept. of Chemistry Munoz, Maria; Universitat Autònoma de Barcelona, Muraviev, Dmitri N.; Universitat Autònoma de Barcelona, Departament de Química

Chemical Communications

Guidelines for referees



ChemComm is a forum for urgent high quality communications from across the chemical sciences.

Communications in *ChemComm* should be preliminary accounts of **original and significant work** in any area of chemistry that is likely to prove of wide general appeal or exceptional specialist interest. The 2012 impact factor for *ChemComm* is **6.37**.

Only a fraction of research warrants publication in *ChemComm* and strict refereeing standards should be applied. Our current rejection rate is around 70%. Acceptance should only be recommended if the content is of such **urgency or impact** that rapid publication will be advantageous to the progress of chemical research.

Routine and incremental work – however competently researched and reported – should not be recommended for publication.

Thank you very much for your assistance in evaluating this manuscript.

General Guidance

Referees have the responsibility to treat the manuscript as confidential. Please be aware of our [Ethical Guidelines](#), which contain full information on the responsibilities of referees and authors, and our [Refereeing Procedure and Policy](#).

Supporting information and characterisation of new compounds

Experimental information must be provided to enable other researchers to reproduce the work accurately. It is the responsibility of authors to provide fully convincing evidence for the homogeneity, purity and identity of all compounds they claim as new. This evidence is required to establish that the properties and constants reported are those of the compound with the new structure claimed.

Please assess the evidence presented in support of the claims made by the authors and comment on whether adequate supporting information has been provided to address the above. Further details on the requirements for characterisation criteria can be found [here](#).

When preparing your report, please:

- comment on the originality, significance, impact and scientific reliability of the work;
- state clearly whether you would like to see the article accepted or rejected and give detailed comments (with references, as appropriate) that will both help the Editor to make a decision on the article and the authors to improve it.

Please inform the Editor if:

- there is a conflict of interest;
- there is a significant part of the work which you are not able to referee with confidence;
- the work, or a significant part of the work, has previously been published;
- you believe the work, or a significant part of the work, is currently submitted elsewhere;
- the work represents part of an unduly fragmented investigation.

Submit your report at <http://mc.manuscriptcentral.com/chemcomm>

Analytical Unit
Department of Chemistry
University Autonomous of Barcelona (UAB)
08193, Bellaterra, Barcelona, Spain.
February 10th, 2014
Tel: +34 935812119
e-mail : dimitir.muraviev@uab.cat

RSC Chemical Communications
Editorial Board

We are sending this original research Communication entitled: “**Simple synthesis of CdS Quantum Dots on multiwall carbon nanotubes: to make CNTs visible**” in order to be considered for publication in your journal.

In the present, work we present for the first time the results obtained from the application of Intermatrix Synthesis technique as an effective method for the in situ synthesis of CdS quantum dots (QDs) on the surface of multiwall carbon nanotubes (MWCNTs), based on the ion exchange nature of this material and tested their feasibility for electrochemical sensing purposes.

Moreover, taking into account the supposition of the preferential formation of CdS-QDs on the MWCNTs surface, it was demonstrated that after modification with QDs the intensity of fluorescent emission appears to be directly proportional to the CNTs concentration in water. This can be used for the detection of CNTs in water samples. Thus, a research path is open to develop and optimize a simple analytical procedure based on the above supposition for the detection of MWCNTs in water, replying to the current necessity of analytical methodologies for the determination and quantification of nanomaterials in environmental samples.

We hope that this Communication would fit and be of interest for publication in RSC Chemical Communications Journal.

With best wishes,

Dmitri N. Muraviev

Cite this: DOI: 10.1039/c0xx00000x

www.rsc.org/xxxxxx

ARTICLE TYPE

Simple synthesis of CdS Quantum Dots on multiwall carbon nanotubes: to make CNTs visible.**Julio Bastos-Arrieta^a, Jose Muñoz^a, Maria Muñoz^a, Mireia Baeza^a, Francisco Céspedes^a and Dmitri N. Muraviev^{*a}**⁵ Received (in XXX, XXX) Xth XXXXXXXXX 20XX, Accepted Xth XXXXXXXXX 20XX

DOI: 10.1039/b000000x

In this communication we report a simple and effective method for the *in situ* synthesis of CdS quantum dots (QDs) on the surface of multiwall carbon nanotubes (MWCNTs), based on the ion exchange nature of this material. These QDs have a favourable distribution over the surface of the nanotubes and their fluorescent properties can be used for detection of MWCNTs in water.

The progress in many fields of the modern technology within the last decade is determined by the rapid development and wide application of various nanomaterials (NMs) and nanocomposites on their base.^{1–4} At the same time, insufficient safety of these materials may result in the uncontrollable release of NMs into the environment.^{5–9} Consequently it results in the serious concerns dealing with^{10,11}:

- 1) the approved higher toxicity of many NM in comparison with their bulk counterparts,
- 2) the absence of the legislation normative for permitted levels of various NMs in water and air
- 3) the absence of the adequate analytical techniques for detection of NMs in the environment.

The last point seems to be the most important one as the solution of this problem would provide the base for the quantitative analytical detection of various NMs and elaboration of the corresponding legislation normative for their permitted levels in the environment. In this regard it is essential to develop the analytical methodology to quantify NMs concentration, for example in water samples. This procedure can be based on the specific properties of the analyte under determination, such as for example Carbon Nanotubes (CNTs), which are known to be the most toxic carbon nanoform in comparison with, e.g. fullerenes and nanodiamonds.^{12,13,14} In this regard the development of analytical techniques permitting their detection in the environment seems particularly important.

CNTs find various applications since their discovery due to their structural properties (almost one-dimensional), stability and high electrical and thermal conductivities. All these features make CNTs a valuable component of different kind of composites, which are used as a base for design of various devices such as, for example electrochemical sensors.^{15, 16, 17} CNTs are known to be partially oxidized and as the result, bear on their surface the carboxylic functional groups. From this viewpoint they can be considered as a “nanoanalog” of fibrous carboxylic ion exchange

materials such as, for example FIBAN K-4.^{18,19} The surface of these materials can be easily modified with metal nanoparticles (MNPs) as it has been shown in our recent publications.^{20,21}

This modification is carried out by using the intermatrix synthesis (IMS) technique^{22,23} representing a simple and effective procedure, which includes two stages based on aquatic chemistry: 1) loading the functional groups with MNPs precursor (e.g., metal or metal complex ions), and 2) *in situ* formation of MNPs in the polymer matrix after reduction of MNPs precursor. Similar methodology can be used for modification of CNTs surface with easily detectable species, such as, for example, quantum dots (QDs).

QDs are known to present quantum confinement effects during light excitation, which gives them interesting optical and semi-conducting properties. Tuning these features and coupled them with its surface modification or using them for the surface modification of CNTs, led to explore the application of these nanocrystals to the field of sensors (fluorescent and biosensors) and to bioassays.^{24–27}

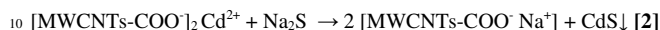
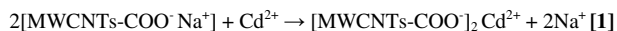
Previous works related to decoration or modification of CNTs with nanocrystals such as Metal NanoParticles (MNPs), usually involve thermal evaporation²⁸, electroless deposition by galvanic replacement²⁹, MNPs hydrosol absorption³⁰, electrochemical deposition³¹. These methods are mainly based on the use of high temperatures or organic solvents, involving a significant environmental impact of the process. There are greener methodologies for the decoration of CNTs with MNPs such as seed-mediated growth^{32,33} in which metal salts solutions can be reduced by a strong reducing agent (e.g. NaBH₄) at room temperature and aqueous solution. However to the knowledge of the authors no information regarding modification of CNTs with QDs can be found in the literature.

Modification of reactive surfaces such as CNTs or multi-wall CNTs (MWCNTs) with QDs can be carried out by taking advantage of their ion exchange functionality and using a slightly modified IMS procedure (see above). In this case the first stage remains absolutely the same (loading the functional groups with NPs precursor), while the second one includes the formation of NPs (QDs) by precipitation reaction (instead of reduction). Moreover, the synthesis of QDs on the surface of MWCNTs provides the final nanocomposite material with additional enhanced properties in terms of its electrocatalytic features (as shown in supplementary information SI.1.1).

The surface modification of MWCNTs with CdS-QDs was carried out using the following two sequential stages^{23,34}:

Stage 1: Loading (sorption) of Cd²⁺ ions (QDs precursors) onto the carboxylic groups of MWCNTs (equation 1), and

Stage 2: Precipitation of CdS-QDs on the MWCNTs surface by adding Na₂S (Equation 2):



As it is clearly seen from Equation (2), after carrying out the QDs formation reaction (precipitation of CdS with Na₂S, see eq.2) on the surface of MWCNTs, the functional groups of the later appear to be regenerated, i.e. are converted back into the Na-form. This means that the QDs formation cycle can be repeated again by using the same reactions (1) and (2) without any additional pre-treatment of MWCNTs. This allows for accumulation of the desired amount of QDs on the surface of MWCNTs.

Supporting information (SI.1) provides more details about the IMS experimental methodology. The raw material consists of commercial MWCNTs from SES®. Figure 1 presents the result of the application of this synthesis route of CdS-QDs on MWCNTs.

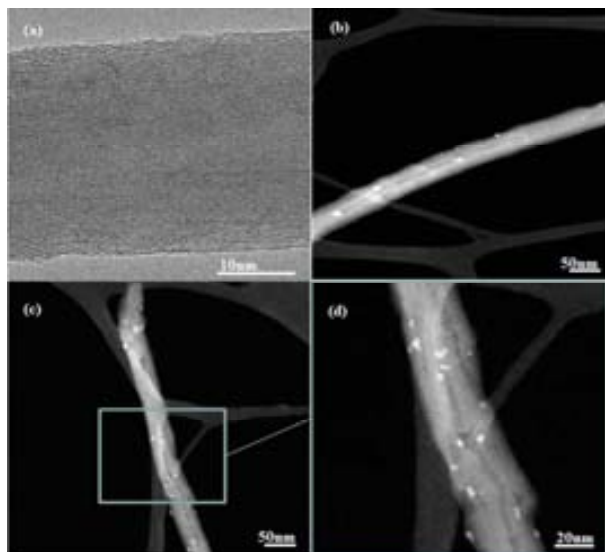


Figure 1: a) HR-TEM raw MWCNT b) HR-(S)TEM CdS-QDs on MWCNTs after one IMS cycle. c) and d) HR-(S)TEM images of CdS-QDs on MWCNTs after two sequential IMS cycles. Magnification of d>>c.

As it is seen in Fig. 1, the microscopic characterization of QD-MWCNTs nanocomposites (see Fig. 1b) confirms that the CdS-QDs are located mainly on the surface of MWCNTs. As it is also seen, QDs are well separated from each other and do not form any visible agglomerates. The raw MWCNTs also contain Fe and Ni catalyst MNPs used by the manufacturer to grow the CNT. These catalysts are located inside the wall of the MWCNTs. In order to differentiate the QDs from the catalyst MNPs the Energy Dispersive X-Ray (EDS) analysis of CdS-QD-MWCNT-

nanocomposites was also performed. The size distribution of the CdS-QDs is another parameter, which can be used for their identification. An average diameter of CdS-QDs is 3nm, while the one of the catalyst MNPs is >10nm. HR-(S)TEM images in Figure 1(c and d) show an increase of CdS-QDs content on the MWCNTs after two consecutive IMS cycles. This is due to the regeneration of the Na-form present on the carboxylic group after one complete IMS, accordingly to equation 2. The corresponding EDS spectra confirm the presence of CdS-QDs and it is presented in supporting information (S2).

The QDs content in the final nanocomposite material was evaluated by the thermogravimetric analysis (TGA) and appeared to equal to 11% weight of CdS-QDs (see supplementary information SI.1.3). As is also seen in Figure 1, despite of a larger amount of QDs accumulated on the MWCNT surface after two sequential loading-precipitation cycles, no evidence of QD agglomerates formation can be detected. Therefore, this fact can be considered as an additional advantage of the synthetic route used.

After the modification of MWCNTs with QDs they acquire optical properties³⁵, in other words unlike QD-free MWCNTs, MWCNT-CdS-QDs nanocomposites demonstrate fluorescence emission spectra and start to be visible. These spectra were determined for different concentrations of CdS-QDs-MWCNTs nanocomposite in aqueous solution. Acquisition parameters are described in supporting information in SI.1.5 Figure 2 presents the schematic diagram of sample preparation procedure for proposed analytical methodology for detection of CNTs in water.

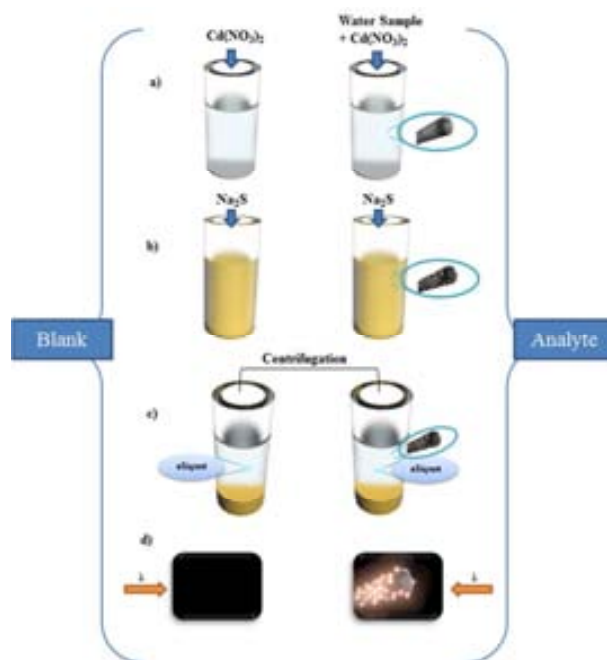


Figure 2: Scheme of analytical procedure for determination of MWCNTs in water. a) addition of Cd(NO₃)₂ aqueous solution to blank and water sample under analysis, b) precipitation of CdS_(s) and formation of CdS-QDs on MWCNTs surface, c) centrifugation, d) aliquot from liquid phases of blank and analyte is analysed on spectrophotometer for detection of MWCNTs due to presence of CdS-QDs.

The procedure is based on the supposition that CdS-QDs can be formed only on the surface of supporting material, such as for example CNTs. The surface of this material serves as both QDs formation medium as it bears the QDs-precursors (Cd^{2+} ions fixed on the carboxylic groups of CNTs) and the QDs-stabilizing medium as it prevents their agglomeration and uncontrollable grows (see Fig.1). Based on this supposition it was also assumed that QDs cannot be formed in the QDs-free aqueous phase (used as blank) as in this case only the formation of CdS macro crystalline precipitate can occur.

Precipitation of CdS in blank was carried out by using the same reagent amount as for IMS of CdS-QDs on MWCNTs. Then, the solution obtained was centrifuged. The aliquot of the resulting upper liquid phase was used as blank solution. An analogous procedure was applied for the water samples containing MWCNTs. After centrifugation, aliquots from the samples containing different MWCNTs concentration (differing by factors 1x, 2x and 3x) were taken for spectrophotometric analysis.

Figure 3 presents the values of fluorescent emission at the wavelength of $\lambda = 405\text{nm}$ for three different concentrations of CdS-MWCNTs nanocomposite (obtained after one QDs loading cycle) in aqueous phase. As it is seen in Figure 3, the fluorescent emission at this particular wavelength appears to be directly proportional to the concentration of analyte (MWCNTs) in the sample. This fact can be used for the quantitative detection of MWCNTs in water samples.

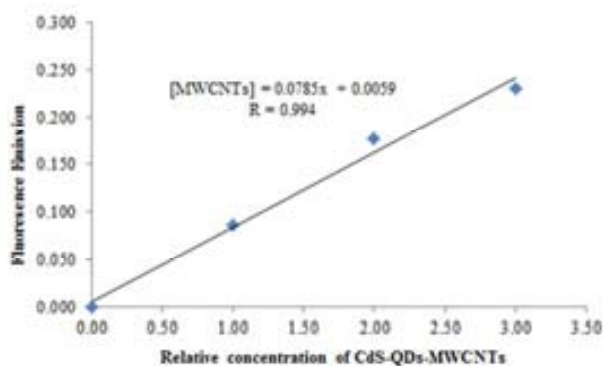


Figure 3: Dependence of intensity of fluorescence emission at wavelength of $\lambda = 405\text{nm}$ on relative concentration of MWCNTs decorated with CdS-QDs. Zero point corresponds to emission of blank (see text).

Consequently, it can be concluded that non-aggressive IMS technique proves to be applicable for the decoration of MWCNTs with QDs what makes them visible and therefore, spectrophotometrically detectable. IMS methodology is an environmentally friendly technique as the amount of reagents used for IMS of QDs on MWCNTs surface can be minimized and only aqueous solutions are used in all cases. In addition it seems important to emphasise that although the results reported in this communication have been obtained with samples containing relatively high concentrations of MWCNTs, they demonstrate the principle possibility of visualization of this NM by using simple procedure shown in Fig.2, what makes detectable its presence in water.

The further enhancement of the IMS of QDs on MWCNTs surface procedure (for example, the use of several sequential metal-loading-precipitation cycles) along with the use of far more sensitive spectrophotometric equipment will allow to substantially decreasing the limit if MWCNTs detection in water. Moreover; the proposed methodology seems to be easily adaptable for visualization of other carbon NMs such fullerenes, nanodiamonds and some others. Moreover, the final distribution of the QDs on the support makes feasible the application of the obtained nanocomposites also in catalysis or electrocatalysis.

Conclusions

The following conclusions can be derived from the results reported in this communication:

1. The IMS technique has been shown to be applicable for the synthesis of CdS-QDs on MWCNTs by precipitation route, what results to the favourable distribution of QDs on the surface of the nanotubes. The functional groups of the MWCNTs are converted back into the initial ionic form (regenerated) after the CdS precipitation stage, what permits to carry out several sequential metal-loading-precipitation cycles to increase the QDs content in the final nanocomposite material.
2. Taking into account the proposed supposition of the preferential formation of CdS-QDs on the MWCNTs surface, it was demonstrated that after modification with QDs the intensity of fluorescent emission at a certain wavelength ($\lambda = 405\text{nm}$) appears to be directly proportional to the CNTs concentration in water. This can be used for the detection of CNTs in water samples.
3. A simple analytical procedure based on the above supposition for the detection of MWCNTs in water has been proposed and experimentally approved.

Notes and references

^a *Departament de Química, Facultat de Ciències, Edifici C-Nord, Universitat Autònoma de Barcelona, 08193 Cerdanyola del Vallès (Bellaterra), Barcelona, Spain. E-mail: dimitri.muraviev@uab.cat*

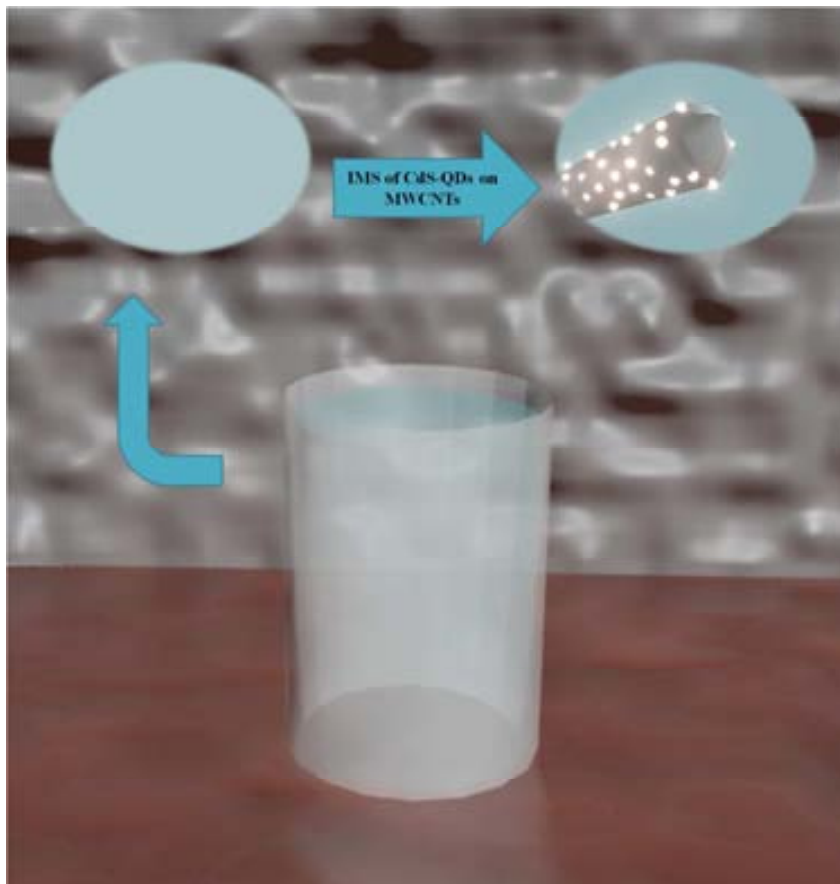
Programa Operatiu de Catalunya (FEDER) is acknowledged for the financial support within the project VALTEC09-02-0058. JB and JM also thank Universitat Autònoma de Barcelona for the personal grants and Servei de Microscòpia of the Universitat Autònoma de Barcelona for the electron microscopy images.

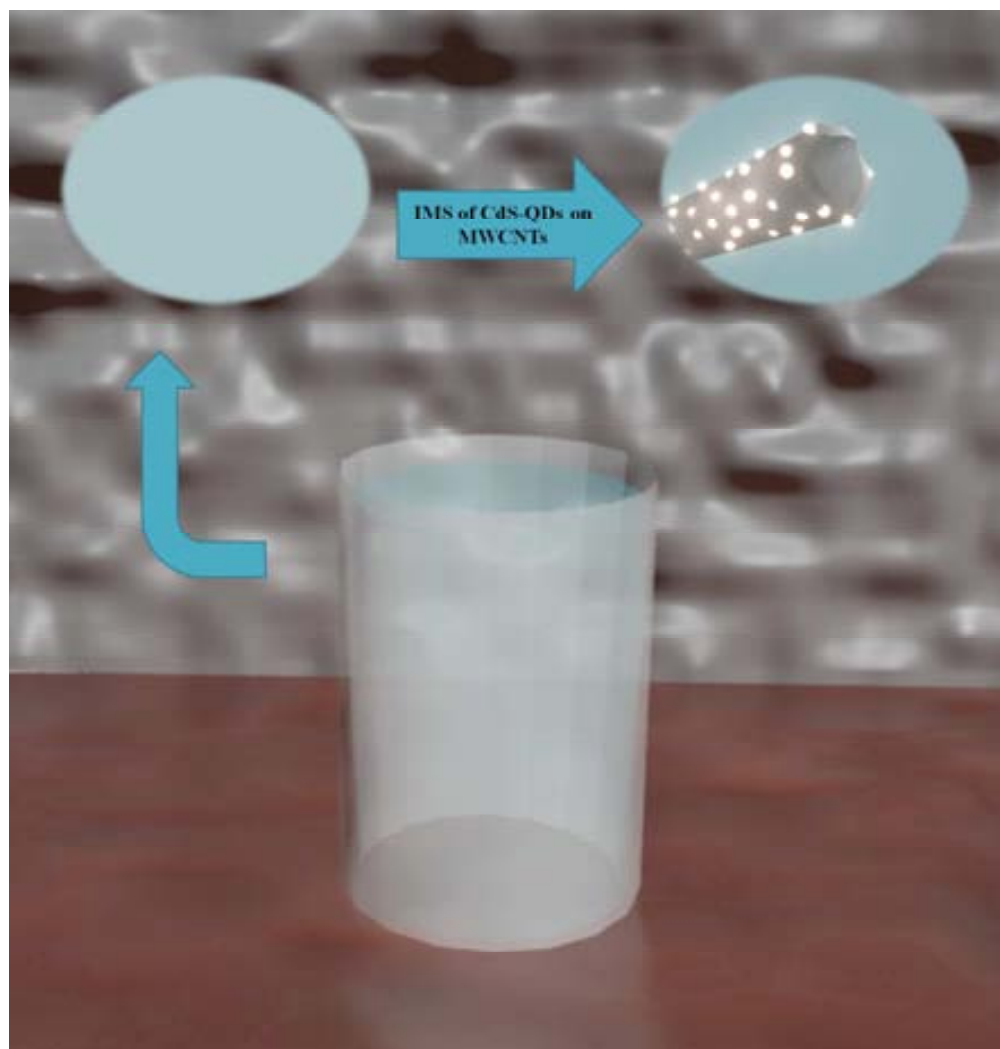
1. P. Xu, X. Han, B. Zhang, Y. Du, and H.-L. Wang, *Chem. Soc. Rev.*, 2014, **43**, 1349–60.
2. F. Hussain, *J. Compos. Mater.*, 2006, **40**, 1511–1575.
3. D. R. Paul and L. M. Robeson, *Polymer (Guildf.)*, 2008, **49**, 3187–3204.
4. J. Kao, K. Thorkelsson, P. Bai, B. J. Rancatore, and T. Xu, *Chem. Soc. Rev.*, 2013, **42**, 2654–78.
5. S. F. Hansen, L. Carlsen, and J. a. Tickner, *Environ. Sci. Policy*, 2007, **10**, 395–404.

6. R. Nijhara and K. Balakrishnan, *Nanomedicine*, 2006, **2**, 127–36.
7. C. Milburn, *Configurations*, 2012, **20**, 53–87.
8. F. Pacheco-Torgal and S. Jalali, *Constr. Build. Mater.*, 2011, **25**, 582–590.
9. K. J. Lee, P. D. Nallathamby, L. M. Browning, C. J. Osgood, and X.-H. N. Xu, *ACS Nano*, 2007, **1**, 133–43.
10. W. L. Robison, *Nanoethics*, 2011, **5**, 1–13.
11. A. Franco, S. F. Hansen, S. I. Olsen, and L. Butti, *Regul. Toxicol. Pharmacol.*, 2007, **48**, 171–83.
12. S. Sharifi, S. Behzadi, S. Laurent, M. L. Forrest, P. Stroeve, and M. Mahmoudi, *Chem. Soc. Rev.*, 2012, **41**, 2323–43.
13. N. Biolabeling and D. Ho, 2009, **3**, 3825–3829.
14. V. N. Mochalin, O. Shenderova, D. Ho, and Y. Gogotsi, *Nat. Nanotechnol.*, 2012, **7**, 11–23.
15. C. Gao, W. Li, H. Morimoto, Y. Nagaoka, and T. Maekawa, *J. Phys. Chem. B*, 2006, **110**, 7213–20.
16. D. Wang, Z.-C. Li, and L. Chen, *J. Am. Chem. Soc.*, 2006, **128**, 15078–9.
17. K. Balasubramanian and M. Burghard, *Small*, 2005, **1**, 180–92.
18. S. Sarkar, E. Guibal, F. Quignard, and a. K. SenGupta, *J. Nanoparticle Res.*, 2012, **14**, 715.
19. J. E. Greenleaf, J. Lin, and A. K. Sengupta, *Environ. Prog.*, 2006, **25**, 300–311.
20. A. Alonso, N. Vigués, X. Muñoz-Berbel, J. Macanás, M. Muñoz, J. Mas, and D. N. Muraviev, *Chem. Commun. (Camb)*, 2011, **47**, 10464–6.
21. A. Alonso, J. Macanás, A. Shafir, M. Muñoz, A. Vallribera, D. Prodius, S. Melnic, C. Turta, and D. N. Muraviev, *Dalton Trans.*, 2010, **39**, 2579–86.
22. P. Ruiz, M. Muñoz, J. Macanás, and D. N. Muraviev, *Chem. Mater.*, 2010, **22**, 6616–6623.
23. D. N. Muraviev, *Contrib. to Sci.*, 2005, **3**, 19–32.
24. S. D. Elliott, M. P. Moloney, and Y. K. Gun'ko, *Nano Lett.*, 2008, **8**, 2452–7.
25. E. Petryayeva, W. R. Algar, and I. L. Medintz, *Appl. Spectrosc.*, 2013, **67**, 215–52.
26. M. P. Moloney, Y. K. Gun'ko, and J. M. Kelly, *Chem. Commun. (Camb)*, 2007, **7345**, 3900–2.
27. D. Bera, L. Qian, T.-K. Tseng, and P. H. Holloway, *Materials (Basel)*, 2010, **3**, 2260–2345.
28. C. Bittencourt, a. Felten, J. Ghijssen, J. J. Pireaux, W. Drube, R. Erni, and G. Van Tendeloo, *Chem. Phys. Lett.*, 2007, **436**, 368–372.
29. H. C. Choi, M. Shim, S. Bangsaruntip, and H. Dai, *J. Am. Chem. Soc.*, 2002, **124**, 9058–9.
30. K. Y. Lee, M. Kim, J. Hahn, J. S. Suh, I. Lee, K. Kim, and S. W. Han, *Langmuir*, 2006, **22**, 1817–21.
31. L. Qu and L. Dai, *J. Am. Chem. Soc.*, 2005, **127**, 10806–7.
32. C. J. Murphy and N. R. Jana, *Adv. Mater.*, 2002, **14**, 80–82.
33. B. Nikoobakht and M. El-Sayed, *Chem. Mater.*, 2003, 1957–1962.
34. P. Ruiz, J. Macanás, M. Muñoz, and D. N. Muraviev, *Nanoscale Res. Lett.*, 2011, **6**, 343.
35. J. S. Son, K. Park, S. G. Kwon, J. Yang, M. K. Choi, J. Kim, J. H. Yu, J. Joo, and T. Hyeon, *Small*, 2012, **8**, 2394–402.

Graphical Abstract

The use of nanomaterials has grown faster than the evaluation of their possible environmental risks. In addition to that, the lack of appropriate analytical techniques for nanomaterials makes the risk assessment even more complicated. We propose a valid method for synthesis of CdS quantum dots in multiwall carbon nanotubes that lead to their determination in water due to fluorescence properties of the final nanocomposite.





566x591mm (72 x 72 DPI)

Supporting Information

SI.1: Experimental

SI.1.1: Electroanalytical Experiments.

All experiments were performed at room temperature (25 °C). Electroanalytical experiments were carried out in a 10 mL glass cell (home-made), using a three-electrode configuration. Electrochemical Impedance Spectroscopy (EIS) measurements were made in a 0.1 M potassium chloride solution containing 0.01 M potassium ferricyanide/ferrocyanide under quiescent condition.

SI.1.1.1 Electrochemical Performance of CdS-QDs on MWCNTs in epoxy composite electrodes.

Regarding the feasibility for the preparation of epoxy composite electrodes with CdS-QDs on MWCNTs, the information of previous studies was taken into account considering that the optimal composition of the transducer material used for the construction of nanocomposite electrode was around 10% of MWCNTs dispersed in epoxy Epotek H77 resin.¹

Basing on our previously obtained results, 10% of conducting material content was considered as the optimum for MWCNTs/epoxy composite electrodes containing SES® CNTs.¹ This composition was also used in this work.

Composite containing	R_Ω (Ω)	R_{ct} (Ω)	C_{dl} (μF)
RawMWCNTs	138.0	530.0	9.02
MWCNTs-CdS - QDs	141.9	408.0	4.20

Table 1: Electrochemical characterization of MWCNTs/epoxy electrodes for the determination of Ohmic Resistance (R_Ω), Charge Transference Resistance (R_{ct}) and Double-Layer Capacitance (C_{dl}) was obtained by Electrochemical Impedance Spectroscopy (EIS).

The electrochemical characterization showed that the incorporation of CdS-QDs leads to a significant improvement of these parameters, as seen in Table 1. The presence of CdS-QDs leads to a remarkable decrease of the C_{dl} value and consequently the reduction of the signal to noise ratio.

SI.1.2: Synthesis of Cd-Quantum Dots(QDs) on multiwall carbon nanotubes (MWCNTs) by co-precipitation technique

The general procedure of synthesis was carried out by loading the raw multiwall carbon nanotubes functional groups with 20mL Cd (NO₃)₂ 0.1M for 30 min. with magnetic stirring. MWCNTs were rinsed with deionized MiliQ water. Then 20mL Na₂S 0.1M were added to promote CdS-QDs precipitation on the MWCNTs surface.

SI.1.3: Metal content by thermogravimetric Analysis of CdS-QDs MWCNTs composites

Thermogravimetric analysis (TGA) were performed on a Netzsch instrument, model STA 449 F1 Jupiter®, with a flow of air. A ~20 mg sample was heated to 1000 °C at 10 °C/min, using flow of air. The mass of the sample was continuously measured as a

function of temperature and the rate of weight loss (d.t.g.) was automatically recorded. The composition of the MWCNTs composite is 11% weight CdS-QDs as showed in figure 1.

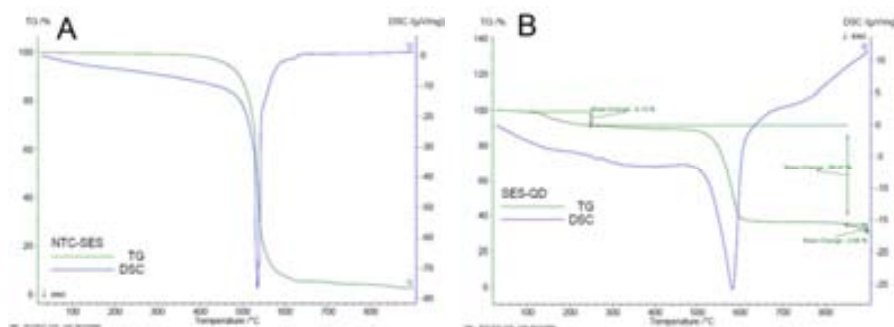


Figure 1: TGA for a) Raw MWCNTs and b) CdS-QDs on MWCNTs

SI.1.4: Electron Microscopy Characterisation: TEM and HR(S)TEM

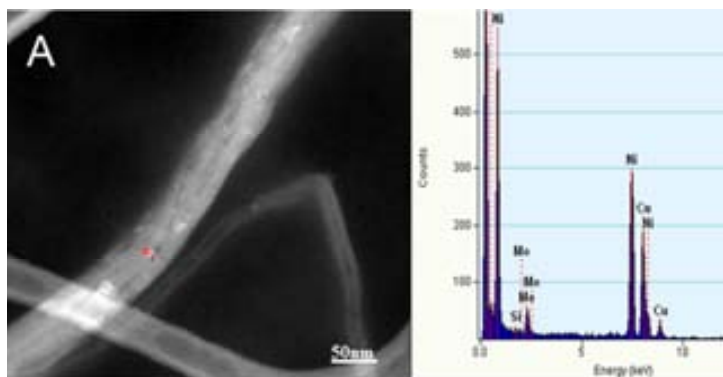
Transmission Electron Microscopy (TEM) images were obtained with the JEM-1400 unit with an acceleration voltage of 120kV. HR(S)TEM images were taken with a FEI Tecnai G2 F20 S-TWIN HR(S)TEM field emission of 200kV with analytical EDX. Sample preparation: A 1 mg of MWCNTs was dispersed in 5 mL of acetone as organic solvent and then placed in ultrasound bath for one hour. Finally, a drop of the solution was placed on a grid and let it dry before TEM analysis.

SI.1.5: Confocal Microscopy

Samples were mounted on bottom-glass culture dishes (MatTek Corp., Ashland) and were examined using a TCS-SP5 (Leica Microsystems, Heidelberg, Germany) confocal laser scanning microscope located in Microscopy Facilities of Universitat Autònoma de Barcelona. Fluorescence Emission Spectra were obtained using a 63x objective with an excitation wavelength of 405nm for all spectra. Recording data has a wavelength range from 425nm to 775nm with a band width of 10nm and a spectral resolution of 7nm. Raw MWCNTs do not present fluorescent emission signal.

SI.2: Energy Dispersive X-Ray (EDX) microanalysis

STEM microscopy shows colour contrast depending on the composition of the sample. The clear zones present a higher weight composition. Combining this technique with EDX analysis under the same frame, EDX spectra evidence the composition difference between the catalyst of the MWCNT and the CdS-QDs as presented in figure 2.



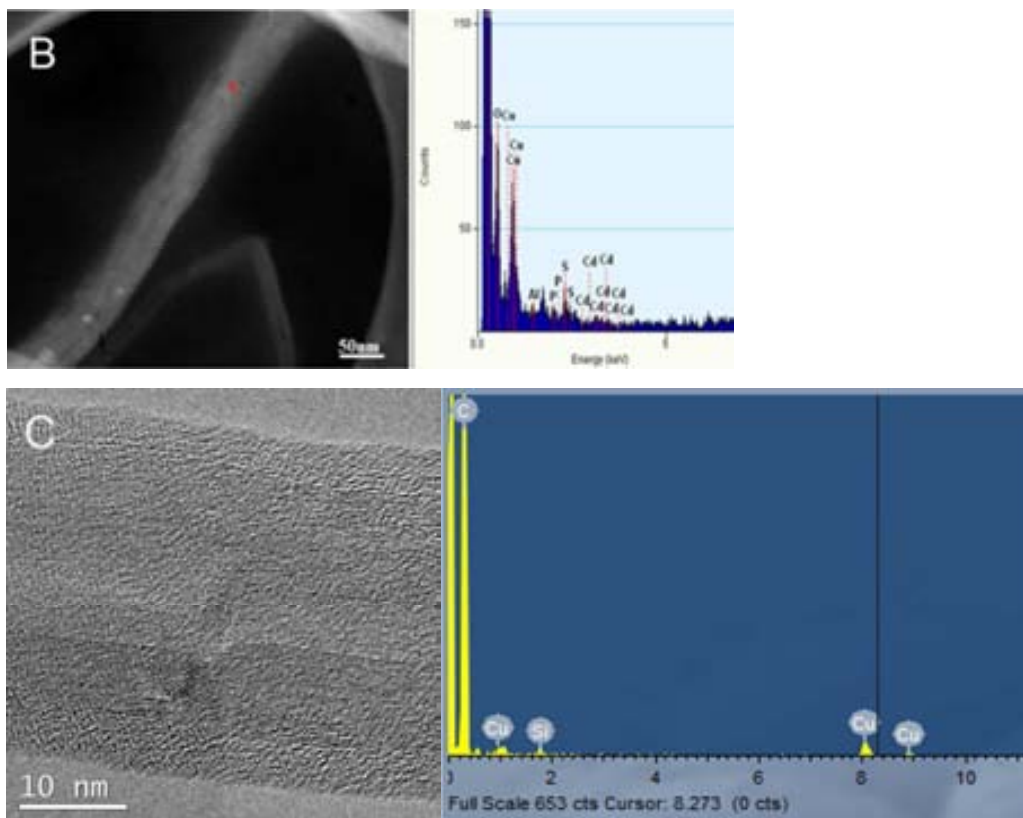


Figure 2: EDX spectra of a) MWNTs Catalyst showing high Ni content. b) CdS-QDs showing the presence of Cd and S and c) raw MWNTs.

References:

1. R. Olivé-Monllau, M. J. Esplandiú, J. Bartrolí, M. Baeza, and F. Céspedes, *Sensors Actuators B Chem.*, 2010, **146**, 353–360.

ANNEX 4

Elsevier Editorial System(tm) for Reactive and Functional Polymers
Manuscript Draft

Manuscript Number: REACT-D-14-00317

Title: Surface modification of gel-type ion exchange polymers with silver nanoparticles by intermatrix synthesis technique

Article Type: Research Paper

Corresponding Author: Dr. Dmitri Muraviev,

Corresponding Author's Institution:

First Author: Dmitri Muraviev

Order of Authors: Dmitri Muraviev; Maria Muñoz; Julio BASTOS ARRIETA

Suggested Reviewers: Arup SenGupta
aks0@Lehigh.edu

Samuel Sánchez
sanchez@is.mpg.de

Yurii Gun'ko
igounko@tcd.ie

Jean-François Lahitte
lahitte@chimie.ups-tlse.fr

Opposed Reviewers:

Dr. Y. Tezuka
Editor-in-Chief *Reactive and Functional Polymers*
Tokyo Institute of Technology, Meguro-Ku, Japan

Barcelona, June 12th, 2014

Dear Prof. Tezuka,

Attached you will find a file with our paper: "**Surface modification of gel-type ion exchange polymers with silver nanoparticles by intermatrix synthesis technique**", which we would like you to consider for publication in the *Reactive and Functional Polymers* journal.

In the present work we report the results obtained in the study of the modification of gel-type polymeric ion exchange matrices with silver nanoparticles. In previous studies, it was demonstrated the bactericide features of these nanocomposite materials. In this article we present a deeper analysis of the data obtained from the characterization of the morphology of the final added value material, demonstrating no significant changes of the initial ion exchange properties of the supporting matrix after Intermatrix Synthesis of silver nanoparticles with a favorable distribution, leading to the appearance of nanoporosity and wrinkle structures on the surface of the polymeric support. In addition it is also demonstrated that the presence of this nanoparticles layer does not essentially affect the mass transfer process of ions in the matrix as the obtained diffusion coefficient value for silver ion for the studied system is very close to the value reported by other researchers in similar systems. In the supplementary information we present a time lapse video of the surface morphology changes of a gel-type resin due to its modification with Ag functional metal nanoparticles by InterMatrix Synthesis

We state that none of the submission has been or will be done to another journal without proper acknowledgment and permission.

We suggest the following experts as potential referees of our paper:

1. Dr. Jean-François Lahitte, Laboratoire de Génie Chimique, Génie des Interfaces et Milieux Divisés, Route de Narbonne, 118, 31062, Toulouse, France.
Fax: 33 0 561556139, E-mail: lahitte@chimie.ups-tlse.fr
2. Prof. Yuri Gun'ko, SNIAM Building, School of Chemistry, Trinity College Dublin, College Green, Dublin 2, Ireland. E-mail: igounko@tcd.ie
3. Dr. Samuel Sanchez Ordóñez, Max Planck Institute for Intelligent Systems
Heisenbergstr. 3; 70569 Stuttgart, Germany. E-mail: sanchez@is.mpg.de
4. Prof. Arup K. SenGupta Department of Civil & Environmental Engineering, 13 E. Packer Av. Lehigh University Bethlehem, PA 18015 U.S.A. E-mail: aks0@Lehigh.edu

We keep looking forward to hearing from you on the acceptability of our paper for publication in your journal.

Sincerely,

Dr. Dmitri N. Muraveiv
Dept. of Analytical Chemistry
Autonomous University of Barcelona
Campus UAB, Bellaterra
E-08193 Barcelona, Spain
Fax: 34-93-5812379; E-mail: Dimitri.Muraviev@uab.es

Surface modification of gel-type ion exchange polymers with silver nanoparticles by intermatrix synthesis technique

*J. Bastos-Arrieta, M. Muñoz and D. N. Muraviev.**

Department of Chemistry, Universitat Autònoma de Barcelona, 08193 Bellaterra, Barcelona,

*Corresponding autor: dimitri.muraviev@uab.cat

ABSTRACT: This communication reports the results obtained by the modification of gel-type ion exchange materials with functional metal nanoparticles having biocide activity. The modification is carried out by using Intermatrix Synthesis technique coupled with Donnan Exclusion Effect what results in the most favourable distribution of silver nanoparticles near the surface of nanocomposite material. The surface of polymer-metal nanocomposite is characterised by the worm-like structure due to the interaction of metal nanoparticles with polymer chains. This interaction leads to the appearance of nanoporosity in the matrix what enhances its mass-transfer characteristics. Moreover, it has been shown that modification of gel-type ion exchangers with silver nanoparticles essentially does not change the ion exchange properties of the initial polymeric matrix.

Keywords: Ion Exchange, Intermatrix Synthesis, Nanoparticles, Nanocomposite, Surface Modification.

1. Introduction

Ion exchange materials[18] find numerous large-scale industrial applications in various fields, such as water treatment[9,23], catalysis[3], and many others. In some instances the efficient use of ion exchangers can be substantially improved by tailored modification with functional metal

nanoparticles (FMNPs) by using the Intermatrix Synthesis (IMS) technique[20]. The first communication about IMS of FMNPs in ion exchange polymeric materials dates back to 1949, in which Mills and Dickinson described the preparation of a weakly basic anion exchange resin containing Copper Metal Nanoparticles (Cu-MNPs or “colloidal copper”) and the use of this polymer-metal nanocomposite to remove oxygen from water based on its interaction with Cu-MNPs.[26] Since then, many studies of the modification of ion exchange resins with MNPs (mainly Cu-MNPs) resulted in the development of a new class of bi-functional ion exchange materials combining both the ion exchange properties determined by the presence of functional groups in the matrix, and the redox properties due to the presence of “colloidal metal” or MNPs in the matrix. They are also known as redoxites and electron exchangers.[27] Redoxites have found wide application in the complex water treatment processes at power stations for the removal of hardness ions by ion exchange and dissolved oxygen by redox reactions with MNPs. However, essentially no information about the sizes and the structures of MNPs in redoxite matrices and the features of their distribution inside polymers can be found in the literature.

The preparation of such materials was based on the use of the IMS technique and involved in the case of weakly basic anion exchange polymers the following two consecutive stages:

(a) metal loading:



(b) metal reduction:



As clearly follows from equation (2), the functional groups of the polymer bearing Cu-MNPs precursors (Cu^{2+} ions) are not protonated to provide the most favourable conditions for formation of amino-complexes with copper ions. This means that they are not bearing any charges and dithionite anions can diffuse deeply into the polymer without any restriction. Therefore, one can quite logically suggest that this provides the conditions for the homogeneous distribution of the Cu-MNPs throughout the polymer matrix.

This type of MNPs distribution was quite appropriate for practical applications of redoxite nanocomposites such as the elimination of oxygen from water at heat power stations (for preventing corrosion of steam turbine materials) as molecular oxygen dissolved in water can diffuse inside the nanocomposite materials and interact with Cu-MNPs.[12,17] However, for some other practical applications of polymer-metal nanocomposites such as for example, reagent-free disinfection of water or heterogeneous catalysis, for obvious reasons this type of MNPs distribution appears to be inappropriate. Indeed, in the first case the size of bacteria to be eliminated from the water does not allow them to deeply penetrate into the nanocomposite material. They can only interact with MNPs located at or near the nanocomposite surface. In the second case, the kinetics of the catalytic reaction strongly depends on the accessibility of catalyst MNPs for reactants. For this reason the surface distribution of catalytically active MNPs has to substantially enhance their properties.[7,8]

One other important point besides MNPs distribution has to be taken into account when designing the modification of ion exchange materials with MNPs. Although MNPs in the final nanocomposite are strongly captured by the polymer, some can escape into the medium, water or the reaction mixture, being treated. The main concerns of the presence of MNPs, or other nanomaterials, in water or air are associated with the following:

- 1) the higher toxicity of many nanomaterials (NMs) in comparison with their larger counterpart;
- 2) the absence of adequate analytical techniques for detection of NMs in the environment, and
- 3) the absence of the legislation normative for permitted levels of various NMs in water and air.

In this respect increase of the safety of NMs and nanocomposites is of particular importance.[21][10] A possible solution of this particular problem has been shown to be the IMS[20] of FMNPs with core-shell structure consisting of a superparamagnetic core coated with a functional metal shell of minimal thickness, which provides the maximal bactericide or catalytic activity.[22,24] The superparamagnetic nature of MNPs provides an additional level of the material safety as MNPs leached from the polymer matrix can be easily captured by magnetic

traps to completely prevent any post-contamination of the treated water. In the case of catalytic applications of polymer-metal nanocomposites this feature of MNPs allows for their easy recovery for reuse or recycling, particularly important in case of noble MNPs. The presence of MNPs does not block the functional groups of the polymer so that the polymer-metal nanocomposite can be also used for the removal of some undesired ions (e.g. hardness ions, iron, nitrates, etc.) from water, which is particularly important in the case of complex water treatment.

Consequently, IMS technique coupled with the Donnan Exclusion Effect (DEE) provides an environmentally friendly route for the modification of reactive polymer surfaces with functional metal nanoparticles (FMNPs).[20] Previous reports on the application of IMS for the preparation of polymer-metal nanocomposites proof the most favourable distribution of the FMNPs near the surface of the host polymeric matrix with no evident agglomerates. IMS main stages include: 1) the immobilization (sorption) of metal or metal complex ions (FMNP precursors) onto the functional groups of the polymer, and 2) their chemical or electrochemical reduction on the polymer matrix.

In this communication we report the results obtained on the further development of IMS technique coupled with DEE (DEEIMS) to produce nanocomposites with desired FMNPs content and also on the study of morphological changes of nanocomposite structure in comparison with the initial (FMNPs-free) polymer.

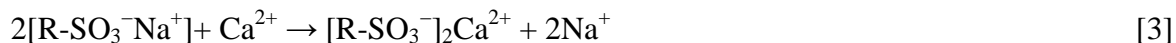
2. Experimental

2.1 Reagents and materials: Metal salts as AgNO_3 , NaBH_4 (Aldrich, Germany), acids and bases were of p.a. grade were used as received. Bidistilled water was used in all experiments.

The ion exchange capacity for the anionic exchanger gel-type polymer (quaternary ammine) and for the cationic exchanger gel-type (sulfonic) were calculated by volumetric titration were $2.1 \text{ meq} \times \text{g}^{-1}$ in both cases.

For both anionic and cationic breakthrough experiments a column with internal diameter of 0.025m was used for an average bed particle diameter of 500 μm . For the breakthrough curve profile for cationic gel-type polymer modified and unmodified with Ag-FMNPs a fixed bed of the resin was placed in the column. A Ca^{2+} solution was introduced with a pump and made go

through the fixed bed particles with a flux rate of 1mL/min. Then, each 2mL of effluent were collected separated samples for the determination of displacement of Na⁺ to Ca²⁺ as described in equation (3).



Similar procedure was followed for anionic breakthrough curve profile. Modified and unmodified with Ag-FMNPs quaternary amine anionic gel-type exchanger were used as fixed bed in the column. Cl⁻ solution was introduced with pump and made go through the fixed bed particles with a flux rate of 1mL/min. Then, each 2mL of effluent were collected separated samples for the determination of displacement of OH⁻ to Cl⁻ as described in equation (4).



2.2 Intermatrix Syntesis of FMNPs.

2.2.1. IMS of Ag-FMNPs on sulfonic gel–type cation exchanger: The general IMS of Ag-NPs was carried out by loading of the functional groups of 400mg the sulfonic gel-type polymer with Ag⁺ by using 0.1 mol×L⁻¹ aqueous AgNO₃ solution (20mL) followed by reduction with 0.1 mol×L⁻¹ aqueous NaBH₄. Some kinetic studies were developed by changing metal loading time at stage 1 of IMS.

2.2.2. IMS of Ag-FMNPs on quaternary ammine gel – type anionic exchanger: IMS of Ag-FMNPs was carried out by the loading the functional groups of the polymer with anions of the reducing agent using 0.1 mol×L⁻¹ aqueous NaBH₄ solution (20 mL) followed by the treatment of the resin with 0.1 mol×L⁻¹ AgNO₃ solution (20mL). The last stage resulted in the formation of the Ag-FMNPs on the polymer matrix.

2.3. Analysis of nanocomposite metal composition: A sample of about 10mg of FMNPs-containing material was immersed in aqua regia (1 mL) to completely dissolve the palladium by oxidation. The solution was filtered through a 0.22 μm Millipore filter and diluted for metal content quantification by Induced Coupled Plasma Optical Emission Spectrometry, ICP–OES (Iris Intrepid II XSP spectrometer Thermo Electron Co) and ICP-MS (Agilent 7500). The average uncertainty of metal ions determination was less than 2% in all cases.

2.4. Scanning Electron Microscopy (SEM) Characterization: Scanning Electron Microscopes (SEM) coupled with an Energy-Dispersive Spectrometer (EDS) Zeiss EVO MA 10 and Zeiss MERLIN FE-SEM (Servei de Microscòpia of Universitat Autònoma de Barcelona). SEM technique was used to obtain the metal distribution profiles across the cross-section of the FMNPs containing materials, morphology of the polymer surface. The nanocomposite samples were prepared by embedding several granules in the epoxy resin followed by cutting and cross-sectioning with a ultramicrotome (Leica EM UC6) using a 35° diamond knife (Diatome) at liquid nitrogen temperature (-160°C).

3. Results and discussion

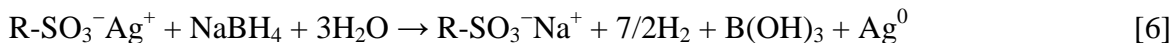
Depending on the final application of interest for these nanocomposites, catalytic or bactericide activity, and with the goal to obtain the most favourable distribution of NPs in the polymer, IMS methodology has been coupled with the DEE (DEEIMS). The distribution of FMNPs near the surface of the nanocomposite material may be considered as really the most favourable for practical application of nanocomposites of this type as it provides an enhanced access of the substrates (in catalytic applications) or bacteria (in water disinfection) to the FMNPs layer of the nanocomposite.

Figure 1 shows distribution of Ag-NPs in the nanocomposite where a desirable metal content is observed mainly on the polymeric surface; this due to DEEIMS methodology as indicated in the following equations:

Metal loading stage:



Metal reduction stage



As it is seen from equation (6), the negatively charged borohydride anions (the actual reducing agent) cannot deeply penetrate into the polymeric matrix bearing the charge of the same sign due to the action of DEE. As the result, the reduction of Ag ions leading to the formation of Ag-

FMNPs proceeds near the surface of the polymer. As it also follows from the same equation, the functional groups of the polymer appear to be regenerated in the course of metal reduction, i.e. are converted back into the initial Na-form (see equation (5)). This means that the metal loading reduction cycle can be repeated without any additional pre-treatment of the polymer what has been shown to lead to the increase of FMNPs layer thickness in the nanocomposite and consequently an increase in the FMNPs content.[2,20] The thickness of Ag-FMNPs layer (I.E., FMNPs content) can be also tuned by changing the time of the metal loading stage.

The system FMNPs-Polymer shows a series of interactions that leads to the increase of the stability of the NPs and reduces the possibility of release, reducing as well the environmental impact of these nanocomposites. This can be explained by the increase of viscosity of the immobilizing media (polymeric support), and the decrease of the energy of particle-particle interaction in FMNPs systems regarding the MNPs prepared in solution.[11]

The IMS of MNPs in non-cross-linked polymers was shown to be accompanied by a strong change of the polymer morphology and the appearance of typical worm-like structure on the surface of the corresponding polymer-metal nanocomposite.[19] Although the rigidity of cross-linked polymer matrix is far higher than that of their non-cross-linked analogues, one can also expect the appearance of similar morphological changes in the case of IMS of MNPs in the matrices of cross-linked polymers. The confirmation of this supposition is shown in Fig. 2. As it is seen in Figs. 2a and 2b, after carrying out the metal-loading-reduction cycle (IMS of MNPS) the initially smooth polymer surface changes its morphology due to the appearance of the worm-like structure similar to that observed in the case of non-cross-linked polymers product of IMS of Cu-FMNPs.[19] As it is also seen in Figs. 2e and 2f, the morphological changes result also in the appearance of nanopores in the gel-type polymer. The appearance of nanoporosity results in turn in increase of the internal surface area what can be one of the factors explaining the excellent performance of these nanocomposites in bactericide assays.[1,2]

The bactericide activity of Ag-FMNPs-cation-exchange polymer nanocomposites with different thickness of Ag-FMNPs layer was tested previously and after 60 minutes contact time the E. Coli activity decreased to zero. Moreover, it has been also shown that the bactericide activity of these nanocomposites does not depend on the thickness of the Ag-FMNPs layer.

Therefore, the preparation the layer with the minimum quantity of FMNPs and with the most favourable distribution provides the same bactericide results at lower production cost and time.[1]

The increase of FMNPs content near the surface of the matrix can be considered as an additional diffusional barrier for the ions to be removed by the nanocomposite material. However, the formation of FMNPs layer is accompanied by formation of nanopores and increase of the surface area by up to 20% in comparison with the initial.[4]

The thickness of the FMNPs layer on cation exchangers can be tuned and optimized within the metal loading stage of the IMS process. As the performance of these nanocomposites for bactericide water treatment does not depend on the thickness of Ag-FMNPs layer the increase of the amount of silver content in nanocomposite appears to be undesirable. An additional argument in favour of this point deals with the better accessibility of the functional groups of the polymer for ions to be removed within a complex water treatment cycle at a minimal FMNPs content.

As it is seen in Fig. 3, the polymer provides an effective stabilization effect towards Ag-FMNPs so that no visible agglomeration of silver nanoparticles can be observed. This fine distribution of the nanomaterial is a very important feature for the bactericide (and catalytic) applications of nanocomposite material.

Therefore, optimization of the Ag-FMNPs content by minimizing the thickness of FMNPs layer combined with an appropriate distribution is a mandatory for the preparation of novel polymer-metal bactericide composite materials. Figure 4 presents SEM images of cross sections of Ag-FMNPs-sulfonic gel-type polymer nanocomposite granules at different times of metal loading stage and, as the result, different thickness of Ag-FMNPs layer.

The values of FMNPs layer thickness obtained from the SEM images of cross-sections of nanocomposite granules (see Fig.4) demonstrate a linear dependence on the metal loading time as it shows in Figure 5. This linear dependence can be used as a sort of calibration curve to determine the thickness of FMNPs layer at any time within the given time interval. The results of this estimation are shown in Table 1.

The results shown in Fig. 4 and Table 1 can also be used for estimation of the diffusion coefficient of Ag^+ ions in the polymer phase and compare it with the value reported by Matuzuru and Wadachi for sulphonated cation-exchanger of a gel-type, which equals $1,3 \times 10^{-7} \text{cm}^2/\text{s}^{20}$.

Under the conditions of experiments carried out in this research, the intra-particle diffusion (in the resin phase) is considered to control the kinetics of ion exchange. The diffusion coefficient of silver ions in this case can be calculated from the models first described by Boyd, Adamson and Mayers[6] and Helfferich[14] and developed by other researchers[15,16] by using for example, the following equation:

$$t = \frac{q^* F r^2}{6 D C_i}, \quad [7]$$

where q^* is the ion-exchange capacity of the resin (mequiv/g), F is the degree of exchange at certain time (s), r is the diffusion distance of the ions into the matrix (cm), D is the diffusion coefficient of Ag^+ ions (cm^2/s) in the resin phase and t is the time of diffusion (in our case it is the metal loading time) and C_i is the concentration of the metal salt solution (mequiv/l).

The F value standing in equation (7) can be calculated by taking into account the thickness of the Ag-FMNPs layer (Δl , see Fig. 4 b, right) as follows:

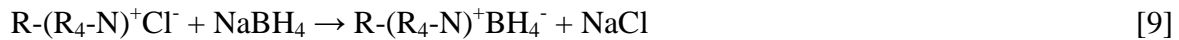
$$F = \frac{r^3 - (r - \Delta l)^3}{r^3} \quad [8]$$

The D_{Ag^+} value calculated by using equations (7) and (8) equals to $3.5 \times 10^{-7} \text{cm}^2/\text{s}$, what is sufficiently close to that reported by Matuzuru and Wadachi (see above). The difference between the calculated and the reported D values can be mainly attributed to the appearance of Ag-FMNPs layer near the surface of the resin beads (see Fig.4) and also by possible differences in the cross linking degree of the polymer matrices and in the other experimental conditions. In other words the resistance of the polymer-metal nanocomposite material towards mass-transfer does not change dramatically in comparison with the initial FMNPs-free polymer.

This conclusion also follows from the results shown in Fig. 6, where the breakthrough curves obtained within a series of experiments on displacement Na^+ with Ca^{2+} ions from the initial polymer (FMNPs-free) and nanocomposite samples containing different amounts of FMNPs are presented. The slope of the curves shown in Fig. 6 qualitatively reflects the kinetic properties of the corresponding material so that the closer it to 90° the faster is the mass transfer process inside the polymer matrix. This means that after DEDIMS of FMNPs the functional groups of the ion exchanger remain almost equally accessible for ions to be removed from the water under treatment. At the same time what it also follows from the results shown in Fig.6, the slowing down of the ions diffusion can be decreased by minimizing the thickness of FMNPs layer moreover the negative impact of this layer is partially compensated by the appearance of nanoporosity in nanocomposite material (see above).

The area marked by the horizontal and vertical dotted lines in Fig. 6 corresponds to the ion exchange capacity, q^* (see eq.5) of the initial polymer and nanocomposite samples. The vertical dotted line has to pass through the inflection point of each breakthrough curve and as it is seen these points for all curves essentially coincide with each other. This means that q^* values of all nanocomposite samples coincide with that of the initial polymer. The q^* value estimated from Fig. 6 appears to equal to $2.0 \text{ meq} \times \text{g}^{-1}$ what is very close the value of $2.1 \text{ meq} \times \text{g}^{-1}$ obtained by the quantitative titration of a certain mass of the initial polymer in the H^+ -form with alkali solution.

Figure 7 presents the breakthrough curve profiles obtained with modified and unmodified Ag-FMNPs anion-exchange resin of gel type. The modification was carried out by DEEIMS of Ag-FMNPs by using the following reactions:



As it clearly follows from the breakthrough curve profiles shown in Figure 7, the displacement of OH^- with Cl^- ions from the FMNPs free anion exchanger and Ag-FMNPs-containing nanocomposite coincide essentially in all points. This means that the kinetics of $\text{OH}^- - \text{Cl}^-$ exchange is the same in both cases. In other words the Ag-FMNPs layer does not create any additional diffusional barrier for exchanging ions. Another conclusion which follows from the breakthrough curves shown in Fig. 7, concerns the equality of ion exchange capacity values of FMNPs free and Ag-FMNPs-containing anion exchanger. The capacity of both samples estimated from the data of Fig. 7 appears to be equal to $2.1 \text{ meq} \times \text{g}^{-1}$ what coincides with the value obtained by titration of a certain mass of the initial polymer in the OH^- -form with acid solution. Comparison of the data shown in Figures 6 and 7 allow to conclude that minimization of the metal loading time allows to decrease the thickness of Ag-FMNPs layer what in turn permits to maintain the ion exchange properties of the ion exchange material unchanged. This is particularly true in the case of anion exchange polymer.

The comparison of DEEIMS versions used for modification of cation exchange (see equations 5 and 6) and anion exchange (see equations (9) and (10)) polymeric matrices leads to a quite logic conclusion: both versions of DEEIMS procedure are in fact the specular reflection of each other. Indeed, in the first case after the loading of the functional groups with metal ions (equation (5)) the polymer is treated with reducing agent (equation (6)), anions of which (the actual reducer) bear the same charge (negative) as the functional groups of the polymer. Due to the action of DEE they cannot deeply penetrate inside the matrix and the reduction of metal ions leading to formation of FMNPs proceeds near the polymer surface (see Fig. 1).

In the case of anion exchange polymer, the first stage of DEEIMS is the sorption of the reducer anions on the positively charged functional groups of the polymer (equation (9)). The second stage (equation (10)) is the treatment of the polymer with solution of positively charged metal ions. Their rejection by the matrix bearing the charge of the same sign does not allow them to deeply penetrate into the polymer and their interaction with reducing agent proceeds (as in the previous case) near the surface of the polymer. It seems important to emphasize that both versions of DEEIMS technique lead to the most favourable distribution of FMNPs near the surface of nanocomposite material, what is particularly important in practical application of such materials for complex water treatment. Note that similar procedure has been also applied for the

synthesis of metal oxide nanoparticles inside ion exchange resins for removal of arsenic from water[13] and for the preparation of heterogeneous catalysts.[5]

Conclusions

The following conclusions can be derived from the results obtained in this study:

1. The surface modification of ion exchange materials with FMNPs by DEEIMS technique has been shown to provide the most favourable distribution of FMNPs in the final nanocomposite materials enhancing their feasible applications such as complex water treatment and heterogeneous catalysis.
2. DEEIMS has been demonstrated to be a universal synthetic methodology applicable for the preparation of bifunctional polymer-metal nanocomposites from polymers of either functionality, i.e. bearing either negatively (e.g., cation exchangers) or positively (e.g., anion exchangers) charged functional groups.
3. The ion exchange capacity of the polymer is not essentially changed after its modification with FMNPs as it follows from the breakthrough curve profiles obtained on the unmodified polymers and modified with FMNPs nanocomposites. As it also follows from these data, the resistance of the matrix towards ions diffusion can be minimized by varying the thickness of FMNPs layer and can reach the same value as that of the unmodified polymer.
4. The modification of polymers with negatively charged functional groups with FMNPs by using DEEIMS technique has been shown to be accompanied by regeneration of the functional groups, i.e. their conversion into the initial Na⁺-form. This permit to easily increase the thickness of FMNPs layer (if required) by carrying out consecutive metal-loading-reduction cycles.
5. Modification of the cation-exchange polymer of gel-type with Ag-FMNPs has been shown to lead to strong modification of the polymer morphology due to the appearance of the woam-like structure on the polymer surface and the nanoporosity, which enhances the rate of mass transfer in the nanocomposite

ASSOCIATED CONTENT

Supporting Information.: Time lapse video of actual IMS of Ag-NPs on cationic gel-type polymer and its corresponding measurement parameters. This material is available free of charge via the Internet at <http://pubs.acs.org>.

AUTHOR INFORMATION

Corresponding Author

Dmitri N. Muraviev. E-mail: dimitri.muraviev@uab.cat

Author Contributions

The manuscript was written through contributions of all authors. All authors have given approval to the final version of the manuscript and all of them contributed equally.

ACKNOWLEDGMENT

Programa Operatiu de Catalunya (FEDER) is acknowledged for the financial support within the project VALTEC09-02-0058. JB also thanks the Autonomous University of Barcelona for the personal grant and Servei de Microscopia of Universitat Autònoma de Barcelona for the SEM and Confocal images..

ABBREVIATIONS

IMS Intermatrix Synthesis, NPs nanoparticles, MNPs metal nanoparticles, FMNPs functional metal nanoparticles, NMs nanomaterials, DEE Donnan Exclusion Effect, DEEIMS intermatrix synthesis technique coupled with Donnan Effect, SEM scanning electron microscopy.

REFERENCES

- [1] A. Alonso, X. Muñoz-Berbel, N. Vigués, J. Macanás, M. Muñoz, J. Mas, et al., Characterization of fibrous polymer silver/cobalt nanocomposite with enhanced bactericide activity., *Langmuir*. 28 (2012) 783–90.
- [2] A. Alonso, N. Vigués, X. Muñoz-Berbel, J. Macanás, M. Muñoz, J. Mas, et al., Environmentally-safe bimetallic Ag@Co magnetic nanocomposites with antimicrobial activity., *Chem. Commun. (Camb)*. 47 (2011) 10464–6.
- [3] P. Barbaro, F. Liguori, Ion exchange resins: catalyst recovery and recycle., *Chem. Rev.* 109 (2009) 515–29.

- [4] J. Bastos-Arrieta, M. Muñoz, P. Ruiz, D.N. Muraviev, Morphological changes of gel-type functional polymers after intermatrix synthesis of polymer stabilized silver nanoparticles., *Nanoscale Res. Lett.* 8 (2013) 255.
- [5] J. Bastos-Arrieta, A. Shafir, A. Alonso, M. Muñoz, J. Macanás, D.N. Muraviev, Donnan exclusion driven intermatrix synthesis of reusable polymer stabilized palladium nanocatalysts, *Catal. Today.* (2012).
- [6] G. Boyd, A.W. Adamson, L.S. Myers, The exchange adsorption of ions from aqueous solutions by organic zeolites. II. Kinetics, *J. Am. Chem. Soc.* 69 (1947) 2836–2848.
- [7] J.M. Campelo, D. Luna, R. Luque, J.M. Marinas, A. a Romero, Sustainable preparation of supported metal nanoparticles and their applications in catalysis., *ChemSusChem.* 2 (2009) 18–45.
- [8] J.M. Campelo, D. Luna, R. Luque, J.M. Marinas, A. a Romero, Sustainable preparation of supported metal nanoparticles and their applications in catalysis., *ChemSusChem.* 2 (2009) 18–45.
- [9] A. Chiavola, E. D'Amato, R. Baciocchi, Ion Exchange Treatment of Groundwater Contaminated by Arsenic in the Presence of Sulphate. Breakthrough Experiments and Modeling, *Water, Air, Soil Pollut.* 223 (2011) 2373–2386.
- [10] J. a Dahl, B.L.S. Maddux, J.E. Hutchison, Toward greener nanosynthesis., *Chem. Rev.* 107 (2007) 2228–69.
- [11] B. Domènech, M. Muñoz, D.N. Muraviev, J. Macanás, Uncommon patterns in Nafion films loaded with silver nanoparticles., *Chem. Commun. (Camb).* 50 (2014) 4693–5.
- [12] N. Ertugay, Y.K. Bayhan, The removal of copper (II) ion by using mushroom biomass (*Agaricus bisporus*) and kinetic modelling, *Desalination.* 255 (2010) 137–142.
- [13] J.E. Greenleaf, J. Lin, A.K. Sengupta, Two novel applications of ion exchange fibers: Arsenic removal and chemical-free softening of hard water, *Environ. Prog.* 25 (2006) 300–311.
- [14] F. Helfferich, *Ion Exchange*, McGraw-Hill Book Co. Inc., New York, 1962.
- [15] F. Helfferich, ION-EXCHANGE KINETICS. 1 III. EXPERIMENTAL TEST OF THE THEORY OF PARTICLE-DIFFUSION CONTROLLED ION EXCHANGE, *J. Phys. Chem.* 66 (1962) 39–44.
- [16] F. Helfferich, Ion-exchange kinetics. V. Ion exchange accompanied by reactions Ion exchange kinetics, *J. Phys. Chem.* 69 (1965) 1178–1187.

- [17] a. a. Kudinov, Y. V. Solodyannikova, O. V. Tsabilev, D. V. Obukhov, Deoxygenation of chemically purified water at thermal power plants, *Power Technol. Eng.* 43 (2009) 131–134.
- [18] S. Kumar, S. Jain, History, Introduction, and Kinetics of Ion Exchange Materials, *J. Chem.* 2013 (2013) 1–13.
- [19] D. Muraviev, J. Macanas, M. Farre, M. Munoz, S. Alegret, Novel routes for inter-matrix synthesis and characterization of polymer stabilized metal nanoparticles for molecular recognition devices, *Sensors Actuators B Chem.* 118 (2006) 408–417.
- [20] D.N. Muraviev, Inter-matrix synthesis of polymer stabilised metal nanoparticles for sensor applications, *Contrib. to Sci.* 3 (2005) 19–32.
- [21] B. Pan, B. Pan, W. Zhang, L. Lv, Q. Zhang, S. Zheng, Development of polymeric and polymer-based hybrid adsorbents for pollutants removal from waters, *Chem. Eng. J.* 151 (2009) 19–29.
- [22] V. Polshettiwar, R. Luque, A. Fihri, H. Zhu, M. Bouhrara, J.-M. Basset, Magnetically Recoverable Nanocatalysts., *Chem. Rev.* (2011).
- [23] N. Ramzan, N. Feroze, M. Kazmi, M. Ashraf, S. Hasan, Performance analysis of cation and anion exchangers in water treatment plant: an industrial case study, *Polish J. Chem. Technol.* 14 (2012) 35–41.
- [24] J. Shi, On the synergetic catalytic effect in heterogeneous nanocomposite catalysts, *Chem. Rev.* 113 (2013) 2139–2181.
- [25] P. Taylor, H. Matsuzuru, Y. Wadachi, Journal of Nuclear Science and Influence of Differences in Resin-Matrix Structure on Ion-Exchange Adsorption of Trace Amounts of Ag (I), Co (II) and Cr (III) Influence of Differences in Resin-Matrix Structure on Ion-Exchange Adsorption of Trace Amou, *J. Nucl. Sci. Technol.* 12 (1975) 344–349.
- [26] P. Xu, X. Han, B. Zhang, Y. Du, H.-L. Wang, Multifunctional polymer-metal nanocomposites via direct chemical reduction by conjugated polymers., *Chem. Soc. Rev.* 43 (2014) 1349–60.
- [27] E. V. Zolotukhina, T. a. Kravchenko, Synthesis and kinetics of growth of metal nanoparticles inside ion-exchange polymers, *Electrochim. Acta.* 56 (2011) 3597–3604.

Figure Captions

Figure 1: (a) High resolution SEM image of nanocomposite bead cross section and (b, c) Line Scan EDS spectra showing distribution of Ag-MNPs (red) in sulfonic gel type cation-exchange resin modified with Ag-FMNPs.

Figure 2: High-resolution SEM images of: a) NPs free granulated polymer. b, c, d, e, f): Ag-FMNPs containing polymer with clearly seen as worm-like structure of nanocomposite surface and nanopores. Magnification $a = b < c < d < e < f$

Figure 3: High-Resolution SEM images of Ag-FMNPs with an average diameter of 33 ± 1 nm on gel type polymer, show distribution of the FMNPs with non-evident agglomerates after surface modification Magnification of $b \gg a$.

Figure 4: SEM images of cross sections of Ag-FMNPs-sulfonic gel-type polymer nanocomposite granules at different times of metal loading stage and thicknesses (Δl) of final FMNPs layer (time of $a < b$).

Figure 5: Thickness of FMNPs layer versus metal loading time.

Figure 6: Breakthrough curves of displacement of Na^+ with Ca^{2+} from FMNPs-free sulfonic cation-exchange resin and nanocomposites obtained after different times of metal loading stage.

Area marked by dotted lines corresponds to ion exchange capacity of resin and nanocomposite samples.

Figure 7: Breakthrough curves of displacement of OH^- with Cl^- ions from FMNPs-free quaternary amine anion-exchange resin (gray) and nanocomposite (dark gray) obtained by DEEIMS technique with metal loading time of 1 minute.

Fiigures

Figure 1

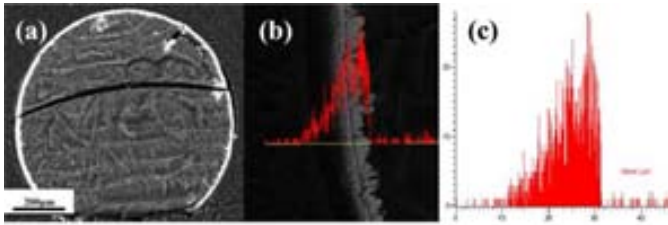


Figure 2:

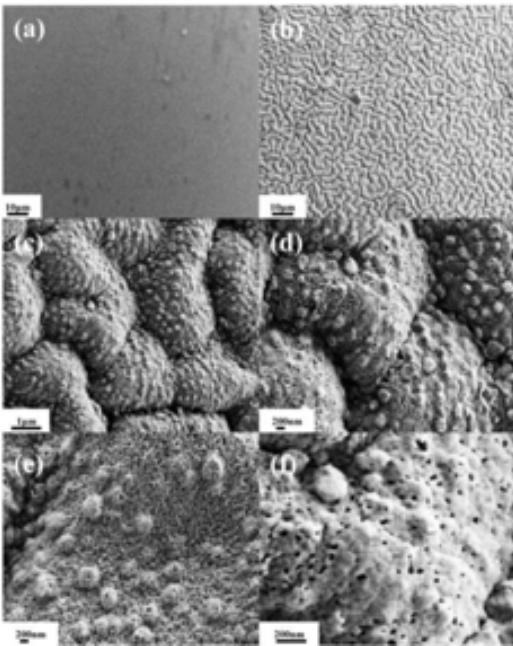


Figure 3:

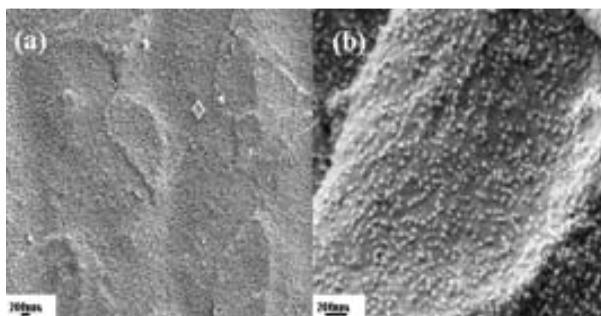


Figure 4:

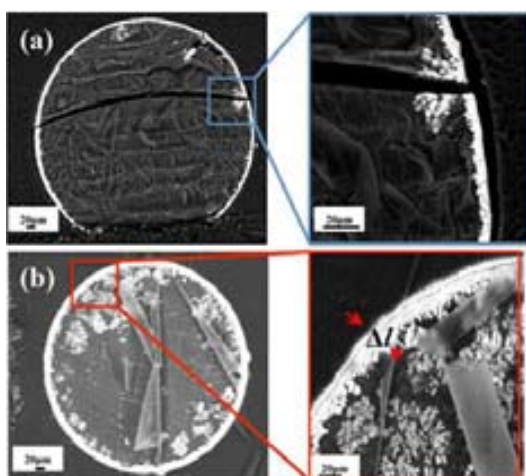


Figure 5:

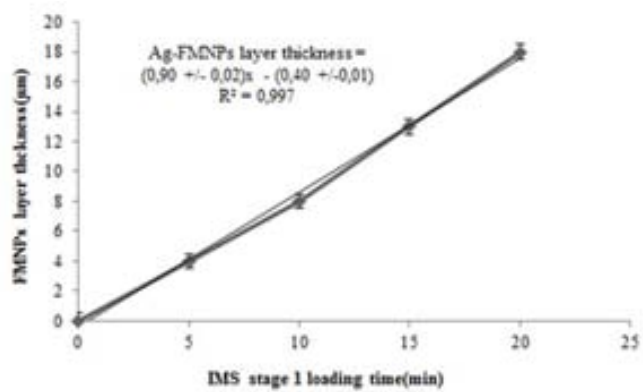


Figure 6:

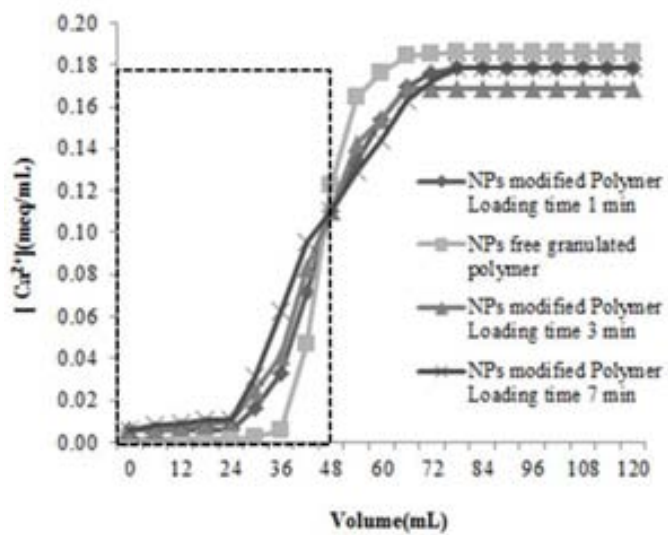
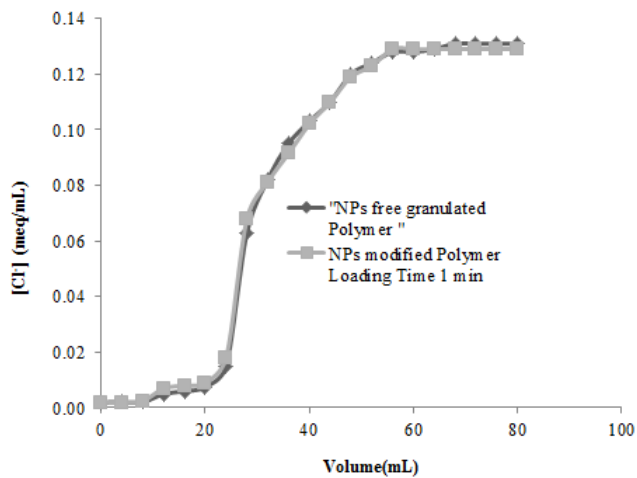


Figure 7:



Tables:

Table 1:

IMS stage 1 loading time (min)	Ag-FMNPs layer thickness μm ($\pm 0.02\mu\text{m}$)
1	0.50
3	2.30
7	5.90

Table 1: Thickness values of Ag-FMNPs layer at low metal loading times determined from Figure 4.

Graphical Abstract

Intermatrix synthesis (IMS) of Ag functional metal nanoparticles (FMNPs) leads to a significant Surface modification of gel – type polymers without changing ion exchange properties of the polymeric support. A) smooth surface confocal 3D image and SEM frame image of raw gel-type cationic resin before IMS B) rough surface confocal 3D image and SEM frame image of gel-type cationic resin containing after IMS of Ag-FMNPs.

